

**CRESTA: Consortium on  
Remote Sensing of Freight Flows in  
Congested Border Crossings and Work Zones**

Final Report

**Prepared for:**

Research and Innovative Technologies Administration  
U.S. Department of Transportation

**Prepared by:**

The Ohio State University (M. McCord, P. Goel, P. Kapat, and C. Merry)  
in collaboration with  
University of Arizona (M. Hickman and P. Mirchandani)  
Michigan Tech Research Institute (C. Brooks and E. Keefauver)  
Center for Automotive Research (R. Wallace)

March 2011

## EXECUTIVE SUMMARY

The objectives of this project were to develop and demonstrate the use of remote sensing and geospatial information technologies to provide useful information for applications related to

- the times trucks incur in various activities (activity times) at international border crossings
- truck movements in and around work zones

We used an empirical approach at specific sites to situate our developments in a context sensitive to the types of issues that would be experienced in practical applications, to validate our results in a realistic setting, and to provide case-study type demonstrations on the value of the approaches developed.

The international border crossing sites chosen were the Ambassador Bridge crossing, connecting Windsor, Ontario, and Detroit, Michigan; the Blue Water Bridge crossing, connecting Sarnia, Ontario, and Port Huron, Michigan; and the Mariposa Port of Entry, connecting Nogales, Sonora, and Nogales, Arizona. The Ambassador and Blue Water Bridge crossings were among the three top land crossings in terms of shipment values in 2008. The Mariposa POE is the designated port of entry for the CANAMEX (Canada-America-Mexico) freight corridor in the western U.S. The work zone site chosen was that associated with the I-10 reconstruction project in Tucson, Arizona. In this project, I-10 was to be widened from six lanes to eight lanes over a 4.5-mile stretch through downtown Tucson. The project, managed by the Arizona Department of Transportation, was expected to have significant impacts on traffic conditions throughout Tucson.

Given the empirically-based approach, our goals in the international border crossing application were to

- apply remote sensing and geospatial technologies to acquire data on truck activity times
- process the acquired data into novel and meaningful information on truck activity times
- use the activity time to develop, estimate, and validate explanatory models of activity times at the gateways
- exploit the validated models to predict responses in activity times to various scenarios on traffic growth and changes in infrastructure and operations at the border crossing facilities

In the work zone application, our goals were to

- apply remote sensing and geospatial technologies to acquire data on the movements of construction vehicles and other vehicles in and around a major construction zone
- process the acquired data to facilitate an understanding of these movements
- document the changes, from preexisting conditions, in vehicle speeds and routing in and around the work zone that occurred during the construction

- identify routing patterns of construction vehicles that would enhance construction operations and reduce construction-related delays to other vehicles

At the Ambassador Bridge and Blue Water Bridge sites, we developed and applied an approach based on electronic geo-fences to estimate times the trucks incurred when undergoing the multiple activities – *e.g.*, approaching the facility, undergoing toll and customs inspection, queuing – associated with traveling through an international border crossing facility.

We produced “activity time” distributions from geo-fence data collected from CEVA Logistics, Inc., trucks over approximately eleven months and indicated the types of information that could be obtained from these distributions. Specifically, we used the results to document greater in overall crossing times for U.S.-bound traffic than for Canada-bound traffic and to demonstrate the usefulness of being able to identify trips that visit duty-free facilities both for fleet management purposes and for refinement of crossing time distributions. We also illustrated how the geo-fence approach can be used to depict different temporal patterns in the crossing times for different directions of traffic at the different crossing sites and to determine time spent in queuing before primary customs inspection and the time spent while undergoing inspection. We noted that the times and the variability of times spent queuing before inspection and when undergoing the inspections are generally greater for U.S.-bound traffic than for Canada-bound traffic. We also documented the temporal stability in inspection times at both crossing sites and for both directions of traffic. Finally, we demonstrated how the data obtained with the geo-fence approach can be used to support “before-and-after” analysis by investigating queuing times prior to and after implementing traffic management systems for U.S.-bound traffic at the Blue Water Bridge crossing site.

In addition, we developed visualization tools to assist in understanding the activity times obtained with the geo-fence approach. We used both open source and proprietary software to produce tools that were used to help us investigate patterns and communicate our results to stakeholders and at conference presentations.

The geo-fence approach takes advantage of existing hardware, software, and communication systems associated with GPS-based on-board data units (OBDU) that are already in use on many truck fleets. These systems automatically record and communicate time-stamped truck locations when events of interest occur, for example, when a truck’s ignition is turned off or on, when the truck travels faster than some threshold speed, when no record has been received in some predetermined time interval. In addition, they trigger a record when the unit determines that the truck has crossed a geo-fence, the virtual perimeter of an electronic polygon, the coordinates of which can be remotely transmitted to the OBDU. Our contributions lay in realizing that several spatially precise geo-fences could be used to provide times associated with important activities, specifying the locations of these geo-fences at the sites used in our empirical study, working through implementation and data processing issues, and demonstrating the types of previously

unavailable information that can be derived from the data and be of use to both fleet managers and facility operators and planners. Since many fleets already use the underlying technologies for management purposes, no additional infrastructure is required to obtain the data associated with the geo-fence approach.

If one has access to a fleet of trucks already using the underlying technologies, the geo-fence approach is an expeditious and low-cost way to produce detailed information on border crossing activity times over long durations. However, if the information is to portray activity times for trucks from a broader population than that from which the data were obtained, the representativeness of the information must be determined. The fleet of CEVA trucks are all FAST (Free and Secure Trade)-certified. We developed ways to compare our CEVA-generated geo-fence results to results we produced from manually collected data, from airborne imagery, from information posted on the U.S. Customs and Border Protection website, and from a data set recently collected by Turnpike Global Technologies and Transport Canada-Ontario region. The screening time comparisons support that the geo-fence results produced from the CEVA data are more representative of distributions for FAST-certified trucks than for non-FAST-certified trucks and that FAST-certified trucks tend to be inspected more quickly than non-FAST-certified trucks. Queuing time comparisons also indicate that the CEVA data are more representative of FAST than non-FAST trucks, although there is some evidence that the results may provide indications of non-FAST truck patterns.

At the Mariposa POE, we did not have access to geo-fence data. To investigate activity times at this site, we extracted information from imagery collected from airborne platforms. Airborne imagery is an attractive approach to obtaining synoptic information on truck activity times, especially for focused time periods of interest. Like the geo-fence approach, no roadside infrastructure is required, and data are, therefore, relatively easy to collect. However, the cost of airborne data collection does not make it useful for ongoing monitoring of truck activity times. Rather, data would be acquired from time to time on a “sampling” basis.

In our empirical study, we used a helicopter equipped with a camera platform and a computer with sufficient memory to store multiple images of points of interest. We used two different camera platforms. One platform was a commercially-available high-resolution camera that obtained imagery containing approximately 5 megapixels at rate of 15 images per second. The second was the ANTAR platform developed by the German Aerospace Center (Deutsches Zentrum für Luft- und Raumfahrt, or DLR). This platform included a high-resolution visual imagery camera that captures imagery of approximately 4 megapixels per image at 3-5 images per second, a high-resolution infrared camera that captures images synchronous images with the visual camera, a differentially-corrected GPS unit, and an inertial measurement unit (IMU) to capture the orientation of the helicopter and the camera platform. We manually analyzed the imagery to produce the number of vehicles arriving to various inspection stations, the number of vehicles in queues at these stations, the time spent by vehicles as they were being inspected at these stations, and the routing of the vehicles to different stations within the POE.

In a concurrent ground-based data collection effort, conducted for a separate study, video cameras were used to collect license plate numbers for trucks upstream and downstream of the POE and truck counts entering and leaving the POE. The license plate data and the truck counts allowed a temporally continuous record of truck volumes, but no direct observation of truck movements within the POE was possible on the ground. The airborne imagery allowed observations within the POE, but for only a limited time period. Using the combined data sets and mathematical modeling, we determined and validated truck routing probabilities within the POE and distributions of truck times at various POE inspection stations.

We were also successful in using the data collected from both the geo-fence and the air-based imagery approaches to develop models of truck activity times. Using the geo-fence derived information and vehicle volume and lane status information obtained from other sources, we developed aggregate, macroscopic models of the queuing time upstream of U.S. primary customs inspection at the Blue Water Bridge site as a function of traffic volumes and numbers of open inspection booths. The coefficients of the models are statistically significant and have the expected signs, which indicate that queuing times increase when traffic increases and the number of open inspection booths decrease. We also developed and calibrated a microsimulation model using the information produced from our airborne data collection studies at the Mariposa POE. However, we were unable to explore “what if” scenarios for the Mariposa POE, since we did not have sufficient data to validate the models.

We conducted several flights to obtain imagery of truck movements around the I-10 work zone site. We again used both a traditional camera platform and the high-resolution ANTAR system mounted on a helicopter for these data collection efforts. Both systems allowed us to determine traffic density and queue lengths through the work zone. The ANTAR system also provided automated geo-referencing, vehicle detection, and vehicle tracking, which allowed the determination of vehicle speed information. The empirical studies supported the value of better technology for airborne traffic data collection, but no major work zone-induced congestion was observed in the empirical study. The absence of the anticipated congestion in the work zone area was primarily attributed to successful traffic demand management and active signal control in the corridor.

In summary, we have demonstrated that remote sensing and geo-spatial information technologies already deployed by many carriers for tracking commercial vehicles can be used to provide information on truck activity times at border crossing facilities and that airborne imagery can provide quantitative measures of traffic conditions in an around work zones.

## TABLE OF CONTENTS

Executive Summary	ii
Table of Contents	vi
Acknowledgments and Disclaimer	viii
List of Tables	ix
List of Figures	xii
Section 1. Introduction, Scope, and Overview	1
1.1 Overview and General Scope	1
1.2 Motivation for Methodological Approaches	2
1.2.1 Motivation for Determining Truck Activity Times at Border Crossings	3
1.2.2 Motivation for Work Zone Analysis	5
1.3 Outreach Efforts	6
1.4 Overview of the Report	9
Section 2. Geo-fence Approach and Results	11
2.1 Description of the Approach	12
2.2 Empirical Setting	13
2.3 Geo-fence Implementations	15
2.3.1 General Approach	15
2.3.2 Geo-fence Implementations	16
2.4 Geo-fence Empirical Results	22
2.4.1 Preprocessing and Trip Chaining	22
2.4.2 Activity and Excess Times	24
2.4.3 Selected Activity Time and Excess Time Results	26
2.5 Visualization of Geo-fence Results	36
2.5.1 Web Based Data Sharing	37
2.5.2 GIS-Based Display Tools for Examining Numerical Results	39
Section 3. Validation of Truck Activity Time Patterns Determined from Geo-fence Results	43
3.1 Supplementary Data for Validation	45
3.2 Customs Screening Validation	51
3.3 Queuing Time Validation	56
3.4 Border Crossing Time Validation	62

Section 4. Airborne Data Collection and Results	74
4.1 Approach and Methodology	74
4.2 Empirical Setting	77
4.3 Selected Results	81
4.3.1 Analysis of License Plate Data	81
4.3.2 Analysis of U.S. Customs and Border Protection Waiting Time Data	87
4.3.3 Analysis of Airborne Imagery	89
Section 5. Modeling of Activity Times	93
5.1 Macroscopic Modeling	93
5.2 Microsimulation Models	97
5.2.1 Model Structure	98
5.2.2 Model Calibration and Application	105
5.2.3 Conclusions	108
Section 6. Analysis of Work Zones	110
6.1 Empirical Setting	110
6.2 Approach and Methodology	112
6.2.1 Imagery and Camera Platform	112
6.2.2 Traffic Analysis Software	114
6.2.3 Traffic Condition Measurement	114
6.2.3.1 Image Processing	114
6.2.3.2 Traffic Density Calculation	124
6.3 Selected Results	127
6.4 Conclusions	129
Section 7. Conclusions	130
References	133
Appendix to Section 1: Summary of Technical Expert Advisory Committee Meetings Held in 2010	136
Appendix to Section 2: Tables in Support of Section 2.4.2	142
Appendix to Section 3: Figures and Tables in Support of Validation Study	152

## ACKNOWLEDGMENTS AND DISCLAIMER

This work was partially supported by the Commercial Remote Sensing and Spatial Information program of the Research and Innovative Technologies Administration, U.S. Department of Transportation, award number #DTOS59-07-H-0001, with additional cost share funds provided by The Ohio State University, the University of Arizona, the Michigan Tech Research Institute, the Center for Automotive Research, and Skycomp, Inc. The authors are also grateful for the data and institutional and personnel support provided by Ray Cossette, Systems Operations Analyst, CEVA Logistics Canada, ULC; Morris Hall, Blue Water Bridge Operations Manager for Michigan Department of Transportation; and Jim Phillips, Senior Customs Manager, General Motors Corporation; and for the insights on operations at the Blue Water Bridge offered by Michael Szuch, Blue Water Bridge Manager for Michigan Department of Transportation.

The views, opinions, findings, and conclusions reflected in this report are the responsibility of the authors only and do not represent the official policy or position of the USDOT, RITA, or any other individual or entity.

## LIST OF TABLES

Table 2.3.2-1: Description of Ambassador Bridge AU08 geo-fences	18
Table 2.3.2-2: Description of Blue Water Bridge AU08 geo-fences	21
Table 2.4.3-1: Border crossing time statistics by bridge crossing and direction, before (Original Distributions) and after (Distributions w/o Duty Free Trips) eliminating trips that crossed through duty-free geo-fence	28
Table 2.4.3-2: Proportion* of Canada-to-US truck trips in data base traversing duty free polygon by hour-of-day and day-of-week at Ambassador Bridge crossing ( <i>*noise added to proportions to preserve confidentiality of information</i> )	29
Table 2.4.3-3: Queuing-induced excess time statistics for roadway sections upstream of customs screening locations by bridge crossing and direction	32
Table 2.4.3-4: Primary customs screening-induced excess time statistics by bridge and direction combination	33
Table 3.2-1: Summary statistics of primary customs screening times of U.S.-bound trucks for FAST and standard/non-FAST truck lanes from ground-based data collection at Blue Water Bridge crossing	51
Table 3.2-2: Summary statistics of distributions of screening times determined from air-photos aggregated by what were considered to be FAST lanes and standard/non-FAST lanes during air-based data collection period; (a) Ambassador Bridge statistics (b) Blue Water Bridge Statistics	54
Table 3.2-3: Probabilities, derived from geo-fence ECDFs, of observing screening times equal to the mean of screening times derived from the air photo- and ground-based data, plus or minus 0.1 [min]; (a) Ambassador Bridge probabilities using air photos (b) Blue Water Bridge probabilities using air photos (c) Blue Water Bridge, U.S.-bound probabilities using ground-based data	55-56
Table 3.3-1: Probabilities derived from geo-fence ECDFs of observing queuing times equal to the mean of queuing times derived from the air photo-data, plus or minus 0.5 [min] (a) Ambassador Bridge probabilities (b) Blue Water Bridge probabilities	57-58
Table 3.3-2: Correlation values between geo-fence derived queuing excess times and CBP-posted delays and between pairs of CBP-posted delays at Ambassador Bridge and Blue Water Bridge Crossings; (a) Ambassador Bridge correlations (b) Blue Water Bridge correlations	60
Table 3.4-1: Summary statistics of crossing time distributions obtained from CEVA geo-fence and Transport Canada Bluetooth data by direction and crossing site	66

Table 4.3.1-1: Summary statistics obtained from license plate data through the Mariposa POE	81
Table 4.3.1-2: Estimated mean and standard deviations of waiting time (service time + queuing time) distributions for the inspection stations produced from Maximum Likelihood Estimation	85
Table 4.3.1-3: Estimated means and standard deviations of waiting time (service time + queuing time) distributions for the inspection stations produced from the MCMC method	86
Table 4.3.3-1: Selected queuing statistics from Mariposa POE	91
Table 5.1-1: Numbers of excess time-hourly volume pair observations for <i>usplazabridge</i> geo-fence, in Canada-to-US direction	95
Table 5.1-2: Summary results of logistic regression models of excess times for various thresholds $T^{thr}$	96
Table 6.2.3.1-1: Actions and results of steps used to generate the digital street map of I-10 used as input for the geo-referencing features of TrafficFinder and ClickTool	115
Table 6.2.3.1-2: Description of navigation file data elements	120
Table 6.2.3.1-3: Steps used to identify vehicles using ClickTool	121
Table 6.3-1: Density of traffic, Westbound I-10	128
Table 6.3-2: Density of traffic, Eastbound I-10	128
Table 6.3-3: Average speed of traffic, Westbound I-10	128
Table 6.3-4: Average speed of traffic, Eastbound I-10	128
Table A2.4.2-1: Free flow speeds for various geo-fences at the Ambassador Bridge	143
Table A2.4.2-2: Free flow speeds for various geo-fences at the Blue Water Bridge	143
Table A2.4.2-3: Free flow speeds for roadway section including toll collection and customs inspection, in the US-to-Canada direction at the Ambassador Bridge	144
Table A2.4.2-4: Free flow speeds for roadway section including toll collection and customs inspection, in the Canada-to-US direction at the Ambassador Bridge	144

Table A2.4.2-5: Free flow speeds for roadway section including toll collection and customs inspection, in the US-to-Canada direction at the Blue Water Bridge	145
Table A2.4.2-6: Free flow speeds for roadway section including toll collection and customs inspection, in the Canada-to-US direction at the Blue Water Bridge	145
Table A2.4.2-7: Activity times for various geo-fences, US-to-Canada direction, Ambassador Bridge	146
Table A2.4.2-8: Activity times for various geo-fences, Canada-to-US direction, Ambassador Bridge	146
Table A2.4.2-9: Activity times for various geo-fences in the US-to-Canada direction at the Blue Water Bridge	147
Table A2.4.2-10: Activity times for various geo-fences in the Canada-to-US direction at the Blue Water Bridge	147
Table A2.4.2-11: Excess times for various geo-fences in the US-to-Canada direction at the Ambassador Bridge	148
Table A2.4.2-12: Excess times for various geo-fences in the Canada-to-US direction at the Ambassador Bridge	148
Table A2.4.2-13: Excess times for various geo-fences in the US-to-Canada direction, Blue Water Bridge	149
Table A2.4.2-14: Excess times for various geo-fences in the Canada-to-US direction, Blue Water Bridge	149
Table A2.4.2-15: Total crossing times in both directions at the two bridges, with and without duty-free trips included	150
Table A2.4.2-16: Total excess times in both directions at the two bridges	150
Table A2.4.2-17: Toll collection and customs inspection gap activity times in both directions at the two bridges	151
Table A2.4.2-18: Toll collection and customs inspection gap excess times in both directions at the two bridges	151
Table A3.2-1: Summary statistics of screening times, by lane, derived from air photos	155
Table A3.2-2: Summary statistics of queuing times, by lane, derived from air photos	156

## LIST OF FIGURES

Figure 2.2-1: The Ambassador Bridge and Blue Water Bridge border crossing sites connecting Michigan and Ontario	14
Figure 2.3.2-1: Ambassador Bridge AU08 geo-fences developed to investigate border crossing activities	17
Figure 2.3.2-2: Blue Water Bridge AU08 geo-fences developed to investigate border crossing activities	20
Figure 2.4-1: Illustration of Regions of Interest (ROI) used to spatially filter data into subsets around the bridge crossings; (a) Ambassador Bridge (b) Blue Water Bridge	22
Figure 2.4.2-1: Illustration of the “crossing-in” and “crossing-out” locations of the <i>bwb_usplazabridge</i> geo-fence at the Blue Water Bridge crossing, US-to-Canada direction	25
Figure 2.4.2-2: ECDF plots used to determine the free flow speed in the US-to-Canada direction for the <i>bwb_usplazabridge</i> geo-fence, Blue Water Bridge crossing site; (a) “crossing-in” speeds (b) “crossing-out” speeds	25
Figure 2.4.3-1: Illustration of geo-fence crossing locations used to determine “border crossing times”; (a) Ambassador Bridge site (b) Blue Water Bridge site	27
Figure 2.4.3-2a: Border crossing time medians by hour-of-day for the four bridge crossing-direction combinations	31
Figure 2.4.3-2b: Border crossing time variability measures by hour-of-day for the four bridge crossing-direction combinations	31
Figure 2.4.3-3: Empirical cumulative distribution functions of screening-induced excess times by time-of-day period, for each border crossing site-direction	34
Figure 2.4.3-4: Empirical cumulative distribution functions of queuing-induced excess times upstream of customs inspection for “before” and “after” DMS implementation periods	35
Figure 2.4.3-5: Empirical cumulative distribution functions of queuing-induced excess times during three time-of-day periods for the “before” and “after” periods	36
Figure 2.5.1-1: Screen shot of VISDAQ web mapping interface of the geographic area encompassing the two border crossing locations used in the geo-fence study	37
Figure 2.5.1-2: VISDAQ interface with results (symbolized geo-fences) from a query of median excess time results at the Blue Water Bridge in the US to CA direction	39

Figure 2.5.2-1: An example of ESRI ArcGIS being used to display the details of CEVA data records for February 16, 2010	40
Figure 2.5.2-2: Example screen shot of a Google Earth visualization of PNT data showing truck locations and direction (symbolized with arrows), speed (size of arrow), and event triggering the data record	41
Figure 2.5.2-3: Example screenshot of a Google Earth visualization using geo-fence polygon extrusion techniques to display geo-fence excess time values by geo-fence for an individual chained truck trip that occurred from Canada to the U.S. on November 4, 2008 with the height of the extrusion symbolizing the amount of excess time	42
Figure 3.1-1: An example of the lane status data on November 19, 2008, collected manually every five minutes at the Blue Water Bridge for U.S. customs lanes	47
Figure 3.1-2: An example of the primary inspection time data collected on November 19, 2008, recorded by lane type at the Blue Water Bridge	48
Figure 3.1-3: Example photos taken from 8/1/2008 field collect at the Blue Water Bridge	49
Figure 3.1-4: Example of queue length data, on November 18, 2008, recorded manually at the Blue Water Bridge for each lane	49
Figure 3.1-5: The queue length graphic used to rapidly estimate queue lengths on the bridge in dynamic traffic situations	49
Figure 3.2-1: Empirical cumulative density functions of screening times, by lane, derived from air photos during the morning, period for the US-bound traffic at the Blue Water Bridge crossing	52
Figure 3.2-2: Empirical cumulative density functions of screening times derived from geo-fence data, by bridge crossing and direction	55
Figure 3.3-1: Scatter plots of CBP-posted delays against geo-fence recorded (CEVA) queuing excess times for FAST trucks, standard/non-FAST trucks, NEXUS passenger vehicles, and standard/non-NEXUS passenger vehicles at the Ambassador Bridge and Blue Water Bridge crossings	59
Figure 3.3-2: Empirical cumulative distributions of geo-fence derived queuing excess times when CPB posting are zero and greater than zero for various traffic classes at Ambassador Bridge and Blue Water Bridge crossings	61
Figure 3.4-1: Comparison of Transport Canada crossing time zones to merged AU08 geo-fences; (a) Blue Water Bridge (b) Ambassador Bridge	63

Figure 3.4-2: Histograms of crossing times (in seconds) obtained from CEVA geo-fence and Transport Canada Bluetooth data by direction (data from February-April 2009); (a) Ambassador Bridge (b) Blue Water Bridge	65
Figure 3.4-3: Histograms of numbers of observations by hour-of-day of CEVA geo-fence and Transport Canada Bluetooth data by direction; (a) Ambassador Bridge temporal patterns (b) Blue Water Bridge temporal patterns	66-67
Figure 3.4-4: Spline function representations for time-of-day modeling	68
Figure 3.4-5: Crossing time trends based on the (partial) marginal effect of the time-of-day variable on crossing times estimated from CEVA and Transport Canada data for both bridges and directions; (a) Ambassador Bridge (b) Blue Water Bridge	69
Figure 3.4-6: Crossing time trends based on the (partial) marginal effect on crossing times of the day-of-month variable estimated from CEVA and Transport Canada data for both bridges and directions; (a) Ambassador Bridge (b) Blue Water Bridge	70
Figure 3.4-7: Crossing time trends based on the partial (marginal) effect of the day-of-week variable on crossing times estimated from CEVA and Transport Canada data for both bridges and directions; (a) Ambassador Bridge (b) Blue Water Bridge	71
Figure 3.4-8: Crossing time trends based on the partial (marginal) effect of month-of-year variable on crossing times estimated from CEVA and Transport Canada data for both bridges and directions; (a) Ambassador Bridge (b) Blue Water Bridge	72
Figure 4.1-1: Example airborne imagery	75
Figure 4.1-2: The ANTAR platform	76
Figure 4.1-3: Registered imagery from the DLR's ANTAR	77
Figure 4.2-1: Geographic location of the Mariposa POE in Arizona	78
Figure 4.2-2: Geographic location of the Mariposa POE with respect to the City of Nogales, AZ	78
Figure 4.2-3: Points of inspection for commercial traffic at Mariposa POE	79
Figure 4.2-4: Mariposa POE process flow diagram	80
Figure 4.3.1-1: Distribution of travel times through the Mariposa POE from license plate data	82

Figure 4.3.1-2: Network representation of inspection sequences within the Mariposa POE	83
Figure 4.3.1-3: An overview of the solution method	84
Figure 4.3.1-4: Estimated composite and individual path distributions	85
Figure 4.3.1-5: Estimated routing probabilities produced from Maximum Likelihood Estimation	86
Figure 4.3.1-6: Estimated routing probabilities produced from MCMC	87
Figure 4.3.2-1: Average number of lanes open by day of week at the Mariposa Port of Entry	88
Figure 4.3.2-2: Average truck delay by day of week at the Mariposa Port of Entry	88
Figure 4.3.2-3: Average truck delay by time of day at the Mariposa Port of Entry	89
Figure 4.3.3-1: Sample cumulative curves for primary inspection (“superbooths”) during two different time periods on Feb. 28, 2008	90
Figure 4.3.3-2: Sample cumulative curves for X-ray inspection during two different time periods on Feb. 28, 2008	90
Figure 4.3.3-3: Sample cumulative curves for exit / weight check during two different time periods on Feb. 28, 2008	91
Figure 4.3.3-4: Histogram of observed service times, primary inspection (superbooths)	92
Figure 4.3.3-5: Histogram of observed service times, exit station	92
Figure 5.1-1: Excess times in geo-fences vs. hourly vehicle volume for Canada-to-U.S. geo-fences at Blue Water Bridge Crossing	94
Figure 5.1-2: Empirical cumulative distribution functions of excess times in <i>usplazabridge</i> geo-fence when there were seven and five primary customs screening truck lanes open	95
Figure 5.2.1-1: Graphical depiction of <i>Station</i> elements in VISSIM: (a) Queue entrance and exit detectors (b) Route and (c) Signal head	99
Figure 5.2.1-2: Graphical depiction of the buffer zone and the corresponding station	101
Figure 5.2.1-3: Graphical user interface for the Mariposa POE	102
Figure 5.2.1-4: Schematic layout of the Mariposa POE network	102

Figure 5.2.1-5: Simulation settings interface	103
Figure 5.2.1-6: Service time distributions interface	103
Figure 5.2.1-7: Schedules interface	104
Figure 5.2.1-8: Event calendar interface	105
Figure 5.2.2-1: Inspection points for trucks at Mariposa POE	106
Figure 5.2.2-2: Mariposa POE simulation process flow	107
Figure 5.2.2-3: Distribution of travel times through the Mariposa POE from license plate data	108
Figure 6.1-1: I-10 Work Zone in Tucson	111
Figure 6.1-2: ADOT flyer on traffic patterns during I-10 construction	112
Figure 6.2.1-1: The ANтар Platform. (a) The camera system with GPS and IMU; (b) the computer and communications infrastructure	113
Figure 6.2.2-1: Registered imagery from the DLR’s ANтар; (a) from TrafficFinder; (b) from ClickTool	114
Figure 6.2.3.1-1: Excerpt from KML file for nodes placed along I-10	116
Figure 6.2.3.1-2: Name file showing name of road segment	116
Figure 6.2.3.1-3: Excerpt from node file, with node numbers and coordinates	116
Figure 6.2.3.1-4: Link file showing segments connecting nodes	117
Figure 6.2.3.1-5: Traffic Finder GUI	118
Figure 6.2.3.1-6: Structure of TrafficFinder configuration file	118
Figure 6.2.3.1-7: Example geotiff file	119
Figure 6.2.3.1-8: Navigation data file	120
Figure 6.2.3.1-9: Configuration file for ClickTool	121
Figure 6.2.3.1-10: ClickTool GUI	122
Figure 6.2.3.1-11: Vehicles.log file	123

Figure 6.2.3.1-12: Output Excel file containing (a) the vehicle and coordinates; and (b) the average vehicle speed	124
Figure 6.2.3.2-1: Vehicle trajectories and their intersection in time-space	125
Figure 6.2.3.2-2: Images in space and time across a set of vehicle trajectories	126
Figure A3.2-1: ECDF of screening times, by lane, derived from air photos at the Ambassador Bridge crossing	153
Figure A3.2-2: ECDF of screening times, by lane, derived from air photos at the Blue Water Bridge crossing	154

## **Section 1. Introduction, Scope, and Overview**

### **1.1 Overview and General Scope**

The objectives of this project were to develop and demonstrate the use of remote sensing and geospatial information technologies to provide useful information for applications related to

- the times trucks incur in various activities (activity times) at international border crossings
- truck movements in and around work zones

For both the border crossing truck activity time application and the work zone truck movement application, our approach was one based on empirically driven developments and demonstrations at specific sites. The site-specific studies allowed us to base our developments in a context sensitive to the types of issues that would be experienced in practical applications, validate our results in a realistic setting, and provide case-study type demonstrations on the value of the approaches developed.

Given this is empirically-based approach, our goals in the international border crossing application were to

- apply remote sensing and geospatial technologies to acquire data on truck activity times
- process the acquired data into novel and meaningful information on truck activity times
- use the acquired data to develop, estimate, and validate explanatory models of activity times at the gateways
- exploit the validated models to predict responses in activity times to various scenarios on traffic growth and changes in infrastructure and operations at the border crossing facilities

In the work zone application, our goals were to

- apply remote sensing and geospatial technologies to acquire data on the movements of construction vehicles and other vehicles in and around a major construction zone
- process the acquired data to facilitate an understanding of these movements
- document the changes, from preexisting conditions, in vehicle speeds and routing in and around the work zone that occurred during the construction
- identify routing patterns of construction vehicles that would enhance construction operations and reduce construction-related delays to other vehicles

The international border crossing sites chosen were the Ambassador Bridge crossing, the Blue Water Bridge crossing, and the Mariposa Port of Entry. The Ambassador Bridge is a privately owned and operated facility (owned by the Detroit International Bridge Company – DIBC) that connects Windsor, Ontario, and Detroit, Michigan. The Blue Water Bridge is a publicly owned

and operated facility (jointly by the Michigan Department of Transportation and the Blue Water Bridge Authority, a Canadian Federal Crown Corporation) that connects Sarnia, Ontario, and Port Huron, Michigan. These border crossings ranked first (Ambassador) and third (Blue Water) among North American land crossings in terms of shipment values in 2008, serving, respectively, 2,885,047 and 1,574,428 trucks that carried approximately \$100 billion and \$80 billion of freight into the U.S. (TOLLROADSnews, 2010; US DOT, 2009). The Mariposa Port of Entry connects Nogales, Sonora, with Nogales, Arizona, and is publicly owned and operated. Mariposa is the designated port of entry for the CANAMEX (Canada-America-Mexico) freight corridor in the western U.S. In 2009, Mariposa handled 276,877 trucks and managed \$6.6 billion of freight imports into the U.S. The work zone site chosen was that associated with the I-10 reconstruction project in Tucson, Arizona. In this project, I-10 was to be widened from six lanes to eight lanes over a 4.5-mile stretch through downtown Tucson. The project, managed by the Arizona Department of Transportation, cost \$200 million and was expected to have significant impacts on traffic throughout Tucson.

We believe we were very successful in using remote sensing and geospatial technologies to collect previously unavailable data and in demonstrating how these data can be used to produce a unique understanding of truck activity patterns at international border crossings. We were also successful in combining several datasets to develop macroscopic models that explain correlations among important variables associated with the variability in the time needed to traverse a border crossing facilities, as well as in producing a simulation-based explanatory model for the Mariposa Port of Entry. However, we did not use these models to explore “what if” scenarios. Macroscopic models lack the ability to reflect the different conditions associated with “what if” scenarios, and we were unable to validate the simulation model sufficiently. For the work zones, we consider our efforts to have been very successful in using advanced remote sensing and spatial information technologies to monitor traffic conditions. Surprisingly, though, the expected construction impacts failed to materialize.

## **1.2 Motivation for Methodological Approaches**

Border crossings and transportation facilities work zones produce delays for commercial trucks and private vehicles. Understanding vehicular movements at these locations is essential to understanding, quantifying, and, ultimately, reducing these delays. However, collecting data at international border crossings and work zones has traditionally been difficult. The added requirement of security at the border crossings, and safety at construction zones, has made data collection even more difficult. Methods that can collect data remotely, using commercially available technologies, and in a manner that reduces the need for on-the-ground infrastructure would be attractive, would be valuable.

### **1.2.1 Motivation for Determining Truck Activity Times at Border Crossings**

Efficient movement of international freight to or from the U.S. is essential for national and regional economic vitality. U.S. border crossings are important nodes in the NAFTA international freight shipment network. The need to ensure the security of freight entering the country and the limited infrastructure that can be constructed at these nodes add time to international freight trips and, equally important, uncertainty in the trip times. Documenting the times and variability in times that trucks incur when crossing international borders is important to facility operators and planners for balancing the primary needs for safety and security with the secondary need to serve their customers. Monitoring trends and discovering changes in the times assist planners and operators in deciding if changes in infrastructure or operations are warranted and in allowing “before-and-after” analyses of infrastructure or operations changes. Planners and operators can also use predictive models as decision support tools to conduct “what-if” analysis. Developing, calibrating, and validating decision support models that predict crossing times under alternative infrastructure configurations and operations policies require extensive and valid data on crossing times. Fleet operators and their customers would likewise benefit from documented crossing times in helping them choose among border crossing sites, determine whether to participate in specific time-saving programs, such as Free and Secure Trade Program, FAST (Customs and Border Protection Agency, 2010), or plan more effectively for the just-in-time arrival of shipments.

Contributing to the magnitude and variability in truck crossing times are the multiple activities involved with international truck crossings – *e.g.*, approaching the facility on freeways or surface streets, paying tolls, waiting in queues, undergoing primary and potentially secondary customs inspection, possibly visiting duty free facilities. Decomposing the overall travel time into its components helps in the identification of the critical activities affecting the overall border crossing times, the management of components of the cross-border trip, and the development of models that are appropriately sensitive to different operations policies and infrastructure improvements and traffic characteristics. For example, studies that predict the effects of increased demand at the border crossing facility require an understanding of how the rates at which trucks are screened at primary inspection (a specific border crossing activity) interact with traffic volumes to produce queuing-induced delays. As another example, for planning and monitoring purposes, it is important to adjust overall crossing times to remove the effect of voluntary activities, such as visiting duty free facilities (another border crossing activity), that add to the observed travel time incurred when crossing the border. Determining whether trucks visit duty free facilities is also of interest to carrier managers, who may wish to investigate the effect of the duty free visits on the fleet’s productivity.

Traditional methods of collecting crossing time data (Neto, et al., 2009, TTI and Battelle, 2002) rely on surveillance personnel or technologies placed at specific locations along roadway infrastructure to record truck identifiers as the trucks pass the recorders. Implementing these methods is complicated at international crossings because border crossing activities include

infrastructure and operations in two countries and may be overseen by multiple international agencies (*e.g.*, customs and border protection, state departments of transportation, private bridge operators). Moreover, the spatial extent of these activities and the temporal variability in the activity times make it difficult to obtain synoptic, representative activity crossing time data: times are only obtained between the fixed surveillance locations. A large amount of equipment or personnel must be deployed for extended periods of time if activity times are to be monitored or if representative samples of these times are to be obtained. New technologies, such as Radio Frequency Identification (RFID) or Bluetooth readers (Sabeen, et al., 2008), used to determine the time that a truck passes a fixed location, offer advantages in more easily re-identifying the truck at a downstream surveillance location. However, these technologies suffer from the same difficulties as traditional methods in decomposing these travel times into components attributable to each of the multiple activities that may occur between two locations.

In addition to the multiple activities involved, not all trucks move through the border crossing facility in the same manner. Some, but not all, drivers may have the time and desire to visit duty free facilities, and some, but not all, shipments are sent to secondary customs inspection. The complexities of some of these activities and interactions among the multiple activities make the modeling of these movements difficult. Indeed, our attempts to use macro-level models, which avoid many of these complexities, did not seem sufficient for decision support purposes. We also investigated a simulation-based approach to modeling. Simulation is a common tool used to model inspection and vehicle movements and to test various operational strategies (Jeannotte, *et al.*, 2004). Simulation tools can capture the physical layout of the facility and can display the possible congestion that occurs in queues at the inspection stations and the vehicle trajectories within and around the port.

In our study, we used two approaches to collect primary data on the truck activity times. In one approach we developed what we call the “geo-fence” approach and demonstrated it at the Ambassador Bridge and Blue Water Bridge crossing sites. As will be discussed in Section 2, this is an attractive approach for collecting truck activity times if one can acquire the cooperation of managers of a fleet of trucks that are equipped with state-of-the-art position, navigation, and timing (PNT) systems and that regularly cross the border. In this case, implementation of the geo-fence approach is relatively easy and inexpensive, and data can be obtained on a continuous basis that allows ongoing data collection and monitoring of truck activity patterns. In the second approach, we developed means to exploit imagery collected from airborne platforms when one does not have access to data supporting the geo-fence approach and demonstrated this approach at the Mariposa POE. As discussed in Section 4, airborne imagery is an attractive approach to obtaining synoptic information on truck activity times, especially for focused time periods of interest. Like the geo-fence approach, no roadside infrastructure is required, and data are, therefore, relatively easy to collect. However, the cost of airborne data collection does not make it useful for ongoing monitoring of truck activity times. Rather, data would be acquired from time to time on a “sampling” basis.

As will be seen in Section 5, when combined with other, more traditional data collection techniques, imagery collected from airborne platforms is also valuable in developing micro-simulation models of activity times at border crossing facilities. We also used airborne imagery at the Ambassador Bridge and Blue Water Bridge crossing sites to support our investigations into the validity of the geo-fence data collected.

### **1.2.2 Motivation for Work Zone Analysis**

Roads near the work sites associated with construction of major transportation facilities have decreased capacities. The movement of trucks and heavy equipment to and from the work sites also tends to disrupt traffic. As a result of traffic controls and network layout, primary queues form at the construction site, and secondary queues form upstream. Additional queues can form on cross-streets and other parallel roadways as drivers choose alternate routes. Such construction projects may therefore create significant delays for drivers. Not surprisingly, mitigating these impacts is a major focus of the traffic control plans instituted during these episodes.

Capturing the impacts of work zones is difficult because the common tools for network monitoring are often disrupted during the construction. Traditional ground sensors, such as loop detectors or intersection cameras, are often removed or otherwise disabled during the construction. As a result, the empirical measurement of traffic volumes, vehicle speeds, queue lengths, and related measures is not usually possible during the event (FHWA, 2006). Rather, traffic simulation or other existing tools are used to estimate these impacts (FHWA, 2009), for the purposes of traffic management and control. In addition, there is little research or documentation of *ex post* evaluation of the effectiveness of work zone operations and management.

Remote sensing and spatial information technologies can be used to provide an alternative method of evaluating impacts of work zones. As the queues associated with construction are inherently spatial in nature, temporally and spatially extensive data from remote sensing and geospatial technologies can be used to monitor traffic patterns during construction and benchmark operations during different work activities. Developing a spatial-temporal characterization of the traffic network from available remote sensing and geospatial technologies would allow an understanding of queuing behavior and provide insights on efficient management of the queues. For example, traffic and construction managers can use these insights to improve traffic signal control during construction and the scheduling of the activities and associated truck and equipment movement around and within the construction site. Likewise, observing truck and vehicle movements at major construction sites, and the associated formation of queues, would assist in developing models to capture the spatial-temporal queuing dynamics; in turn, these models can be used to identify construction design and staging logistics to decrease vehicle delays.

### 1.3 Outreach Efforts

In addition to our technical developments, we engaged in multiple outreach activities. We held the following outreach meetings:

- Meetings with project sponsor, Research and Innovative Technologies Administration, U.S. Department of Transportation, Washington, DC: January 14, 2008, January 13, 2009
- Meetings of the Technical Expert Advisory Committee and other stakeholders:
  - Northern and Southern Border Committee Members and Stakeholders, February 9, 2009, Ann Arbor, MI (report referenced below)
  - Southern Border Committee Members and Stakeholders , April 27, 2010, Tempe, AZ (summary appears in Appendix to Section 1)
  - Northern Border Committee Members and Stakeholders; June 11, 2010 , Ann Arbor, MI (summary appears in Appendix to Section 1)
- Meetings with General Motors Corporation and CEVA Logistics, Inc. to discuss results and plans for future work, Detroit, MI: August 1, 2007; December 18, 2008,
- Meeting and presenting study results with the GM Carriers Association, January 27, 2009, Detroit, MI
- Meetings with CEVA Logistics to discuss technical details on geo-fence data and updated geo-fence implementations: March 21, 2007, Southfield, MI; September 12, 2007, Ann Arbor, MI; April, 21, 2008, Ann Arbor, MI
- Meetings with Blue Water Bridge managers to brief them on the study, understand traffic and inspection flow patterns at the site, and gain permission for collecting data from a bridge location: January 24, 2008 and August 1, 2008, Port Huron, MI
- Visit to Ambassador Bridge U.S. Plaza area with Detroit International Bridge Company personnel, for a view of current and intended future operations through U.S. Customs and the new I-75 interchange leading to the bridge, February 9, 2009

We made the following technical presentations at conferences and meetings:

- Annual meetings of the Transportation Research Board (TRB), Washington, DC:
  - “Freight Flow Modeling at Border Crossings for Congestion Mitigation,” M. McCord, January 13, 2008
  - “Emerging Tools for Visualization,” T. Erickson and C. Brooks, January 13, 2008
  - “Truck Activity Time Patterns at International Borders Documented with Advanced Location and Geospatial Technologies: Empirical Results at the Ambassador and Blue Water Bridges,” M. McCord, P. Goel, C. Brooks, P. Kapat, R. Wallace, D.E. Keefauver, January, 11, 2009

- “Sharing Large Geospatial Databases and Imagery via Open Source Visualization Tools.” D. E. Keefauver, January 11, 2009
- “Remote Sensing at Border Crossings: Understanding Freight Flows,” M. McCord, January 10, 2010
- “Advanced Applications of Remote Sensing and Geospatial Decision Support Tools for Transportation Applications.” C. Brooks and R. Shuchman, January 10, 2010
- “Truck Activity Times at International Border Crossings Using Redesigned Geofences and Existing Onboard Systems,” M. McCord, P. Goel, C. Brooks, P. Kapat, R. Wallace, H. Dong, January, 11, 2010
- “Data Collection and Calibration of Simulation Models of Border Inspection Facilities,” D. Anjos, P. Mirchandani, M. Hickman, S. Lee, and Y.-C. Chiu, January 11, 2010
- North American Traffic Monitoring Exhibition and Conference (NATMEC), Washington, DC: “Truck Flow Management with Aerial Imagery,” (poster presentation) M. Hickman, P. Mirchandani, S. Lee, August 6-8, 2008
- Institute for Operations Research and Management Sciences (INFORMS), Washington, DC: “Simulation Modeling and Remote Sensing Data for a Port of Entry,” P. Michandani, D. Anjos, Y.-C. Chiu, M. Hickman, S. Lee, B. Bustillos, Y. Jang, B. Esmer, October 11, 2008
- North American Freight Flow Conference, (TRB-sponsored conference) Irvine, CA:
  - “Empirical Truck Activity Times at International Crossings from Position and Timing Data and Geospatial Information Systems,” (poster presentation) M. McCord, P. Goel, C. Brooks, R. Wallace, September 16, 2009
  - “Using Advanced Geospatial Visualization Tools for Freight Flow Measurement and Analysis for Congestion Mitigation at International Border Crossings.” D. E. Keefauver, C. Brooks, and K. Stephens, MTRI. TRB North American Freight Flows Conference: Understanding Changes and Improving Data Sources, Irvine, CA, September 16, 2009
- UCGIS Winter Meeting, Washington, DC: “Documenting Truck Times at International Borders with Advanced Location and Geospatial Technologies,” M. McCord, February 5, 2009
- Ohio Transportation Engineering Conference, Columbus, OH : “Investigating Truck Crossing Times at International Borders with Advanced Technologies,” M. McCord, P. Goel, C. Books, P. Kapat, D.E. Keefauver, R. Wallace, October 28, 2008
- Center for Energy, Sustainability and the Environment workshop, The Ohio State University, Columbus, OH: “Transportation Engineering at The Ohio State University,” (poster presentation) B. Coifman, M. McCord, P. Goel, R. Mishalani, December 3, 2008
- The Ohio State University Civil Engineering Alumni breakfast at the Ohio Transportation Engineering Conference, Columbus, OH: “Department of CEEGS Federally Funded Transportation Projects,” M. McCord and B. Coifman, October 29, 2008

- In Step, In Line, On Time: Regional Strategies for Trade, Security, and Mobility Challenges at the US-Canada Border, U.S. DOT Region V University Transportation Center (NEXTRANS) Conference, West Lafayette, IN:
  - “Documenting Truck Activity Times at International Crossings using Available Technologies “ and “How academia can fill the data and information gaps to facilitate integrated, coordinated and performance based operation and governance of the border region” M. McCord, November 16, 2009
  - “Empirical Truck Activity Times at International Crossings from Position, Navigation and Timing Data and Geospatial Information Systems,” (poster presentation), M. McCord, P. Goel, C. Brooks, R. Wallace, September 16, 2009
- 2010 Ohio Conference on Freight, Toledo, OH:
  - “Freight Research at The Ohio State University: Selected Projects,” M. McCord, September 14, 2010
  - “Exploiting Geo-fences to Document Truck Activity Times at the Ambassador and Blue Water Bridge Gateways,” M. McCord, September 15, 2010

We prepared the following papers, reports, and technical documents.

- McCord, M., P. Goel, P. Kapat, C. Brooks, R. Wallace, H. Dong, “Empirical Evidence of Decreased Truck Queuing Times from Traffic Management Changes at the Blue Water Bridge using Geo-fence Derived Data,” working paper, 2010
- McCord, M., P. Goel, C. Brooks, P. Kapat, R. Wallace, H. Dong, D.E. Keefauver, “Documenting Truck Activity Times at International Border Crossings Using Redesigned Go-fences and Existing Onboard Systems. “ *Transportation Research Record*, 2162, 81-89, 2010
- McCord, M., P. Goel, C. Brooks, R. Wallace, “Empirical Truck Activity Times at International Crossings from Position and Timing Data and Geospatial Information Systems,” paper submitted in conjunction with TRB North American Freight Flow Conference, Irvine, CA, 2009
- “Report on Initial Findings, Challenges, and Future Potential Opportunities of CRESTA: Consortium on Remote Sensing of Freight Flows in Congested Border Crossings and Work Zones,” prepared by The Ohio State University, University of Arizona, Michigan Tech Research Institute, for the Research and Innovative Technologies Administration, U.S. Department of Transportation, December 21, 2007
- “Report on the Technical Expert Advisory Committee and Local Stakeholders Meeting – Held February 9, 2009,” prepared by CRESTA: The Consortium on Remote Sensing of Transportation Activities – The Ohio State University, Michigan Tech Research Institute, University of Arizona, Center of Automotive Research; submitted to U.S. DOT/Research and Innovative Technologies Administration, Washington, DC, June 2009

- D. Anjos, “Interfacing VISSIM and ARENA Systems for Modeling Vehicle-Processing Facilities,” MS Project Report, Department of Systems and Industrial Engineering, April 2009
- Liang, J., M.R. McCord, and P.K. Goel, “Truck Screening Time Analysis of the U.S.-Canada International Border,” working paper, The Ohio State University, September 2009
- Dong, H., M.R. McCord, and P.K. Goel, "Empirical Truck Activity Times and Excess Times at International Crossings using Electronic Geo-fences," working paper, The Ohio State University, December 2009.
- McCord, M. P. Goel, P. Kapat, H. Dong, and J. Liang, “Manual for Extracting Travel Information from Geo-fence Database on International Border Crossings,” The Ohio State University, [http://www.stat.osu.edu/~pkapat/bc/CRESTA\\_Manual.pdf](http://www.stat.osu.edu/~pkapat/bc/CRESTA_Manual.pdf) , 2009.
- B. Esmer, “An Analysis of Gamma Mixtures for Service Networks.” MS Thesis, Department of Systems and Industrial Engineering, University of Arizona, December 2010

#### **1.4 Overview of the Report**

In Section 2, we present the geo-fence approach to determining truck activity times and describe our implementation of the approach at the Ambassador Bridge and Blue Water Bridge crossing sites. We present the overall sets of numerical results obtained on multiple activity times and excess times – the times in excess of the free flow times associated with traversing the distance between points delimiting the areas in which the activities takes place. We also present subsets of the empirical data to indicate how the geo-fence approach can be used to investigate specific activity time patterns of interest. We conclude Section 2 with a discussion of tools we developed to visualize activity and crossing times.

In Section 3, we present multiple ways of indirectly validating the geo-fence results. There is little doubt about the ability of the PNT devices used to determine valid times and locations of the truck observations. Therefore, the investigations center on the ability of the activity times determined from the specific fleet of trucks from which data are collected – which are all enrolled in the FAST (see, Customs and Border Protection Agency, 2010) program and, therefore, have the opportunity to benefit from expedited inspections at the crossing – to lead to valid conclusions on activity time patterns for that fleet and for a broader population of trucks using the international crossings. Because of the uniqueness of the information provided by the geo-fence approach, we could not directly verify that the patterns produced actually represent patterns of a broader set of trucks. However, we developed ways to indirectly support the reasonableness of the patterns derived from the geo-fence data.

In Section 4, we describe our approach to developing crossing and activity times from a combination of airborne imagery, ground-based data collection, and mathematical modeling.

Unlike the geo-fence approach, the cost of collecting airborne imagery makes this approach infeasible for ongoing data collection and monitoring. However, by implementing the approach at the Mariposa POE, we demonstrate how it can be used for special studies. We determined the routing of individual vehicles and the distributions of service times at the various stations within the POE, as well as the overall distribution of travel times from the entrance to the exit of the POE.

In Section 5, we use data collected from the geo-fence approach and data on traffic volumes and numbers of operating inspection booths to develop aggregate, macroscopic models of the time involved with queuing upstream of primary customs inspection as a function of traffic volumes and numbers of open inspection booths. The coefficients of the models are statistically significant and have the expected signs, which indicate that queuing times increase when traffic increases and the number of open inspection booths decrease. However, the aggregate models are not capable of supporting “what if” analysis outside of a narrow range of conditions. In the second part of Section 5, we develop a microsimulation model that exploits the information produced from the airborne data collection studies that can be used to analyze and visualize the operations at a border crossing site. A model was developed and calibrated from the data collected at the Mariposa POE.

Section 6 summarizes our work zone study. Several flights were made over the I-10 Tucson work zone. Two different airborne camera platforms were used: a traditional camera platform and the high-resolution ANTAR system loaned to us from the German Aerospace Agency, Deutsche Zentrum für Luft- und Raumfahrt (DLR). Both systems allowed us to measure traffic density and queue lengths through the work zone. Moreover, the ANTAR system uses geo-referenced imagery and automated vehicle detection and tracking to generate vehicle speed information. The ANTAR system provides higher-resolution imagery through the work zone. While proving the value of better technology for airborne traffic data collection, no major work zone-induced congestion was observed in the empirical study. This “success” in work zone operations is primarily attributed to successful traffic demand management and active signal control in the corridor.

We present concluding remarks in Section 7. Overall, we believe we have made a convincing case for a novel application of remote sensing and geospatial technologies that are already in use by many careers to collect truck activity time information at border crossing facilities. We have also shown that remotely sensed data obtained from airborne platforms can provide unique quantitative measures of traffic conditions in an around work zones.

## Section 2. Geo-fence Approach and Results

In this section, we present our geo-fence approach to determining truck activity times at international border crossings. We describe the general methodology and its advantages in Section 2.1. In Section 2.2 we present the setting for the empirical implementation of the approach in which we collect data from a specific fleet of trucks that regularly traverse the U.S.-Canada border using the Ambassador and Blue Water Bridges. In Section 2.3 we present the various iterations we undertook when specifying the geo-fence locations until we settled on the novel specifications used in this study. We then describe the details of this final set of geo-fences.

We present empirical results on activity time patterns obtained from the geo-fence data in Section 2.4. We first describe additional data processing that was required to produce the results. We also describe our approach to producing “excess times,” which are the differences between the actual travel times obtained using the geo-fence approach and the times it would take to traverse the sections between the geo-fence boundaries under free-flow conditions. Considering activity times, rather than actual travel times, can facilitate comparisons with other activities, other crossing sites, and the different directions of traffic. We present empirical results and investigate a subset of the results that address specific questions of interest. An investigation of the overall border crossing times indicates more variability in the times for U.S.-bound traffic than for Canada-bound traffic. We also demonstrate the usefulness of being able to identify trips that visit duty-free facilities both for fleet management purposes and to refine crossing time distributions. We illustrate how the geo-fence approach can be used to depict different temporal patterns in the crossing times for different directions of traffic at the different bridge crossing sites. In addition, we use the data obtained from the geo-fence approach to determine time spent in queuing before primary customs inspection and the time spent while undergoing inspection. We notice that the times and the variability of times spent queuing before inspection and when undergoing the inspections are generally greater for U.S.-bound traffic than for Canada-bound traffic. We also document the temporal stability in inspection times at both crossing sites and for both directions of traffic. Finally, we show how the data obtained with the geo-fence approach can be used to support “before-and-after” analysis by investigating queuing times prior to and after implementing traffic management systems for U.S.-bound traffic at the Blue Water Bridge crossing site.

In Section 2.5, we describe visualization tools we developed to assist in understanding the activity times obtained with the geo-fence approach. We used both open source and proprietary software to produce tools that were used to help us investigate patterns and communicate our results to stakeholders and at conference presentations.

## 2.1 Description of the Approach

The geo-fence approach we developed for use at the Ambassador Bridge and Blue Water Bridge border crossing sites takes advantage of existing hardware, software, and communication systems associated with a GPS-based on-board data unit (OBDU) that are already in use on many truck fleets. These systems automatically record and communicate time-stamped truck locations when events of interest occur. For example, the freight hauler cooperating in this study uses a system that sends a data record from each of its trucks when a truck's ignition is turned off or on, when the truck travels faster than some threshold speed, when no record has been received in some predetermined time interval, when the truck has not moved in some specified time interval, or when any of a number of several other defined events occurs. In addition to a time stamp, latitude, and longitude, each data record includes a vehicle identifier, instantaneous speed at the time of the event, odometer reading, heading, textual information on the type of event that triggered the data record or "ping" (e.g., "ignition on," "time send"), and several other data elements.

Information other than that discussed in this report could conceivably be used to investigate truck movements. Indeed, before developing our final specifications for data collection (see below), as a proxy for customs inspection time we used elapsed time between when the truck's engine was turned off and when it was turned on (two data elements saved automatically in the truck's GPS log) while the truck was located in the vicinity of primary customs inspection locations (Liang, *et al.*, 2009). In the geo-fence approach we exploit the records triggered when a truck's GPS system determines that the vehicle has crossed an electronic geo-fence. A geo-fence is the virtual perimeter of an area (a polygon) that defines a region of interest (ROI). The coordinates of the points that define the geo-fence are remotely transmitted to the OBDU (see below). Using the GPS system, the unit determines its current location at a very high frequency against the electronic geo-fence boundary to determine if the truck has entered or exited a geo-fence. Once the OBDU determines that it has entered or exited a geo-fence, a crossing data record is transmitted to a database with the type of information described above. Of interest for this study are the time stamp, name of the geo-fence crossed, an indication of whether the crossing was into or out of the geo-fence (to provide direction), and the speed of the vehicle when the geo-fence was crossed.

By using the unique identifier of the truck in the data records and additional logic, one can identify and examine records for the various geo-fences crossed during an individual truck trip and the direction of crossing. These matched records form a chained trip. By taking the difference in crossing times for a pair of crossing records in the chained trip, the travel time between the corresponding locations is determined. Thus, specifying geo-fences at strategic locations that delineate activities of interest in the truck trip yields the travel time between these strategically selected locations, and the times incurred in the activities can be determined.

Since many fleets use the underlying technologies for management purposes, no additional infrastructure is required to obtain these records. For example, prior to its involvement in this effort, CEVA Logistics, Inc., the freight hauler that provided empirical data for this study, was already using geo-fences that indicated when its trucks were in the vicinity of an international border. However, because they were implemented for other purposes, the existing geo-fences did not provide information on general crossing times that could be used for monitoring or for decomposition into multiple activities (see Section 2.4). Our contributions lay in realizing that several spatially precise geo-fences could be used to provide times associated with important activities, specifying the locations of these geo-fences at the sites used in our empirical study, working through implementation and data processing issues, and demonstrating the types of previously unavailable information that can be derived from the data and be of use to both fleet managers and facility operators and planners.

## **2.2 Empirical Setting**

As mentioned in Section 1, we demonstrated the use of the geo-fence approach at the Ambassador Bridge and Blue Water Bridge border crossing sites. These two bridges connect Michigan and Ontario (see Figure 2.2-1) and provide a vital link for moving freight between the United States and Canada.

The Ambassador Bridge, owned by the Detroit International Bridge Company, a privately held company, has four undivided lanes. It is the busiest international crossing in North America in terms of trade volume: more than 25% of all merchandise trade between United States and Canada crosses the bridge (Ambassador Bridge Facts, 2010). Approximately 2.3 million trucks used this crossing in 2009 (Szuch, 2010; TOLLROADSnews, 2010). Completed in 1929, this bridge connects Windsor, Ontario on the south with Detroit, Michigan on the north. On the U.S. side, the bridge is now linked to two major freeways (I-96 and I-75). Truck traffic previously had to pass through Detroit City streets to reach the bridge from I-75, but a major redesign of the U.S. plaza, completed in July 2009, now allows direct access from I-96 and I-75 on the American side. Currently, traffic coming off the Ambassador Bridge on the Canadian side must travel through heavily populated residential and business areas on Huron Church Road in Windsor, before accessing Canadian Highway 401, which continues on to Toronto and beyond.

Since 1997, the Blue Water Bridge has consisted of two one-way spans, each with three lanes. The bridge is jointly owned by the Michigan Department of Transportation and the Blue Water Bridge Authority, a Canadian Federal Crown Corporation. This facility runs roughly east to west between Port Huron, Michigan and Sarnia, Ontario. On the U.S. side, it connects with Interstates 94 and 69, and on the Canadian side it connects directly with Highway 402, which merges with Highway 401 at London, Ontario. In 2008, it was the third largest (as measured by total value of freight) North American international gateway and second busiest crossing between the U.S. and

Canada (U.S. Department of Transportation, 2010). In 2009, approximately 1.35 million trucks used this crossing (TOLLROADSnews, 2010; Blue Water Bridge Info, 2010).

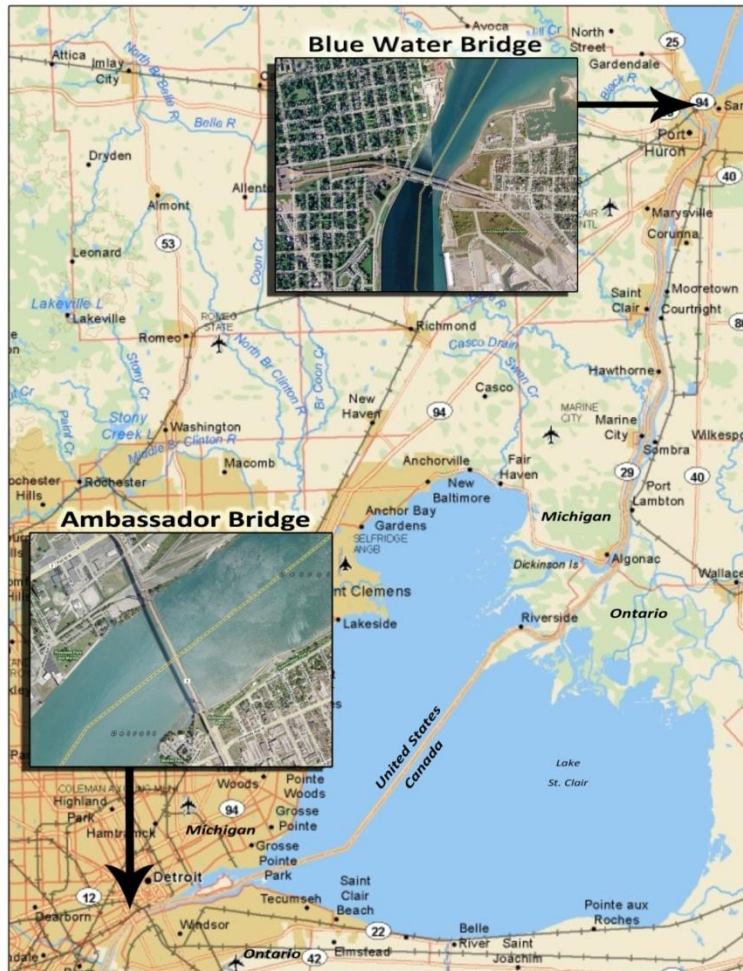


**Figure 2.2-1:** The Ambassador Bridge and Blue Water Bridge border crossing sites connecting Michigan and Ontario *Map copyright ©2009 DeLorme.*

CEVA Logistics, Inc., served as the source of geo-fence data used in our study. Formed in 2007 from the merger of TNT Logistics and EGL Global Logistics, CEVA Logistics is a major logistics provider within the North American automotive industry. It is a global business with significant operations in Europe, Middle East, Africa, North and South America, Asia, and Australia, with approximately 46,000 employees worldwide. The company uses owner operators, as well as employee drivers, for its fleet. CEVA was brought into the project at the recommendation of the Global Customs group within General Motors. After an initial meeting with CEVA, we determined that CEVA (through its geomatics provider, WebTech Wireless, Vancouver, British Columbia) was able and willing to provide the type and volume of data needed for the geo-fence based approach that we wanted to develop. CEVA collaborated in

several iterations of different geo-fence implementations, as we gained insights into what was needed to employ the geo-fence approach for the collection of truck activity times.

## **2.3 Geo-fence Implementations**

### **2.3.1 General Approach**

As mentioned above, prior to its involvement in this project, CEVA was using basic geo-fences to indicate when its trucks were in the vicinity of an international border. For this study additional geo-fences were specified to allow estimation of times the trucks incurred in various activities associated with the international crossing. To implement these refined geo-fences, the polygon boundaries were digitized on top of aerial photography and satellite imagery using a combination of available GIS products. For each specification of the geo-fences, we digitized these boundaries on top of the high-resolution imagery available in Google Maps (the same satellite imagery and aerial photography that is available in Google Earth), using Google's "MyMaps" function (Google Maps, 2010). Once digitized, we e-mailed our first two sets of geo-fence specifications directly to CEVA Logistics as KML (Keyhole Markup Language) files using the e-mailing function that exists within MyMaps. KML is an open-source geospatial data transmission standard, approved by the Open Geospatial Consortium (OGC) (Google Code, 2010). Our CEVA collaborator then re-digitized the specifications into mapping software provided by WebTech Wireless for transmittal to the truck OBDUs. CEVA then transmitted the digitized specifications to its fleet. Sometimes, this re-digitization step introduced minor changes in the geo-fences.

We digitized our third set of geo-fence specifications in Google Maps as before. However, this time we imported the KML file into ESRI's ArcGIS software, using the commercial Arc2Earth program (Arc2Earth, 2010). Once in ArcGIS, we adjusted the geo-fence boundaries to fully ortho-rectified aerial photography we had obtained from the United States Geological Survey, the Michigan Center for Geographic Information, and the US Department of Agriculture. These additional steps provided more precise boundaries than our earlier process of drawing geo-fences using only Google Maps or Google Earth, where the absolute positional accuracy of displayed imagery is typically secondary to user-friendly displays of interesting geographic data. At the suggestion of our CEVA collaborator, we then worked directly with their geomatics service provider, WebTech Wireless, to ensure that our detailed geo-fences would be loaded exactly onto the OBDUs. To accomplish this goal, we sent to WebTech the refined geo-fences as shapefiles, another common spatial data standard originally developed by ESRI and now available as a publicly available read/write standard. WebTech was able to ingest the shapefiles directly into its mapping software and transmit the boundaries to CEVA's entire vehicle fleet via cellular data transmission in less than 24 hours. Working directly with the geomatics service provider in this way also ensured that all CEVA trucks received the latest geo-fence specifications at the same time.

### 2.3.2 Geo-fence Implementations

Before the project began, CEVA Logistics was using geo-fences in the vicinity of international border crossings for company purposes. We call these “SU07” geo-fences because they were the operational geo-fences when the project began in summer 2007. The SU07 geo-fences were centered at the U.S.-Canada border and only covered limited areas. At the Ambassador Bridge crossing, the geo-fence included the main body of the bridge, part of the approach highways, toll collection facilities, customs inspection facilities, and part of the departure highways for both directions. At the Blue Water Bridge crossing, the geo-fence primarily covered the bridge itself. Although of use for CEVA operations, the geo-fences were not helpful in providing information on the multiple activities around the international crossing sites. In addition to covering limited areas, the times in the SU07 data records were rounded to the minute. Rounding times to the minute would affect the precision of the actual times, especially for the Blue Water Bridge crossing, where the geo-fences covered such a limited area with little impediment to travel.

After working with the data obtained from the S07 geo-fences, we recognized the potential of specifying additional geo-fences to determine the time incurred in the multiple activities associated with an international crossing. As a result, in autumn 2007 we specified and implemented “AU07” geo-fences. In these geo-fences, we extended the spatial coverage of the geo-fences to cover approach roadways and separated the approach roadways from the toll collection and primary customs inspection facilities and the segments associated with queuing before these facilities. These geo-fences could be used to monitor aggregate crossing times at the facility and in the direction of travel over time. Descriptions of the SU07 and AU07 geo-fences and summaries of empirical data obtained from them can be found in (Dong et al., 2009).

The AU07 geo-fences allowed us to collect aggregate crossing time data by bridge and direction of travel. However, the grouping of many facilities in one geo-fence did not allow a disaggregate analysis of several activity times. After working with the data collected from the AU07 geo-fences, we realized the potential of the geo-fence approach to obtain fine resolution information. In winter 2008, we specified a new set of geo-fences to obtain this fine resolution. However, when we started analyzing initial data from the “WI08” geo-fences, we learned that the re-digitization step, discussed in Section 2.3.1 above, led to some specification errors in the geo-fences, and that the fences were not loaded simultaneously onto the fleet’s OBDUs. Since these data were from a mixture of two different sets of fences, WI08 fences did not produce the desired information. After trying to overcome the erroneous implementations through post-processing, we decided that it would be more productive to re-implement the geo-fences. We therefore refined the WI08 specifications in autumn 2008 and implemented AU08 geo-fences, using a more refined geo-fences design and uploading process, as discussed in Section 2.3.1 above.

Ambassador Bridge Crossing Geo-fences: The AU08 geo-fences at the Ambassador Bridge crossing are shown in Figure 2.3.2-1 and described in Table 2.3.2-1.

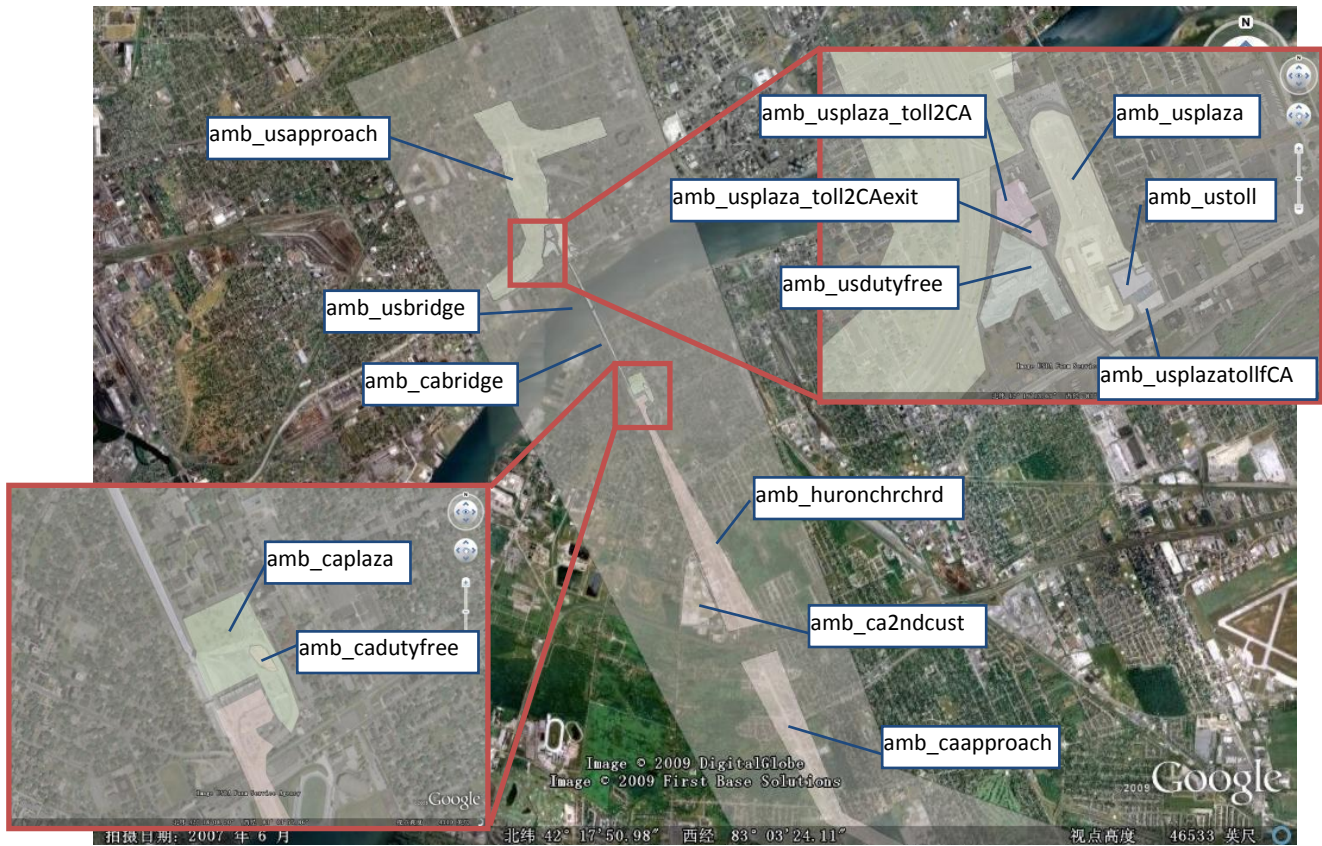


**Figure 2.3.2-1:** Ambassador Bridge AU08 geo-fences developed to investigate border crossing activities

The “amb\_usapproach” geo-fence was designed to capture the travel time spent on connecting roadways approaching the border crossing facility in the US-to-Canada direction and departing from the facility in the Canada-to-US direction. The “amb\_caapproach” and “amb\_huronchrchrd” geo-fences were designed to capture the parallel activities in the opposite direction, namely, approaching the facility in the Canada-to-US direction and departing the facility in the US-to-Canada direction.

The “amb\_cadutyfree” geo-fence was placed on the Canadian side of the border to allow an estimate of the time spent in the duty-free facility in the Canada-to-US direction. The “amb\_usdutyfree” geo-fence was placed on the US side of the border to record the time spent in the duty-free facility in the US-to-Canada direction. Construction associated with the Ambassador Gateway project (Michigan Department of Transportation, 2009), which occurred during our data collection effort, changed the location of the US duty-free facility. Crossings of

the “amb\_usdutyfree” geo-fence were still recorded and processed, but we could not associate these crossings with a trip visiting the duty-free facility.

**Table 2.3.2-1:** Description of Ambassador Bridge AU08 geo-fences

Geo-fence Name	Geo-fence Function by Direction		Length* (Miles)
	US to CAN	CAN to US	
amb_usapproach	Highway approaches	Highway departures	1.19
amb_usdutyfree	The US duty-free facility and surrounding roadway	NA	0.20
amb_usplaza_toll2CA	Upstream approaches of toll collection	NA	0.04
amb_usplaza_toll2CAexit	Road segment after toll	NA	0.04
amb_usplaza	NA	Upstream approaches of customs inspection	0.62
amb_ustoll	NA	Upstream approaches of toll collection	0.02
amb_usplaza_tollfCA	NA	Road segment after toll	0.02
amb_usbridge	Bridge segment between Toll collection and Customs inspection	Bridge segment before Toll collection and Customs inspection	0.44
amb_cabridge	Bridge segment between Toll collection and Customs inspection	Bridge segment before Toll collection and Customs inspection	0.71
amb_caplaza	Upstream approaches of customs inspection	Include duty-free facility and surrounding roadway	0.10
amb_cadutyfree	NA	Duty-free facility and surrounding roadway	0.06
amb_huronchrchrd	Highway departures	Highway approaches	2.16
amb_ca2ndcust	Secondary inspection	NA	0.54
amb_caapproach	Highway departures	Highway approaches	4.42

*\* based on median of difference of odometer readings between bounding geo-fence crossings*

To better evaluate and separate the travel time spent in toll collection, customs inspection, and the queuing time incurred from toll collection and customs inspection activities, we set one geo-fence boundary slightly upstream and another geo-fence boundary slightly downstream of the toll collection locations, and similarly for the customs inspection locations. The gaps between

these consecutive geo-fences boundaries were designed to allow an approximation of the time spent paying tolls and undergoing customs inspections. We placed the “amb\_usplaza\_toll2CA” geo-fence upstream of the toll collection facility for Canada-bound traffic to capture possible queuing times upstream of the facility. The southern segment of this fence was just upstream of the toll facilities. The northern segment of the “amb\_usplaza\_toll2CAexit” geo-fence was just downstream of the toll facility. The time between these two geo-fence crossings would be primarily composed of time associated with toll collection.

Similarly, we placed the “amb\_ustoll” geo-fence upstream of the US-bound toll facilities to capture queuing times associated with toll collection in the Canada-to-US direction. The southern segment of this fence was just upstream of the toll facilities. The northern segment of the “amb\_usplaza\_tollfCA” geo-fence was just downstream of the toll facility. The time between these two crossings would be primarily composed of time associated with toll collection for US-bound traffic.

We placed the “amb\_caplaza” geo-fence upstream of the primary customs facilities for Canada-bound traffic to capture queuing time upstream of the facilities. The southern segment of the fence was just upstream of the facilities. The northern boundary of the “amb\_huronchrchrd” crossing was just downstream of the facilities. The time between these two crossings would be primarily composed of time associated with primary inspection for Canada-bound traffic. In the same way, we placed the “amb\_usplaza” geo-fence upstream of the U.S. primary inspection facilities to capture inspection-induced queuing in the Canada-to-US direction. The southern segment of the fence was just upstream of the facilities. The time incurred between this crossing and the northern crossing of the “amb\_ustoll” geo-fence, which was just downstream of the facilities, would primarily consist of time associated with primary inspection for U.S.-bound traffic.

The “amb\_ca2ndcust” geo-fence was designed to identify US-to-Canada trucks sent to secondary customs inspection, even though it was not needed for this task. From the initial geo-fences, we knew that the database of truck’s GPS logs regularly contained additional vehicle location records (*e.g.*, the engine was turned off and on, the truck stopped and started) generated for CEVA’s vehicle tracking and security related needs. The latitudes and longitudes of these location records could be used to determine if the truck had traveled within our “post-processing” polygons surrounding the secondary customs facilities. If so, we would deduce that the truck had been sent to secondary customs. We used the “amb\_ca2ndcust” geo-fence for validation of this “post-processing” procedure. We did not encode geo-fences in the OBDUs in the AU08 geo-fences to identify trucks sent to secondary inspection in Canada-to-US direction at the Ambassador Bridge crossing or in either direction at the Blue Water Bridge crossing site. Instead, we used our post-processing software in these cases. Conducting post-processing analysis, rather than implementing additional geo-fences, may be desirable so as to reduce data

transmission costs incurred when producing additional records associated with crossing geo-fences. More examples for such post-processing are provide in Section 2.4.1.

Blue Water Crossing Geo-fences: The AU08 geo-fences at the Blue Water Bridge crossing are shown in Figure 2.3.2-2 and described in Table 2.3.2-2.

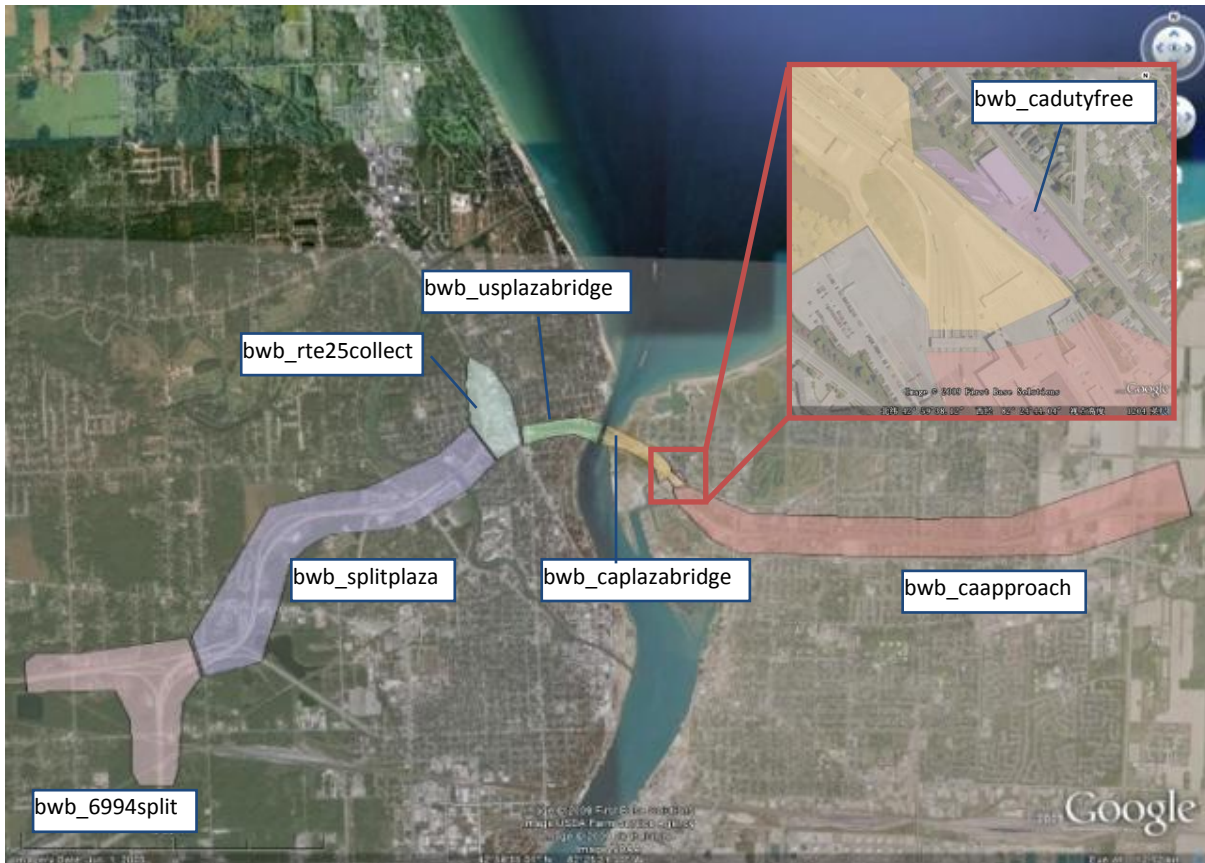


**Figure 2.3.2-2:** Blue Water Bridge AU08 geo-fences developed to investigate border crossing activities

The “bwb\_6994split” and “bwb\_splitplaza” geo-fences were designed to capture the times spent on connecting roadways approaching the border crossing facilities in the US-to-Canada direction and departing the facilities in the Canada-to-US direction. The “bwb\_caapproach” geo-fence was designed to capture the parallel activities in the opposite direction.

The “bwb\_cadutyfree” geo-fence surrounded the duty-free facilities for US-bound trips. The “bwb\_usplazabridge” and “bwb\_caplazabridge” geo-fences covered the US and Canadian sides of bridge, respectively, and were designed to capture the times the trucks incurred when crossing the bridge. We did not implement a duty-free geo-fence in the US-to-Canada direction, because the location of duty free facility was not well understood at that time.

**Table 2.3.2-2:** Description of Blue Water Bridge AU08 geo-fences

Geo-fence Name	Geo-fence Function by Direction		Length* (Miles)
	US to CAN	CAN to US	
bwb_6994split	Highway approaches	Highway departures	1.32
bwb_splitplaza	Highway approaches	Highway departures	3.00
bwb_rte25collect	Upstream approaches of toll collection	Road segment downstream of customs inspection	0.25
bwb_usplazabridge	Bridge segment between Toll collection and Customs inspection	Upstream approaches of customs inspection	0.61
bwb_caplazabridge	Upstream approaches of customs inspection	Bridge segment between Toll collection and Customs inspection	0.71
bwb_cadutyfree	NA	Duty-free facility and surrounding roadway	0.07
bwb_caapproach	Highway departures	Highway approaches	4.10

\* based on median of difference of odometer readings between bounding geo-fence crossings

We placed the “bwb\_rte25collect” geo-fence upstream of the toll collection facility for Canada-bound traffic to capture possible queuing times upstream of the facility. The eastern segment of this fence was just upstream of the toll facilities. The western segment of the “bwb\_usplazabridge” geo-fence was just downstream of the toll facility. The time between these two geo-fence crossings would be primarily composed of time associated with toll collection. Similarly, we placed the “bwb\_caapproach” geo-fence upstream of the US-bound toll facilities to capture queuing times associated with toll collection in the Canada-to-US direction. The western segment of this fence was just upstream of the toll facilities. The eastern segment of the “bwb\_caplazabridge” geo-fence was just downstream of the toll facility. The time between these two crossings would be primarily composed of time associated with toll collection for US-bound traffic.

We placed the “bwb\_caplazabridge” geo-fence upstream of the primary customs facilities for Canada-bound traffic to capture queuing time upstream of the facilities. The eastern segment of the fence was just upstream of the facilities. The western boundary of the “bwb\_caapproach” crossing was just downstream of the facilities. The time between these two crossings would be primarily composed of time associated with primary inspection for Canada-bound traffic. In the same way, we placed the “bwb\_usplazabridge” geo-fence upstream of the U.S. primary inspection facilities to capture inspection-induced queuing in the Canada-to-US direction. The western segment of the fences was just upstream of the facilities. The time incurred between this crossing and the crossing of the “bwb\_rte25collect” geo-fence, which was just downstream of

the facilities, would primarily consist of time associated with primary inspection for U.S.-bound traffic.

## 2.4 Geo-fence Empirical Results

### 2.4.1 Preprocessing and Trip Chaining

As mentioned above, we collected data from CEVA trucks to investigate the activity times incurred by these trucks at the Ambassador Bridge and Blue Water Bridge crossing sites. CEVA trucks operate over much of North America. Rather than ask CEVA to select data for the two empirical crossings of interest to us, CEVA had WebTech Wireless send us all of CEVA's North American data on daily basis. Because of limitations on the number of records that could be sent per data file, WebTech Wireless divided each daily set of data into four .csv (comma separated value) files. We imported the daily .csv data files directly into a PostGreSQL relational database using a SQL import scripting routine that helped automate the data import process and provided a level of data scrubbing to eliminate any information that CEVA regarded as sensitive to operations and personnel. The imported data were housed on a secure server. Periodically, new data were filtered into the subset of records whose locations fell within pre-determined logical regions of interest (ROI) focused on areas around the two bridge crossings (see Figures 2.4-1a and 2.4-1b). These spatially filtered subsets of the original data were delivered to other members of the project team via a secure FTP site.



(a) Ambassador Bridge

(b) Blue Water Bridge

**Figure 2.4-1:** Illustration of Regions of Interest (ROI) used to spatially filter data into subsets around the bridge crossings

The records of interest in this study were the geo-fence crossing records for trucks traversing the international border. However, geo-fence crossing records were produced whenever the truck crossed a geo-fence boundary, even if the truck was only traveling locally and not crossing the border. In addition, if a geo-fence boundary that was intended to be parallel to the roadway was placed too close to the roadway, GPS location errors might indicate that the truck crossed the same geo-fence multiple times on a trip. Similarly, the same geo-fence boundary would be crossed by multiple trucks each day. Therefore, we needed to preprocess the selected data to identify the crossing records with individual truck trips that traversed the border. To do this we “chained” consecutive records to form a sequence of records for trips that traversed the border. We chained not only the records indicating the crossing of a geo-fence boundary, but all the consecutive records associated with the truck trip.

In general, we sorted data by the truck identifier (entry in the *vehicleid* field), odometer reading (entry in the *odometer* field), and time stamp (entry in the *datestamp* field). We then examined the differences in the odometer and time stamp of consecutive records. If these differences exceeded corresponding odometer and time stamp thresholds (we used 10 km and one hour), we considered that the earlier record was associated with end of one set of chained trip records, and the later threshold was associated with the beginning of the next set of chained trip records. We then examined the field that indicated whether the truck was in Michigan or Ontario (entry in the *state\_abbr* field) when the record was generated. If this entry changed from MI to ON or from ON to MI in the set of chained trip records, we considered the trip to have traversed the border. If not, the set of chained trip records was discarded from further analysis. To filter out the multiple crossings of the same geo-fence resulting from GPS errors and closely aligned geo-fences, we used the first crossing record indicating that the truck was entering a geo-fence of interest (crossing into the geo-fenced polygon) and the last crossing record indicating that the truck was exiting the geo-fence (crossing out of the geo-fenced polygon) in the chained set of trip records as the geo-fence crossing records to determine activity times.

Because we were interested in using the geo-fence based data to represent activity times for regulatory compliant trucks attempting to expeditiously cross the border, we also cleaned the data of trips that incurred extra time that would indicate that the trucks did not satisfy these conditions. For example, we controlled for trucks visiting duty-free facilities (explained in more detail below), sent to secondary customs inspection (discussed above), or just parked for long durations. For some of these regions, existing geo-fences were used; for others, we constructed additional polygons, not present on the OBDUs, by identifying locations of long-term parking. Chained trip records that entered these polygons were flagged for special processing. In addition, other GPS errors (possibly due to malfunctioning units) resulted in some geo-fence crossing records not appearing in the database. We handled such “incomplete” sets of chained trip records on a case-by-case basis during the analysis. Details of the trip chaining and cleaning can be found in McCord, *et al.* (2009).

## 2.4.2 Activity and Excess Times

As discussed above, we found the differences between the times for a specified pair of geo-fence crossings on an individual trip that crossed the border to approximate the time of the primary activity that occurred between the pair of geo-fence crossings. In addition to these activity times, we computed "excess times" for these activities. "Excess times" are similar to "delays" that might be considered in traditional traffic engineering studies. (We prefer the term "excess time" in this context because of the negative connotation associated with the term "delay," whereas much of the increased time being captured at the border is the result of truck and driver screening at the border, which are necessary for safety and security.) As will be seen below, by controlling for different distances and infrastructural conditions, these excess times allow more consistent and meaningful comparisons across different border crossing sites and in different directions than do the original activity times.

The excess time between a specified pair of geo-fence crossings for a truck trip is calculated as the time incurred between the geo-fence crossings on the trip minus the free-flow travel time corresponding to the roadway section between the geo-fence crossings. The free-flow time is the time that the truck would incur if there were no impediments to travel over the roadway, such as customs inspection or toll collection facilities, traffic control devices, or traffic congestion. The free-flow time is determined by dividing the distance the truck traveled between the geo-fence crossings by the free-flow speed for the roadway section between these records. The distance traveled is obtained from the odometer readings in the geo-fence crossing data records.

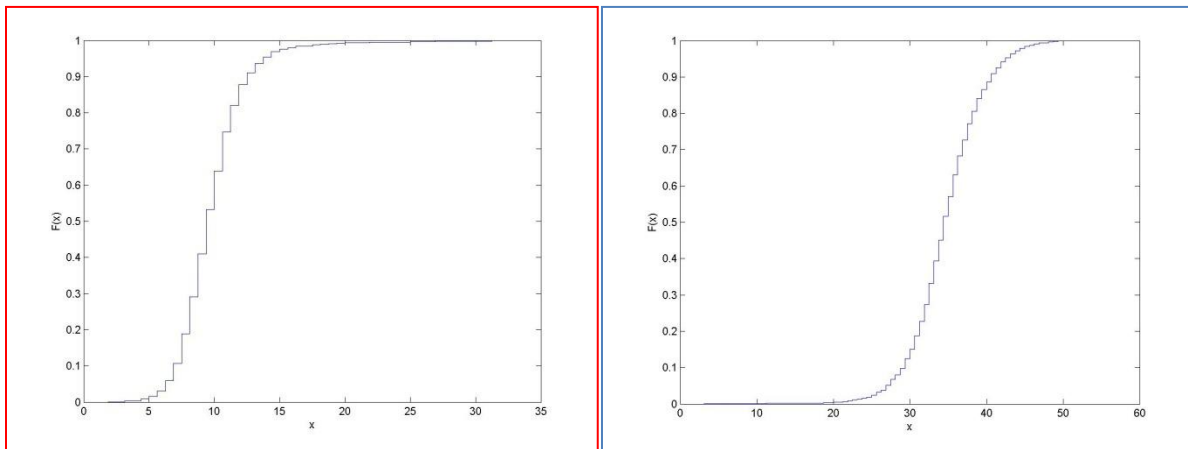
The free-flow speed could be determined in a variety of ways, and future work could be devoted to comparing alternative approaches and specifying a preferred method. In our analysis, the truck speeds that appear in the data records were used to determine the free-flow speeds. When considering an uninterrupted roadway segment between a pair of geo-fence crossings, we determined the 85<sup>th</sup> percentile values of the empirical cumulative distribution functions (ECDFs) of speeds at each of the two geo-fence crossings, and considered the larger of these two 85<sup>th</sup> percentile values as the free flow speed of the roadway section. The 85<sup>th</sup> percentile speed was considered because of its common use in traffic engineering and was selected as appropriate for first-cut analysis after investigation of the empirical distributions of truck speeds in the data records. We used the greater of the two 85<sup>th</sup> percentile values because the lower speed would be more likely to be affected by congestion or operations on the roadway section considered or on an adjacent roadway section.

To illustrate, consider trips in the US-to-Canada direction at the Blue Water Bridge crossing site that pass the two segments of the "bwb\_usplazabridge" geo-fence intersecting the roadway (see Figure 2.4.2-1). The empirical cumulative distribution functions (ECDFs) of the "crossing-in" (upstream) and "crossing-out" (downstream) speeds, as obtained from the geo-fence crossing

data records are shown in Figure 2.4.2-2. The 85<sup>th</sup> percentile speeds for “crossing-in” and “crossing-out” records were 12.5mph and 39.4 mph. respectively. We rounded the higher speed to 40 mph and considered this as the free flow speed of the roadway section within the “bwb\_usplazabridge” geo-fence. In this case, the lower “crossing-in” speeds are attributed to the effects of the toll collection facility, which is immediately upstream of the “crossing-in” geo-fence location.



**Figure 2.4.2-1:** Illustration of the “crossing-in” and “crossing-out” locations of the *bwb\_usplazabridge* geo-fence at the Blue Water Bridge crossing, US-to-Canada direction



(a) “crossing-in” speeds

(b) “crossing-out” speeds

**Figure 2.4.2-2:** ECDF plots used to determine the free flow speed in the US-to-Canada direction for the *bwb\_usplazabridge* geo-fence, Blue Water Bridge crossing site

As discussed above, we placed geo-fences just upstream and just downstream of toll collection and primary customs inspection facilities. In these cases the facilities were actually in "gaps" between pairs of geo-fences, rather than being inside of a polygon formed by the geo-fence. To determine the free-flow speed in these gaps, where traffic flow was interrupted by the facilities, we chose the higher of the free-flow speeds for the upstream and downstream roadway sections, where the free-flow speeds on the upstream and downstream sections were determined as described above.

The free-flow speeds for the geo-fences, as well as the toll collection and customs inspection gaps, are tabulated in Appendix to Section 2. The free-flow speeds compared favorably to posted speed limits, where we obtained information on the posted speed limits. (For example, the posted speed limit for the roadway section discussed above and illustrated in Figure 2.4.2-1 was 30 mph, whereas we determined a free-flow speed of 40 mph using our approach.) These comparisons and more detailed explanation of how we determined the free-flow speeds can be found in (Dong, *et al.*, 2009).

After computing the activity times and excess times for each truck trip for the geo-fences, we formed the distributions of the times for the specific geo-fence or gap. Summary measures of the distributions of the activity times and excess times are presented in Appendix to Section 2.

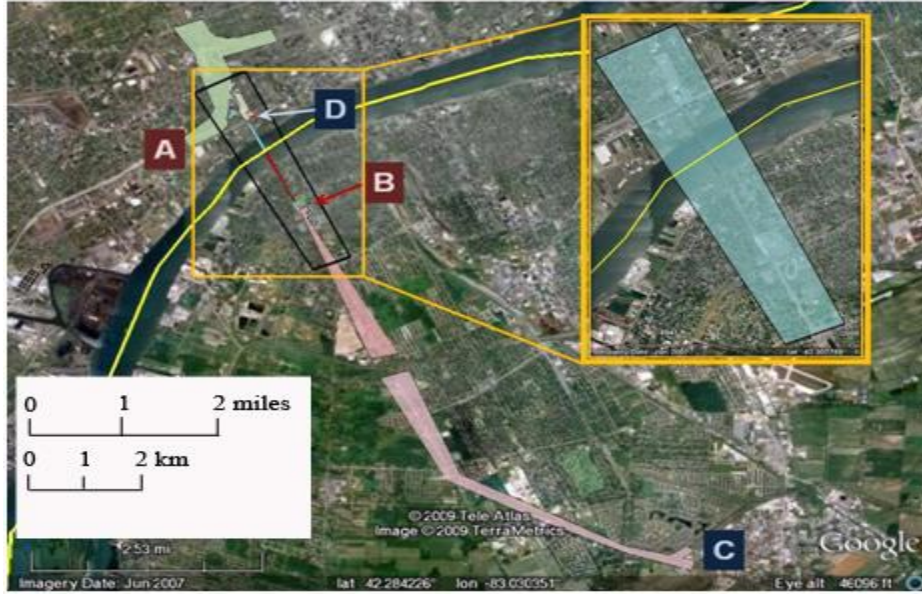
### **2.4.3 Selected Activity Time and Excess Time Results**

As mentioned above, summary statistics for activity times and excess times appear in Appendix to Section 2. In this section, we illustrate the types of information that can be produced from these distributions, in some cases, with additional processing.

Border Crossing Times: In Figures 2.4-3.1a and b, we illustrate geo-fence crossing locations used to determine overall "border crossing times." For example, a border crossing time for a US-to-Canada trip at the Ambassador Bridge site was determined as the time between the record of geo-fence crossing at the point marked A and the record of geo-fence crossing at the point marked B. In the Canada-to-US direction, a crossing time was determined as the time between geo-fence crossings at C and D. Similarly, at the Blue Water Bridge site, the border crossing times were determined between geo-fence crossings at locations E and F in the US-to-Canada direction and G and H in the Canada-to-US direction.

There are other points where one could enter the geo-fences marking the beginning of the border crossing trips at the Ambassador Bridge (Fig. 2.4.3-1a). These entrances would produce slightly different results than those presented here. For illustrative purposes, we limit the analysis to trips travelling between the specified locations. At the Blue Water Bridge (Fig. 2.4.3-1b), the limited access of Highway 402 covering the polygon beginning at location "G" restrains the entry points for U.S.- bound traffic. There are two important access locations for Canadian-bound traffic at

the Blue Water Bridge crossing, indicated by the two “E” locations, but the crossing times are similar for the trips entering these two locations, and the results are pooled in the empirical results presented in this section. In this way, the illustrative empirical results relate to homogeneous traffic patterns.



(a) Ambassador Bridge site



(b) Blue Water Bridge site

**Figure 2.4.3-1:** Illustration of geo-fence crossing locations used to determine “border crossing times”

We present the 50<sup>th</sup> -percentile (median) and the 90<sup>th</sup> -percentile values of the distributions of the thousands of border crossing times between the locations specified above, by facility (Ambassador Bridge crossing site or Blue Water Bridge crossing site) and direction (into US or into Canada) in the Table 2.4.3-1 columns denoted “original distributions.” We also present the median distances traveled between the specified fences, as obtained by odometer readings in the data records.

Uncertainty in crossing times can be more onerous to shipment planning than increases in crossing time that are known in advance, especially for shipments serving scheduled production runs using just-in-time delivery schemes. To quantify the uncertainty of the crossing time for a shipment during the period, we used the difference in the 90<sup>th</sup>-percentile and 50<sup>th</sup>-percentile values. The difference, which is similar to the so-called buffer measure, (see, *e.g.*, Texas Transportation Institute, 2008; Turnbull, 2005), represents the spread or variability in the distribution. This measure is more useful than the standard deviation in depicting variability in highly skewed distributions with much longer right tails than left tails. These variability measures are also presented in Table 2.4.3-1.

**Table 2.4.3-1:** Border crossing time statistics by bridge crossing and direction, before (Original Distributions) and after (Distributions w/o Duty Free Trips) eliminating trips that crossed through duty-free geo-fence

	Original Distributions				Distributions w/o Duty Free Trips	
	Ambassador Bridge Crossing		Blue Water Bridge Crossing		Ambassador Bridge Crossing	Blue Water Bridge Crossing
	US to CAN	CAN to US	US to CAN	CAN to US	CAN to US	CAN to US
Number of Records	9195	8619	3797	3892	7674	2860
Median Distance [km (mi)]	4.34 (2.70)	15.62 (9.70)	9.98 (6.20)	9.43 (5.86)	15.62 (9.70)	9.43 (5.86)
Median Time [min](50%-ile)	11.12	22.55	9.10	11.77	22.63	11.62
90th Percentile Time [min](90%-ile)	19.73	35.17	12.13	26.07	35.22	24.93
Time Variability [min] (90%-ile - 50%-ile)	8.62	12.62	3.03	14.30	12.58	13.32

The 50<sup>th</sup>- and 90<sup>th</sup>-percentile values in the table are difficult to compare across bridge crossing-direction pairs because the types of roadway traversed and the distances traveled vary by bridge

and direction. However, the variability in the values is more comparable. These values indicate that the crossing times are much more variable for trips entering the U.S. than for trips entering Canada at both crossings. These results are consistent with expectations of those familiar with truck shipments at these crossings. As such, they provide a general validation of the approach, but they also illustrate how this variability can be quantified.

Use of Duty Free Information: The duty free polygons can be used to determine if a truck passed through the duty free area on its trip and the amount of time a truck spent in the area. In Table 2.4.3-2, we illustrate our presentation of the proportion of Canada-to-US, Ambassador Bridge trips that passed through the duty free geo-fences by time-of-day and day-of-week. (We have added noise to these proportions to protect the confidentiality of the information.) CEVA has indicated that this type of information is quite useful for fleet management purposes.

**Table 2.4.3-2:** Proportion\* of Canada-to-US truck trips in data base traversing duty free polygon by hour-of-day and day-of-week at Ambassador Bridge crossing

	0-2	2-4	4-6	6-8	8-10	10-12	12-14	14-16	16-18	18-20	20-22	22-24	Day
<b>Sun</b>								0.31	0.09	0.09	0.13	0.23	0.20
<b>Mon</b>	0.31	0.17	0.05	0.06	0.21	0.08	0.09	0.06	0.05	0.09	0.26	0.10	0.08
<b>Tue</b>	0.30	0.10	0.08	0.14	0.17	0.08	0.08	0.06	0.06	0.06	0.11	0.16	0.09
<b>Wed</b>	0.25	0.23	0.18	0.13	0.25	0.07	0.05	0.07	0.10	0.04	0.05	0.14	0.12
<b>Thu</b>	0.19	0.26	0.08	0.16	0.22	0.11	0.06	0.06	0.09	0.12	0.21	0.27	0.11
<b>Fri</b>	0.12	0.22	0.17	0.07	0.21	0.11	0.02	0.04	0.07	0.10	0.11	0.34	0.08
<b>Hour</b>	0.23	0.19	0.12	0.11	0.21	0.09	0.08	0.08	0.07	0.07	0.16	0.20	0.10

*\*noise added to proportions to preserve confidentiality of information*

For facility planning and operations, the border crossing times of interest are for those trips where drivers try to minimize times. Therefore, it is important to eliminate the added time of visiting duty-free facilities when presenting distributions of border crossing times. We eliminated Canada-to-US trips that passed through the duty-free fence and recomputed border crossing time distributions statistics. These summary statistics are presented in the “Distributions w/o Duty Free Trips” columns of Table 2.4.3-1. It should be noted that the lane alignments at the AMB plaza on the Canadian side make it possible that some trips passing through the duty-

free fence did not actually stop at the duty-free site. By using a travel time threshold through this fence or other information in the data records (*e.g.*, “engine on” and “engine off” indications), one could eventually determine whether a truck stopped at the duty free facility. Distinguishing between trucks that stopped and did not stop would allow a more refined correction to the travel time distribution. Comparison of the statistics of the “without duty free trips” distributions with the corresponding statistics of the “original” values at the Blue Water Bridge crossing shows that controlling for the voluntary diversion of visiting duty free facilities led to a decrease in the 90<sup>th</sup> percentile and measure of variability in the crossing time distribution at the site.

Temporal Variability in Border Crossing Times: The data can also be used to investigate temporal differences in crossing times. In Figures 2.4.3-2a and 2b, we plot the median (50<sup>th</sup> -percentile values) and variability measures (90<sup>th</sup> -percentile minus the 50<sup>th</sup> -percentile) by hour-of-day of the border crossing times for the four bridge crossing-direction combinations. The results should be considered illustrative of the types of information that can be obtained from the geo-fence approach at this time. More in-depth analysis would be needed before time-of-day patterns could be considered validated. For example, the high variability measures for U.S.-bound trips at the Blue Water Bridge crossing at 13h and 14h are surprising. Upon further investigation, it seems that these high variability measures may be attributable to some trucks spending a large amount of time parked along Highway 401 in the approach fence, prior to entering the toll gate. To have this effect on the variability measure, the proportion would need to be small enough not to substantially affect the median, but large enough to affect the 90<sup>th</sup> -percentile. Although we successfully eliminated many of these types of anomalies in our data cleaning and trip chaining steps, the fact that some of them remain in the processed data highlights the need for additional effort to be devoted to robust data cleaning before use in an operational setting. Additionally, the locations of such parking sites can change over time and the data cleaning step needs to be updated accordingly. Despite the caution advised for interpreting these two sets of numerical results, the plots provide a strong indication that time-of-day trends can be captured by this approach and that these trends may vary by bridge and direction.

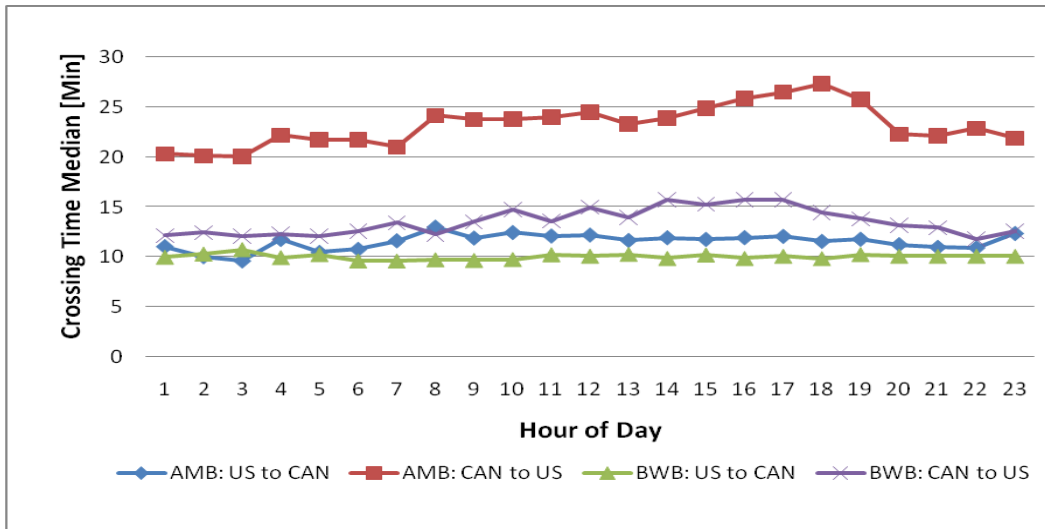


**Figure 2.4.3-2a:** Border crossing time medians by hour-of-day for the four bridge crossing-direction combinations

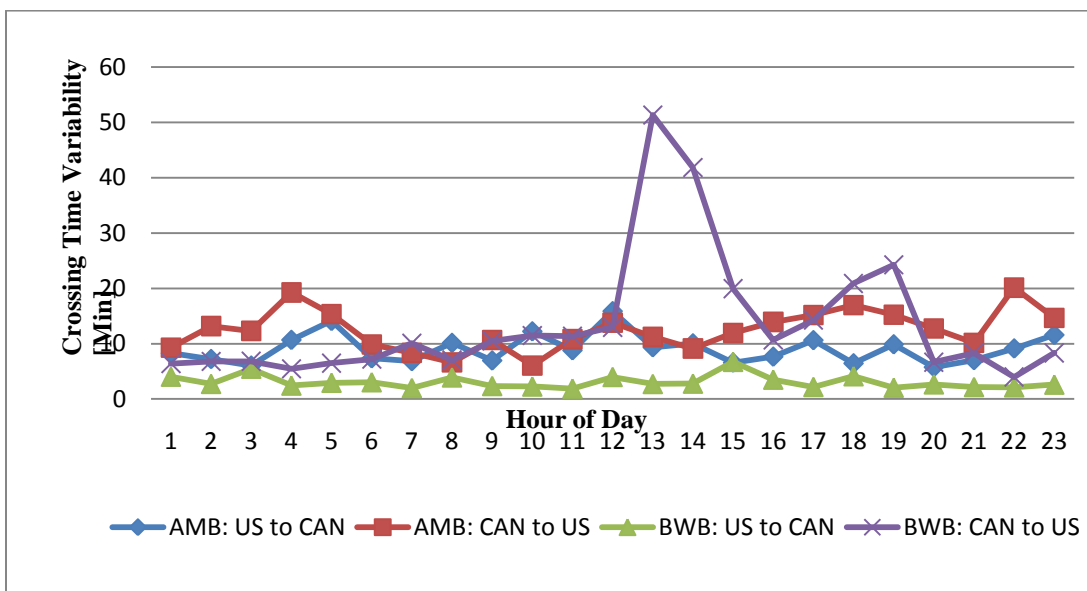


**Figure 2.4.3-2b:** Border crossing time variability measures by hour-of-day for the four bridge crossing-direction combinations

Queuing-induced Excess Times Upstream of Primary Customs Inspection: We described above our approach to determining excess times from activity times and free flow speeds. The summary statistics of excess times, by border crossing site and direction combination, on roadway sections between the exiting (downstream) crossing of the geo-fence immediately upstream of the primary customs screening location and a geo-fence crossing approximately 1 km (0.6 mi) farther upstream are presented in Table 2.4.3-3. Because the geo-fence crossing immediately upstream of the customs screening location is placed very close to the screening

facility (see Figures 2.3.2-1 and 2.3.2-2) the excess times determined in this way would primarily be caused by traffic queuing upstream of the customs facilities. (At times, queues extend farther than one kilometer upstream, so the results are not necessarily representative of all the queuing that occurs. However, they allow comparisons over roadway sections of approximately equal length.) The results indicate markedly longer queuing-induced excess times and more variability in the excess times for trips entering the U.S. than for trips entering Canada, regardless of which crossing is used.

**Table 2.4.3-3:** Queuing-induced excess time statistics for roadway sections upstream of customs screening locations by bridge crossing and direction

	Queuing Induced Excess Time			
	Ambassador Bridge		Blue Water Bridge	
	US to CAN	CAN to US	US to CAN	CAN to US
Number of Records	6869	5721	2652	1974
Median Distance [km (mi)]	1.30 (0.81)	1.00 (0.62)	1.14 (0.71)	0.97 (0.60)
Median Time [min](50%-ile)	0.78	3.67	0.46	2.13
90th Percentile Time [min] (90%-ile)	5.53	14.88	1.86	12.18
Time Variability [min] (90%-ile - 50%-ile)	4.74	11.21	1.40	10.05

Primary Customs Screening Times: For each border crossing site and direction combination, we intentionally specified the first geo-fence upstream of the primary customs screening station and the first geo-fence downstream to be close to the station (see Figures 2.3.2-1 and 2.3.2-2). The times between these geo-fence crossings would represent the times incurred when trucks traversed the segments that included customs screening. By subtracting free-flow times, as discussed above, we determined the excess times on these segments. These excess times would primarily result from customs screening time, with some contribution from the increased times resulting from decelerating to and accelerating from the stop required for inspection. In Table 2.4.3-4, we present the summary statistics for these screening-induced excess times by border crossing site and direction combination. As with the queuing-induced excess times of Table 2.4.3-3, the screening-induced excess times and the variability in the times are greater when entering the U.S. than when entering Canada, regardless of the crossing. Indeed, the increased screening-induced excess times would suggest longer inspection times when entering the U.S. than when entering Canada and, using queuing-theory language, these longer service times are a likely contributor to the longer queues and delays, assuming that arrival rates are roughly similar. (Small differences in service times can lead to relatively large differences in delays if the demand is sufficiently high.)

**Table 2.4.3-4:** Primary customs screening-induced excess time statistics by bridge and direction combination

	Screening Induced Excess Time			
	Ambassador Bridge		Blue Water Bridge	
	US to CAN	CAN to US	US to CAN	CAN to US
Number of Records	6826	4840	2613	1946
Median Distance [km (mi)]	0.05 (0.03)	0.02 (0.01)	0.03 (0.02)	0.04 (0.02)
Median Time [min](50%-ile)	1.10	1.22	0.93	1.46
90th Percentile Time [min] (90%-ile)	1.94	2.36	1.42	2.93
Time Variability [min] (90%-ile - 50%-ile)	0.84	1.14	0.49	1.47

Our Technical Expert Advisory Committee particularly commented on the information we could produce on screening times. It appears that this is truly new information. To illustrate further the type of information one can produce on screening times with the geo-fence approach, in Figure 2.4.3-3, we present the empirical cumulative distribution functions (ECDFs) of the screening induced excess times for the four bridge crossing-directions by three periods of day, what we call Morning (7:00 am – 2:00 pm), Afternoon (2:00 pm – 9:00 pm), and Night (9:00 pm – 7:00 am). No apparent difference is seen in the distributions by time of day, when controlling for the border crossing site and direction. That is, unlike crossing times, screening times appear very homogeneous throughout the day.

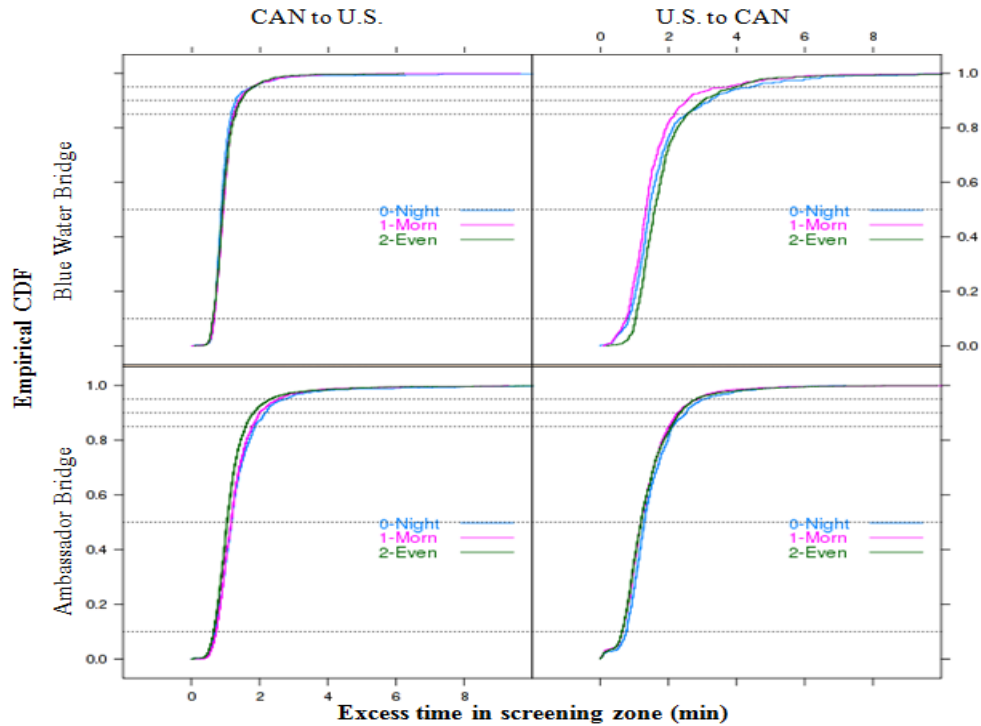


**Figure 2.4.3-3:** Empirical cumulative distribution functions of screening-induced excess times by time-of-day period, for each border crossing site-direction

Before-and-after analysis: The geo-fence approach can also be used to monitor trends or changes in performance of conditions. As an example, during the course of this project, we discovered that, in an attempt to improve traffic flow in the Canada-to-US direction at the Blue Water Bridge site, the Michigan Department of Transportation (MDOT) installed new dynamic message signs (DMS) at the U.S. primary customs inspection locations, as well as at other upstream locations on the U.S. side of the bridge. The new DMS replaced older, less flexible information signs that had operational difficulties. Our understanding is that, by being able to provide dynamic updates on the inspection lane status to traffic upstream of the inspection facilities, inspection lanes can now be assigned much more easily to FAST-certified trucks and NEXUS passenger cars in response to real-time traffic conditions. The expectation was that this would reduce delays upstream of the primary customs inspection. (More details on the actual implementation of the DMS and the motivation for the systems can be found in McCord, *et al.*, 2010).

Queuing-based excess times “before” and “after” implementation of the DMS system can be compared to investigate whether there is evidence consistent with the hypothesis that the DMS system would produce more efficient traffic flow. The new DMS system was considered fully operational on April 13, 2009, but our understanding is that installation and testing were conducted before that date. We, therefore, consider a “transition period” from March 1, 2009 to April 13, 2009 to separate the period considered to be “before” installation of the new DMS

system from the period considered to be "after" installation of the system. In Figure 2.4.3-4, we present the empirical cumulative density functions (EDCFs) of the excess times on the roadway section upstream of primary customs inspection location (*i.e.*, in the *bwb\_caplazabridge*) geo-fence, see Figure 2.3.2-2) for the “before” and “after” periods. The “before” period was considered to cover the period from October 1, 2008 (the approximate date when we first began collecting data with our AU08 geo-fences) to February, 28, 2009 (the day before the beginning of the “transition” period). The “after” period was considered to cover the period from April 13, 2009 (after the DMS system was considered operational) to June 17, 2009 (the last date for which we had processed geo-fence data when conducting this analysis). There were 1100 and 533 excess time values in the before and after periods, respectively.

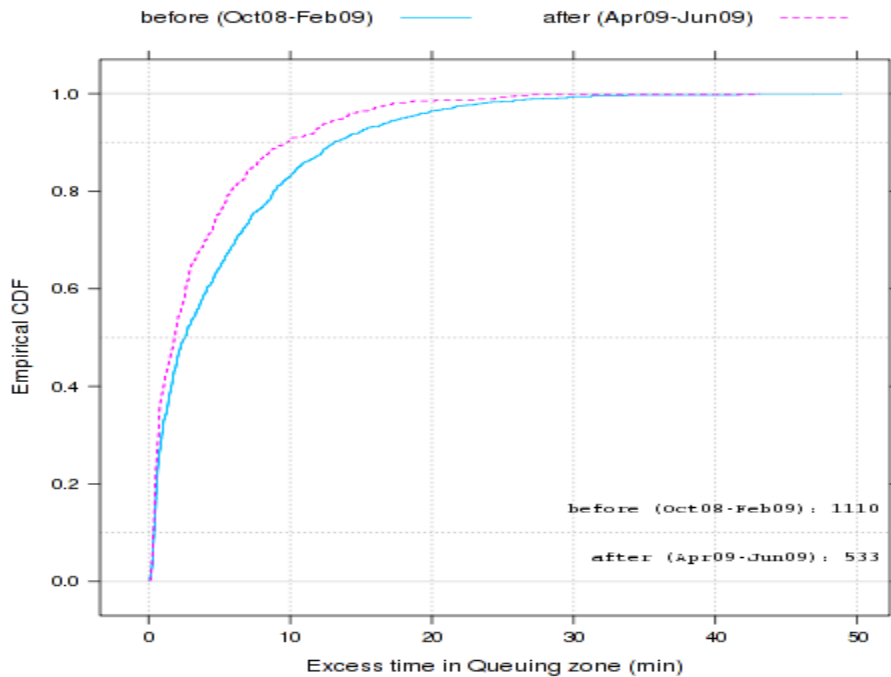


**Figure 2.4.3-4:** Empirical cumulative distribution functions of queuing-induced excess times upstream of customs inspection for “before” and “after” DMS implementation periods

The shift to the left in the “after” EDCF indicates decreased queuing times in the “after” period. The median (50<sup>th</sup>-percentile) value is reduced from 2.6 minutes for the “before” period to 1.8 minutes for the after period, and the 90<sup>th</sup>-percentile value is reduced from 13.1 minutes to 9.8 minutes. The value of the variability measure (90<sup>th</sup>-percentile minus 50<sup>th</sup>-percentile) is reduced from 10.5 to 7.9 minutes.

As seen in the time-of-day border crossing time plots (Figure 2.4.3-2), overall crossing times were seen to be highest for US-bound traffic at the Blue Water Bridge facility in the mid-afternoon and early evening. Assuming that much of the temporal pattern in increased crossing times is attributable to a similar temporal pattern in queuing times, the queuing delays would also

be expected to be highest in this period, and the DMS and traffic management changes would be expected to have the greatest benefit in this period. In Figure 2.4.3-5, we plot the ECDFs of the queuing-induced excess times for the “before” and “after” periods for three time periods: 7:00 am – 2:00 pm (Morning), 2:00 pm – 9:00 pm (Afternoon), and 9:00 pm – 7:00 am (Night). As expected, these plots show that the queuing delays for both the “before” and “after” periods were greatest in the “afternoon” period. The plots also show that the greatest reduction in the delays from the “before” to “after” period occurred in this period, when reductions were most needed.

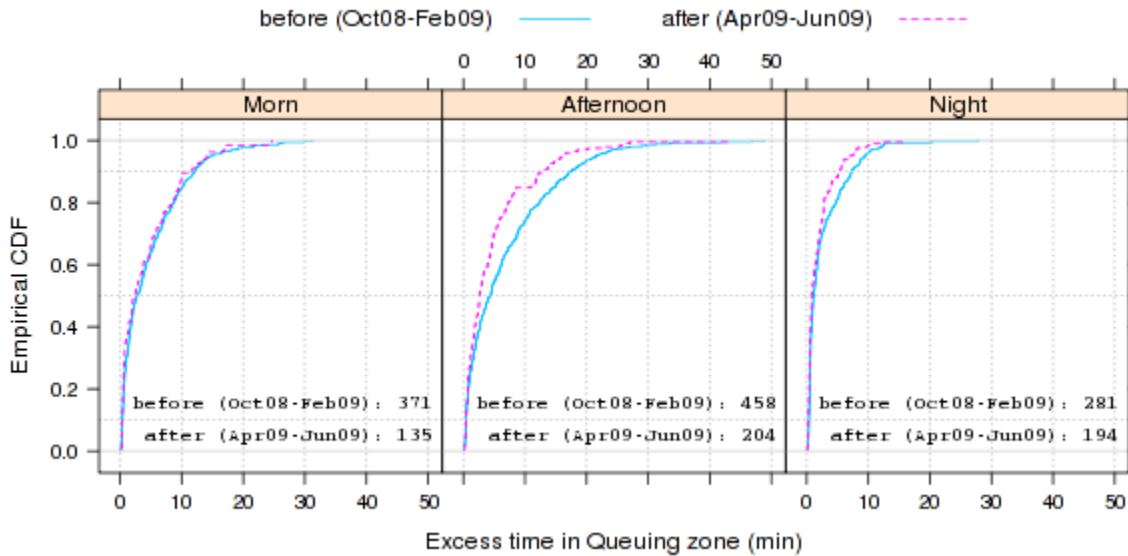


**Figure 2.4.3-5:** Empirical cumulative distribution functions of queuing-induced excess times during three time-of-day periods for the “before” and “after” periods

In McCord *et al.* (2010), we investigate data on traffic volumes and the number of inspection lanes open, obtained from other sources, as well as customs inspection excess times obtained from our geo-fence data to demonstrate that these factors cannot be considered to cause the changes in the “before” and “after” period distributions. The conclusion is that there is strong evidence that the DMS system had the intended effect of decreasing queuing-induced excess times. The point to be illustrated here is that the excess time data required to conduct this type of analysis, which have previously been costly and institutionally difficult to produce, can be provided by the geo-fence approach.

## Section 2.5 Visualization of Geo-fence Results

To facilitate interpretation and sharing of our geo-fence results, we developed and applied several geo-spatial visualization tools. We utilized both open source and commercial proprietary software to develop two major classes of visualization tools. One class focused on interactive

web-based applications for querying, retrieving, and sharing analysis results over the internet. The other class of tools focused on geospatial data display methods using desktop GIS techniques that were developed to provide a better understanding of interesting patterns and results of our analysis. These tools were used both for internal discussions on understanding crossing time data, and also for sharing results at Technical Expert Advisory Committee and sponsor review meetings.

## 2.5.1 Web Based Data Sharing

We developed an interactive web-based visualization tool for sharing study results. The “Visualization System for Data Analysis and Query” (VISDAQ) tool provides a prototype interactive method of querying, retrieving, and displaying our results via the internet in an advanced geo-spatial setting. In Figure 2.5.1-1 we present a screen shot of the tool’s starting interface to show the area where the two bridges are located, the tool parameters that enable users to choose the bridge and directions to show excess time, and instructions to the user. VISDAQ’s capabilities are focused on enabling users to be able to access and visualize the excess time results at the two border crossing sites. The tool is currently capable of displaying excess time results, but the open source framework was designed to be able to integrate other study results, such as activity times by geo-fence. The excess time results were selected as being demonstrative of data that users of a future current and historical crossing time tool would want to access in an online tool. The tool’s display of summary excess time results is available at <http://apache.mtri.org/VISDAQ/> as an example of the capabilities of VISDAQ.

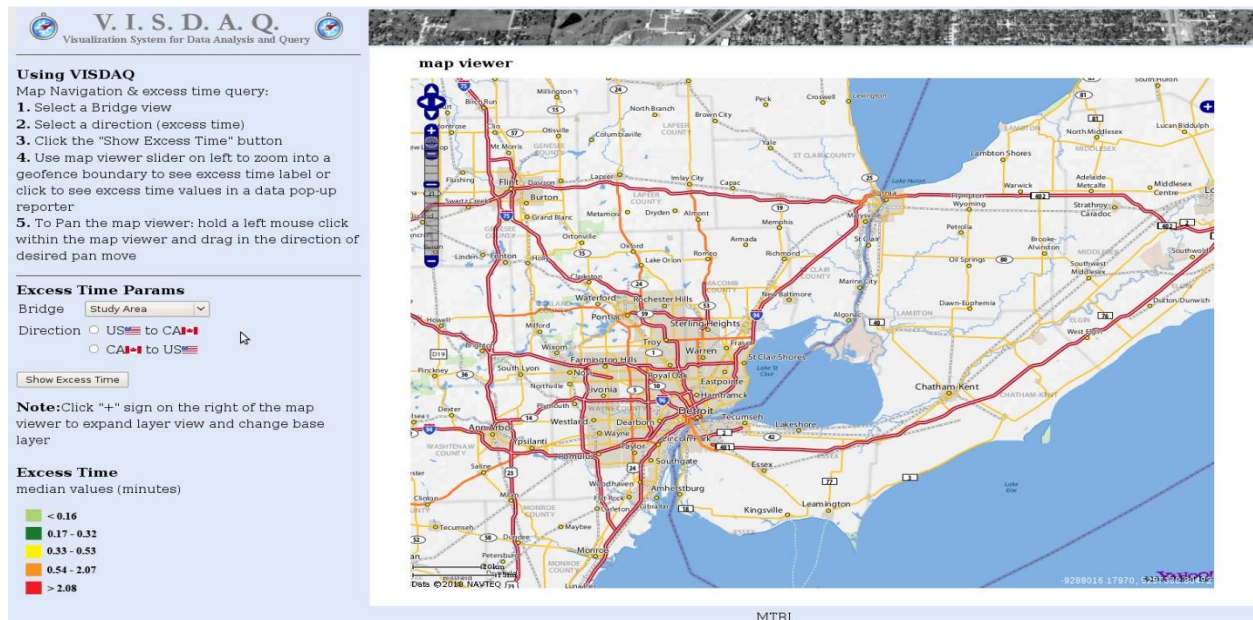


**Figure 2.5.1-1:** Screen shot of VISDAQ web mapping interface of the geographic area encompassing the two border crossing locations used in the geo-fence study

The VISDAQ web mapping application is composed of four primary open-source software components (Figure 2.5.1-2), namely:

- PostgreSQL with the PostGIS extension: PostgreSQL provides the underlying relational database software for storing data such as excess times. PostGIS is an extension to PostgreSQL that provides the capability of storing geo-spatial data, such as (geofences and PNT records. (For additional information, see <http://www.postgresql.org/> and <http://postgis.refractions.net/>)
- GeoServer: GeoServer is the server software that sends data to the front end user web mapping application. (For additional information, see <http://geoserver.org/display/GEOS/Welcome>).
- OpenLayers: OpenLayers is the collection of mapping software libraries that enable the displaying of an interactive web mapping interface that works on most modern web browsers. (For additional information, see <http://www.openlayers.org>).
- Javascript: Javascript provides the underlying software code for VISDAQ that ties the mapping functionality into data displays.

VISDAQ presently provides users the ability to query and visualize the median excess times associated with geo-fences at the Ambassador Bridge and Blue Water Bridge sites. It could also display other summary data, such as mean, standard deviations, and percentile values, if those data were loaded into PostgreSQL for use in the mapping interface. The user is prompted with a choice of border crossing site and direction of travel. The application then queries the backend PostgreSQL databases via Geoserver, which provides a visualization of the median excess time by color coding the geo-spatial displays of the geo-fences according to the median value (see Figure 2.5.1-2 for an example). We have designed the infrastructure to be easily expandable in future versions to process the input data and provide requested statistical values (not just median ones) for user selected time periods, such as a particular day or consecutive set of days. This type of setup could be the foundation for a tool accessible to multiple stakeholders interested in being able to query historical excess time and other queuing data at border crossings. The VISDAQ infrastructure is also designed to be easily expanded to additional locations and to easily and quickly display other border crossing data, such as activity times for particular geo-fences. Figure 2.5.1-2 shows an illustration of VISDAQ being used to display symbolized median excess time in minutes, with the user having queried the values for a particular geo-fence (“bwb\_caapproach” – the Blue Water Bridge Canadian Approach geo-fence, U.S. to Canada direction).

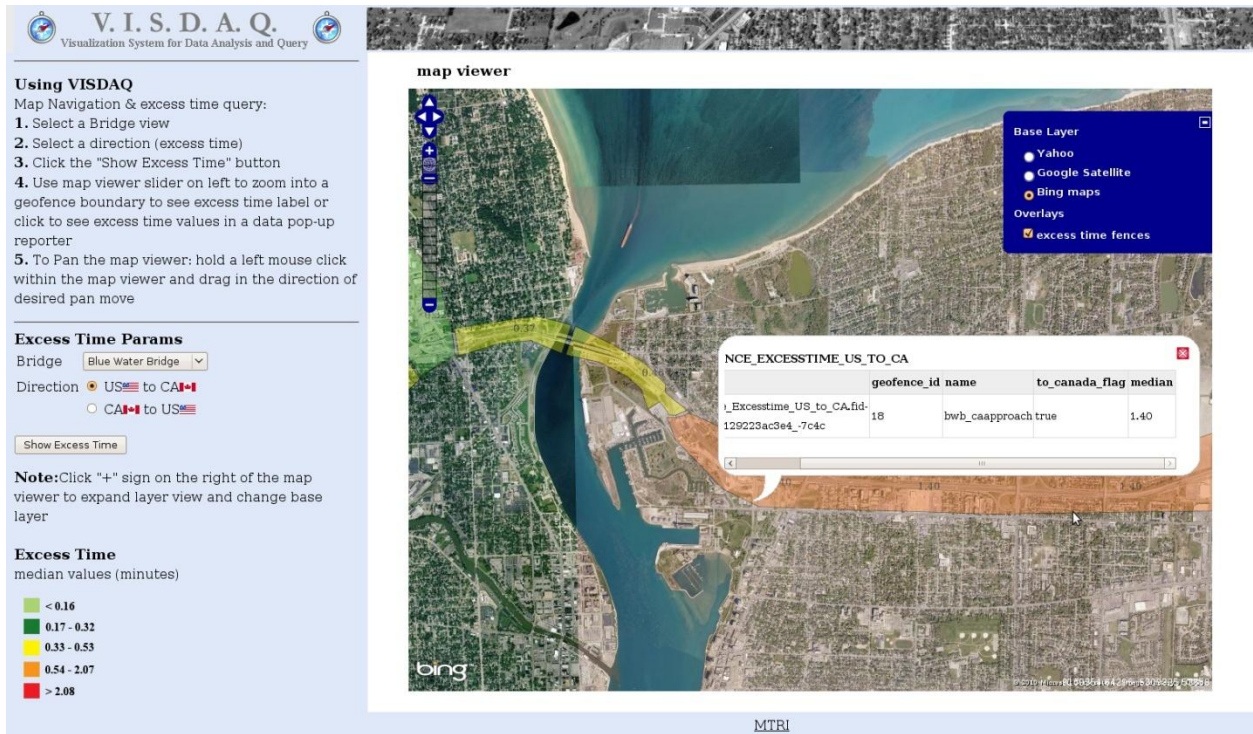


**Figure 2.5.1-2:** VISDAQ interface with results (symbolized geo-fences) from a query of median excess time results at the Blue Water Bridge in the US to CA direction

## 2.5.2 GIS-Based Display Tools for Examining Numerical Results

In addition to the VISDAQ web-based application, we developed various GIS-based displays that have provided unique view of data and have assisted in analyzing and communicating input data and processed output.

ESRI's ArcGIS: Commercial GIS software, Environmental Systems Research Institute's Desktop ArcGIS (versions 9.2 and 9.3), was regularly used to analyze the integrity and patterns of the CEVA data used in this study. ArcGIS was used to refine AU08 geo-fences described in Section 2 by enabling the digitizing of precise geo-fence boundaries on ortho-rectified aerial imagery. By using ArcGIS to map the GPS derived positions of the truck data, we noticed that some geo-fence boundaries were placed so close to roadway boundaries that the combination of mapping and GPS accuracy errors produced many "in" and "out" geo-fences records when the truck traveled along a roadway section that we intended to be contained within a single geo-fence. In the top right portion of Figure 2.5.2-1, the multiple green triangle points are illustration of multiple geo-fence crossing "in" and "out" records along the amb\_usplaza geo-fence, whereas we had intended the geo-fences to be designed so that all the records would occur at a single entrance and a single exit to the geo-fence. Displays such as this made it clear that we needed to provide additional logic in our data processing to determine the activity times defined by some

geo-fences, such as the “amb\_usplaza” geo-fence (the Ambassador Bridge’s U.S. plaza area for in-bound trucks from Canada).

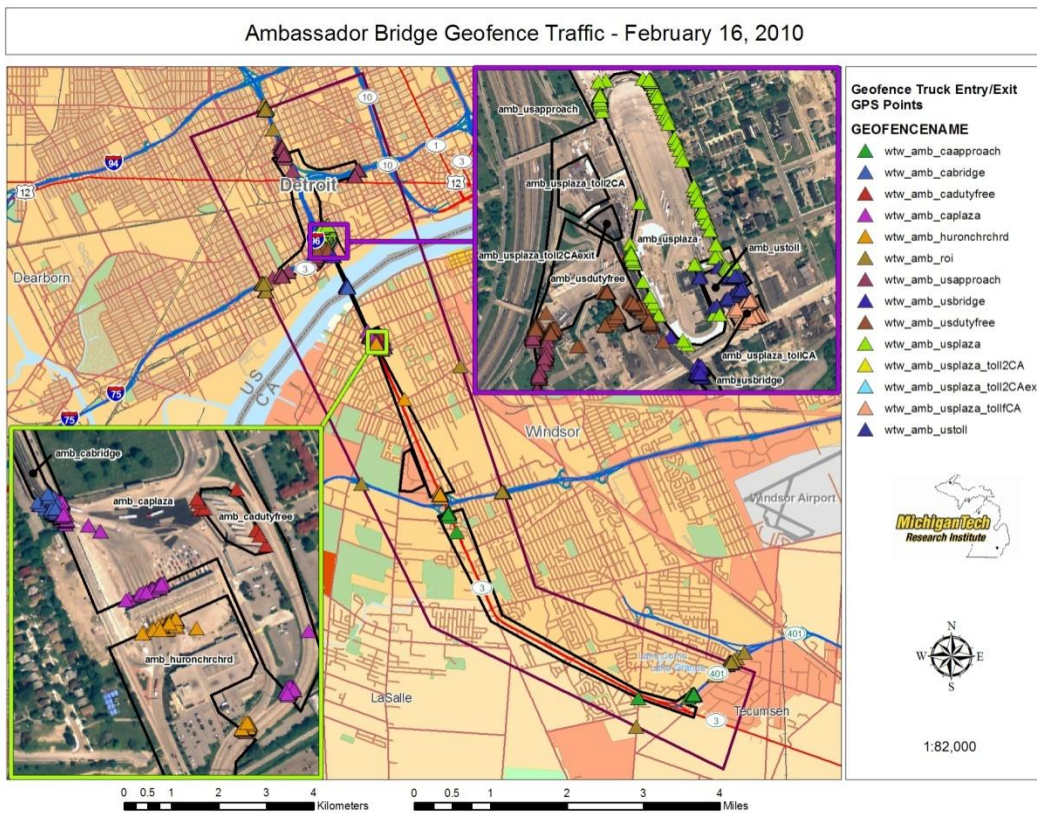


**Figure 2.5.2-1:** An example of ESRI ArcGIS being used to display the details of CEVA data records for February 16, 2010

Google Earth: We used Google Earth, the popular “3-D virtual globe” geospatial data viewer application, to produce visualizations that helped to illustrate crossing times and examples of information available in the PNT data. We developed example data displays using Google Earth’s temporal animation modules to view truck movement patterns and study results such as excess time calculations. Figure 2.5.2-2 shows how Google Earth can be used to display attributes of PNT data such as location, direction of travel, truck speed, and event causing the data record to be generated. Figure 2.5.2-3 shows an example visualization of excess time for U.S-bound traffic at the Ambassador Bridge, with the amount of excess time for an individual truck trip being represented by the height of the extruded geo-fence-based polygon. The Figure portrays a single screenshot of excess times for a truck that crossed from Canada to the U.S. on November 4, 2008, and had an excess time of 5.99 minutes in the amb\_usplaza geo-fence. The record is contained in a 6-month database from 9/29/2008 to 4/1/2009 comprised of 4424 chained trip records, where excess times were calculated in minutes for each geo-fence crossed by the trucks for each chained record. We also created a time-based visualization of these

records, which we displayed as animated video files at Technical Expert Advisory Committee meetings and professional meetings (for an example of an animated video available for download, please see [ftp://ftp.mtri.org/pub/OSU\\_Freight/Video/Excesstime\\_November2008\\_ON2MI.wmv](ftp://ftp.mtri.org/pub/OSU_Freight/Video/Excesstime_November2008_ON2MI.wmv) ). Data displayed in Google Earth for these visualizations were developed as Google Earth KML (Keyhole Markup Language) files. (KML is now an open standard.) Given the popularity of Google Earth, with over 400 million unique activations in 2008 (<http://2008.geowebconference.org/youtube> ), we recommend this format continue to be used to share transportation research results.

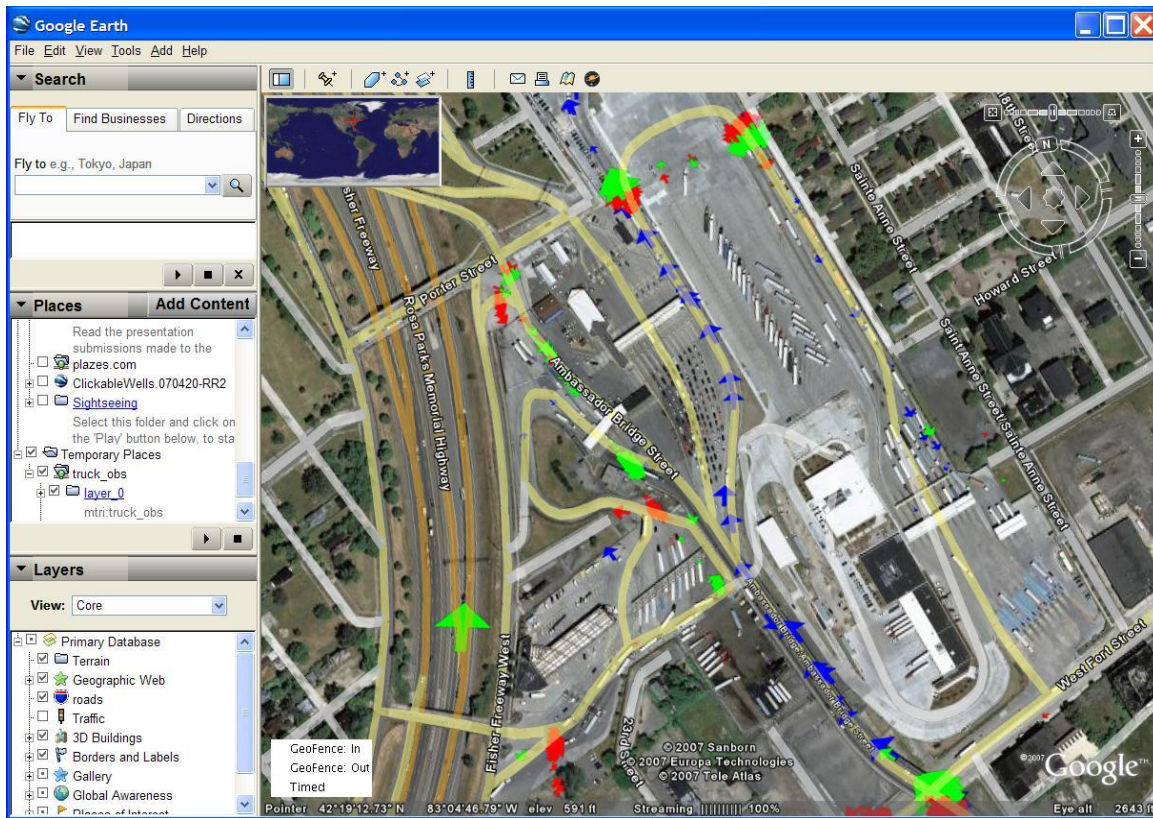


**Figure 2.5.2-2:** Example screen shot of a Google Earth visualization of PNT data showing truck locations and direction (symbolized with arrows), speed (size of arrow), and event triggering the data record (green = entering geofence, red = exiting geofence, blue = time send)

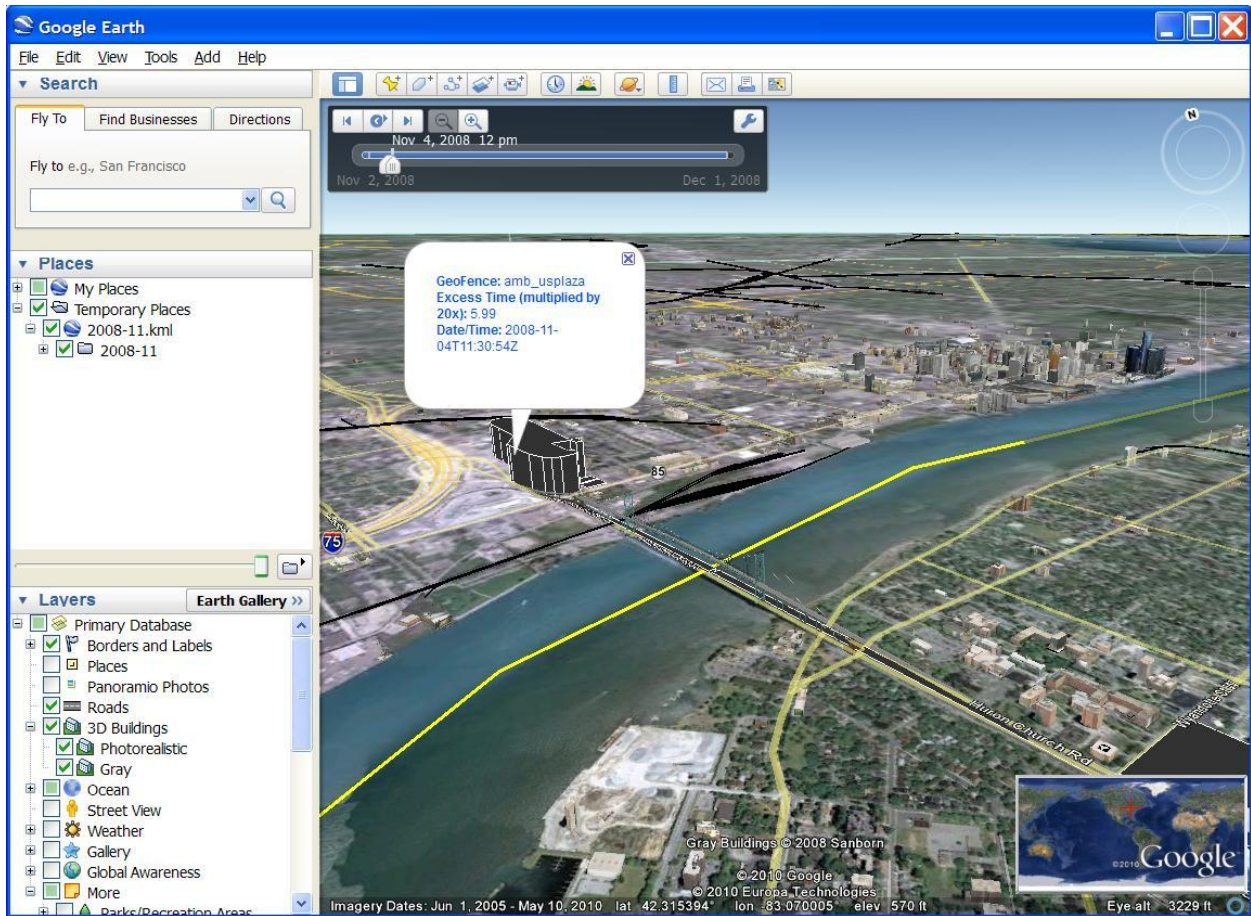


**Figure 2.5.2-3:** Example screenshot of a Google Earth visualization using geo-fence polygon extrusion techniques to display geo-fence excess time values by geo-fence for an individual chained truck trip that occurred from Canada to the U.S. on November 4, 2008 with the height of the extrusion symbolizing the amount of excess time

These data were dynamically displayed using the time feature of KML data in Google Earth, and the extrusion heights (in meters) were set to 20 times the actual excess time value (in minutes) to make larger values more obvious as taller extrusions. A single geo-fence crossing time value is highlighted with an excess time of 5.99 minutes for that individual truck trip at the amb\_usplazageofence on 11/4/2008.

### **Section 3. Validation of Truck Activity Time Patterns Determined from Geo-fence Results**

In this section, we discuss our efforts to “validate” the use of the geo-fence data. We have no real concerns about the activity times we collected validly representing the true activity times the individual trucks incurred between a specified pair of geo-fences. The position, navigation, and timing (PNT) systems used are standard and well accepted technologies. Similarly, the use of geo-fences is not new. Indeed, the central appeal of our approach is that these technologies are well established and already in use for other purposes. It is worth noting that we are considering the validity of the times in terms of fractions of minutes, not to the exact second. Even though the PNT clocks are extremely accurate, the GPS location systems have inherent noise, and mapping systems may also involve error between the recorded and actual locations of the geo-fence crossing signals. In any case, the envisioned uses of these results do not require a second-level precision of the truck being at the intended location. The contributions in this project lay in the innovative application of these existing remote sensing and geo-spatial technologies to obtain unprecedented information on activity times at border crossings.

The primary means of assuring the validity of the patterns in the specific activity times we obtained was by having our Technical Expert Advisory Committee and other stakeholders examine the results and verify that they are reasonable. Perhaps the most telling verification that the results passed this test was the comment of our CEVA and General Motors stakeholders that they would use our results to determine the amount of time that their trucks require to cross the borders. (We cautioned them to consider the entire distributions and not only the medians in times before making any changes based on our data.)

Since the GPS technology is well tested and broadly employed, there is consensus about the ability of the recorded geo-fence crossing times to validly represent the actual times that these trucks crossed the geo-fences. Indeed, the Transport Canada-Ontario Region’s pilot project on Border Wait Times, discussed in Section 3.1 and used for validation as described in Section 3.4, also used carriers’ GPS-based digital tractor logging systems (Shallow, 2008). Rather than the ability of the GPS-based technology to provide accurate data records, the primary validation issue in this project was one of the ability of these FAST-certified CEVA trucks to serve as probe vehicles for the underlying conditions at the border crossing.

We collected data from only CEVA trucks. As mentioned above, CEVA shipments and drivers are FAST-certified. Therefore, they may not be expected to represent all truck conditions when FAST trucks were not mixed with other types of vehicles in the traffic stream. In addition, although CEVA trucks regularly traverse the border at the crossings investigated, they represent only a small proportion of FAST-certified trucks traversing these crossing. In 2007, approximately 18% and 12.5% of all truck traffic at the Ambassador Bridge and Blue Water Bridge sites, respectively, were FAST-certified (Bradbury, 2010; Canadian Border Services Agency, 2008). Using monthly truck volumes data, regularly prepared by the Public Bridge Operators Association and obtained through Blue Water Bridge Operations Manager (Szuch,

2010; TOLLROADSnews, 2010), we determined that there were, respectively, approximately 2.1 million and 1.2 million truck crossings at the two sites between October 2008 and August 2009. If we assume the same 18% and 12.5% FAST-certified percentages as in 2007, we calculate approximately 376,000 and 150,000 FAST-certified truck crossings during this period. During this same period, we compiled approximately 19,000 and 8,000 CEVA truck crossings at the two sites. Based on these numbers, our CEVA crossings data represents approximately 0.9% of total truck crossings and 5% of FAST-certified crossings at the Ambassador Bridge site and 0.7% of total truck crossings and 6% of FAST-certified crossings at the Blue Water Bridge site.

Given the specific nature of most CEVA shipments, we were interested in validating the ability of the activity time distributions produced from the CEVA geo-fence data to provide meaningful information for conditions that were assumed. Conducting any direct validation would have been difficult because of the uniqueness of the data we collected. The geo-fence data were collected over several months. Indeed, one of the most attractive features of the geo-fence approach is its ability to provide information over long observation periods for monitoring of conditions. Given the sampling over long durations, this approach implies that the distributions summarized in Sections 2.4.2 and 2.4.3 represent a mixture of varying conditions over the data collection period. The overall variability would result from trends over time, seasonal effects such as monthly cycles, day-of-week and time-of-day effects, and higher frequency variations about the trends due to short term effects of changes in operating conditions at the primary inspection lanes and security levels set by the Department of Homeland Security, as well as traffic incidents. For example, changing economic conditions during our data collection period led to changing traffic levels using the crossings and, therefore, trends in the traffic delays during the data collection period. On the other hand, traffic incidents could cause increased times on a more random basis, or changing security alerts might change inspection conditions on an unpredictable basis; this would result in changing inspection rates and changing queuing times. Therefore, the distributions derived from the geo-fence data can only give an indication of the likelihood of the activity times that would be expected to occur, and one cannot directly compare times obtained with from some independent observation technique at a specific time with those obtained from the CEVA data over many months of observation.

Nevertheless, we indirectly validated the ability of the distributions to portray general conditions of activity times for FAST-certified trucks and, to some degree, other vehicles at the crossing. Again, we used our Technical Expert Advisory Committee and stakeholders to assess, on multiple occasions, the validity of the general patterns we obtained. They confirmed the reasonableness of our results that inspection times, queuing times, and variability in total border crossing times would tend to be longer when entering the U.S. than when entering Canada. They also confirmed that, as we found, queuing times would be lower in the nighttime than in the daytime. There were times when our experts and stakeholders expressed interest in the patterns we found – and surprise in our ability to produce information they believed was otherwise

unavailable (*e.g.*, the temporal stability in the primary customs screening time distributions) – but there were no instances where they disagreed with our results.

In the rest of this section, we discuss quantitative approaches to indirect validation of the patterns we found. In Section 3.1, we describe supplementary data sources used in our validation. In Section 3.2, we describe the use of air photos and ground-based, manually observed data to demonstrate that primary customs screening times are lower for FAST-certified trucks than for the general truck population. We then show that the FAST-certified screening times are more likely to be realized than the general truck screening times if probabilities are calculated from our geo-fence derived distributions. Because our geo-fence data are collected from FAST-certified trucks, these results are consistent with what would be expected if our screening time results are representative of the general population of FAST-certified screening times. In Section 3.3, we use the air photos to demonstrate that FAST-certified queuing times are lower than queuing times for the general truck population. As with the screening time analysis, the FAST queuing times are more likely than the general truck population queuing times to be realized if probabilities are calculated from our geo-fence derived distributions. We also show that the CEVA derived queuing times are correlated with delay estimates posted by the U.S. Customs and Border Protection, further supporting that valid information is being produced in our geo-fence derived distributions. In Section 3.4, comparing the temporal patterns in crossing times obtained from our CEVA data and the Transport Canada data, it is shown that our FAST-certified data are representative for day-of-week and day-of-month patterns, but are different for time-of-day effects, particularly at the Ambassador Bridge. Before presenting these comparisons, we first describe the data used in these comparisons

### **3.1 Supplementary Data for Validation**

In this subsection, we describe the multiple sets of data used to produce information that could be compared to the results we derived from the FAST-certified CEVA trucks using the geo-fence approach.

Air-based digital imagery: We acquired airbased images at both bridges that allowed us to track a subset of trucks through the geo-fence sections upstream of primary customs screening and in the screening area itself. Specifically, we collected aerial imagery at the Blue Water Bridge and Ambassador Bridge crossings on May 5<sup>th</sup> and May 20<sup>th</sup> of 2009. Our project partner, Skycomp, Inc., conducted aerial surveys for the purpose of collecting data for specified traffic movements, using a time-lapse photographic approach to record traffic movements in the study area. High-resolution digital camera was used to collect imagery (jpeg format at 10MB per photo) for approximately an hour at each bridge in the morning and in the afternoon, taking photos every two seconds, alternating between the two sides of the border, resulting in a spacing of 4 seconds for each side. Skycomp coordinated the flights with the FAA beforehand to minimize potential perceived security issues with an airplane “loitering” over international bridges for extended periods of time.

The Skycomp photography is oblique. Thus it is neither geo-referenced nor ortho-rectified. After collecting the requested imagery, SkyComp used a process called “photo alignment” to prepare the images for extraction of relevant traffic data. Each border crossing was divided into “zones” that corresponded to our geo-fences or the gaps between geo-fences by overlaying our geo-fences on the survey area image. Sample photographs of the survey area were printed and “marked up” to provide guidance for the data reduction personnel at SkyComp, who use a software suite called “SkyComp SkyTracker2” for data reduction. The SkyTracker2 was used to track each vehicle beginning at one of the origins; using a marker, vehicles were identified in subsequent photos as each vehicle traveled through the aerial survey area. The software marks the same two physical locations on each photo (point 1 and point 2); it then exports a data table that creates the x, y coordinates of each location marked in each image. This information, along with the pixel size in each image was then processed through the photo- alignment utility. This utility stacks all of the images with point 2 in the same pixel location, and then rotates all the images so that point 1 is on the same azimuth. Each time the vehicle is marked, a record is written to a table that includes the vehicle ID, vehicle type, location of the vehicle (pixel x, y address), photo name, zone and lane. After each vehicle was successfully tracked to one of the destinations, the data reduction personnel recorded this information in the software. Throughout the course of data reduction, an analyst performed quality control checks for each of the movements.

Using the process described above, individual trucks were tracked through the sequence of images by placing a cursor on the truck in the image and mouse-clicking to automatically record relative coordinates, time of the image, and a truck identifier. Tables from the SkyTracker2 software were then imported into databases for the purpose of calculating zone travel times. These tables allowed an automatic determination of the first and last time a truck was inside a specified geo-fence (or a geo-fence gap). We then used this information to approximate the “air photo-derived” times that the trucks were undergoing primary screening and the times that they were in the geo-fence upstream of primary customs screening. Because of the labor intensive nature of the process, not all trucks could be tracked. Therefore, rather than having two small samples from each of the two flights, we decided to obtain a larger sample from the May 20<sup>th</sup> flights.

Upon receipt of the oblique aerial imagery and truck activity time databases from Skycomp, we geo-referenced approximately 30 percent of the imagery from the Blue Water Bridge crossing and 5 percent of the imagery from the Ambassador Bridge crossing. We geo-referenced the imagery in the event that we would need a reasonable estimate of distance travelled between consecutive photos to extract speed information from oblique images. We did not ultimately use vehicle speeds or distance travelled, but the effort also allowed us to perform a secondary quality control check on air-based data during our geo-referencing efforts. This additional quality check detected a few (approximately three percent, as measured by the vehicles tracked without error) minor errors in the originally processed records (*e.g.*, trucks mislabeled, geo-fence location incorrectly specified). With this two step quality check, we believe that the air photo-derived travel and inspection times during the survey period are highly reliable. In Section 3.2, we

discuss how we used these data in our investigations of primary customs screening times and queuing times in both directions at both bridges.

Ground-based, manually collected data: We conducted ground-based data collection for U.S.-bound truck traffic at the Blue Water Bridge site for 3 hours on 8/1/2008 (primarily a dry run for our data collection approach), 8 hours on 8/8/2008, 8.5 hours on 11/18/2008, 4 hours on 11/19/2008, 7 hours on 5/5/2009, and 7 hours on 5/20/2009. The Michigan Department of Transportation operators at the Blue Water Bridge granted us access to the MDOT floor of the U.S. Blue Water Bridge building, which provided a view of U.S.-bound traffic and all 13 inspection lanes. We recorded information on primary inspection screening times for trucks, including whether lanes were servicing only FAST-certified (FAST) trucks or “All Trucks” (later called standard/non-FAST trucks for compatibility with other data sets.). Figure 3.1-1 is an example of our lane status data, which were updated every five minutes.

	A	B	C	D	E	F	G	H	I	J	K	L	M	N
1	Blue Water Bridge Collect													
2	11/19/2008													
3	LANE STATUS							LANES						
4		1	2	3	4	5	6	7	8	9	10	11	12	13
5	Time													
51	6:45 - 6:50	AT	AT	AT	AT	AT	AT	F	N	C	C	C	X	X
52	6:50 - 6:55	AT	AT	AT	AT	AT	AT	F	N	C	C	C	X	X
53	6:55 - 7:00	AT	AT	AT	AT	AT	AT	F	N	C	C	C	X	X
54	7:00 - 7:05	AT	AT	AT	AT	AT	AT	F	N	C	C	C	X	X
55	7:05 - 7:10	AT	AT	AT	AT	AT	AT	F	N	C	C	C	C	X
56	7:10 - 7:15	AT	AT	AT	AT	AT	AT	F	N	C	X	C	C	X
57	7:15 - 7:20	AT	AT	AT	AT	AT	AT	F	N	C	X	C	C	C
58	7:20 - 7:25	AT	AT	AT	AT	AT	AT	F	N	C	X	C	C	C
59	7:25 - 7:30	AT	AT	AT	AT	AT	AT	F	N	C	X	C	C	C
60	7:30 - 7:35	AT	AT	AT	AT	AT	X	F	N	C	X	C	C	X
61	7:35 - 7:40	AT	AT	AT	AT	AT	X	F	N	C	X	C	C	X
62	7:40 - 7:45	AT	AT	AT	AT	AT	X	F	N	C	X	C	C	X
63	7:45 - 7:50	AT	AT	AT	AT	AT	X	F	N	C	X	C	C	X
64	7:50 - 7:55	AT	AT	AT	AT	AT	X	F	N	C	X	C	C	X
65	7:55 - 8:00	AT	AT	AT	AT	AT	X	F	N	C	X	C	C	X
66	8:00 - 8:05	AT	AT	AT	AT	AT	X	F	N	C	X	C	C	X
67	8:05 - 8:10	AT	AT	AT	AT	AT	X	F	N	C	X	C	C	X
68	8:10 - 8:15	AT	AT	AT	AT	AT	X	F	N	C	X	C	C	X
69	8:15 - 8:20	AT	AT	AT	AT	AT	X	F	N	C	X	C	C	X
70	8:20 - 8:25	AT	AT	AT	AT	AT	X	F	N	C	X	C	C	X
71	8:25 - 8:30	AT	AT	AT	AT	AT	X	F	N	C	X	C	C	X
72	8:30 - 8:35	AT	AT	AT	AT	AT	X	F	N	C	X	C	C	X
73	8:35 - 8:40	AT	AT	AT	AT	AT	X	F	N	C	X	C	C	X
74	8:40 - 8:45	AT	AT	AT	AT	AT	X	F	N	C	X	C	C	X
75	8:45 - 8:50	AT	AT	AT	AT	AT	X	F	N	C	X	C	C	X
76	8:50 - 8:55	AT	AT	AT	AT	AT	X	F	N	C	X	C	C	C
77	8:55 - 9:00	AT	AT	AT	AT	AT	X	F	N	C	X	C	C	C
78	9:00 - 9:05	AT	AT	AT	AT	AT	X	F	N	C	X	C	C	X
79	9:05 - 9:10	AT	AT	AT	AT	AT	X	F	N	C	X	C	C	X
80	9:10 - 9:15	AT	AT	AT	AT	AT	X	F	N	C	C	C	C	X
81	9:15 - 9:20	AT	AT	AT	AT	AT	F	F	N	C	C	C	C	X
82	9:20 - 9:25	AT	AT	AT	AT	AT	F	F	N	C	C	C	C	X
83	9:25 - 9:30	AT	AT	AT	AT	AT	F	F	N	C	C	C	C	X
84	9:30 - 9:35	AT	AT	AT	AT	AT	F	F	N	C	C	C	C	X
85	9:35 - 9:40	AT	AT	AT	AT	AT	F	F	N	C	C	C	C	X
86	9:40 - 9:45	AT	AT	AT	AT	F	C	C	N	C	C	C	C	X
87	9:45 - 9:50	AT	AT	AT	AT	F	C	C	N	C	C	C	C	X
88	9:50 - 9:55	AT	AT	AT	AT	F	C	C	N	C	C	C	C	X
89	9:55 - 10:00	AT	AT	AT	AT	F	C	C	N	C	C	C	C	X

*Legend: AT = “All Trucks”, F = “Fast”, C = “Cars”, N = “NEXUS”, X = “Closed”*

**Figure 3.1-1:** An example of the lane status data on November 19, 2008, collected manually every five minutes at the Blue Water Bridge for U.S. customs lanes

An example of collected data on inspection times is provided in Figure 3.1-2. In this figure, *Ptime* represents the primary inspection processing time for each truck in each lane. As an example, the first truck in lane one took 1 minute and 10 seconds to go through primary

inspection. These data were used in our investigations of screening times, as discussed below in Section 3.3.

Blue Water Bridge Primary Inspection Processing Times  
 Collected Tuesday, November 19, 2008 from 6:48am to 10:08am  
 Time begins at radiation sensor pass until truck leaves inspection booth  
 Lane status color key: ALL TRUCKS FAST TRUCKS

TIME	LANE 1	LANE 2	LANE 3	LANE 4	LANE 5	LANE 6	LANE 7
Start	6:49:58	6:49:25	6:48:01	6:49:10	6:53:47	6:51:16	6:48:44
Stop	6:51:08	6:51:37	6:49:35	6:51:15	7:00:46	6:51:42	6:49:26
Ptime	0:01:10	0:02:12	0:01:34	0:02:05	0:06:59	0:00:26	0:00:42
Start	6:52:03	6:51:43	6:52:17	6:51:20	7:02:19	6:53:45	6:50:03
Stop	6:53:20	6:52:58	6:53:29	6:53:20	7:03:56	6:54:35	6:51:23
Ptime	0:01:17	0:01:15	0:01:12	0:02:00	0:01:37	0:00:50	0:01:20
Start	6:53:46	6:56:34	6:56:50	6:56:05	7:11:48	6:56:19	6:51:29
Stop	6:55:08	6:58:02	6:58:36	6:57:27	7:19:45	6:56:50	6:52:24
Ptime	0:01:22	0:01:28	0:01:46	0:01:22	0:07:57	0:00:31	0:00:55
Start	7:03:17	7:02:20	7:12:59	6:57:39	7:19:52	7:01:40	6:52:32
Stop	7:09:10	7:03:24	7:14:37	6:59:26	7:21:00	7:04:21	6:53:15
Ptime	0:05:53	0:01:04	0:01:38	0:01:47	0:01:08	0:02:41	0:00:43
Start	7:09:47	7:04:17	7:15:09	7:03:38	7:21:52	7:04:35	6:53:32
Stop	7:11:48	7:06:05	7:16:05	7:05:17	7:24:20	7:06:02	6:55:29
Ptime	0:02:01	0:01:48	0:00:56	0:01:39	0:02:28	0:01:27	0:01:57
Start	7:16:17	7:07:21	7:16:39	7:06:50	7:26:39	7:06:12	6:56:09
Stop	7:20:11	7:09:10	7:18:18	7:08:37	7:28:32	7:07:26	6:56:50
Ptime	0:03:54	0:01:49	0:01:39	0:01:47	0:01:53	0:01:14	0:00:41
Start	7:21:19	7:09:12	7:18:50	7:09:01	7:29:21	7:08:08	6:57:33
Stop	7:22:15	7:10:27	7:20:41	7:13:59	7:29:40	7:09:32	6:58:27

**Figure 3.1-2:** An example of the primary inspection time data collected on November 19, 2008, recorded by lane type at the Blue Water Bridge

In addition, we recorded visible queue length and took photographs to document queue status. For illustration purposes, Figure 3.1-3, shows the traffic status at the Blue Water Bridge on August 1, 2008, which was an Ontario provincial holiday. Hence there was relatively heavy car traffic on this day. At the request of Customs and Border Processing, we did not take any photographs of CBP agents conducting vehicle inspections. Figure 3.1-4 shows an example of the manually collected queue length data on November 18, 2008, relative to labeled reference points on the bridge. Data were updated every five minutes. Figure 3.1-5 shows the queue length estimation reference points as segments A-M, with distances in feet from the primary inspection booths. The field crews could visually estimate the queue and reference locations on the bridge when viewing from the MDOT building (near the center of Line A). We did not find any specific use for the manually observed queue length data in the analyses we discuss below, but the data were helpful in understanding queuing patterns for U.S.-bound traffic at this site.



**Figure 3.1-3:** Example photos taken from 8/1/2008 field collect at the Blue Water Bridge

	A	B	C	D	E	F	G	H	I	J	K	L	M	N	
1	Blue Water Bridge Collect														
2	11/18/2008														
3	Queue Lengths														
4															
5	Time	1	2	3	4	5	6	LANES	7	8	9	10	11	12	13
6	3:00 - 3:05														
7	3:05 - 3:10														
8	3:10 - 3:15														
9	3:15 - 3:20														
10	3:20 - 3:25														
11	3:25 - 3:30	B	E	B	NQ	E	E	D	NQ	B	C	C	C	X	
12	3:30 - 3:35	B	B	E	E	E	C	B	NQ	E	E	D	C	X	
13	3:35 - 3:40	B	B	E	E	E	F	NQ	NQ	E	E	D	C	X	
14	3:40 - 3:45	NQ	B	C	E	E	NQ	NQ	NQ	E	F	F	E	X	
15	3:45 - 3:50	C	D	D	E	E	D	NQ	NQ	E	E	E	E	X	
16	3:50 - 3:55	C	C	H	E	D	B	NQ	NQ	E	E	E	E	X	
17	3:55 - 4:00	NQ	NQ	M	NQ	NQ	NQ	NQ	NQ	H	G	G	F	X	
18	4:00 - 4:05	NQ	NQ	F	F	C	NQ	E	NQ	F	F	F	F	X	
19	4:05 - 4:10	NQ	NQ	E	F	E	F	E	NQ	E	J	F	F	X	
20	4:10 - 4:15	B	F	B	E	E	F	B	NQ	G	F	F	F	X	
21	4:15 - 4:20	C	B	E	F	F	B	C	NQ	G	I	E	F	X	
22	4:20 - 4:25	C	B	E	E	G	E	NQ	NQ	F	E	G	G	X	
23	4:25 - 4:30	C	B	E	F	E	B	NQ	NQ	F	E	F	E	X	
24	4:30 - 4:35	B	B	E	B	E	B	NQ	NQ	F	E	F	E	X	
25	4:35 - 4:40	B	E	E	C	C	G	H	NQ	E	J	G	E	X	
26	4:40 - 4:45	B	B	C	B	E	C	F	NQ	F	I	G	F	X	
27	4:45 - 4:50	C	C	C	E	E	F	F	NQ	J	H	G	F	X	
28	4:50 - 4:55	F	C	E	E	E	E	F	NQ	G	H	G	F	X	
29	4:55 - 5:00	C	E	J	E	I	E	E	NQ	F	F	F	E	X	
30	5:00 - 5:05														
31	5:05 - 5:10	C	E	C	E	F	F	F	NQ	F	F	E	E	X	
32	5:10 - 5:15	C	C	C	E	NQ	F	F	NQ	F	G	F	E	X	
33	5:15 - 5:20	B	E	E	C	A	E	E	NQ	F	E	E	D	X	
34	5:20 - 5:25	B	E	E	C	E	E	E	NQ	E	E	E	D	X	
35	5:25 - 5:30	B	E	C	E	C	F	E	NQ	E	F	F	E	X	
36	5:30 - 5:35	NQ	F	F	E	B	E	E	NQ	F	F	E	E	X	
37	5:35 - 5:40	C	C	E	E	NQ	E	E	NQ	C	F	E	E	X	
38	5:40 - 5:45	NQ	C	E	E	NQ	C	C	NQ	D	D	E	C	X	
39	5:45 - 5:50	C	C	E	E	NQ	B	D	NQ	E	E	E	E	X	
40	5:50 - 5:55	C	E	E	E	C	E	C	NQ	F	F	D	D	X	
41	5:55 - 6:00	C	C	E	E	E	C	NQ	A	D	D	C	B	X	
42	6:00 - 6:05	C	E	E	NQ	E	NQ	NQ	B	G	G	F	F	X	
43	6:05 - 6:10	F	E	F	E	F	U	F	NQ	H	B	B	B	X	

**Figure 3.1-4:** Example of queue length data, on November 18, 2008, recorded manually at the Blue Water Bridge for each lane



**Figure 3.1-5:** The queue length graphic used to rapidly estimate queue lengths on the bridge in dynamic traffic situations

Customs and Border Protection on-line postings: We also used data posted at the U.S. Customs and Border Protection website (<http://apps.cbp.gov/bwt/>) on delays and lane status. We downloaded these data from 10/07/08 to 06/10/09. The website posts near real-time information on delays for FAST-certified trucks, standard (all/non-FAST-certified) trucks, NEXUS passenger vehicles and standard (all/non-NEXUS) passenger vehicles for U.S.-bound traffic. Postings are updated approximately every hour, although the exact time of the update depends on the crossing, as well as on the availability of information. As a result, the downloaded data contain several instances where either no information was available or a posted delay is a duplicate of the previously available information. Such missing or redundant records were purged before using the downloaded data in our analyses below. We downloaded 4924 (3824), 7244 (5574), 4951 (3243), and 7245 (5577) postings, respectively, for FAST trucks, non-FAST trucks, NEXUS, and standard/non-NEXUS passenger vehicles at the Ambassador (Blue Water) Bridge crossing.

Whenever we had data points available, we paired the value of the screening time and queuing excess time determined from the geo-fence data for an individual CEVA truck with the CBP posting at the time the CEVA vehicle exited the geo-fence immediately upstream of primary customs inspection. In this way, we produced 3863 (1585), 4510 (1668), 3791 (1175), and 4505 (1671) pairs of matched data points for FAST trucks, non-FAST trucks, NEXUS, and non-NEXUS vehicles at the Ambassador (Blue Water) Bridge crossing.

The CBP border wait time postings are very aggregate, generally rounded to the nearest five minutes. Moreover, in discussing these postings with our technical experts and stakeholders, the posted delays are difficult to interpret, since they are not defined precisely and it appears that the delays are determined subjectively. Our stakeholders believe our values were more objectively determined and more useful because of the specificity as to the locations to which the times correspond. As such, they believe our values are more useful for planning purposes. Nevertheless, one would expect some positive relationship between our excess times and the CBP-posted delays. In Section 3.3 below, we discuss how we used these data in our investigations of queuing times for U.S.-bound traffic and for determining FAST inspection lanes.

Transport Canada-Ontario Region's Pilot Project on Border Wait Times Measurements: In collaboration with Turnpike Global Technologies (TGT), Transport Canada-Ontario region initiated a pilot project to develop a system to estimate commercial vehicles wait times at Southern Ontario Border crossings, times (Shallow, 2008). The system uses data elements derived from a carrier's GPS-based digital tractor logs of TGT's data logging system, which has been programmed to record vehicle movement, stop times and delays, throughout a pre-defined border perimeter zones, as well as at specified locations of interest within a crossing plaza. These data logs are downloaded to Blue-tooth enabled base station readers located at Canada and U.S. exit points, as soon as the vehicle completes the crossing (Sabeau and Jones, 2009). The data are transmitted immediately, processed within minutes, posted to a dedicated Web-portal, and stored

for subsequent temporal pattern and trends analysis. Over time, the number of fleets participating in this pilot project has increased to more than 50, with a mix of both FAST certified and standard commercial vehicles. A member of this project team, who was also a member of our Technical Expert Advisory Committee, provided a subset of the database to us for possible validation and comparison of temporal patterns of crossing times. In Section 3.4, we compare results produced from the Transport Canada/TGT to results produced by our geo-fence approach.

### 3.2 Customs Screening Validation

Having faster screening time at primary customs inspection is one of the advantages of enrolling in the FAST program. Therefore, the screening times for FAST-certified trucks would be expected to be different, and lower, than screening times for trucks that are not FAST-certified. Since our geo-fence data were obtained from FAST-certified trucks, our distributions should resemble screening times obtained from FAST trucks more than distributions obtained from non-FAST trucks. (We note again that shipments must also be FAST-certified. In cases of mixed loads, this requirement will lead to FAST-certified drivers not being able to use FAST lanes. Therefore, not all of our CEVA trucks would be screened in FAST-certified lanes.)

We confirmed that there truly were differences in FAST and non-FAST trucks. As described above, on multiple occasions we manually collected screening times for U.S.-bound trucks at the Blue Water Bridge crossing along with indication of whether the lanes were reserved for FAST trucks or for “non-FAST/All trucks.” We present summary statistics from these ground-based data collection efforts in Table 3.2-1. It is clear from these results that the FAST trucks tended to be screened more quickly than the non-FAST trucks and that there was less variability (as represented by the 90<sup>th</sup> – 50<sup>th</sup> percentile value) in the FAST trucks distributions.

**Table 3.2-1:** Summary statistics of primary customs screening times of U.S.-bound trucks for FAST and standard/non-FAST truck lanes from ground-based data collection at Blue Water Bridge crossing

	BWB CAN to U.S.							
	18 Nov 2008		19 Nov 2008		5 May 2009		20 May 2009	
	FAST	non-FAST	FAST	non-FAST	FAST	non-FAST	FAST	non-FAST
# of trucks	88	349	96	296	132	575	148	559
mean	2.07	2.62	1.10	2.45	1.85	2.73	2.25	2.62
50% (min)	1.68	2.03	0.77	1.85	1.38	1.92	1.48	2.00
90% (min)	3.40	4.68	1.90	4.87	2.75	5.12	3.37	4.87
90%-50%	1.72	2.65	1.12	3.02	1.37	3.20	1.88	2.87

We could determine the times that the trucks tracked in the air photos traversed the primary customs screening region by lane. As an example, in Figure 3.2-1, we present the empirical

cumulative distribution functions (ECDFs) of the screening times derived by lane in the morning period for the US-bound traffic at the Blue Water Bridge crossing. The figure shows that the screening times are markedly faster in lane 7 than in the other lanes. The Customs and Border Protection postings we downloaded (see above) stated that there was one FAST lane open during this time period. Our ground-based observations confirmed that lane 7 was the only FAST lane operating during this period.

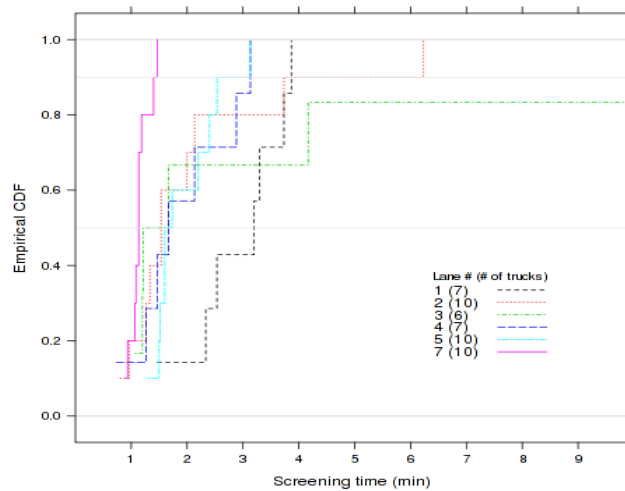


**Figure 3.2-1:** Empirical cumulative density functions of screening times, by lane, derived from air photos during the morning period for the US-bound traffic at the Blue Water Bridge crossing

In some, but not all, of the other sets of air photos, we found similarly distinct indications of which lanes were operating as FAST lanes during the period in which we collected aerial imagery. Some, but not all, of these indications could be supported by our ground-based observations and the CBP data. (As mentioned above, we only had CBP postings for US-bound traffic and only had ground-based observations for U.S.-bound traffic at the Blue Water Bridge.) ECDFs similar to Figure 3.2-1 and summary statistics of the screening times derived from the air photos, by lane, are presented in Appendix Section 3.2. Based on our analysis of the plots of the ECDFs and the summary statistics, along with our ground-based observations and CBP data when available, we estimated which lanes were serving as the FAST lanes during the period of air-based data collection. Specifically, at the *Ambassador Bridge* site:

- for the *U.S.-bound* traffic in the *morning* period, the distribution of air photo-derived screening times indicated three lanes as processing trucks faster than other lanes. CBP data indicated that there were three FAST lanes in operation, and we considered lanes 29,

30, and 31 to be the FAST lanes. We note that lanes 29, 30, and 31 are physically separated from the other lanes.

- for the *U.S.-bound* traffic in the *afternoon* period, the indications from the air photo-derived distributions were not as clear as those in the morning period. The CBP again posted that there were three FAST lanes in operation. The air-based distributions again indicated that lanes 30 and 31 were processing trucks more quickly than other lanes, but lane 25 seemed to be processing trucks more quickly than lane 29. However, given the physical positioning of the lanes, we again assumed that lanes 29, 30, and 31 were serving as FAST lanes during this period.
- for the *Canada-bound* traffic in the *morning* period, from the air photo-derived distributions we could not identify any set of lanes as clearly processing trucks more quickly than any other set of lanes. To be conservative in our analysis below we chose the lane with the lowest median screening time, lane 10 (which was also the lane with the lowest 90<sup>th</sup> percentile screening time) to be the FAST lane.
- for the *Canada-bound* traffic in the *afternoon* period, the situation was the same as in the morning period, and we again chose the lane with the lowest median screening time (which again was the lane with the lowest 90<sup>th</sup> percentile screening time) as the FAST lane. This was lane 9 this time, and we selected it to represent the FAST lane.

At the *Blue Water Bridge* site:

- for the *U.S.-bound* traffic in the *morning* period, as discussed above, the distribution of air photo-derived screening times in one lane was clearly lower than the others, CBP data indicated that there was one FAST lane open, and our ground-based observations confirmed that lane 7 was the FAST lane. We, therefore, considered lane 7 to be the FAST lane.
- for the *U.S.-bound* traffic in the *afternoon* period, from the air photo-derived distributions we could not identify any set of lanes as clearly processing trucks more quickly than any other set of lanes. The CBP data indicated that there was only one FAST lane open. Our ground-based data indicated that lane 7 was again serving as a FAST lane and that lane 4 changed status from serving FAST trucks to serving standard/non-FAST trucks during the period. We therefore, did not consider air photo-derived data from lane 4 in our analysis and considered lane 7 to be the FAST lane during this period.
- for the *Canada-bound* traffic in the *morning* period, the distribution of air photo-derived screening times indicated that lane 13 was processing trucks more quickly than the other lanes. We, therefore, considered lane 13 to be the FAST lane during this period.
- for the *Canada-bound* traffic in the *afternoon* period, the distributions of air photo-derived screening times indicated that lanes 13 and 15 were processing truck more quickly, and we considered these as the FAST lanes during this period.

We present summary statistics for the FAST and standard/non-FAST truck lanes, as determined above, in Table 3.2-2.

**Table 3.2-2:** Summary statistics of distributions of screening times determined from air-photos aggregated by what were considered to be FAST lanes and standard/non-FAST lanes during air-based data collection period

(a) Ambassador Bridge statistics

	CAN to U.S.				U.S. to CAN			
	Morning		Afternoon		Morning		Afternoon	
	FAST	non-FAST	FAST	non-FAST	FAST	non-FAST	FAST	non-FAST
Lane #	29-31	22-28	29-31	22-27	10	3-9,12	9	3-8,10-12
# of trucks	30	60	30	60	7	38	5	40
mean	1.10	2.26	1.16	1.62	0.84	1.58	0.55	1.34
50% (min)	1.05	1.73	0.80	1.40	0.80	0.98	0.53	1.03
90% (min)	1.52	4.25	2.56	2.69	1.17	2.58	0.71	1.98
90%-50%	0.47	2.52	1.76	1.29	0.37	1.60	0.17	0.95

(b) Blue Water Bridge statistics

	CAN to U.S.				U.S. to CAN			
	Morning		Afternoon		Morning		Afternoon	
	FAST	Non-FAST	FAST	non-FAST	FAST	non-FAST	FAST	non-FAST
Lane #	7	1,2,4,5	7	1-3,5	13	15-18	13,15	16-18
# of trucks	10	40	10	40	7	48	46	43
mean	1.14	2.35	2.03	2.56	0.76	1.14	0.80	1.72
50% (min)	1.13	1.70	1.20	1.87	0.60	0.88	0.70	1.67
90% (min)	1.41	3.75	3.03	4.23	1.12	1.92	1.33	2.96
90%-50%	0.27	2.05	1.83	2.36	0.52	1.04	0.63	1.29

In Figure 3.2-2, we present the ECDFs of the screening times obtained from our geo-fence data. As mentioned above, the ECDFs portray the variability of conditions over nine months. The observations obtained from the air photos and ground-based observations only cover a few different periods. Therefore, we cannot expect the distributions to match. However, the distributions derived from the geo-fence data can be considered to give the probability of the conditions during a relatively short, random observation period. We used a very small interval (plus or minus 0.1 minutes) around the mean FAST and standard/non-FAST screening times determined from the air photos and the ground-based data collection to calculate the probabilities of observing these screening times. (We use the means to represent the conditions at the time and assume that the ECDFs portray the probabilities of these conditions.) We present these probabilities in Table 3.2-3.

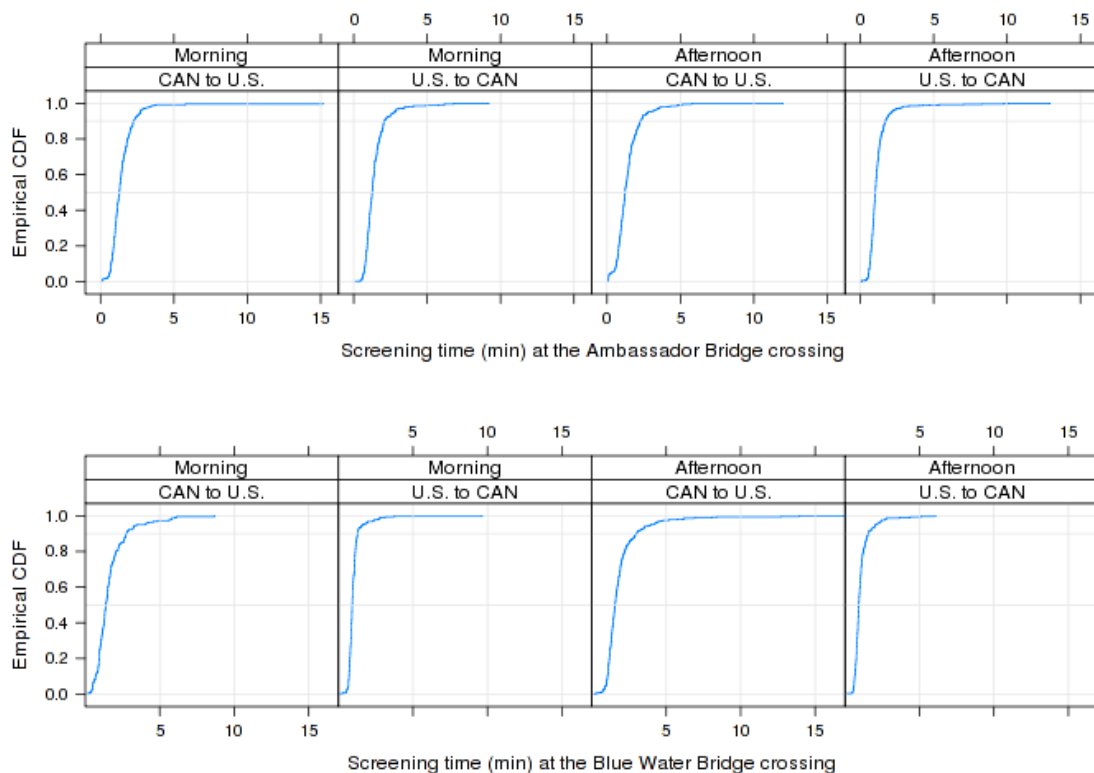


**Figure 3.2-2:** Empirical cumulative density functions of screening times derived from geo-fence data, by bridge crossing and direction

**Table 3.2-3:** Probabilities, derived from geo-fence ECDFs, of observing screening times equal to the mean of screening times derived from the air photo- and ground-based data, plus or minus 0.1 [min]

(a) Ambassador Bridge probabilities using air photos

	CAN to U.S.				U.S. to CAN			
	Morning		Afternoon		Morning		Afternoon	
	FAST	non-FAST	FAST	non-FAST	FAST	non-FAST	FAST	non-FAST
Lane #	29-31	22-28	29-31	22-27	10	3-9,12	9	3-8,10-12
# of trucks	30	60	30	60	7	38	5	40
air-photo mean (min)	1.10	2.26	1.16	1.62	0.84	1.58	0.55	1.34
probability under CEVA distribution	0.157	0.040	0.153	0.078	0.163	0.091	0.079	0.111

(b) Blue Water Bridge probabilities using air photos

	CAN to U.S.				U.S. to CAN			
	Morning		Afternoon		Morning		Afternoon	
	FAST	non-FAST	FAST	non-FAST	FAST	non-FAST	FAST	non-FAST
Lane #	7	1,2,4,5	7	1-3,5	13	15-18	13,15	16-18
# of trucks	10	40	10	40	7	48	46	43
air-photo mean (min)	1.14	2.35	2.03	2.56	0.76	1.14	0.80	1.72
probability under CEVA distribution	0.109	0.027	0.071	0.024	0.318	0.206	0.323	0.01

(c) Blue Water Bridge, U.S.-bound probabilities using ground-based data (CEVA ECDFs based on Monday-Thursday, 6 am to 10 pm data)

	BWB CAN to U.S. (6:01 am – 9:59 pm, M-R)							
	18 Nov 2008		19 Nov 2008		5 May 2009		20 May 2009	
	FAST	non-FAST	FAST	non-FAST	FAST	non-FAST	FAST	non-FAST
# of trucks	88	349	96	296	132	575	148	559
ground data mean (min)	2.07	2.62	1.10	2.45	1.85	2.73	2.25	2.62
probability under CEVA distribution	0.051	0.024	0.122	0.025	0.095	0.019	0.041	0.024

Of the 12 FAST/non-FAST comparisons, the probabilities are higher (and, typically, much higher) of observing the FAST distribution means than the non-FAST distribution means for all but the US-to-Canada afternoon flight comparison at the Ambassador Bridge. That is the air-based and ground-based observations support that the CEVA data better depict FAST-based screening times, as would be expected.

### 3.3 Queuing Time Validation

From inspection of our air photos, there was important queuing upstream of primary customs inspection only on the Blue Water Bridge, in the Canada-to-U.S. direction in both periods. It also appeared that one set of trucks, assumed to be FAST trucks, could by-pass the longer queues and more directly access screening lanes, which still had some queuing on the Blue Water Bridge in the afternoon in the U.S.-to-Canada direction.

We attempted to quantify this activity from the truck tracking we conducted in the air photos. We were able to track most of the trucks we observed undergoing primary customs screening through the geo-fence immediately upstream of primary customs. (We could not track the trucks that were already in the upstream geo-fence when we began our observation period.) From the

truck identifier, we could associate the time of truck in the geo-fence upstream of customs screening with the lane in which the truck was subsequently screened. We call the travel times in the upstream geo-fence “queuing times,” even if there was no queuing until arriving at primary customs screening. Given our designation of screening lanes as being FAST or non-FAST, as described above, we could then determine the distributions of times in the upstream geo-fence for the FAST and non-FAST trucks.

We present the mean queuing times for trucks that were screened in the FAST lanes and for those screened in the standard/non-FAST lanes in Table 3.3-1. We note that the FAST truck queuing times were shorter than the non-FAST truck queuing times for all bridge crossing-direction-time periods except the U.S.-to-Canada direction at the Ambassador Bridge site (for both morning and afternoon observation periods). The geo-fence immediately upstream of customs inspection for Canada bound traffic at the Ambassador Bridge is very short, approximately 0.10 miles long (see Figure 2.3.2-1 and Table 2.3.2-1), and there was not much room for important queues to build up in this area. (In hindsight, we should have attempted to image and track trucks farther upstream in this direction.) The fact that the FAST queuing times were lower than the non-FAST queuing times supports our observations in the air photons and also lends support to our determination of FAST and non-FAST screening lanes.

Similar to what we did above for screening times, we used the distributions of CEVA geo-fence derived travel times in the upstream geo-fence for the time period (Monday-Thursday, am or pm) to calculate the probabilities of observing the air photo-derived times (using plus or minus 0.5 minutes). These probabilities are presented in Table 3.3-1. As with the screening times, it appears that FAST trucks incur less queuing time than standard/non-FAST trucks, at least in the geo-fence immediately upstream of primary screening, and that it was much more likely to observe the FAST truck queuing than the standard/non-FAST truck queuing when using our geo-fence derived distributions. That is, our geo-fence results are more like the air photo-derived results for FAST trucks than for standard/non-FAST trucks. Since the CEVA trucks are all FAST-certified, this result is consistent with expected performance of valid geo-fence results.

**Table 3.3-1:** Probabilities derived from geo-fence ECDFs of observing queuing times equal to the mean of queuing times derived from the air photo-data, plus or minus 0.5 [min]

(a) Ambassador Bridge probabilities

	CAN to U.S.				U.S. to CAN			
	Morning		Afternoon		Morning		Afternoon	
	FAST	non-FAST	FAST	non-FAST	FAST	non-FAST	FAST	non-FAST
Lane #	29-31	22-28	29-31	22-27	10	3-9,12	9	3-8,10-12
# of trucks	53	69	16	40	7	38	5	40
air-photo mean (min)	6.34	11.34	2.49	4.30	1.78	1.30	0.27	0.25
probability under CEVA distribution	0.081	0.024	0.169	0.071	0.134	0.139	0.505	0.505

(b) Blue Water Bridge probabilities

	CAN to U.S.				U.S. to CAN			
	Morning		Afternoon		Morning		Afternoon	
	FAST	non-FAST	FAST	non-FAST	FAST	non-FAST	FAST	non-FAST
Lane #	7	2,4,5	7	1-3,5	13	15-18	13,15	16-18
# of trucks	14	4	5	31	7	48	46	43
air-photo mean (min)	3.71	21.75	4.93	10.19	1.50	1.87	5.16	9.29
probability under CEVA distribution	0.058	0.009	0.066	0.044	0.724	0.527	0.020	0.007

To further indirectly investigate the validity of the geo-fence results, we compared our results with the Customs and Border Protection (CBP) postings on delays in the Canada-to-U.S. direction. We would expect the excess times in the geo-fence upstream of primary customs inspection to represent queuing delays. Queuing delay would be expected to constitute the principal component of the posted CBP delays.

In Figure 3.3-2, we present scatter plots of the CBP-posted delays for FAST trucks, non-FAST trucks, NEXUS vehicles, and non-NEXUS vehicles against CEVA excess times in the geo-fence immediately upstream of primary customs screening at the two border crossing sites. (We discussed above the aggregate nature of the CBP-posted delays, where the postings are provided in five-minute increments.) The very low number of nonzero postings at the Blue Water Bridge for both FAST and NEXUS vehicles - 24 out of 1585 postings and 6 out of 1175 postings, respectively - is noticeable. The extremely low number of non-zero CBP postings, the fairly large values of geo-fence derived excess times when the CBP postings were zero, and the fact that this low number of zero postings did not occur at the Ambassador bridge lead us to believe that posting for FAST and NEXUS vehicles at the Blue Water Bridge site were representing something different than true delays at this site.

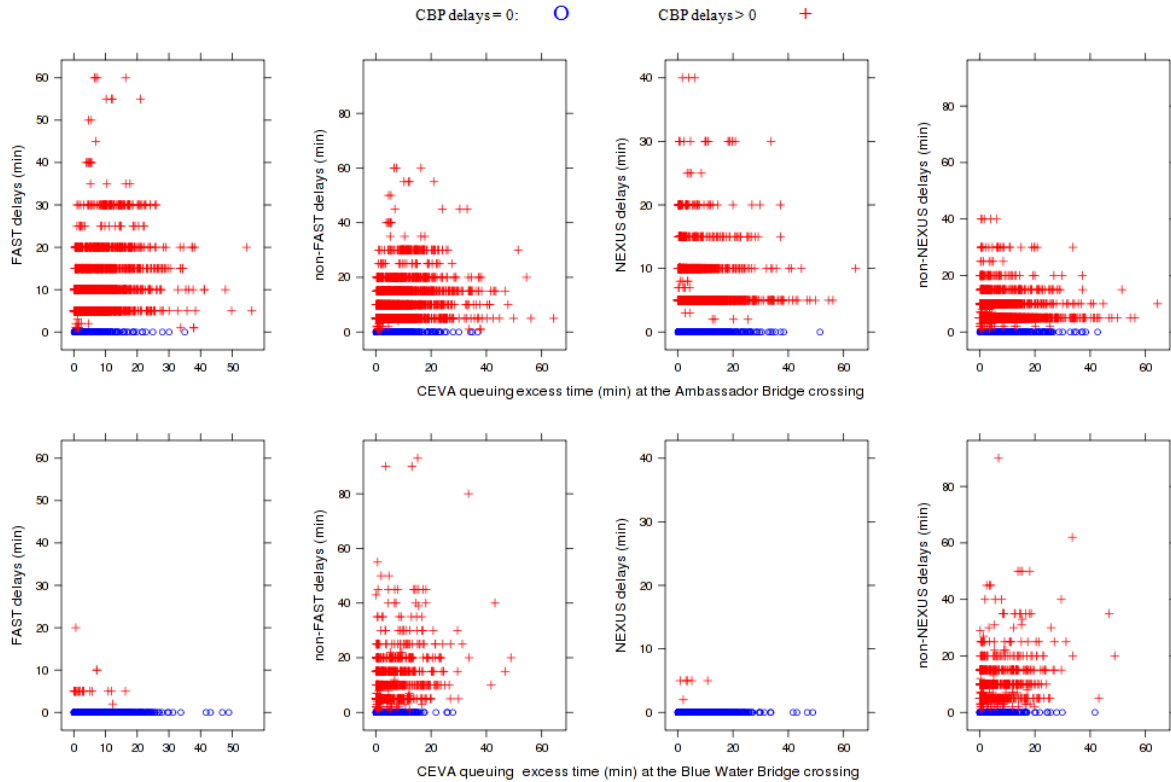


**Figure 3.3-1:** Scatter plots of CBP-posted delays against geo-fence recorded (CEVA) queuing excess times for FAST trucks, standard/non-FAST trucks, NEXUS passenger vehicles, and standard/non-NEXUS passenger vehicles at the Ambassador Bridge and Blue Water Bridge crossings

In Table 3.2.-2 we present the empirical Pearson’s correlation values between the geo-fence derived excess times and the various CBP delay postings and between the various pairs of CBP postings. The positive correlation between geo-fence derived excess times and CBP-posted delays for FAST trucks at the Ambassador Bridge crossing, especially given that estimates provided by the CBP postings are rounded to five minutes and that the postings are not designed to represent exactly the same phenomena as our excess times, supports the validity of the geo-fence data to represent conditions for FAST trucks at the crossing, as expected. There is a similarly positive correlation between the CEVA and standard/non-FAST trucks at the Ambassador Bridge site. Although the air photo-derived results demonstrate that the queuing times are appreciably different, it is conceivable that delays would be correlated: When FAST queuing times decrease, the standard/non-FAST times may also decrease, which is observed when comparing Canada-to-U.S. morning and afternoon air-photo derived queuing times in Table 3.3-1. This would occur if FAST and non-FAST trucks have similar arrival patterns and bridge operators manage the two classes of delays in tandem. The similar correlation value between CEVA-derived excess times and CBP postings for standard/non-FAST trucks at the Blue Water Bridge make this an interesting possibility. However, the extremely high and positive correlation between the CBP postings for FAST and standard/non-FAST delays makes

us hesitate in proclaiming that the CEVA-derived geo-fence data are as representative of patterns in the standard/non-FAST truck delays as they are of patterns in the FAST truck delays. Additional investigation would be warranted.

**Table 3.3-2:** Correlation values between geo-fence derived queuing excess times and CBP-posted delays and between pairs of CBP-posted delays at Ambassador Bridge and Blue Water Bridge Crossings

(a) Ambassador Bridge correlations				
	FAST	non-FAST	NEXUS	non-NEXUS
CEVA	0.376	0.353	0.064	0.034
FAST		0.977	0.138	0.099
non-FAST			0.087	0.143
NEXUS				0.717

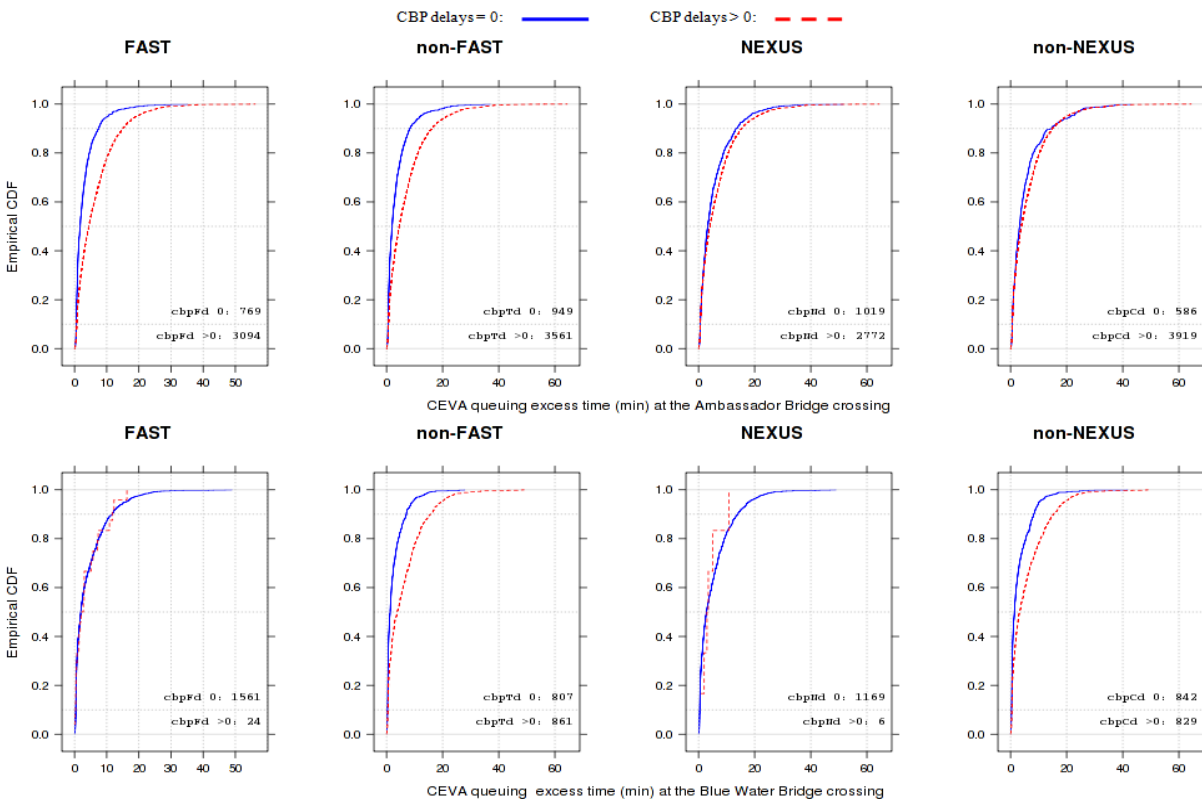
  

(b) Blue Water Bridge correlations				
	FAST	non-FAST	NEXUS	non-NEXUS
CEVA	-0.011	0.380	-0.01	0.349
FAST		0.072	0.299	-0.006
non-FAST			-0.011	0.529
NEXUS				-0.018

The low correlations of the geo-fence derived excess times with the CBP postings for NEXUS and standard/non-NEXUS passenger vehicles indicates that the geo-fence delays would not be useful in portraying delays for non-commercial vehicles at the Ambassador Bridge. This is not inconsistent with expectations because of the separation of truck and passenger vehicles in the section of roadway upstream of primary customs inspection.

The correlation values are low between CEVA-derived excess times and CBP postings for FAST and NEXUS vehicles at the Blue Water Bridge. However, this low correlation is a consequence of the extremely small number of CBP non-zero delay postings for these vehicle classes mentioned above. We note that the correlation values between CEVA-derived excess times and CBP delays are very close to those between CEVA and FAST trucks and CEVA and standard/non-FAST trucks at the Ambassador Bridge site. Given that the correlation between the Blue Water CBP postings for standard/non-FAST trucks and standard/non-NEXUS passenger vehicles is not nearly as strong as the correlation between Ambassador CBP postings for FAST and standard/non-FAST vehicles, it would appear that CEVA derived excess time patterns would be indicative of all traffic patterns at the Blue Water Bridge. Again, the air photo-derived results clearly show that FAST times and non-FAST queuing times would not be the same, and the same would be expected for passenger vehicles. However, it is possible that, when delays to one class of vehicles increases, delays to another class of vehicles also increases, and that the CEVA data can represent these patterns.

We also used a more aggregate categorization of the CPB postings to support the validity of the geo-fence data to portray conditions of some portion of the general traffic stream. In Figure 3.3-2, we present the empirical cumulative distribution functions (ECDFs) of the geo-fence derived excess times at the two border crossing sites when the CPB postings for the various traffic streams were zero and when they were greater than zero. At the Ambassador Bridge crossing (Figure 3.3-2a), it is clear that the geo-fence derived excess times were higher when the CPB posting for FAST trucks were greater than zero than when they were zero, and similarly for the non-FAST trucks. This is not the case for the passenger vehicle postings. These plots further support that the geo-fence data are providing valid information on the FAST truck traffic and, through CBP's correlation of FAST and non-FAST truck traffic, perhaps non-FAST truck traffic at this crossing. At the Blue Water Bridge crossing (Figure 3.3-2b), the plots show that the geo-fence derived excess times were higher when the CPB postings for non-FAST trucks were greater than zero than when they were zero, and similarly for the non-NEXUS vehicles. Although no such distinction is apparent for the FAST trucks and NEXUS vehicles, this is likely a result of the extremely, and possibly unreasonably, low number of non-zero postings for these vehicle classes. That is, the geo-fence delays seem to be providing valid information on the general U.S. bound traffic stream at the Blue Water Bridge crossing.



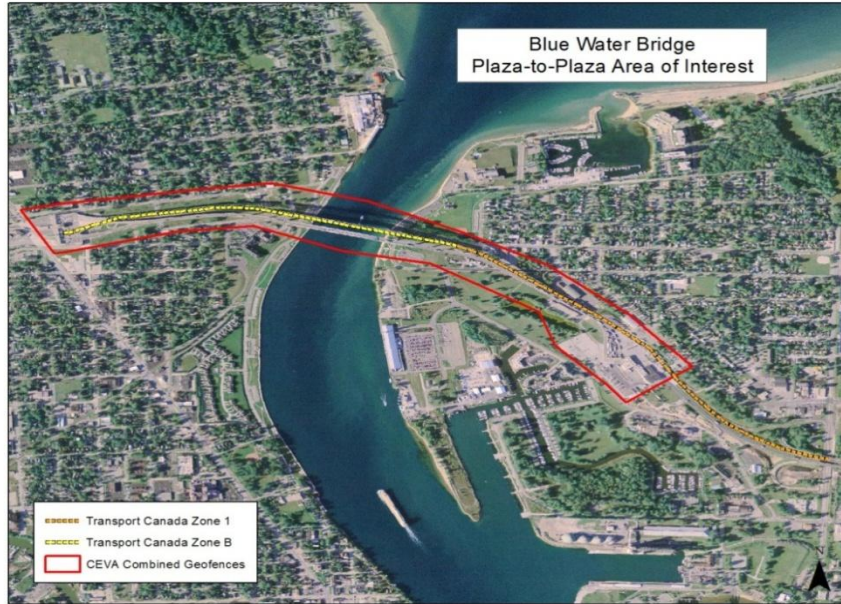
**Figure 3.3-2:** Empirical cumulative distributions of geo-fence derived queuing excess times when CPB posting are zero and greater than zero for various traffic classes at Ambassador Bridge and Blue Water Bridge crossings

In addition to the results presented in this subsection, the statistical significance of the expected relationships seen in Section 5.1, where queuing excess times increase with increasing traffic demand on the system and decreasing number of inspection booths open, also support the validity of the queuing times derived from the geo-fence approach to represent conditions for, at least, FAST trucks.

### **3.4 Border Crossing Time Validation**

The Transport Canada (TC) Bluetooth data discussed above contained travel time information from a wider range of trucks than the CEVA fleet that was used to produce the geo-fence data considered in this study. However, the TC data did not contain information on the multiple activities we were able to investigate with the geo-fence data; nor did the data allow comparisons between the exact same locations we used in our geo-fence derived data. Nevertheless, we could compare the processed information to investigate the degree to which the geo-fence derived results from the single CEVA fleet corresponded to the TC Bluetooth derived results from a broader truck population. We note that the TC data, although collected from a broader sample of trucks, are not claimed to be representative of the entire truck population at the border crossing sites.

In the following comparisons of results obtained from the CEVA geo-fence data and results obtained from the TC Bluetooth data, we use overall crossing times results for February to March 2009. The CEVA geo-fence crossing times were determined from the AU08 geo-fences used in this study to match the Transport Canada crossing-time analysis “zones” (as Transport Canada called them) as closely as possible, specifically between the locations indicated in Figures 3.4-1a and b. The Transport Canada data had duty-free times removed, so we used data with duty-free times removed as explained in Section 2.



(a) Blue Water Bridge



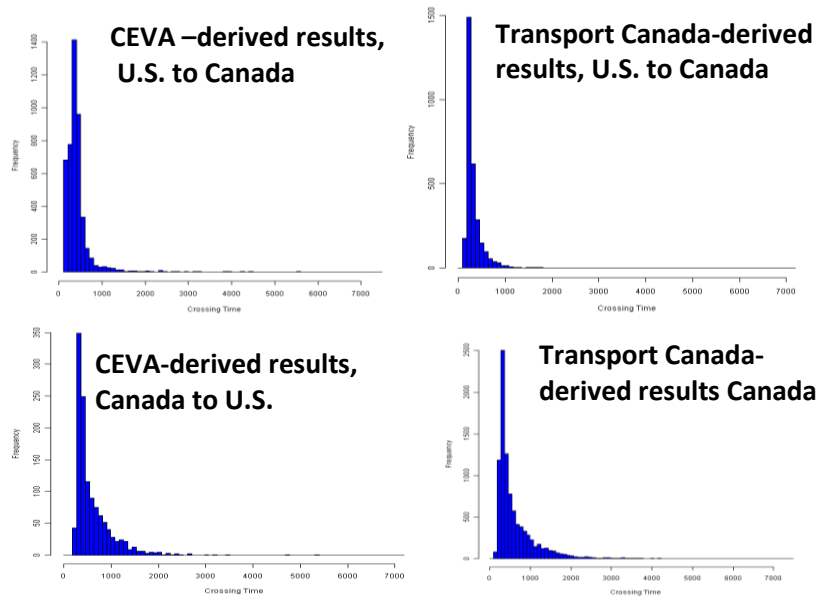
(b) Ambassador Bridge

**Figure 3.4-1:** Comparison of Transport Canada crossing time zones (dashed lines) to merged AU08 geo-fences (red outline)

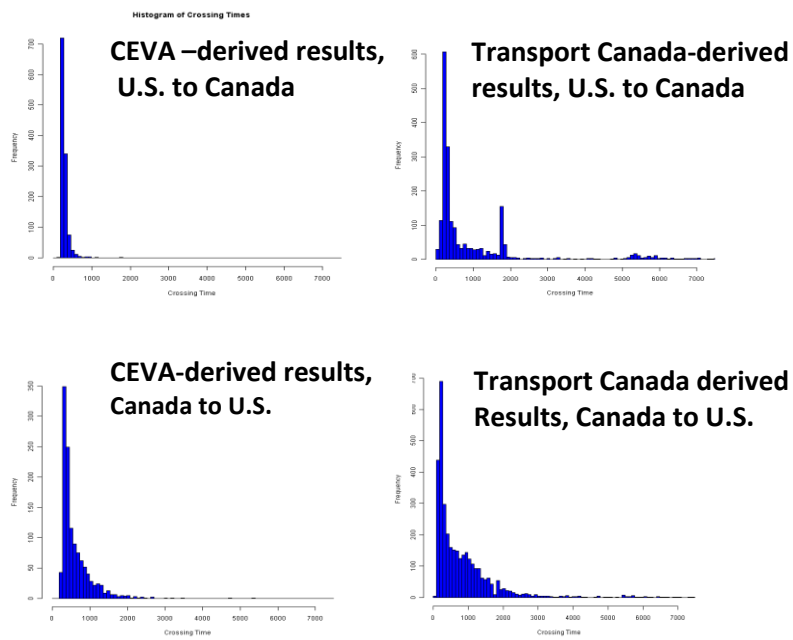
Histograms of the crossing time data for the different bridge crossing sites and directions from the two data sources are presented in Figure 3.4-2. In Table 3.4-1, we present the median (50<sup>th</sup> percentile), 90<sup>th</sup> percentile, 90<sup>th</sup> percentile minus 50<sup>th</sup> percentile values (to represent variability, as in Section 2). The magnitudes of the percentile times cannot be directly compared, since the actual locations between which crossing times are determined are different in the two data sets. However, the general shapes of the CEVA and TC histograms for both directions of traffic at the Ambassador Bridge crossing (Figure 3.4-2a) are similar, and the similarity of the variability measures seen in Table 3.4-1 are striking.

The TC histogram for the Blue Water U.S.-to-Canada direction indicates a bimodal distribution not seen in the CEVA histogram, with several observations of high crossing times. This difference might be attributed to the difference in the locations of the CEVA geo-fences and the TC zones. Specifically, in Figure 3.4.1a, it appears that the TC zone may include the location of the secondary vehicle inspection facilities for Canada-bound traffic, whereas the final CEVA geo-fence crossing is located before the secondary vehicle inspection site. The extra time incurred by Canada-bound vehicles sent to secondary inspection would then appear in the right tail of the TC histogram but not in the tail of the CEVA histogram.

The shapes of the histograms for the Blue Water Canada-to-U.S. direction are more similar than the shapes of the U.S.-to-Canada histograms, but there are again more large times in the TC histogram than in the CEVA histogram. This observation is also manifested by the large discrepancy in the CEVA and TC 90<sup>th</sup> percentile and variability (90<sup>th</sup> percentile – 50<sup>th</sup> percentile) values in Table 3.4-1, while the medians are similar. Again, the difference in the right tails of the distribution might be attributable to the difference in the CEVA geo-fence crossing and the TC zone, this time at the beginning of the trip. When cleaning the CEVA data (see Section 2.4.1), we observed some vehicles parking or spending what appeared to be voluntary extra time upstream of the beginning of the initial geo-fence crossing used in this comparison. These extra times would be more likely to appear in TC histograms than in the CEVA histograms.



(a) Ambassador Bridge



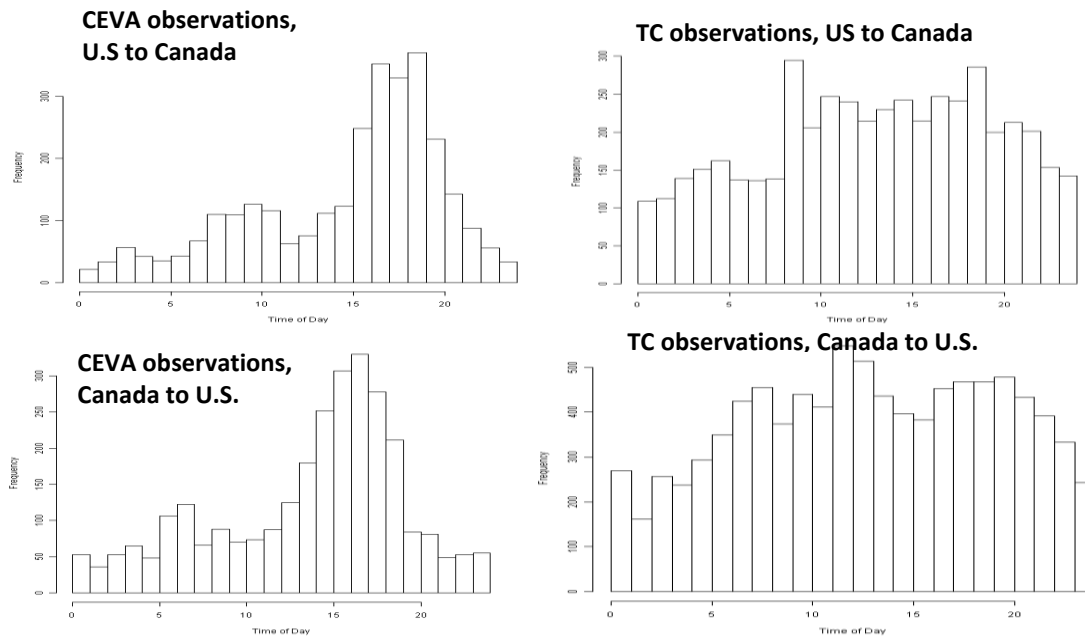
(b) Blue Water Bridge

**Figure 3.4-2:** Histograms of crossing times (in seconds) obtained from CEVA geo-fence and Transport Canada Bluetooth data by direction (data from February-April 2009)

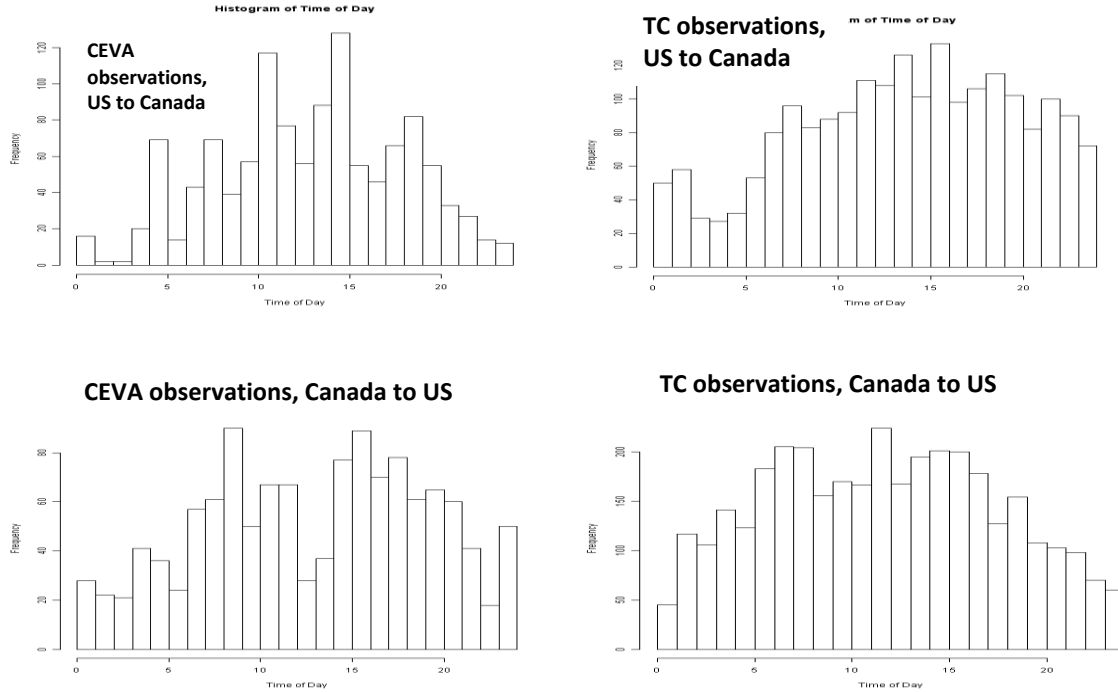
**Table 3.4-1:** Summary statistics of crossing time distributions obtained from CEVA geo-fence and Transport Canada Bluetooth data by direction and crossing site (data from February-April 2009)

	Ambassador Bridge Crossing				Blue Water Bridge Crossing			
	CAN-to-US		US-to-CAN		CAN-to-US		US-to-CAN	
	CEVA	TC	CEVA	TC	CEVA	TC	CEVA	TC
# observations	2872	9215	2987	4656	1238	3514	1187	2050
50%ile [min]	12:47	6:54	4:15	6:00	7:17	8:42	4:19	5:30
90%ile [min]	26:42	20:48	8:37	10:12	18:24	30:18	6:04	33:50
90%ile -50%ile [min]	13:55	13:54	4:22	4:12	11:07	21:36	1:45	28:20

Because of temporal differences in crossing times seen in Section 2.4.3, the comparisons of the CEVA and TC data might also be affected by the differences in the temporal distributions of the two data sets. In Figure 3.4-3, we plot histograms of the numbers of observations by hour-of-day, defined by the time the truck was at the location specified to be the starting location for the crossing time determination. The histograms indicate different temporal patterns in the two data sets, which is understandable, since the CEVA data are dominated by traffic related to the automotive industry, where the TC data are composed of a more diverse mixture of freight traffic.



(a) Ambassador Bridge temporal patterns



(b) Blue Water Bridge temporal patterns

**Figure 3.4-3:** Histograms of numbers of observations by hour-of-day of CEVA geo-fence and Transport Canada Bluetooth data by direction for Ambassador Bridge and Blue Water Bridge crossings

To control for the impacts of the temporal differences in overall summary statistics of crossing times, we investigated the effect of various temporal factors on crossing time and the variability in those crossing times for each of these two data sets. We decomposed the variability in the crossing times into factors accounting for hour-of-day, day-of-month, day-of-week, and month-of-year effects. A generalized additive model of the form in Equation (3.4-1) was chosen to allow for possible nonlinear effects of the variables upon the crossing time.

$$\text{CrossingTime}_i = \beta_0 + s_1(\text{TimeofDay}_i) + s_2(\text{DayofMonth}_i) + f_3(\text{DayofWeek}_i) + f_4(\text{Month}_i) + \epsilon_i \quad (3.4-1)$$

Day-of-week was a categorical variable with seven categories—one for each day of the week. Month was another categorical variable with three categories, one each for February, March, and April, the three months for which we had both CEVA and TC data. The time-of-day and day-of-week variables were both represented as cubic-spline functions  $s_1$  and  $s_2$ , respectively, as we assume that the trends in these effects will be smooth. The term ‘smooth’ here indicates that the trend has no sharp, sudden discontinuities. Day-of-week and month are both categorical additive effects. The  $\beta_0$  term is an additive constant, and  $\epsilon_i$  is the unexplained error in the model for the  $i^{\text{th}}$  individual truck crossing.

Some aspects of our specification are noteworthy. First, the splines function for the time-of-day variable is not a continuous, periodic function: the beginning and end points of the spline function do not necessarily match up with each other, as indicated in the top frame of Figure 3.4-4. We would expect the time-of-day function to be periodic because, for instance, trips that start before midnight one day do not experience extraneous increases or decreases in crossing time when the new day begins compared to trips that end shortly before midnight or begin shortly after midnight. This representation is presented for illustration purposes, but was not used in the model fitting stage. Rather, we used a “wrap-around” spline function with a period three times that of the original spline function, as indicated in middle frame of Figure 3.4-4. This approach ultimately produced a new spline function, illustrated in the bottom frame of Figure 3.4-4, that was used in the model estimation.

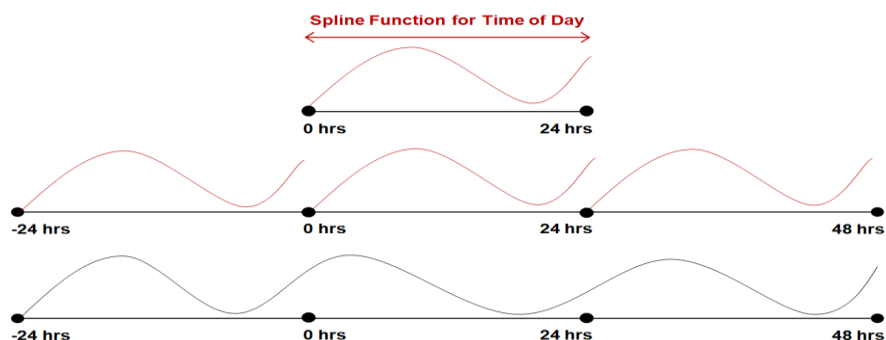
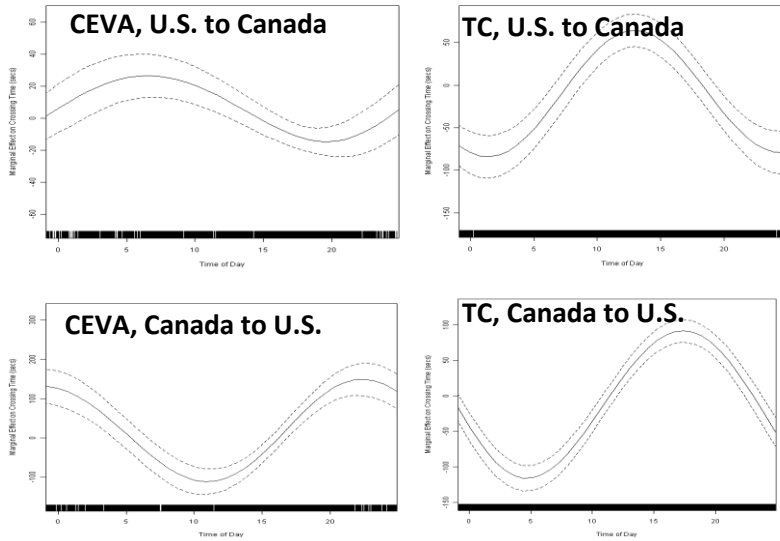


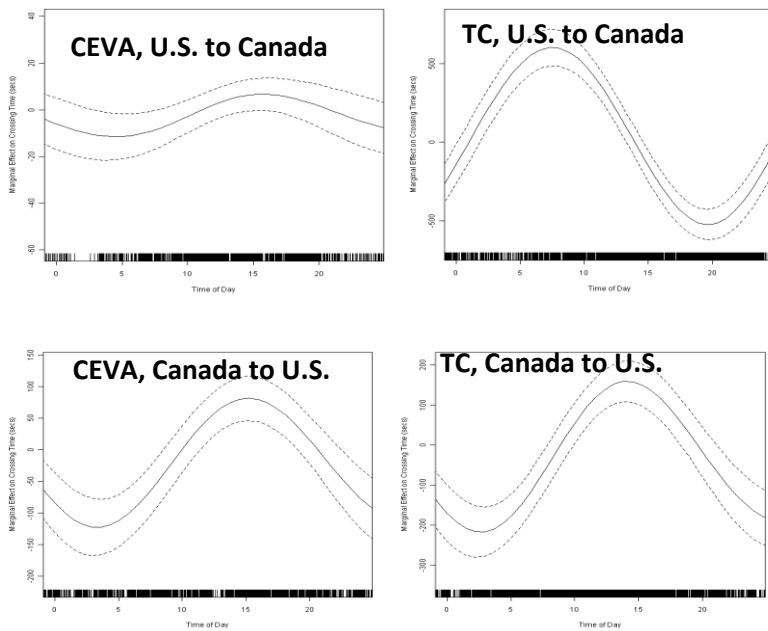
**Figure 3.4-4:** Spline functions representations for time-of-day modeling

Since different months have different numbers of days, we quantified the day-of-month variable by normalizing by the number of days in the month. For example, November 15 would be considered 0.5 (the 15<sup>th</sup> day, divided by the 30 days in November). We did not use the “wrap-around” approach for the day-of-month splines function, since continuity from the end of one month to the beginning of the next month would not necessarily be expected.

The marginal effect on crossing time (in seconds), by the time-of-day, day-of-month, day-of-week, and month are presented by direction and border crossing site in Figures 3.4-5 through 3.4-8, respectively, for CEVA and TC data sets for comparison purposes. The solid curves portray the mean values, and the dashed lines indicate the 95% confidence intervals. Similarities in the patterns associated with these variables are associated with similar patterns (peaks and valleys) in the curves. The narrow confidence intervals (tightness between the dashed curves in the figures) for the time-of-day and day-of-month, in Figures 3.4-5 and Figure 3.4-6, respectively, indicate the statistical significance of these effects. Indeed, all the parameters considered in the model were found to be highly statistically significant. However, collectively, they only explain about 5% of the variance in the data, thereby limiting the explanatory power for predicting an individual truck’s crossing time.

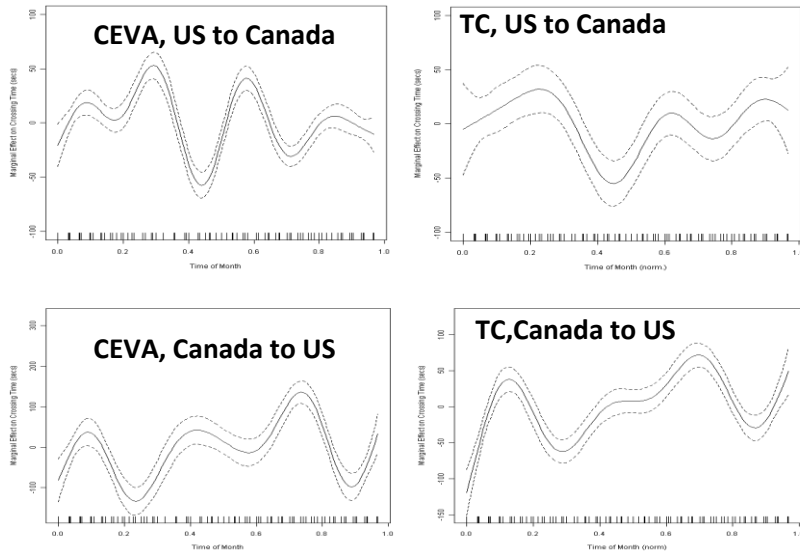


(a) Ambassador Bridge

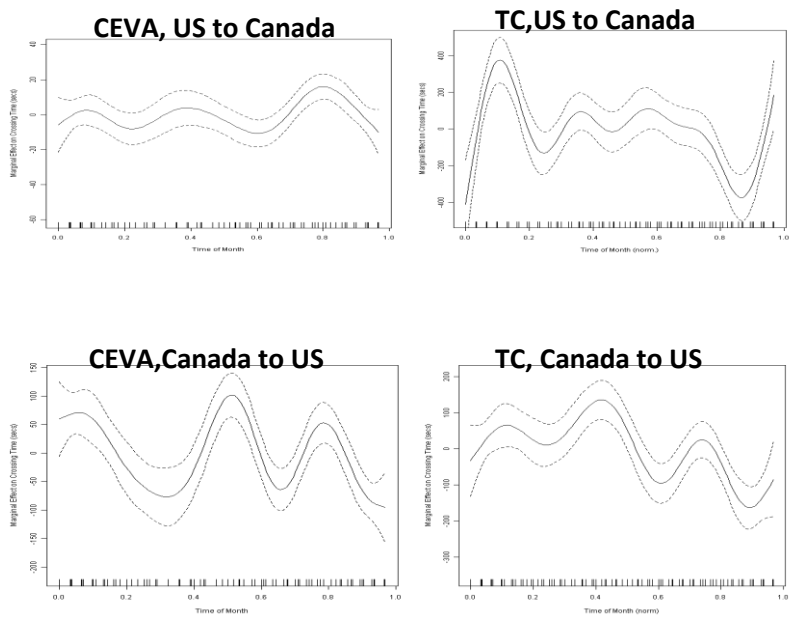


(b) Blue Water Bridge

**Figure 3.4-5:** Crossing time trends based on the (partial) marginal effect of the time-of-day variable on crossing times estimated from CEVA and Transport Canada data for both bridges and directions

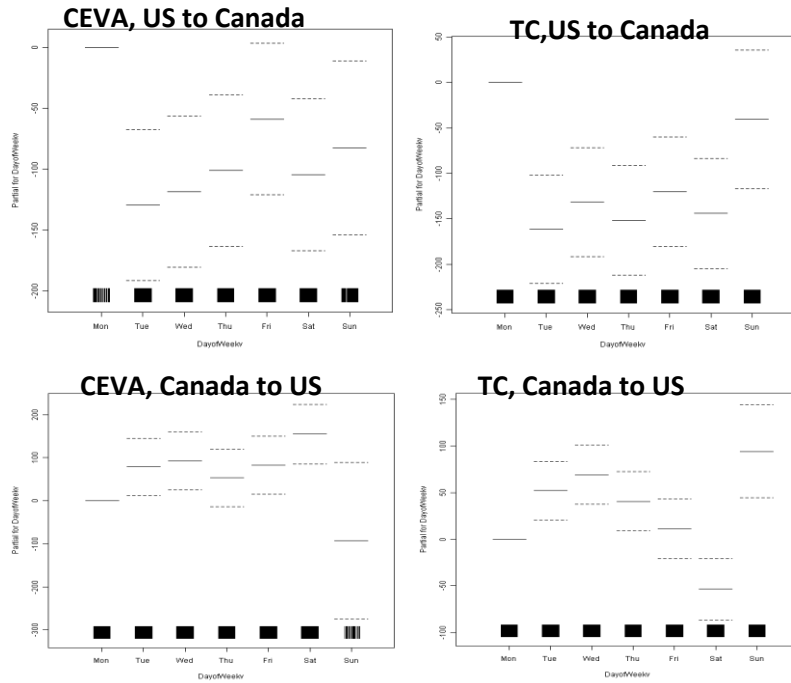


(a) Ambassador Bridge

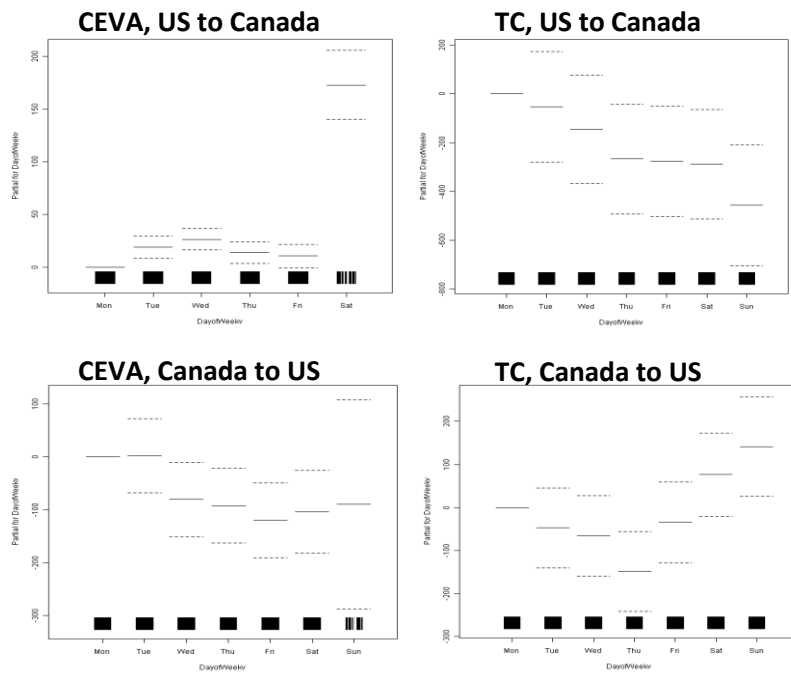


(b) Blue Water Bridge

**Figure 3.4-6:** Crossing time trends based on the (partial) marginal effect on crossing times of the day-of-month variable estimated from CEVA and Transport Canada data for both bridges and directions

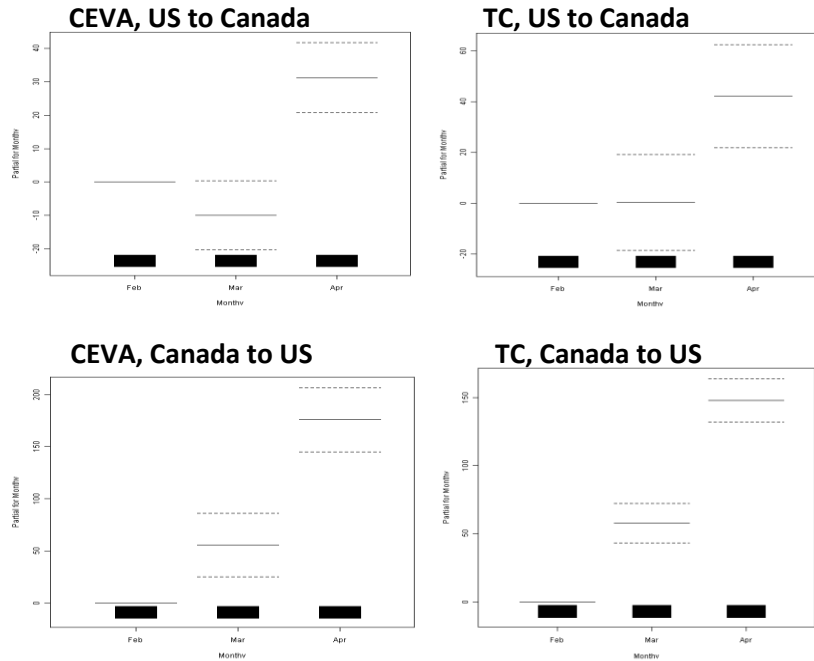


(a) Ambassador Bridge

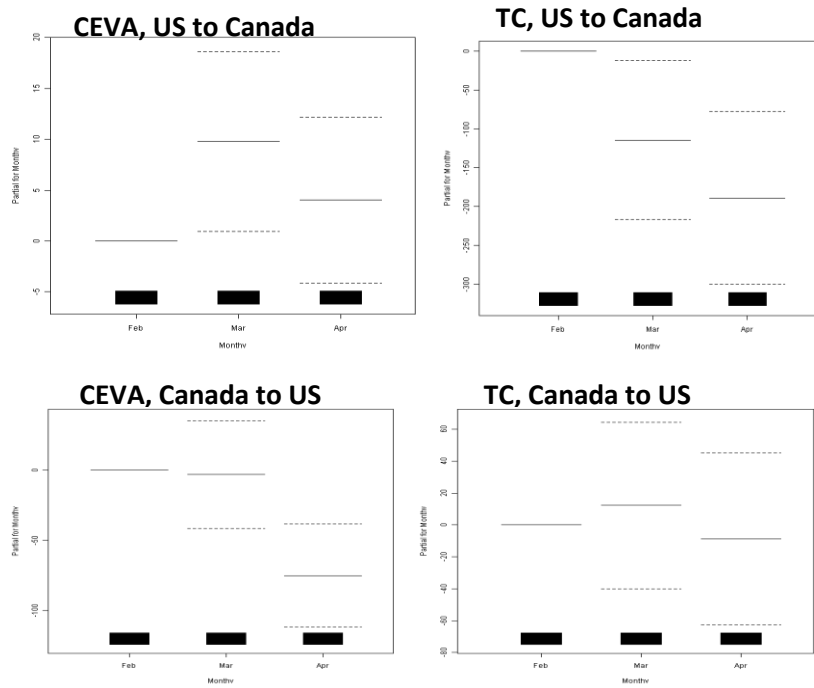


(b) Blue Water Bridge

**Figure 3.4-7:** Crossing time trends based on the partial (marginal) effect of the day-of-week variable on crossing times estimated from CEVA and Transport Canada data for both bridges and directions



(a) Ambassador Bridge



(b) Blue Water Bridge

**Figure 3.4-8:** Crossing time trends based on the partial (marginal) effect of month-of-year variable on crossing times estimated from CEVA and Transport Canada data for both bridges and directions

The shapes of the corresponding curves indicate similarities between the CEVA-derived and TC-derived time-of-day patterns for Canada-to-U.S. traffic at the Blue Water Bridge crossing site, day-of-month patterns for both directions of traffic at the Ambassador Bridge crossing site and for the Canada-to-U.S. traffic at the Blue Water Bridge crossing site, day-of-week patterns (for weekdays, since we had little CEVA data on weekends) for U.S.-to-Canada traffic at the Blue Water Bridge crossing site, and for monthly patterns for both directions of traffic at both crossing sites.

Although, the other comparisons showed little similarity between the CEVA and TC patterns, we were surprised at the degree of similarities in the two data sets for so many comparisons, given the difference in the types of trucks seen in the two distributions. Further comparisons of the two data sets are recommended for the future, with a goal of determining how the two sets could complement each other to provide a more complete picture of crossing and activity time patterns at the two sites.

## Section 4. Airborne Data Collection and Results

### 4.1 Approach and Methodology

In contrast to the geo-fence approach presented in Section 2, we also investigated a second approach to collect data remotely to analyze truck activity times at border crossings. This second method uses airborne data collection, supplemented by more traditional ground data, to track truck movements in and around international border crossings. We investigated this approach at the border between Nogales, Arizona and Nogales, Sonora, along the US-Mexico border. As mentioned in Section 2, the geo-fence approach to estimating activity times at a border crossing requires access to data provided by a fleet of trucks that regularly traverse the border. The airborne data collection method discussed in this section does not require accessibility to such data.

In this approach aerial photography is utilized to capture truck movements. Our empirical study was conducted at the Mariposa port-of-entry (POE). We were interested in an area beginning just a few miles before and after the Mariposa Port-of-Entry (POE), as well as specific movements within the port. We used a helicopter to obtain the aerial photography because a helicopter allows low-speed motion and hovering over points of interest. A camera platform and a computer with significant memory to store camera images were attached to the helicopter. This configuration allowed us to capture and store significant quantities of digital imagery with multiple frames per second from these locations.

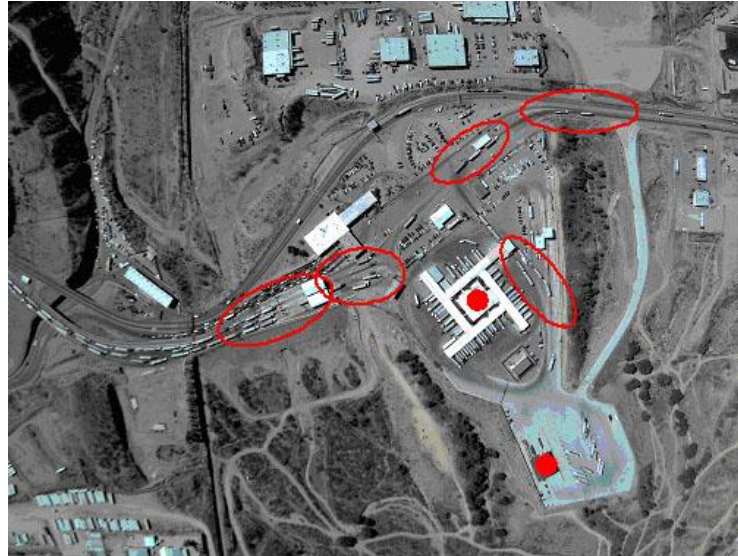
Two different camera platforms were used. In one airborne data collection effort, we used a commercially-available high-resolution camera that obtained imagery containing approximately 5 megapixels at a rate of 15 images per second. The imagery was transferred from the camera to the computer hard drive for later processing. In this case, we manually analyzed the imagery to produce the following data:

- the number of vehicles arriving to various stations, approaching and within the POE
- the number of vehicles in queue at these stations
- the time spent by vehicles as they were being inspected at these stations; and
- the routing of the vehicles to different stations within the POE

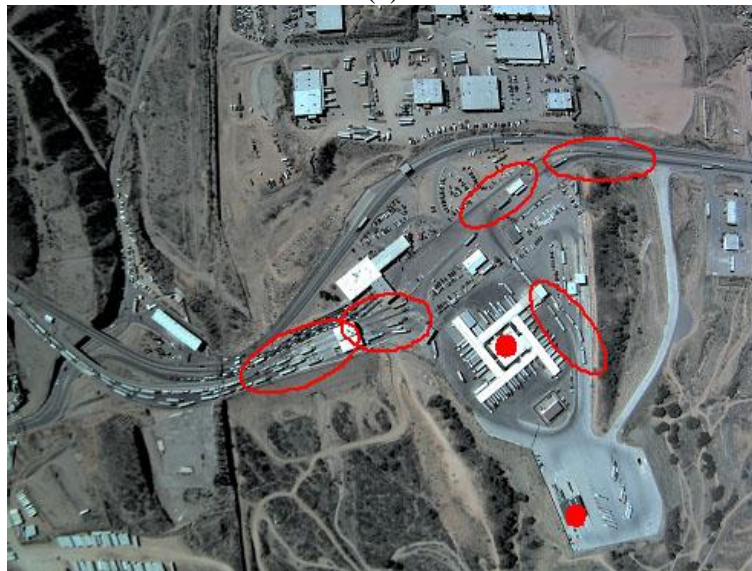
An example of the imagery is shown in Figure 4.1-1 to illustrate the data analysis approach. Figure 4.1-1a shows one image taken over the Mariposa POE at a specific reference time, and Figure 4.1-1b shows a similar image taken exactly 15 seconds later. The red ovals in the image indicate the locations of queues and vehicle movements that were recorded; these locations experienced frequent truck movements, with arrivals and departures occurring at a frequency of seconds up to a few minutes. The red dots on two of the larger buildings indicate inspection stations where truck movements were more infrequent, due to the duration of the inspection times. In these cases, only the number of vehicles in service (or in queue) could be recorded.

With this platform, we collected data on four separate flights over the Mariposa POE in Nogales, AZ. These flights were conducted in the mornings and afternoons on each of February 27 and 28, 2008. In each case, the helicopter traveled in and around the POE for approximately 1.5-2 hours. The specific dates and times were chosen to correspond directly with a separate study that was

also examining commercial vehicle movements around the Mariposa POE. That study used ground data collection methods, including: (1) video camera collection of license plate numbers for trucks, at multiple locations on the Mexican and on the US side, before and after traveling through the POE; and (2) counts of truck movements entering and leaving the POE.



(a)



(b)

**Figure 4.1-1:** Example airborne imagery. Image (a) is taken 15 seconds before image (b). Red ovals indicate queue and truck movement locations; red dots indicate queue locations only

The synchronous ground and airborne data collection provided an opportunity to enhance each data source significantly. The license plate data and the truck counts allowed a temporally continuous record of truck movements on these two days, but no direct observation of truck movements within the POE was possible on the ground. The airborne imagery, in contrast, allowed a limited temporal record of truck movements, generally with a maximum of 5-10

contiguous minutes every half hour during the flights. The airborne data were thus collected over much shorter durations than were the related ground-based data collection; nonetheless, specific truck movements and activities within the POE could be recorded. Combined, the two data collection efforts significantly improve the quality of data for this border crossing.

In our second airborne data collection effort, we used the ANTAR platform developed by the German Aerospace Center, Deutsches Zentrum für Luft- und Raumfahrt (DLR). This platform included: (1) a high-resolution visual imagery camera that captures imagery of approximately 4 megapixels per image at 3-5 images per second; (2) a high-resolution infrared camera, capturing synchronous images with the visual camera; (3) a differentially-corrected GPS unit; and, (4) an inertial measurement unit (IMU) to capture the orientation of the helicopter and the camera platform. The ANTAR platform is illustrated in Figure 4.1-2. The ANTAR system was used to collect imagery from the Mariposa POE on December 12, 2008.

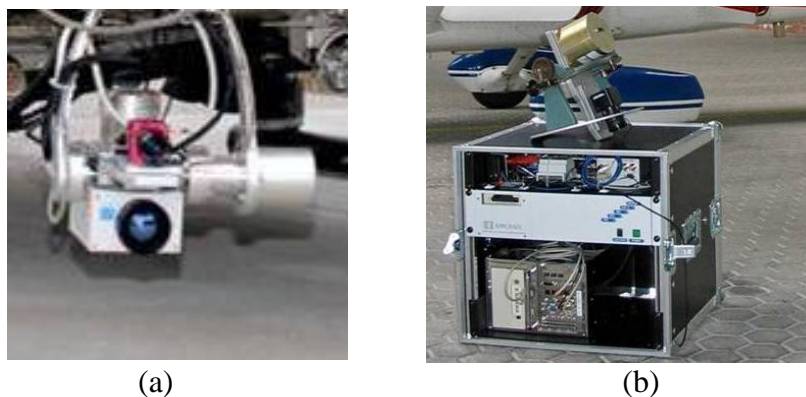


**Figure 4.1-2:** The ANTAR platform. (a) the camera system with GPS and IMU; (b) the computer and communications infrastructure

The ANTAR system also includes a computer with a digital roadway database that provides a reference roadway system for the analysis and allows the platform to automatically register the imagery to geographic coordinates. Because the imagery included the latitude, longitude, elevation, and orientation of the camera, the roadway database could be used to geo-locate a vehicle found in the image onto the reference roadway system. In this way, the exact real-world coordinates of a vehicle in a given image could be identified. By comparing vehicle coordinates between images separated by a known period of time, the speed of the vehicle can also be determined.

The DLR also provided a license to use two software tools that they created to analyze the ANTAR imagery. These include *TrafficFinder*, a software tool to automatically detect and record vehicle speeds and trajectories from the visual imagery, and *ClickTool*, a software tool that has similar features, but allows the user to manually specify the vehicles to be tracked in the imagery. The capabilities of ANTAR, *TrafficFinder* and *ClickTool* are shown in Figure 4.1-3. The imagery has been automatically georeferenced, in that the coordinates of all points in the image have been tied directly to coordinates on the earth. For this reason, the orientation of the images has been

adjusted. In the ClickTool image, one may also note small markers in the image. The markers indicate vehicles that have been tracked across successive images.

(a) from TrafficFinder

(b) from ClickTool

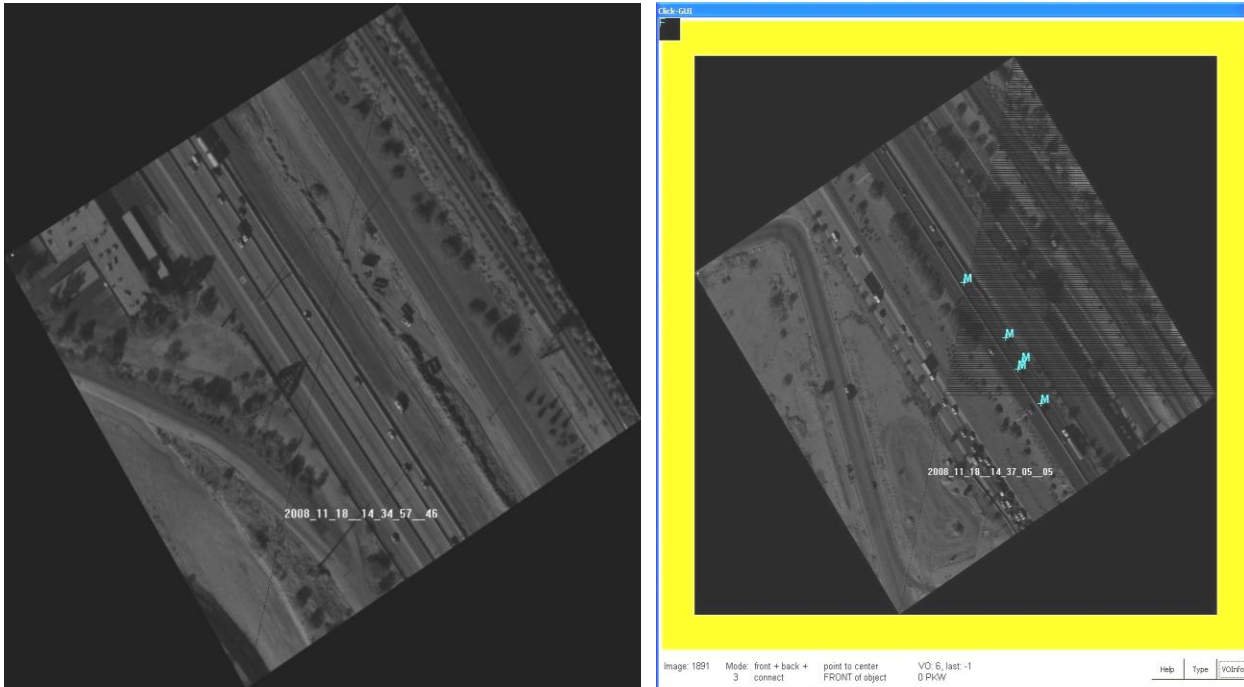


**Figure 4.1-3:** Registered imagery from the DLR’s ANTAR

For the analysis of the Mariposa POE, we did not use the advanced vehicle tracking features of the TrafficFinder and ClickTool software. Rather, we conducted a manual analysis of these images, again gathering data on the number of vehicles approaching each POE station, the number of vehicles in queue, the time spent in inspection for each vehicle, and the routing of vehicles between different stations within the POE.

## 4.2 Empirical Setting

The Mariposa Port-of-Entry (POE) facility, located in Nogales, Arizona is a critical crossing for freight flows into the mid-western and western U.S from Mexico. The port of Nogales handles truck movements across the border as well as the transfer of shipments between Mexican and US trucks. Nogales is the designated port of entry for the CANAMEX (Canada-America-Mexico) freight corridor in the western U.S. In 2009, Mariposa handled 276,877 trucks, and managed truck imports of \$6.6 billion in freight into the U.S. Mariposa ranks 42<sup>nd</sup> among ports in the nation in terms of the total value of imports and exports of freight and is the largest port (among land and air) in Arizona.

Figure 4.2-1 shows the location of the Mariposa POE within Arizona. A more detailed map of the local area is shown in Figure 4.2-2. The Mariposa POE is located west of the city of Nogales, and trucks accessing Mariposa into and out of Mexico must travel a designated access road in Sonora, Mexico.



**Figure 4.2-1:** Geographic location of the Mariposa POE in Arizona

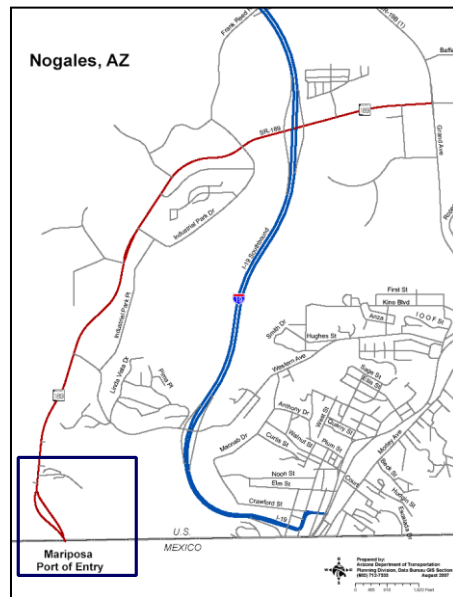


**Figure 4.2-2:** Geographic location of the Mariposa POE with respect to the City of Nogales, AZ

The Mariposa POE processes both non-commercial and commercial vehicles and allows both classes of vehicles to enter the POE from 8 AM to 7 PM on weekdays and allows commercial vehicles to enter from 8 AM to 6 PM on Saturdays. The POE remains open until the last vehicle that entered the port is processed. . In this study, we were only concerned with the processing of commercial vehicles entering the US from Mexico.



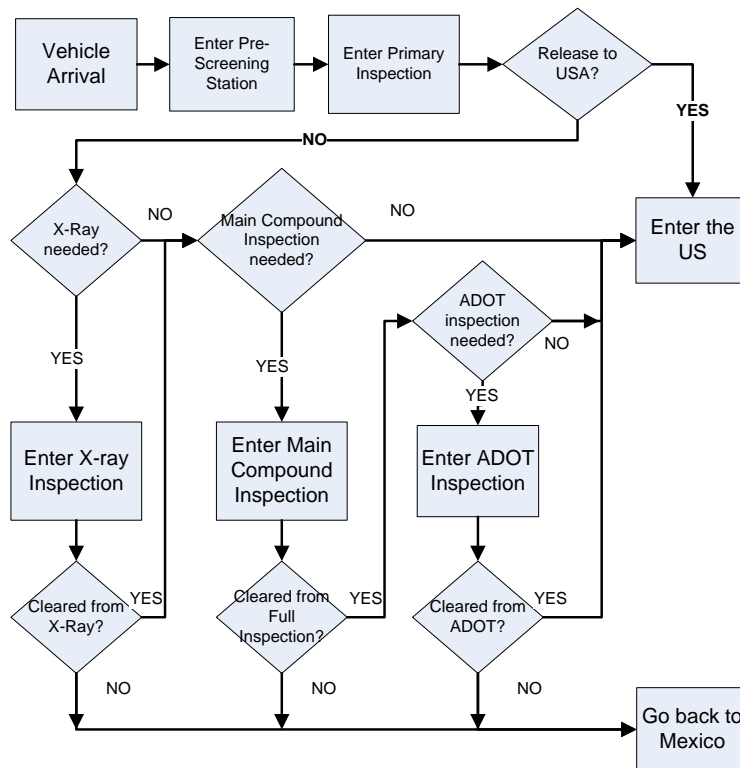
**Figure 4.2-3:** Points of inspection for commercial traffic at Mariposa POE 1: Pre-screening stations; 2: Primary inspection; 3: Secondary inspection; 4: X-ray inspection; 5: Arizona Dept. of Transportation (ADOT) inspection; 6: Final exit and weight check station

Figure 4.2-3 illustrates the various points of inspection at the facility. For the commercial inbound lanes, vehicles enter the facility through the pre-screening stations, where a first assessment of vehicles and their documentation is performed. There are four of these stations, but not all are always open. One of these four stations is a “FAST” lane, which processes vehicles with pre-approved documentation (named for the “Free and Secure Trade” Program, run by the US Customs and Border Protection). At the pre-screening stations, a first assessment on the documentation of the vehicles is performed. Before each truck arrives at the POE, a document from the Mexico inspection stations is sent to the POE in the US containing information about each specific vehicle and the products it carries. This information is then verified at the pre-screening stations once the vehicles arrive. One of the ways to verify this information is by weighing the vehicles (a “weigh-in motion” inspection). A safety inspection, as well as a drug screening inspection, is also performed. If trucks fail these latter tests, they will be directed to the ADOT lot for verification.

From the pre-screening inspection, all vehicles proceed to one of the four “superbooths” at the primary stations (primary inspection), where a more thorough inspection is performed. Vehicles can then take different routes. They either proceed directly into the US or enter one of three main inspection facilities: the secondary, the X-ray, or the ADOT inspection stations. Trucks can be inspected at one, two or all of these three stations, in sequences that may vary depending on the vehicle and the merchandise it carries. At the secondary station, trucks undergo two main types of inspections: a full inspection, in which the entire load in the truck is inspected, or a regular inspection through which samples of the truckloads are analyzed. Trucks may also be submitted to a hazardous materials and weapons inspection.

The X-ray inspection contains three booths. At the primary inspection, it is determined whether a truck will need the X-ray inspection or not. At the ADOT compound, the ADOT’s Motor Vehicle Division (MVD) safety inspection and other federal inspections are conducted. Vehicles may also need a revision of their documentation, which can be done at various points in the facility.

Thus, there is no unique path of vehicles through the facility, since exceptions may occur and sequences may vary. For that reason, based on information gathered during a visit to the facility in September 2007 and based on previous studies performed at Mariposa POE (*Esmer, 2009*), some assumptions were made in modeling the facility. Figure 4.2-4 summarizes the process flow diagram of the facility. The figure is in line with a previous study conducted at the facility (*Esmer, 2009*).



**Figure 4.2-4: Mariposa POE Process Flow Diagram**

## 4.3 Selected Results

### 4.3.1 Analysis of License Plate Data

An analysis of the ground-based data allows us to develop a preliminary sense of the operations of the Mariposa POE, even without specific knowledge of the detailed service information for each inspection location within the POE. For this reason, our first step was to analyze license plate data to gain this perspective. Later, this perspective can be used to provide some validation of the airborne data collection at the Mariposa POE.

License plate data for trucks approaching the Mariposa POE from Sonora and exiting the POE to the US were collected for two days in February 2008 from video cameras positioned on both sides of the border. The imagery allowed us to identify a total of 287 trucks that were observed by both the Mexican-based and US-based cameras.

Summary statistics for the total travel time (which includes the inspection delays at the POE) are shown in Table 4.3.1-1. A histogram of the travel time distribution is shown in Figure 4.3.1-1. From Table 4.3.1-1, one may note that the average traversal time of vehicles on the two days of data collection is 58.5 minutes. However, the median crossing time is significantly shorter, at just under 36 minutes. In Table 4.3.1-1, quartiles of this distribution are also given. The quartiles suggest that the overall distribution of travel times is heavily skewed. The high concentration of short travel times – about 50% of the travel times are under 36 minutes – indicates trucks that move through the POE fairly quickly. However, the very long tail indicates that there are some very long travel times through the POE, accounting for the high average travel time and the very large standard deviation of travel times (58 min). This skewed distribution of travel times is very apparent in Figure 4.3.1-1.

**Table 4.3.1-1:** Summary statistics obtained from license plate data through the Mariposa POE

Average Travel Time	58.5 min
Standard Deviation	58.3 min
Minimum	6.2 min
Maximum	430.9 min
25 <sup>th</sup> percentile	19.5 min
50 <sup>th</sup> percentile	35.8 min
75 <sup>th</sup> percentile	76.7 min

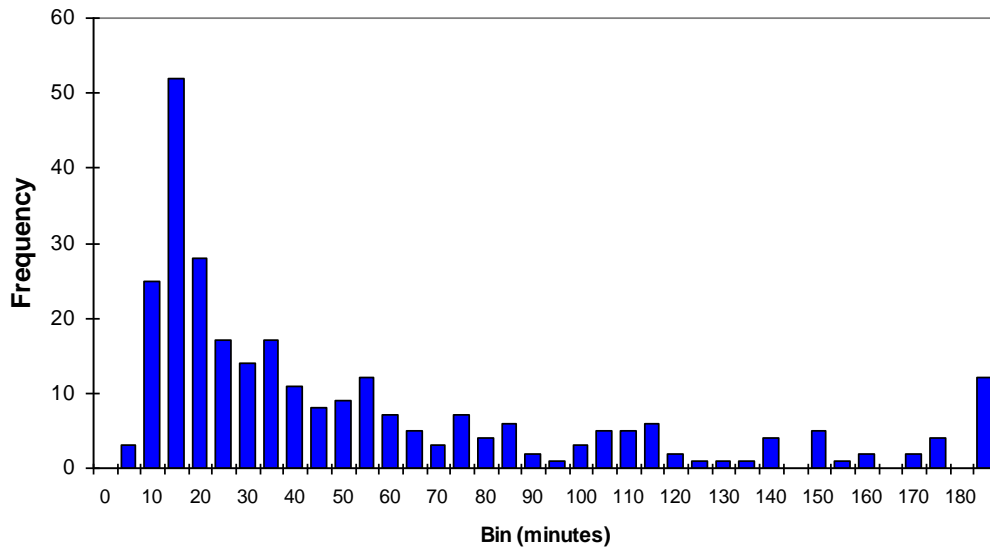


**Figure 4.3.1-1:** Distribution of travel times through the Mariposa POE from license plate data

A more careful examination of Figure 4.3.1-1 suggests that there may be a few factors affecting this distribution of travel times. Certainly, the path a truck takes *within* the POE affects the observed total travel time. For example, the initial spike in travel times between 10-20 minutes may simply reflect vehicles that experience primary inspection and then are permitted to exit directly to the US. Alternately, other smaller “spikes” in the distribution may reflect vehicles that are required to travel through X-ray, or through secondary inspection, or through the ADOT inspection.

To examine these potential factors more carefully, we considered the possible paths of trucks through the POE. We posited that the distribution shown in Figure 4.3.1-1 actually reflects a composite distribution that is composed of the sum of simple distributions for each path. That is, each path has its own statistical distribution of the time through the POE. Then, the weighted combination of the individual path distributions yields the observed composite distribution in Figure 4.3.1.1. “Weights” associated with each path distribution correspond to the probability that a truck actually follows that path through the POE.

The logic associated with the Mariposa POE can be represented as a network for which vehicles enter and ultimately exit the POE for the US. In between, a vehicle can be routed through some sequence of inspections, as indicated in Figure 4.2.4. The inspection sequences can be represented by the network shown in Figure 4.3.1-2.

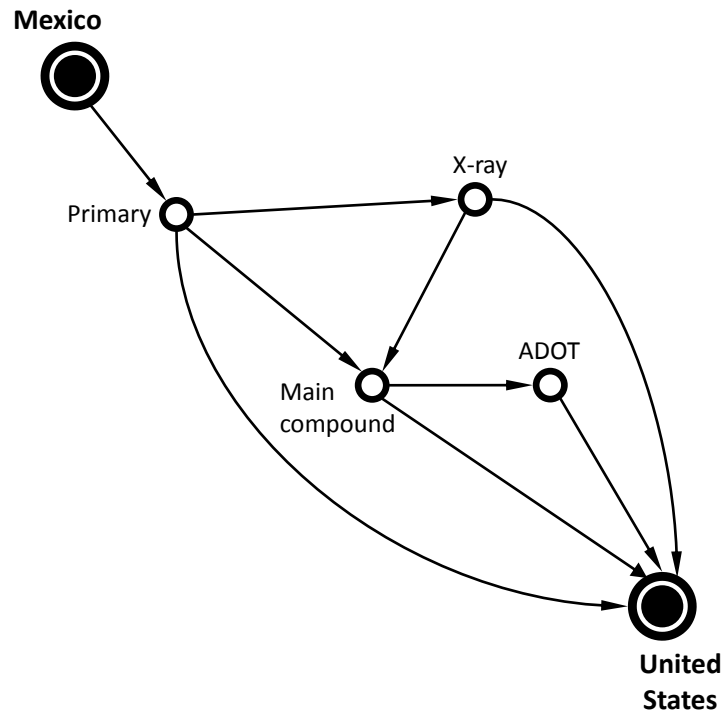


**Figure 4.3.1-2:** Network representation of inspection sequences within the Mariposa POE

Using the POE travel time data from the license plate observations, we determined the travel time distributions by path (inspection sequence) and the probabilities of a truck being routed along the different paths.

The probability density function for travel times given in the composite as  $f(t)$  can be identified as the sum of the weighted probability density functions for the travel times on the different paths. Let  $g$  represent the total number of possible paths through the POE; then, the distribution  $f(t)$  is given as:

$$f(t) = \pi_1 \cdot f_1(t | \theta_1) + \pi_2 \cdot f_2(t | \theta_2) + \dots + \pi_g \cdot f_g(t | \theta_g) \quad (4.3.1.1)$$

where  $\pi_i$  is the probability that a truck is assigned to path  $i$ ,  $f_i(t|\theta_i)$  is the travel time distribution along path  $i$ , and  $\theta_i$  is the set of parameters associated with the probability distribution  $f_i(t|\theta_i)$ . The goal of this part of the research is to determine the values of the routing probabilities ( $\pi_i$  for each path  $i$ ) and the values of the parameters  $\theta_i$  associated with each path's probability distribution  $f_i(t|\theta_i)$ .

In our scenario, Figure 4.3.1-2 indicates that there are six different paths to get through the POE (i.e.,  $g = 6$ ). These are: (1) Primary to exit; (2) Primary to X-ray to exit; (3) Primary to main compound to exit; (4) Primary to X-ray to main compound to exit; (5) Primary to main compound to ADOT to exit; and, (6) Primary to X-ray to main compound to ADOT to exit. However, because some of these paths use common segments with other paths (e.g., two paths share the link connecting the main compound to the exit), the routing probabilities and the parameters of the composite distributions must be estimated carefully. Further details on the

theory and methods used in this analysis are described by Esmer (2009). What follows is a brief summary and the results.

To estimate the routing probabilities (the  $\pi$ 's) and the distribution parameters (the  $\theta$ 's), a common set of mixture methods was used. Figure 4.3.1-3 illustrates the steps to find a solution. The graphical analysis at the top involved determining the possible paths. Then, using the *composite* travel time distribution, we calculate statistical parameters for individual stations.

There are two statistical techniques that are used to decompose the waiting time distributions of the paths from the total time distribution. The expectation-maximization (EM) algorithm provides a point estimate of the parameters (the  $\pi$ 's and the  $\theta$ 's) by maximizing the likelihood (*i.e.*, using maximum likelihood estimation). The Markov Chain – Monte Carlo (MCMC) technique provides not only point estimates, but full distributions for the unknown parameters. When compared, the EM algorithm requires more prior information about the parameter values than does the MCMC algorithm.

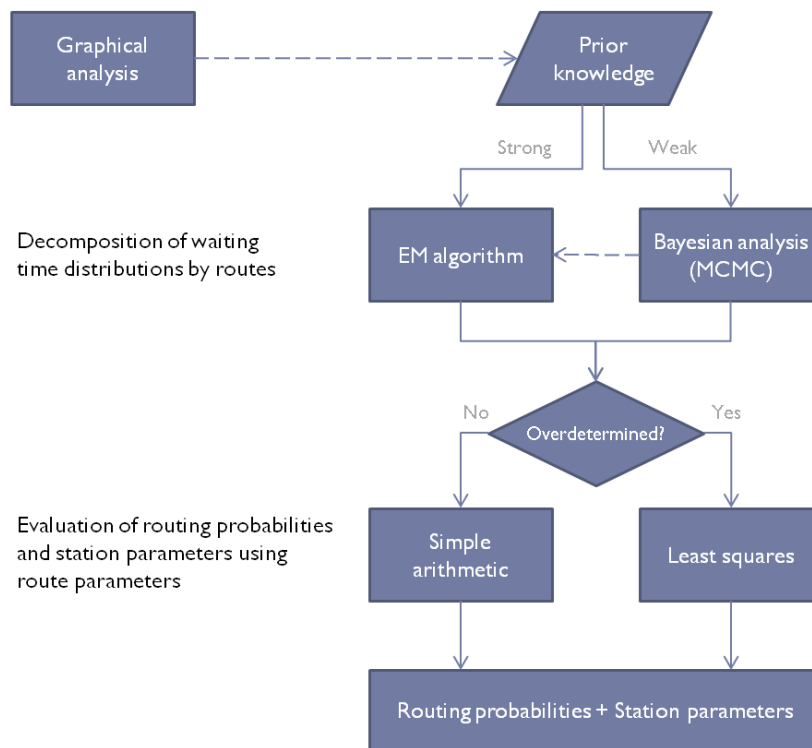


**Figure 4.3.1-3:** An overview of the solution method

Once the distributions for the paths are obtained, the parameters for the individual stations in the POE can also be evaluated. If the number of paths is equal to the number of unknown parameters, then the system can be solved by linear algebra. If the number of paths is greater than the number of unknowns, we can use the method of least squares to obtain the parameters for each station.

For this analysis, we assumed that the travel-time distribution of each path through the POE could be modeled using a gamma distribution and applied maximum likelihood estimation to estimate the means and standard deviations of the total time at each station in the POE.. These

means and standard deviations are given in Table 4.3.1-2. Figure 4.3.1-4 depicts the estimated individual travel time distributions associated with each path through the POE and the resulting estimated composite travel time distribution. (Note that the travel times through the POE are negligible compared with the waiting and inspection times; as a result, these travel times are not explicitly considered.) Probabilities of proceeding to the next station, conditional on having finished processing at a station, are overlaid on the original network for the POE in Figure 4.3.1-5.

**Table 4.3.1-2:** Estimated mean and standard deviations of waiting time (service time + queuing time) distributions for the inspection stations produced from Maximum Likelihood Estimation

Station	Mean (min)	Standard Deviation (min)
1 – Primary inspection	18.64	8.34
2 – X-ray	30.01	10.95
3 – Main compound inspection	62.31	18.65
4 – ADOT inspection	105.8	33.31

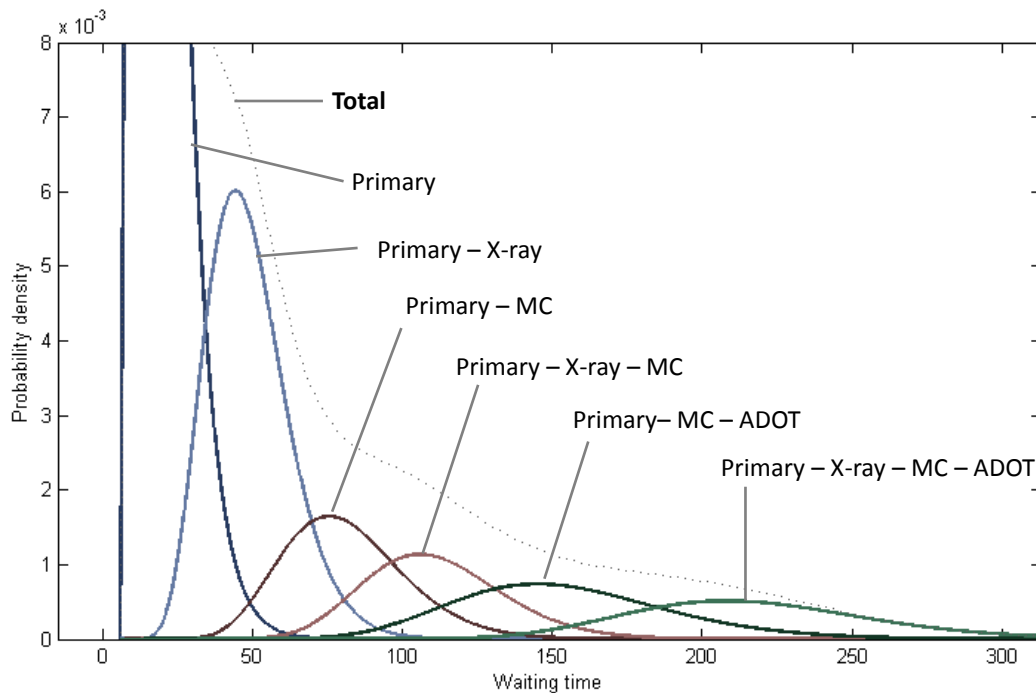


**Figure 4.3.1-4:** Estimated composite and individual path distributions

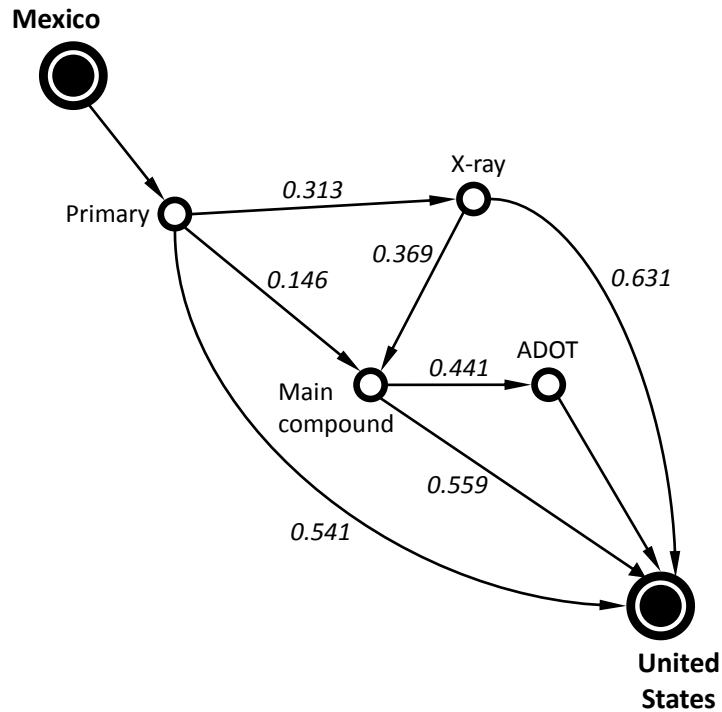


**Figure 4.3.1-5:** Estimated routing probabilities produced from Maximum Likelihood Estimation

Estimates of waiting time distributions and routing probabilities were also produced using the MCMC algorithm. These results are shown in Table 4.3.1-3 and Figure 4.3.16, respectively.

**Table 4.3.1-3:** Estimated means and standard deviations of waiting time (service time + queuing time) distributions for the inspection stations produced from the MCMC method

Station	Mean (min)	Standard Deviation (min)
1 – Primary inspection	16.28	7.19
2 – X-ray	32.89	23.08
3 – Main compound inspection	68.35	36.49
4 – ADOT inspection	123.43	32.55

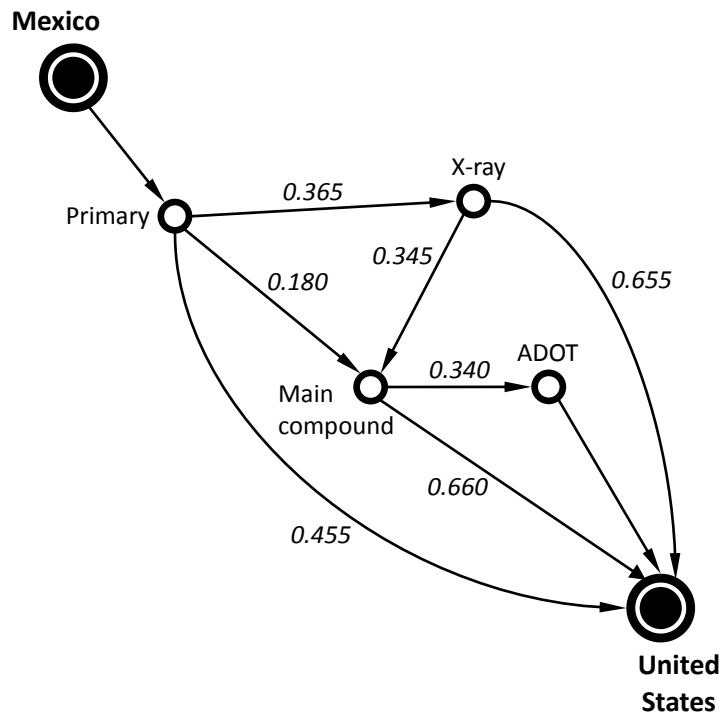


**Figure 4.3.1-6:** Estimated routing probabilities produced from MCMC

By comparing the results in Tables 4.3.1-2 and 4.3.1-3 and those in Figures 4.3.1-5 and 4.3.1-6, one notices that the Expectation Maximization (EM) and The Markov Chain – Monte Carlo (MCMC) methods produced similar results. However, as mentioned before, the MCMC technique also provides distributions for the parameters, whereas EM provides only the expected value of each parameter. Further analyses and results are given in Esmer (2009).

#### 4.3.2 Analysis of U.S. Customs and Border Protection Waiting Time Data

As discussed in Section 3, we downloaded estimates of border waiting times posted by the U.S. Customs and Border Protection (US Customs and Border Protection, 2010). These CBP postings are usually updated every hour and include the maximum number of lanes available for passenger and commercial vehicles, the number of lanes open, and the estimated delays for vehicles entering the U.S. for “standard” commercial and passenger vehicles and for commercial and passenger vehicles that have special pre-clearance (NEXUS-qualified passenger vehicles, and FAST-qualified commercial vehicles).

The Mariposa POE has infrastructure for three “standard” lanes and one FAST-capable lane entering the primary inspection. From our downloaded data, we calculated the average numbers of standard and FAST lanes open by weekday from February 2008 to October 2009. We plot these averages in Figure 4.3.2-1. As one can see, the average number of lanes open for “standard” trucks is about 1.8 on normal weekdays and drops to about 1.6 on Saturdays and 1 on Sundays.

These results suggest that the actual lanes in use at any time can be less than the full 3 lanes for standard trucks. However, this “average” can be a bit misleading: there are significant seasonal variations in the number of trucks approaching the POE. The number of trucks in the peak produce months of January-April is much higher than in late summer and early fall. The number of lanes would be expected to drop in March-October period contained in our data. In addition, the drop-off in lane availability on Saturdays and Sundays can be attributed to the lower truck flow on the typical weekend; these lower flows are due in part to the limited hours of operation of the POE on Saturdays and Sundays. Figure 4.3.2-1 indicates that the FAST lane is always open to trucks, on all days of the week, but with the same limitations on hours of operation.

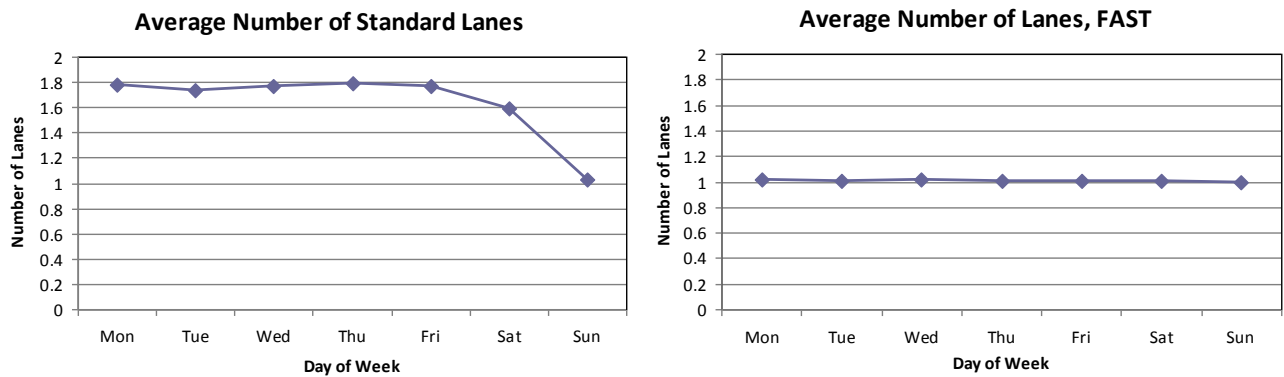


**Figure 4.3.2-1:** Average number of open lanes by day of week at the Mariposa Port of Entry

A similar analysis could be made of the average delay for the different facilities by day of week. Figure 4.3.2-2 provides average delays for these same lane groups. The average delay on weekdays averages 25-28 minutes, with a slightly higher average (over 31 min) on Mondays. Again, these averages can be misleading; it is not uncommon to have much higher delays during the peak produce season in the early spring, but much lower delays at other times of the year. In contrast, the FAST lanes rarely experience delay, with delays averaging less than 1 minute on most days, and only about 4 minutes on Sundays. There are clear advantages in reductions in delay for trucks to participate in the FAST program.

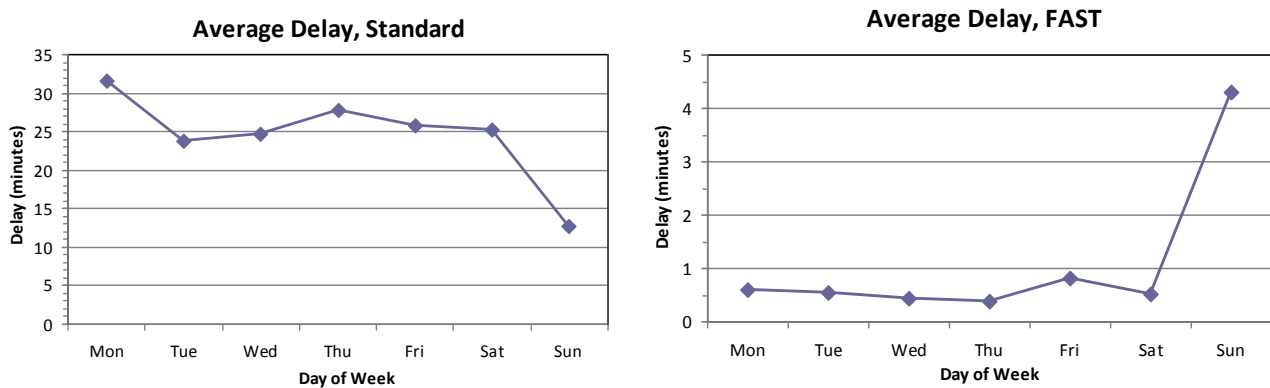


**Figure 4.3.2-2:** Average truck delay by day of week at the Mariposa Port of Entry

Figure 4.3.2-3 plots the average “delay” by hour of day for the average weekday. We assume that this delay is comprised of the time that a vehicle enters the initial queue at the border crossing until the time it enters the initial (primary) inspection. The data in the figure indicate relatively small delays in the early morning hours, with significant increases in delay approaching the noon hour and continuing into the evening. This pattern is fairly consistent in different seasons: truck arrivals tend to experience much less delay in the mornings than in the afternoons.

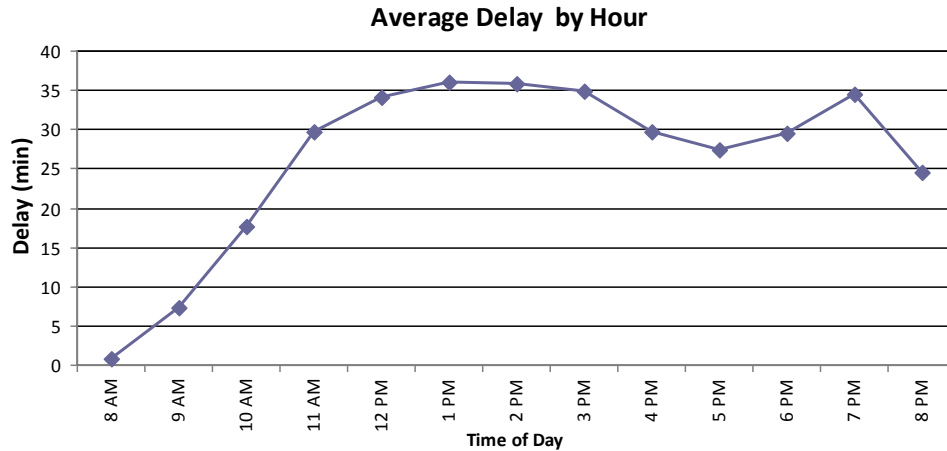


**Figure 4.3.2-3:** Average truck delay by time of day at the Mariposa Port of Entry

While one might be tempted to make a direct comparison of the values determined from the CBP data (Figure 4.3.2-3) to the values determined from the license plate data (Tables 4.3.1-1 and 4.3.1-2), this is not exactly a valid comparison. The license plate waiting time data reflect the records from license plates as the trucks approach the primary inspection. Many trucks may have queued well before their license plates are read. As a result, the average delays observed in Figure 4.3.2-3 would be expected to be, on average, longer than the average waiting time delays observed from the license plate study. This is observed in these data.

As discussed in Section 3, we do not have a good sense of how the CBP arrives at their estimates, and the CBP data are aggregated on an hourly basis and for all trucks through the POE. More disaggregate information underlying these aggregate waiting time estimates, describing the routing of trucks through the port of entry, and the specific delays and processing times associated with these routes through the POE, would be more useful for both estimating travel times, and represent the only data available for estimating routing through the POE. Airborne imagery is our primary data collection method to achieve this information, and is discussed in the next section.

### 4.3.3 Analysis of Airborne Imagery

Using the airborne imagery, we investigated the queuing behavior and service times within the Mariposa POE. For several of the queuing locations within the POE and the times at which the images were obtained, we calculated the cumulative number of vehicles that had arrived and the cumulative number of vehicles that had departed. Using a common technique for queuing

analysis (Mannering *et al.*, 2009), we estimated the average number of vehicles in the queue across the observation period and the average vehicle waiting time in the queue.

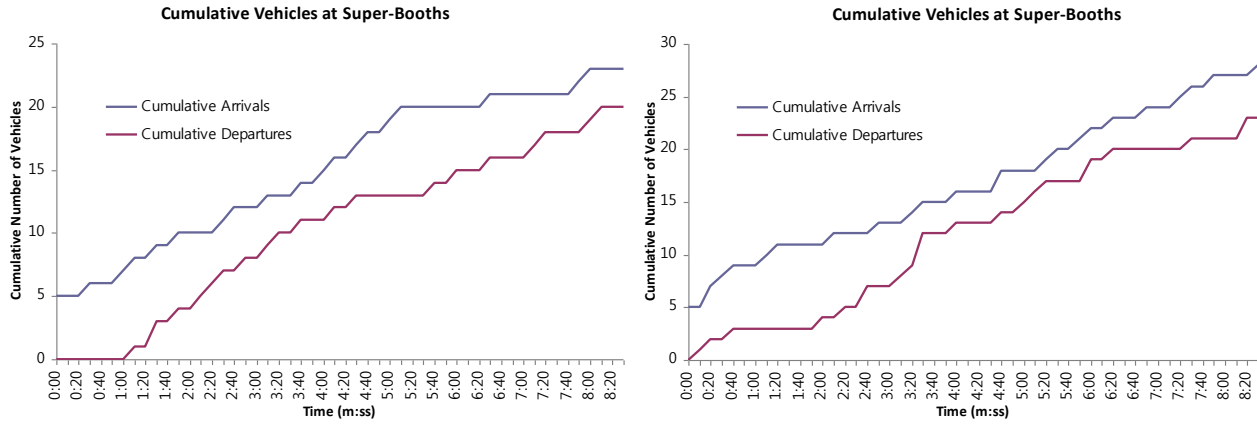


**Figure 4.3.3-1:** Sample cumulative curves for primary inspection (“superbooths”) during two different time periods on Feb. 28, 2008

Figure 4.3.3-1 shows the cumulative vehicle curves for the primary inspection sites at the Mariposa POE, measured on two different times on February 28, 2008. In these diagrams, the vertical distance between the cumulative arrival curve and the cumulative departure curve is the count of vehicles in the queue at the corresponding time, and the horizontal distance between curves is the waiting time in the queue for the corresponding vehicle. One can see in these cases that there is a fairly consistent queue of 2-8 vehicles. The variability in these values depends on variations in both the arrival rate to the queue, shown through changes in the slope of the cumulative arrival curves, and service times of vehicles, shown through changes in the slope of the cumulative departure curves. Similar cumulative vehicle curves are shown for the X-ray station in Figure 4.3.3-2 and for the exit station in Figure 4.3.3-3.

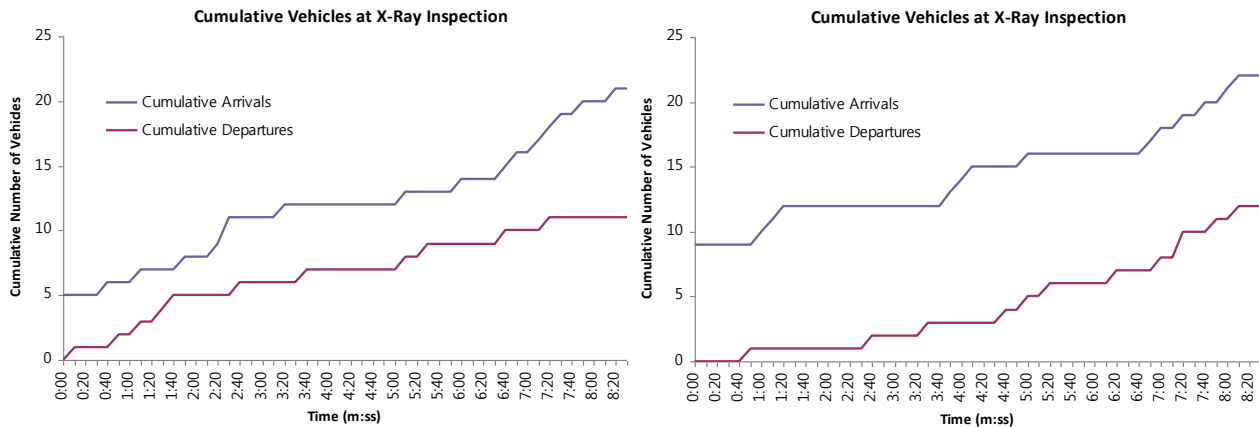


**Figure 4.3.3-2:** Sample cumulative curves for X-ray inspection during two different time periods on Feb. 28, 2008

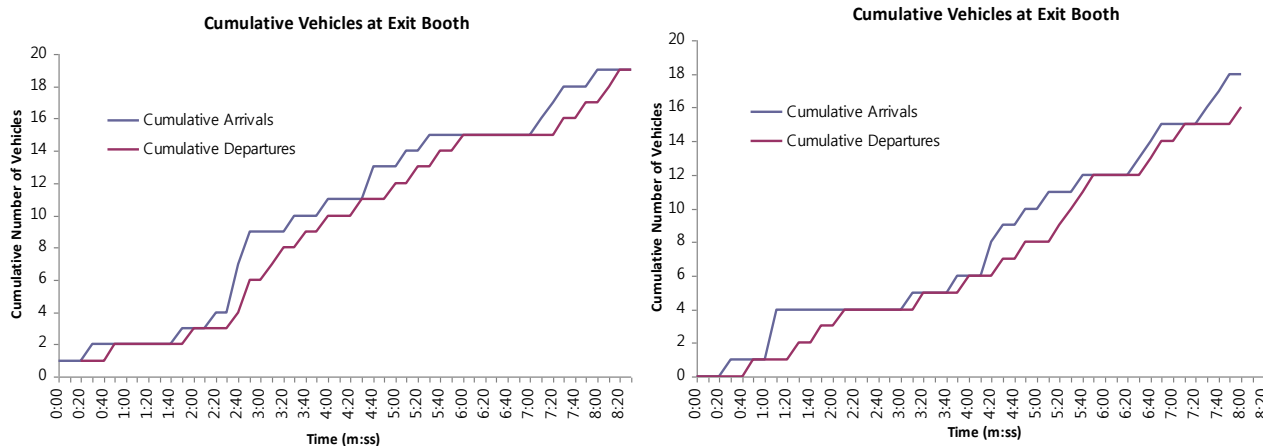


**Figure 4.3.3.3:** Sample cumulative curves for exit / weight check during two different time periods on Feb. 28, 2008

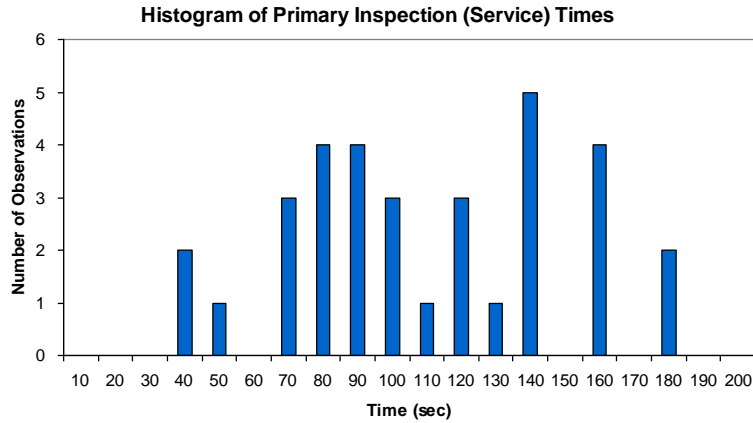
Table 4.3.3-1 provides summary statistics for the average truck arrival rate, average truck waiting time, and average queue length at the primary inspection, X-ray inspection, and exit booth at the Mariposa POE. As is consistent with some of the routing, the arrival rate to the X-Ray inspection is lower than the rate to the main entrance (primary inspection) and to the exit booths. Curiously, given our sample of imagery, the arrival rates at primary inspection and at the exit booth are not equal; naturally, one might expect these to be equal in an equilibrium over a full day. Waiting times are longest for primary inspection and for the X-ray inspection, due to the longer processing times at these facilities when compared with processing times at the exit booth. Similarly, queue lengths are longer at these locations than at the exit booth.

**Table 4.3.3-1:** Selected queuing statistics from Mariposa POE

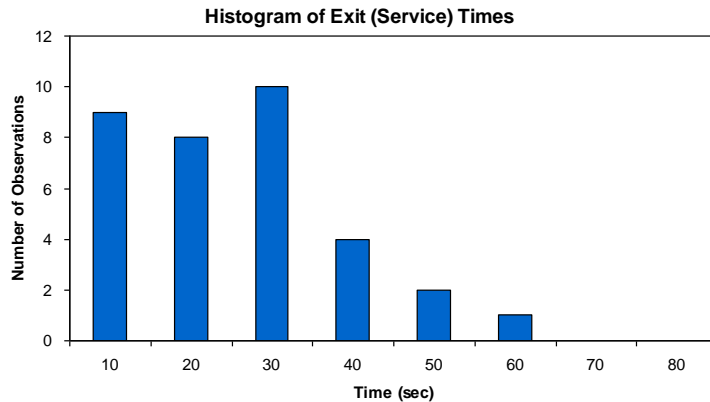
	Primary Inspection	X-Ray Inspection	Exit Booth
Average Arrival Rate (veh/min)	2.39	1.84	2.06
Average Waiting Time (sec)	125.9	231.7	28.1
Average Waiting Time (min)	2.10	3.86	0.47
Average Queue Length (veh)	5.01	7.11	0.97

Figure 4.3.3-4 shows a histogram of observed service times for primary inspection. In this case, the average service time is 110 seconds, and the standard deviation of the service times is 39 seconds. The distribution of service times for the X-Ray inspection only contains 9 observations, so illustrating its distribution is not very meaningful. The distribution has an average service time

of 248 seconds and a standard deviation of 103 seconds. The histogram of service times for the exit station is shown in Figure 4.3.3-5. The average service time at the exit station is 26 seconds and the standard deviation of the distribution is 13 seconds.



**Figure 4.3.3-4:** Histogram of observed service times, primary inspection (superbooths)



**Figure 4.3.3-5:** Histogram of observed service times, exit station

These data provide useful inputs to validate the estimated distributions for service times, conducted previously. Based strictly on a visual comparison, we believe the models estimated with the airborne imagery and validated using these manual observations from the airborne imagery show the value of combining air- and ground-based data collection. In this case study, we have shown that data collected from airborne platforms can provide good disaggregate data on the specific processes occurring within the POE, and we can estimate distributions of service times for various stations in the POE. These can be shown to match more extensive ground-based data, including license plate data and ground counts.

## Section 5. Modeling of Activity Times

The data obtained from the geo-fence based approach described in Section 2 and from the combined air- and ground-based study described in Section 4 could also be used to develop models of activity times at the border crossings. We investigated the development of both aggregate (macroscopic) and disaggregate (microsimulation) models. In the macroscopic models, we fit aggregate relationships between meaningful explanatory variables of activity times and the response in the activity time. In the disaggregate models, we developed microsimulation models of individual truck movements through the gateway facilities to determine the times the trucks incurred in the various activities.

### 5.1 Macroscopic Modeling

From the Michigan Department of Transportation (MDOT), we received hourly traffic volumes entering the U.S. at the Blue Water Bridge border crossing from 08/01/08 to 01/31/09. The data were received in hard copy format, with each day's hourly volumes on a single sheet. We scanned each of these sheets as a black and white PDF file at 600 dots per inch (dpi), then used the built-in Optical Character Recognition (OCR) software of Adobe Acrobat Pro version 9 to convert them to text tables. These text tables were imported into Excel and saved as spreadsheet files, which could then be used to calculate hourly traffic volume information of interest. We checked each file for OCR character recognition errors but found very few errors using the Acrobat OCR software. This process was used after an initial development period; we initially scanned the first month of data as multi-page tiff image files (also at 600 dpi), and then used Microsoft Office Document Imaging's OCR capability to create text files for each page. (This capability was available as a built-in module of Microsoft Office 2003.) That text could be saved into a text file and imported into an Excel spreadsheet. We found that the Acrobat Pro OCR software had fewer errors, though, and eventually processed all the data using that method.

As discussed in Section 3.1, we also downloaded the status of the open lanes from the U.S. Customs and Border Protection website (<http://apps.cbp.gov/bwt/>) from 10/07/08 to 06/10/09. In Figure 5.1-1 we present scatter plots of the excess times in the Canada-to-US geo-fences for individual trucks against the hourly volumes corresponding to the hour-of-day when the trips occurred. (The hour of a trip was determined as the hour in which the truck exited the *uspalazabridge* geo-fence, *i.e.*, when the truck arrived at primary customs inspection.) From the plots, it appears that the *usplazabridge* geo-fence is the geo-fence with the strongest response of excess time to traffic volume. As described in Section 2, the *usplazabridge* geo-fence delimits the roadway section where U.S.-bound vehicles queue upstream of primary customs inspection at the Blue Water Bridge site. The scatter plot shows a general relationship of increasing excess time with increasing hourly volume.

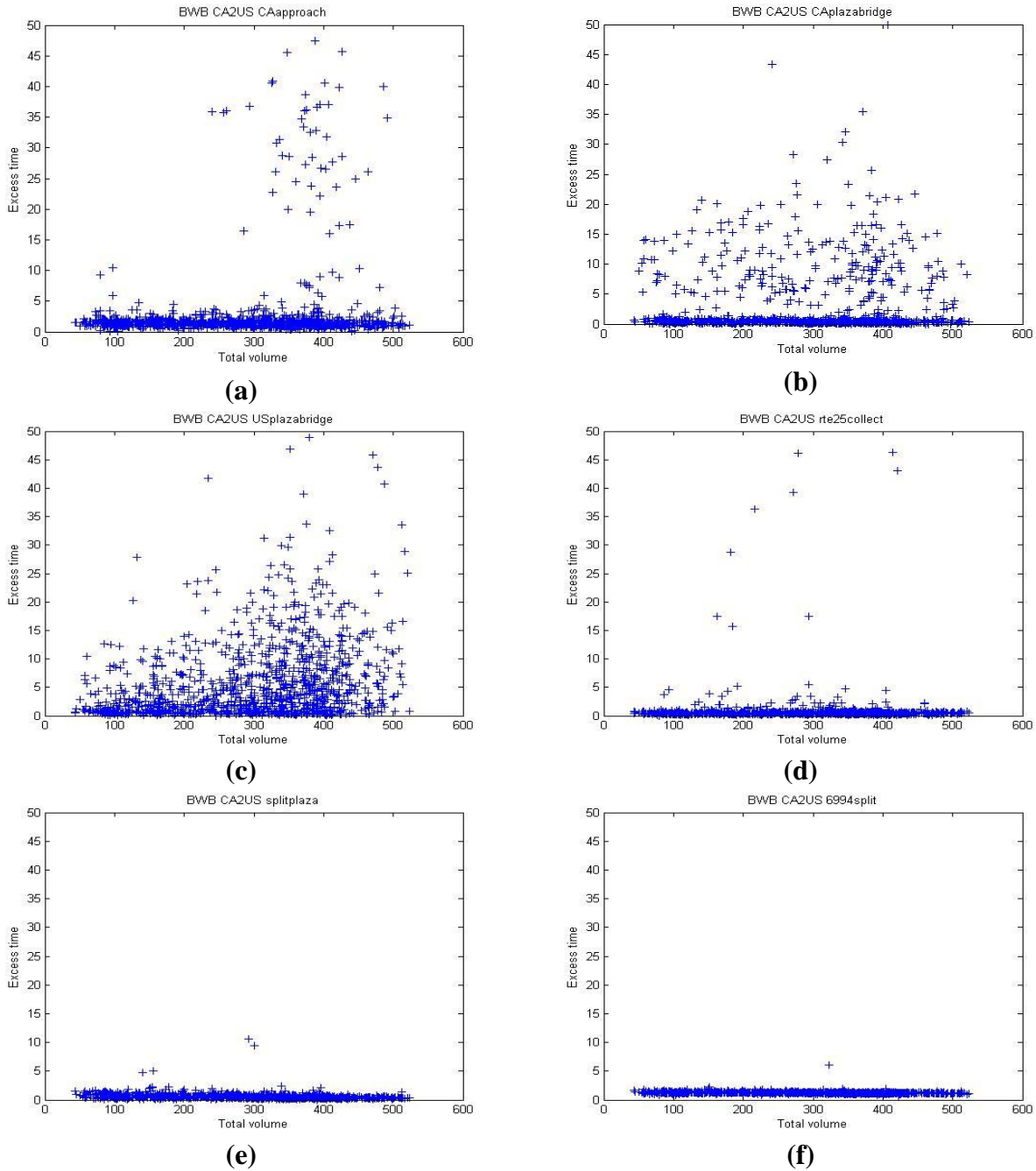


**Figure 5.1-1:** Excess times in geo-fences vs. hourly vehicle volume for Canada-to-U.S. geo-fences at Blue Water Bridge Crossing; (a) caapproach, (b) caplazabridge, (c) usplazabridge (d) rte25collect, (e) splitplaza, and (f) 6994split

To investigate the relationship between volume and excess time upstream of primary customs screening, we determined median hourly volume and median excess time and formed the two-way cross-classification table of the numbers of excess time-hourly volume pairs that fell in the following four paired categories: (*above median volume, above median excess time*), (*below median volume, above median excess time*), (*below median volume, below median excess time*),

(below median volume, above median excess time). The results appear in Table 5.1-1. Using a hypergeometric setup conditional on the specified marginals, it can be shown that the probability of observing as many or more observations in the (above median volume, above median excess time) category – which, in turn, uniquely determines the values in the other cells, since the median imposes that the marginal values be (approximately) equal – is on the order of  $10^{-6}$ . That is, there is strong evidence that higher hourly volumes are associated with higher excess times in the queuing area in that hour.

**Table 5.1-1:** Numbers of excess time-hourly volume pair observations for *usplazabridge* geo-fence, in Canada-to-US direction

		Total Volume		Marginal
		$\leq$ Median**	$>$ Median**	
Excess Time	$\leq$ Median*	265	150	415
	$>$ Median*	150	265	415
Marginal		415	415	830

\* Median Excess Time = 3.3063 [min], \*\* Median Volume = 307.5 [veh/hr]

We also wished to investigate the effects of the numbers of open lanes on the excess times in the queuing region. In Figure 5.1-2, we plot the empirical cumulative density functions (ECDFs) of the excess times when there were seven and five truck lanes in operation at the time that the truck whose excess time was recorded exited the *usplazabridge* geo-fence. The ecdf curves clearly indicate that there was less queuing excess time when there were seven lanes open than when there were five lanes open.

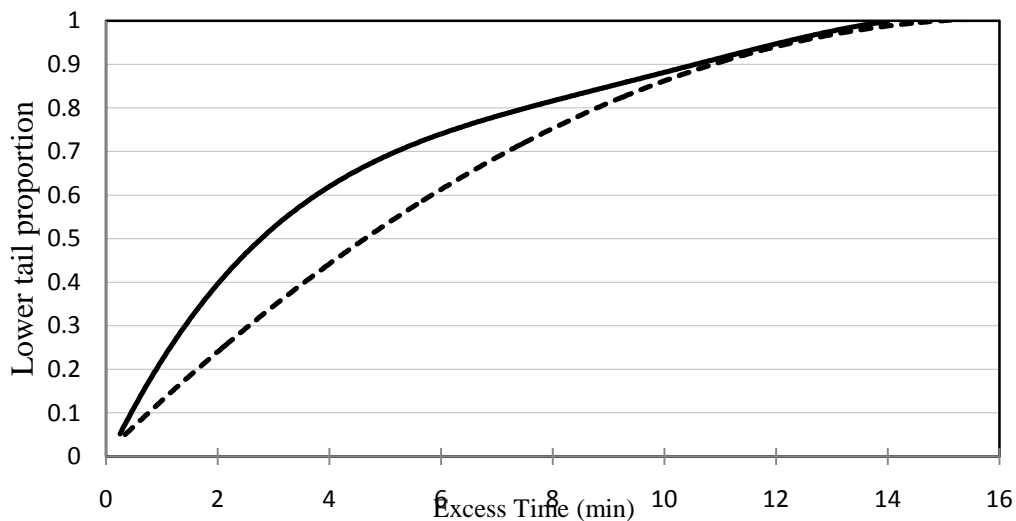


**Figure 5.1-2:** Empirical cumulative distribution functions of excess times in *usplazabridge* geo-fence when there were seven and five primary customs screening truck lanes open

In an attempt to quantify the effects of both the traffic volume and number of lanes open on the geo-fence derived excess queuing times, we fit various linear regression models and logistic regression (see. e.g., McCullagh and Nelder, 1989) models to the data.

The discretization of the response variable in the logistic regression model produced slightly, but not appreciably better results. We therefore present results of the logistic regression models to illustrate the approach and results. The models are of the form:

$$\Pr(t^{exc} > T^{thr}) = \exp(\beta_0 + \beta_1 X_1 + \beta_2 X_2 + \dots + \beta_K X_K) / [1 + \exp(\beta_0 + \beta_1 X_1 + \beta_2 X_2 + \dots + \beta_K X_K)] \quad (5.1.1)$$

where  $\Pr(t^{exc} > T^{thr})$  represents the probability that an excess time  $t^{exc}$  in the queuing geo-fence on a specific trip is greater than an exogenously chosen threshold time  $T^{thr}$ ;  $X_1, X_2, \dots, X_K$  are  $K$  independent (explanatory) variables associated with the trip that are believed to affect the value of the excess times; and  $\beta_0, \beta_1, \beta_2, \dots, \beta_K$  are coefficients of the model.

We used maximum likelihood estimation (see, e.g., Ben Akiva and Lerman, 1985) to fit several specifications of the general formulation in equation (5.1.1) for various values of  $T^{thr}$ . The best results are summarized in Table 5.1-2.

**Table 5.1-2:** Summary results of logistic regression models of excess times for various thresholds  $T^{thr}$  (t-statistics of coefficient estimates are placed in parentheses below the estimated coefficient value)

Variable	Estimated Coefficients (t-statistics) for Threshold Value $T^{thr}$ (min)				
	$T^{thr} = 2$	$T^{thr} = 3$	$T^{thr} = 6$	$T^{thr} = 8$	$T^{thr} = 12$
Constant	-1.89 (-5.69)	-1.62 (5.18)	-1.89 (-6.09)	-2.38 (-7.30)	-2.80 (-7.41)
Truck Volume Per Truck Lane	0.087 (4.59)	0.061 (3.47)	0.055 (3.14)	0.063 (3.36)	0.043 (2.01)
Passenger Vehicle Volume per Passenger Vehicle Lane	0.028 (4.02)	0.022 (3.47)	0.009 (1.68)	0.008 (1.56)	0.009 (1.71)
$LL(\beta^*)$	-532.9	-555.6	-522.7	-460.1	-336.3
$LL(C)$	-562.4	-574.9	-531.9	-470.5	-341.1
$LL(0)$	-575.3				

$LL(\beta^*)$ : log-likelihood function value when determining probability that trip excess time is above  $T^{thr}$  using maximum likelihood coefficient estimates

$LL(C)$ : log-likelihood function value calculated when assuming probability that trip excess time is above  $T^{thr}$  equals the proportion of trips falling above  $T^{thr}$

$LL(0)$ : log-likelihood function value calculated when assuming probability that trip excess time is above  $T^{thr}$  equals 0.5

The coefficients in the estimated models all have the expected signs and are significantly different from zero at the 0.10 significance level, and generally at a much lower level. That is, the results exhibit the expected correlation of excess times with volume and number of open lanes. Similarly, each estimated model produces a significantly better fit than simpler models at a significance level lower than 0.01, where the simpler models are those in which the probability that an excess times is above the threshold  $T^{thr}$  is either given by 0.5 or by the proportion of observations above  $T^{thr}$ . However, when we conducted “cross-validation” assessments of the predictive performance of these models – where we estimated models using a subset of the data, applied the estimated models to predict the response variable using the same independent variables for the subset of (“holdout”) data not used in the estimation, and compared the predicted value of the response value to the observed value – the performance of these models was not satisfactory. In addition, the aggregate models would not be useful when trying to predict performance under entirely different infrastructure conditions. We concluded that the aggregate empirical models support the concept that increased demand (increased traffic volume) or decreased capacity (decreased number of open lanes) is associated with higher queuing times, but that additional models would be needed for predictive decision support. We also investigated a microsimulation approach to modeling border crossing times as described in the following sub-section.

## **5.2 Microsimulation Models**

Simulation is a common tool used to model port facilities, and to test various operational strategies (Jeannotte et al., 2004). Similar to parts movements in manufacturing processes, a truck moves through the port, from inspection station to inspection station, until either all its inspections are completed and it is cleared to exit, or it is stopped (and appropriately dealt with) when an inspection “fails.” The path taken by each truck through the port may take it to one or several inspection facilities. Because we are also dealing with traffic and vehicle flows, existing traffic simulation tools may be useful in describing and visualizing these movements. These tools can capture the physical layout of the facility and can display the possible congestion that occurs in queues at the inspection stations and the vehicle trajectories within and around the port. Such traffic simulation tools are typically oriented toward “discrete-time” simulations, modeling the specific movement of vehicles over relatively short, but constant time increments.

We combined a traditional microscopic traffic simulation tool, VISSIM (PTV, 2007a), using a Visual Basic .NET interface, with a Visual Basic (VB) computer model (code) for representing the specific inspection, routing, and queuing behaviors that occurs at border crossing facilities. The intent was to use the interface to capture explicitly the inspection and review processes that occur in the port, while also capturing the dynamics of truck movements in VISSIM. One of the major tasks of the research team was to integrate VISSIM and VB models effectively to

represent the inspection processes and the truck movements through the port facility. This section discusses the resulting microsimulation tool.

Once the inspection processes are understood and the building blocks for the simulation models are designed and coded, the models must be calibrated with real data. Collecting data non-intrusively, or remotely, can prove to be effective in the port operations setting. There are at least two major ways to collect data non-intrusively. First, one may collect information on truck arrivals and departures at the port, giving total arrival rates, departure rates, and the overall time required to traverse through the port. The total port traversal times can be collected remotely in several ways. We used license plate reading and matching. Second, one may use a remote airborne camera to observe the actual operations within the port, such as truck trajectories through the port, truck waiting times and inspection processing times. From observations of various truck movements and queuing behaviors at the port, the distributions of travel times and processing times can be generated.

### **5.2.1 Model Structure**

The queuing and server logic were implemented in Visual Basic.NET (VB.NET) that controls VISSIM via its Component Object Model (COM) (PTV, 2007b). Using the COM interface in VISSIM, this framework allows in a “faster-than-real-time” simulation speed. The VB.NET user interface allows the simulation inputs to be adjusted as a function of time, which is a crucial property for server scheduling in the queuing models. Because of the object-oriented structure of VB.NET, different components of the simulation (stations, buffer zones, etc.) were developed as programming classes. Currently the resulting simulation can be set up for any facility with minimal modifications.

Simulation Classes: A scaled aerial image of the Mariposa inspection facility was used as a reference to create the traffic network of the facility. Routes, reflecting the possible movements of trucks through the facility, are the primary building blocks within VISSIM. The details about the routes were obtained from previous on-site observations, and from tracking trucks through the facility using the airborne imagery described in Section 4.

There are three programming classes in the VB.NET code that remain unchanged regardless of the simulation application: *Station*, *BufferZone*, and *EventCalendar*. These classes, each of which is discussed below, do not need to be modified when implementing the general simulation tool for different border crossing facilities unless the queuing logic needs to change. The specific parameters associated with each of these classes will change, of course, depending on the facility, but the classes themselves are more generic.

*Station:* The station class holds the information about the current server status, server types, serving time distributions, route links that represent the station queue lanes, detectors, vehicle queues, and any buffer zone connections. All of the station queuing logic is implemented in this class.

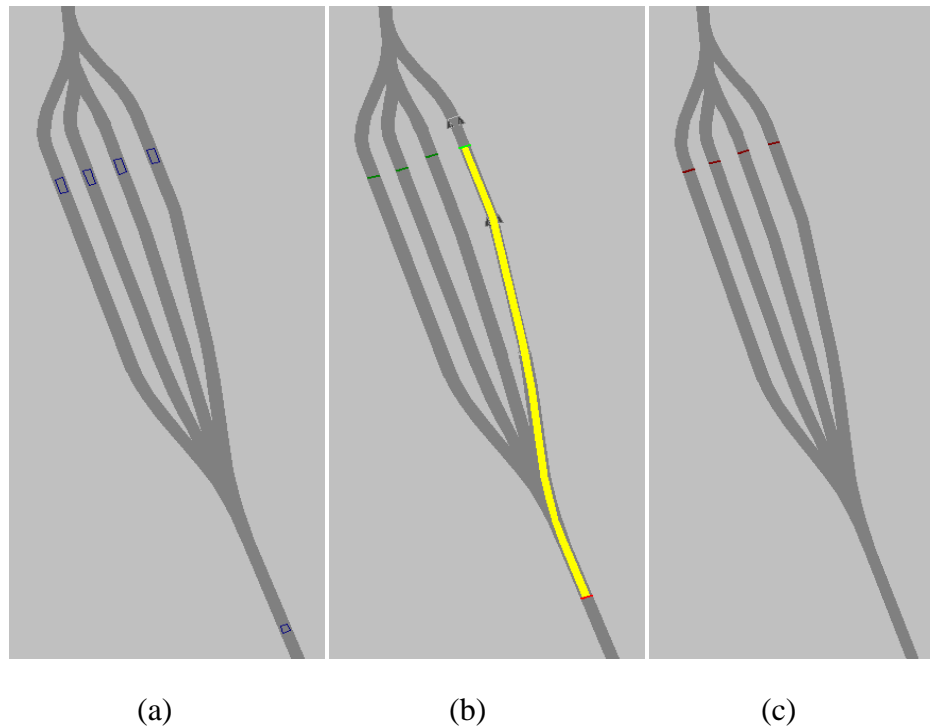


**Figure 5.2.1-1:** Graphical depiction of *Station* elements in VISSIM: (a) Queue entrance and exit detectors (b) Route and (c) Signal head

The *Station* class in VISSIM has three elements: (i) queue entrance and exit detectors; (ii) routes (or paths in the *Station*); and, (iii) traffic signals. These elements are depicted in Figure 5.2.1-1. Figure 5.2.1-1(a) shows a single detector at the queue entrance (to the lower right) where trucks enter to a set of parallel service stations. There are also other detectors, one at each service station, termed the exit detectors. Considering that the traffic flow is upwards in the image, the detector at the bottom right is the entrance detector that signals that the vehicle is about to enter a queue. Once a vehicle passes that point, its vehicle ID is added to a pre-queuing list. At each time step, the speeds of the vehicles on this list are checked. If the speed indicates that a vehicle has stopped in that time step, that time is recorded in the *EventCalendar* as the beginning of the vehicle's queuing time. It should be noted that if the last vehicle in the queue is stationary behind the entrance detector, it will not be considered queued by the model. Therefore, it is best to place the entrance detector as far as possible upstream from the queuing station.

The four detectors that are placed immediately before the signal heads are the server detectors. Vehicles detected at these locations occupy a server. If there are no servers available, vehicles wait until a server becomes available. Servers are allocated to vehicles by the first-in-first-out rule. Stations can have mobile or stationary servers. Mobile servers can serve vehicles that wait in any of the queuing lanes, whereas stationary servers only serve the vehicles on the lane where

they are stationed. To avoid vehicles getting stuck in a queue without service, if the servers are stationary, the number of open lanes is set equal to the number of servers.

From the entrance detector, a truck is assigned to a specific queue for service based on a given probability of entering that queue. The opening or closing of lanes is accomplished by changing the intra-station routing probabilities to a non-zero value or to a value of zero, respectively. Each open route in the station (see Figure 5.2.1-1(b)) is assigned a particular probability that a truck will be placed on that route. Guiding the vehicles intelligently is an important function of these probabilities. This guidance can be handled, for example, through the use of “send to shortest queue” rule. With this rule, rather than being assigned to queuing lanes according to static routing probabilities, the vehicles are assigned using dynamically updated probabilities. The number of vehicles in each lane is known at each time step, and these numbers are used to update the intra-station routing probabilities dynamically. Tests showed that the routing logic (e.g., send to shortest queue, or choosing a queue purely randomly) makes a significant difference in the time trucks spend in queue and in service in the simulation. As a result, this queue assignment method requires careful calibration.

Two vehicle classes, *cleared* and *not cleared*, are created in VISSIM. Before a vehicle approaches a station, its status is changed to *not cleared (NC)* using the upstream detectors. The signal heads, shown in Figure 5.2.1-1(c), are programmed to stop the vehicles with *NC* status. Once the vehicle is released by the server, its status is updated to *cleared*. Since the signal head only stops the *NC* vehicles, *cleared* vehicles can move directly on to the next station.

Within the VB.NET logic, serving time distributions can be selected from one of the following probability density functions: Beta, Chi-squared, F, Gamma, Normal, and Uniform. These distributions are implemented from the COM library of Microsoft Excel. Therefore, Microsoft Excel must be installed on the computer that is to run the developed simulation tool.

*BufferZone*: A buffer zone is the space where vehicles may be parked before entering an inspection station queue. Figure 5.2.1-2 shows the buffer zone and the corresponding inspection station (the ADOT inspection lot) in Mariposa. The vehicles are queued in the fan-shaped space that branches into two lots. As soon as a server becomes available in the ADOT station, the next vehicle in the buffer zone is sent into this queuing area (one of the lanes on the lower part of the figure), where the server became available. This process follows the first-in-first out logic.

*BufferZone* class is very similar to *Station* class, but it is simpler, since it does not have servers that require time to “serve” trucks – the trucks simply wait until a server becomes available in the subsequent *Station*. In this way, the *BufferZone* is associated with specific *Stations* where the service actually takes place. Additionally, the *BufferZone* contains components to communicate with the associated *Stations*, so that a truck leaves the *BufferZone* when the server in the *Station* becomes available.

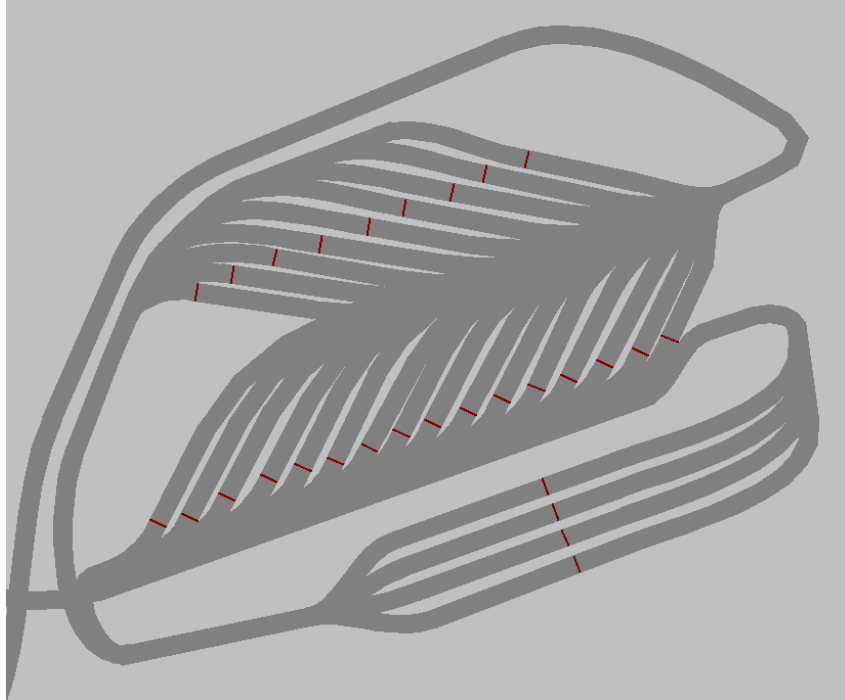


**Figure 5.2.1-2:** Graphical depiction of the buffer zone (top) and the corresponding station (bottom)

*EventCalendar*: Every event that is scheduled in the stations and the buffer zones is logged by the event calendar. Each row of the event calendar contains the following data, organized in columns: Vehicle ID, Station ID, Process type, Time. The Vehicle and Station IDs are numbers specifying the elements being simulated. Process type reflects the specific action to be taken at the given time: either *queuing* or *releasing*. Time denotes the time at which the event occurs. The *EventCalendar* object holds this data set and exports it as a tab-delimited text file. Any information related to facility performance can be derived from this file using a spreadsheet editor or a scientific computing environment.

Graphical User Interface: Every inspection facility has a different layout. Therefore, the graphical user interface (GUI) of the simulation is customized accordingly. Figure 5.2.1-3 shows the GUI for the simulation developed for the Mariposa Port of Entry.

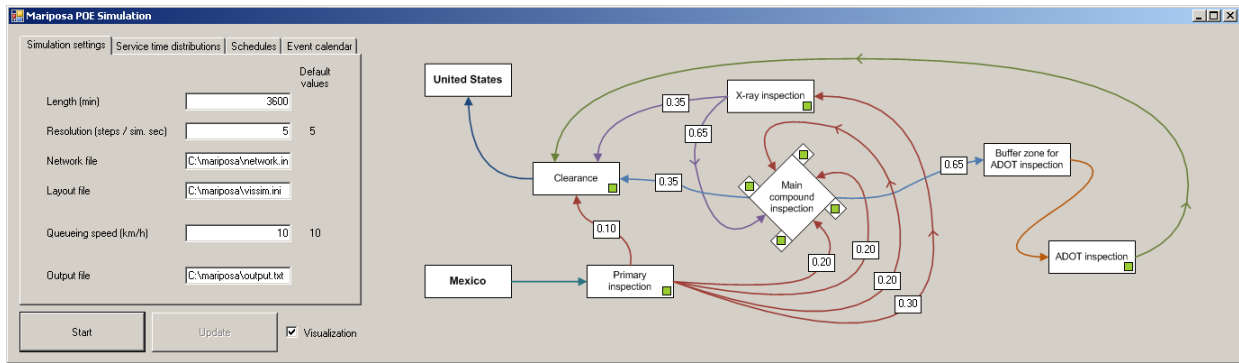


**Figure 5.2.1-3:** Graphical user interface for the Mariposa POE

On the right of Figure 5.2.1-3 is the schematic layout of the inspection network (see Figure 5.2.1-4). Arcs that have the same colors indicate the same origin, and the routing probabilities on arcs of the same color must add to one. Routing probabilities can be set using the text boxes on the arcs. These values can also be updated while the simulation is running. Small green squares on the corners of the station boxes show server availability. The numbers under the boxes show the number of available servers and the number of total servers, separated by a slash (“/”).

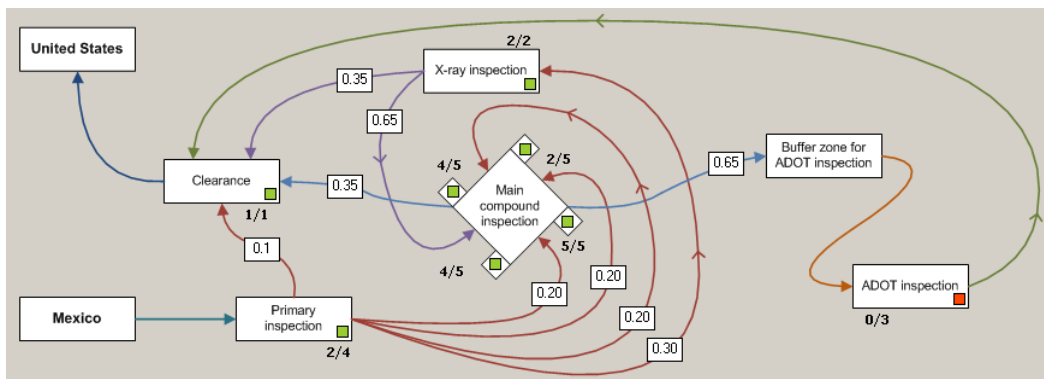


**Figure 5.2.1-4:** Schematic layout of the Mariposa POE network

Detailed simulation parameters can be entered using the tabbed form on the left of the GUI. The first tab (Simulation settings, see Figure 5.2.1-5) allows the specification of the simulation length, simulation resolution, the queuing speed, the location of the associated network file, VISSIM layout file, and output file (for the *EventCalendar*). The resolution gives the number of time steps per second in the simulation. A higher resolution produces smoother vehicle motions, but the execution time for the simulation is much higher. The lower limit for the resolution depends on the network, specifically on the level of communication between VISSIM and the VB.NET code. VISSIM communicates with the code at the end of each time step; if the resolution is too low, more than one vehicle can pass at a detector in one time step. In VISSIM, the variable that logs vehicles on the detector can only hold one vehicle ID at a time step. If two or more vehicles pass during a time step, the variable returns nothing, which causes serious

problems in the program logic. Therefore, having a sufficiently large resolution is important to avoid such problems.

The visualization feature is attractive when one wants to understand the detailed movements being simulated. However, using the visualization feature increases the run time significantly. If not needed, this feature can be turned off using the checkbox on the bottom-right corner.

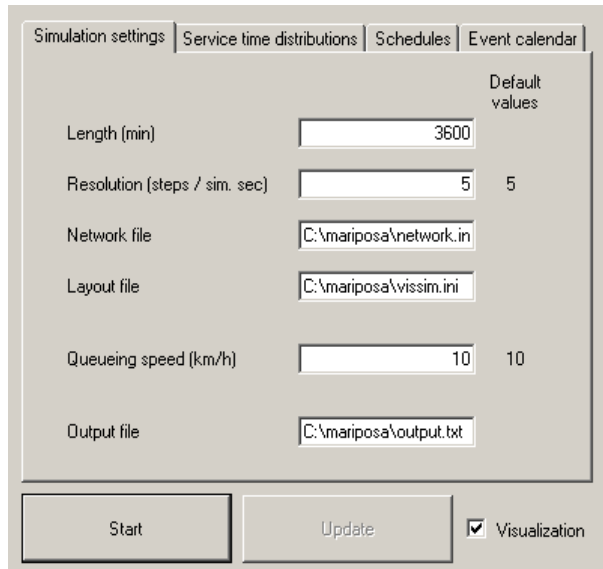


**Figure 5.2.1-5:** Simulation settings interface

The next simulation parameter tab (shown in Figure 5.2.1-6) is used to input the values of the service time distributions. A shift parameter is included in addition to general parameters. The shift parameter is used to shift the distribution by a deterministic value (positive means a shift to the right). Different parametric probability density functions can be chosen using the drop-down menu.

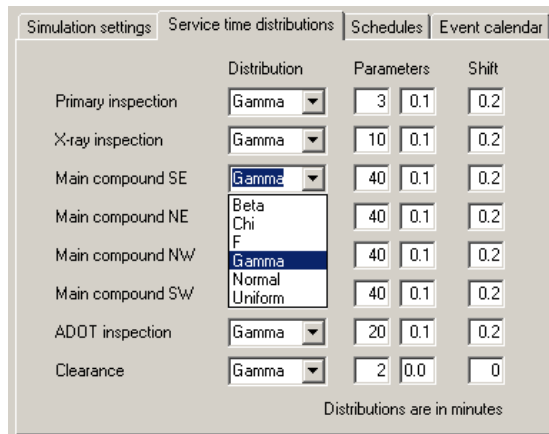


**Figure 5.2.1-6:** Service time distributions interface

The schedules for the servers and the vehicle inputs can be input using the Schedules tab (see Figure 5.2.1-7). The scheduling parameters are entered by a series of comma-delimited values. Each consecutive pair of numbers designates the time and the number of servers after the denoted time. For example, if the input in one box is “0, 4, 5, 6, 12, 3”, the schedule for the servers are as follows:

<u>Time interval</u>	<u>Number of servers</u>
0 – 5	4
5 – 12	6
> 12	3

The inputs in Figure 5.2.1-7 indicate a constant number of servers for the full simulation length.

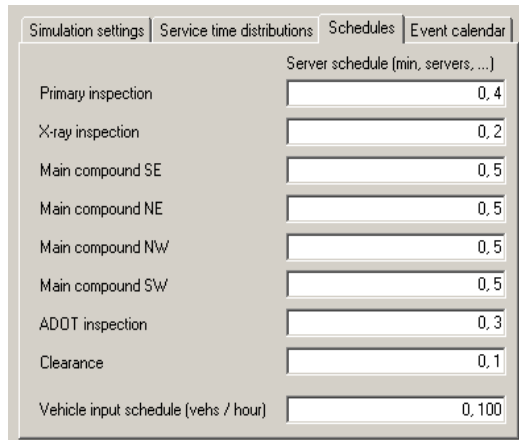


**Figure 5.2.1-7:** Schedules interface

Finally, the Event calendar tab keeps a record of queue and release events. A sample screenshot of the calendar during a run is shown below in Figure 5.2.1-8. These data are sent to the output file once the simulation concludes.

Vehicle ID	Facility type	Facility ID	Process	Time
1	Station	0	Queue	95.2
2	Station	0	Queue	106.8
1	Station	0	Release	127.4
2	Station	0	Release	134.2
3	Station	0	Queue	136
1	Station	2	Queue	151
3	Station	0	Release	164.4
2	Station	4	Queue	182.8
4	Station	0	Queue	201.8
5	Station	0	Queue	228
2	Station	1	Queue	230.4

**Figure 5.2.1-8:** Event calendar interface

## 5.2.2 Model Calibration and Application

Using this simulation framework, we simulated activities at the Mariposa Port-of-Entry. This site was described in Section 4. We obtained sufficient information and data to calibrate the micro-simulation model for the Mariposa POE. However, we did not have sufficient data to validate the simulation model – there was no subsequent data available for a validation. We discuss this model and the modeling effort in some detail in the subsections that follow.

Mariposa Port-of-Entry: The specific stations, routing, service times, and other related features of the Mariposa POE are described in Section 4.3.1. Figure 5.2.2-1 shows the various points of inspection at the facility.



**Figure 5.2.2-1:** Inspection points for trucks at Mariposa POE. 0: Pre-screening; 1: Primary inspection; 2: Secondary inspection; 3: X-ray inspection; 4: ADOT inspection; 5: Final inspection and weight check.

Commercial vehicles enter the facility through the pre-screening stations (point 0), where an initial assessment of vehicles and their documentation is performed. There are four pre-screening stations, but not all are always open. One is a FAST lane, which processes vehicles with pre-approved documentation. Before a FAST truck arrives at the POE, a document from the Mexico inspection stations is sent electronically to the POE on the US side. The document contains information about the vehicle and the product(s) it carries. This information is then verified at the pre-screening stations once the vehicle arrives. One of the ways to verify this information is by weighing the vehicles (a “weigh-in motion” inspection). In contrast, non-FAST trucks simply present information when they arrive, leading to a possible slowdown in their pre-screening. A safety inspection, as well as a drug screening inspection, is also performed on all trucks and drivers. If trucks or drivers fail these tests, they will be directed to the Arizona Department of Transportation (ADOT) lot for further verification.

From the pre-screening inspection, all vehicles proceed to one of the four “superbooths” at the primary inspection stations (point 1), where a more thorough inspection is performed. After undergoing this inspection, vehicles can then take different routes. They either proceed directly

into the US (point 5) or enter one of three main inspection facilities: a secondary inspection facility (point 2), an “X-ray” facility which contains three booths (point 3), or the ADOT inspection stations (point 4) for the ADOT Motor Vehicle Division (MVD) safety inspection and other federal inspections. Vehicles may also need a revision of their documentation, which can be done at various points in the facility. Trucks can be inspected at one, two or all three inspection points, in sequences that may vary depending on the vehicle and the product(s) it carries. At the secondary inspection station, trucks undergo two main types of inspections: a full inspection, in which the entire load in the truck is inspected, or a regular inspection, in which samples of the truckloads are analyzed. Trucks may also be submitted to a hazardous materials and weapons inspection.

We modeled the facility using information gathered during a visit to the facility in September 2007 and from previous studies performed at the Mariposa POE (Villalobos et al., 2006). Figure 5.2.2-2 summarizes the process flow diagram of the facility, which corresponds to the logic implemented in the simulation model.

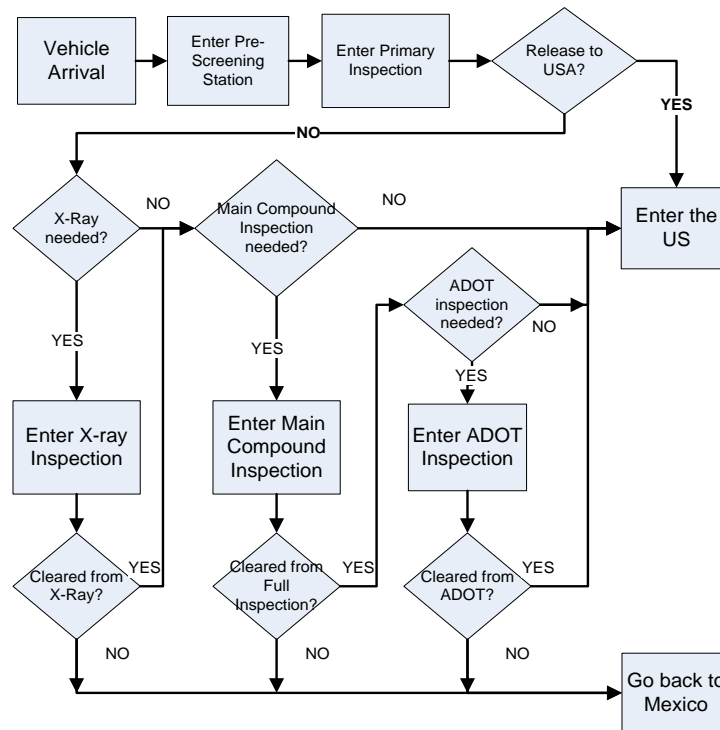


**Figure 5.2.2-2:** Mariposa POE simulation process flow

The data obtained from the February 2008 field data collection, described in Section 4, were used to calibrate the Mariposa POE simulation model. In particular, the truck traversal times sampled from the license plate data and the air photos collected from flights over the POE were used to derive truck arrival rates and inspection time distributions and the routing probabilities through the POE. The video data from cameras posted just before and directly after the Mariposa

POE were analyzed manually to estimate the license plate numbers and letters, along with a time stamp for the vehicle observation. The license plate data were matched, assuming five of the six characters on the license plate could be matched directly and that the sixth character could be either matched directly or matched subject to a small plausible error in interpretation (e.g., 4 for A, 8 for B, etc.). From this matching, we derived the total time for the truck to traverse the entire POE. A histogram of these travel times is given in Figure 4.3.1-1 and is reproduced below in Figure 5.2.2-3.

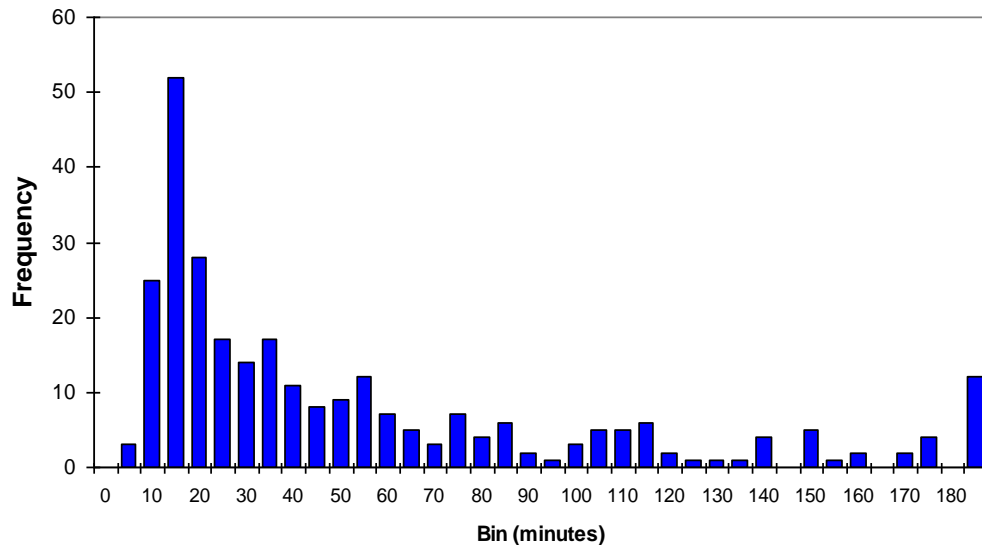


**Figure 5.2.2-3:** Distribution of travel times through the Mariposa POE from license plate data

As was noted and described in Section 4.3.1, these data were separated into subsets based on what we understood were different paths through the POE. Specific distributions for processing times within the POE were considered. The generation of these distributions is described in Section 4.3.3. The net result was a set of path routing fractions (see Section 4.3.1) and a set of distributions for specific inspections within the POE (Section 4.3.3). The path routing fractions and inspection distributions allowed us to calibrate the Mariposa POE simulation model.

### 5.2.3 Conclusion

This section illustrates the type of simulation model that may be developed for ports-of-entry. It is clearly possible to model such a system by combining a traffic simulation software, such as VISSIM, with a model that handles discrete events (e.g., the start and end times and places of vehicle inspections) using other software. In our case, we developed code in VB.NET. The result is a calibrated tool that can be used to simulate the operations, and potential operational improvements, at an international border crossing. In addition, the application of the simulation to the Mariposa Port of Entry shows that non-intrusive (remote) data collection can be used to

calibrate such a simulation model. The primary data elements required for the simulation models include:

- data on the full traversal time from entry to exit at border crossing facility
- estimates of the distribution of inspection times at specific stations within the facility
- estimates of the fraction of trucks that are diverted from one inspection station to another within the facility

The procedure for developing the integrated model combining off-the-shelf modeling systems and using synchronized inter-process communication, the approaches for remotely collecting data, and the methodologies for model calibration introduced in this research effort can be used to develop models for any border crossing facility -- in fact, any facility where vehicles arrive and undergo complex vehicle processing.

## **Section 6. Analysis of Work Zones**

During construction of major transportation facilities, roads near the work sites have decreased capacities, and the movement of trucks and heavy equipment also tend to disrupt traffic. As a result of traffic controls and network layout, primary queues form at the construction site, and secondary queues form upstream. Additional queues can form on cross-streets and other parallel roadways as drivers choose alternate routes. Such projects may, therefore, create significant delays for drivers. Not surprisingly, mitigating these impacts is a major focus of the traffic control plans instituted during these construction activities.

Capturing the impacts of work zones is difficult because the common tools for network monitoring are often disrupted during the construction. Traditional ground sensors, such as loop detectors or intersection cameras, are often removed or otherwise disabled during the construction. As a result, the empirical measurement of traffic volumes, vehicle speeds, queue lengths, and related measures is not usually possible during the event (FHWA, 2006). Rather, traffic simulation or other existing tools are used to estimate these measures (FHWA, 2008; FHWA, 2009), for the purposes of traffic management and control. In addition, there is little research or documentation of *ex post facto* evaluation of the effectiveness of work zone operations and management.

The use of remote sensing and spatial information technologies can provide an alternative method of evaluating impacts of work zones. As the queues associated with construction are inherently spatial in nature, temporally and spatially extensive data from imagery and other Position-Navigation-Timing (PNT) technologies can be used to monitor traffic patterns during construction and benchmark operations during different work activities. Developing a spatial-temporal characterization of the traffic network from available PNT technologies would allow an understanding of queuing behavior and provide insights on efficient management of the queues. For example, traffic managers can use these insights to improve traffic signal control during construction. Traffic and construction managers can use this information to improve scheduling of the activities and associated truck and equipment movement around and within the construction site. Likewise, observing truck and vehicle movements at major construction sites, and the associated formation of queues, would assist in developing models to capture the spatial-temporal queuing dynamics; in turn, these models can be used to identify construction design and staging logistics to decrease vehicle delays.

### **6.1 Empirical Setting**

The Interstate I-10 work zone in Tucson was located between 29<sup>th</sup> Street on the south end and Prince Road on the north. The location of the work zone is illustrated on a map in Figure 6.1-1. I-10 is the only major freeway running through the City of Tucson and Pima County. Just south of the work zone, I-10 connects to I-19, which runs from Tucson to the Mexican border in Nogales, AZ. I-10 handles significant through traffic, as well as being a local distributor to the northwest and southeast of the central city of

Tucson. Generally, as can be seen in the figure, I-10 Westbound runs to the north and slightly west, and I-10 Eastbound runs to the south and slightly east, in this alignment.

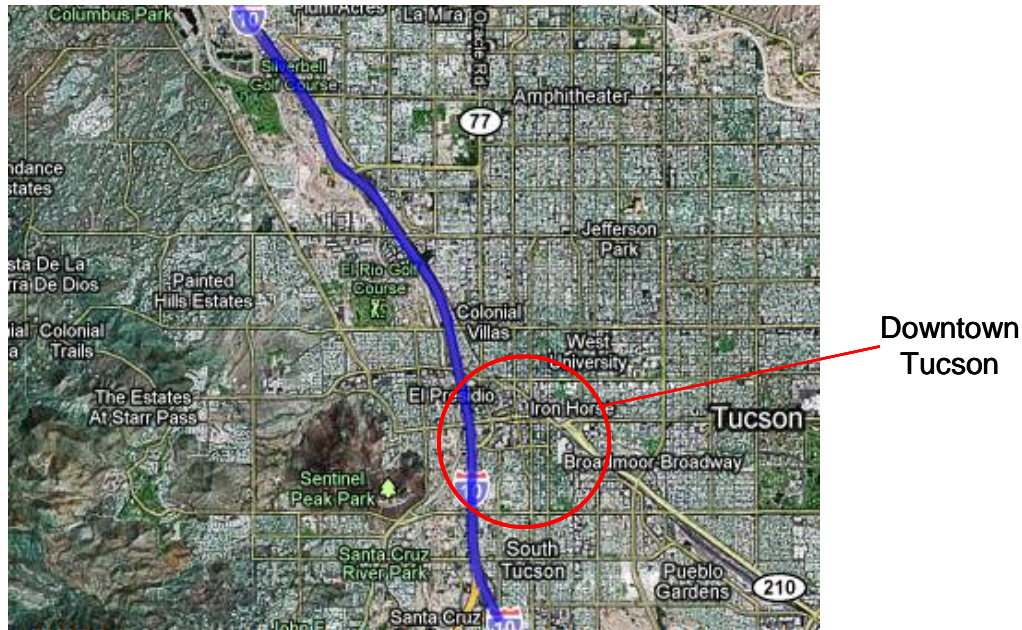


**Figure 6.1-1:** I-10 Work Zone (blue line) in Tucson

The project was designed to widen this section of I-10 from three lanes in each direction (a 6-lane cross-section) to four lanes in each direction (an 8-lane cross-section). The project was conducted in stages, essentially widening one-half of the facility while diverting traffic either onto the other half of the existing freeway or onto the frontage roads. The frontage roads had been widened to three lanes in each direction in anticipation of this project. On I-10 itself, all entrance and exit ramps between 29<sup>th</sup> Street and Prince Road were closed, and only two through lanes in each direction were maintained. This policy meant that all traffic remaining on I-10 was restricted to travel the full distance through the work zone. Traffic wishing access to or from cross-streets along I-10 in the work zone was required to travel on the frontage roads through the entire project area. A schematic summarizing this traffic activity is shown in Figure 6.1-2. Because of the expected high demand on the frontage roads, along with the frequent traffic signals along these roads, it was anticipated that major congestion would occur along the frontage roads and the cross-streets. The Arizona Department of Transportation (ADOT) constructed an Interim Traffic Operations Center (ITOC) at the south end of the project, where freeway cameras could be monitored and traffic signal operations managed, 24 hours a day, 7 days a week.

The project broke ground in the spring of 2007 and continued until September 2009. Originally slated to take 36 months, about 3 months were saved from the project schedule due to more efficient construction staging and methods.

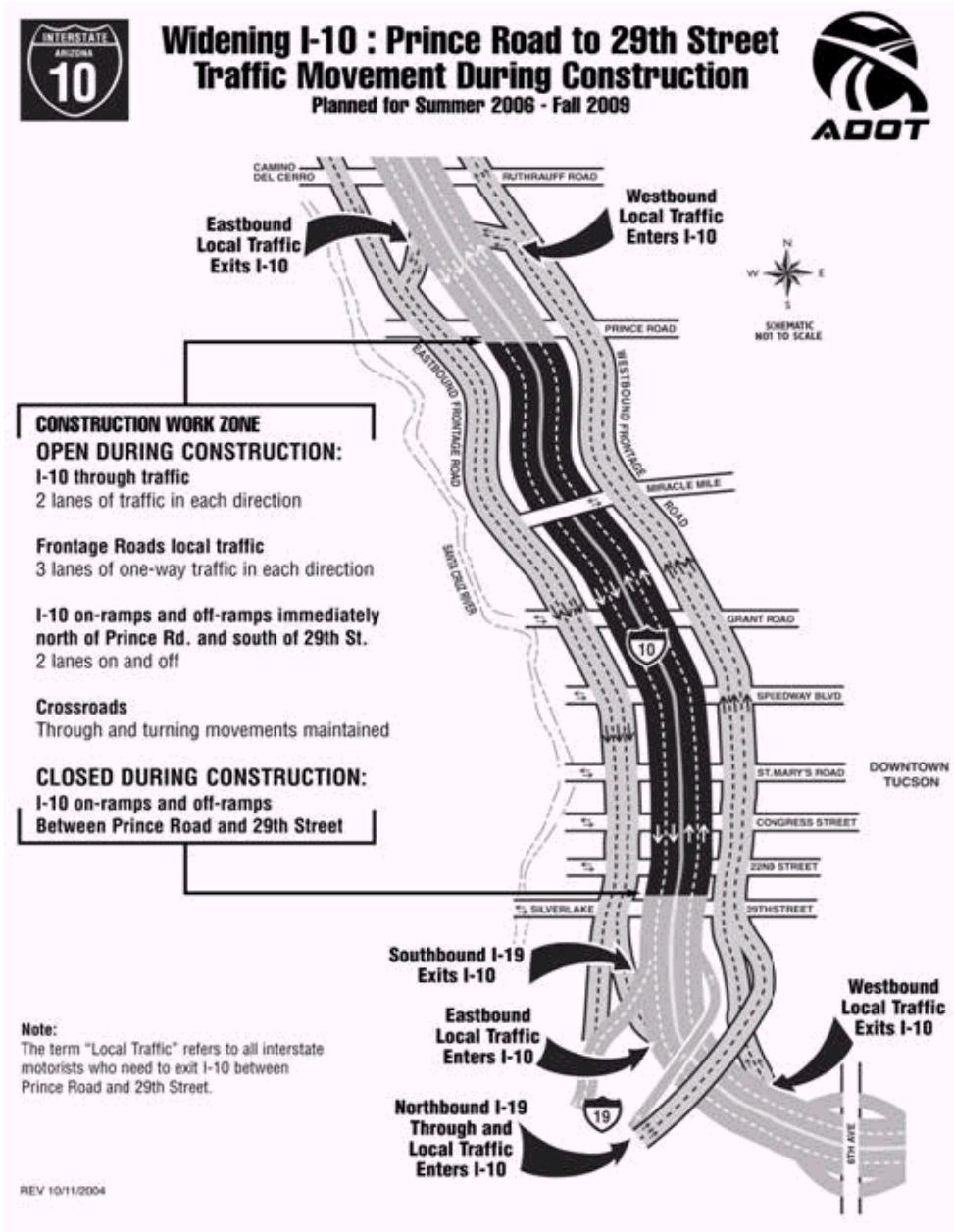


Figure 6.1-2: ADOT flyer on traffic patterns during I-10 construction

## 6.2 Approach and Methodology

### 6.2.1 Imagery and Camera Platform

The goal of the work zone thrust was to collect and to analyze imagery taken from an aircraft flying over the I-10 work zone. Three sets of flights were undertaken. The first set of flights was conducted on September 14, 2007, and the other two sets of flights were conducted in close proximity to each other, one on November 18, 2008 and the other on December 2,

2008. On September 2007, only about 10 minutes of video from the I-10 work zone was available; the video on this day was taken as part of a data collection effort for other purposes. On November 18, 2008, we took approximately 2 hours of video over a contiguous time period from helicopter flights over I-10. On December 2, about two hours of video were taken directly over the I-10 work zone.

The imagery from the September 2007 flight was obtained using a more traditional camera platform, including both a commercial off-the-shelf digital video camera (720x480 pixel resolution, at 30 frames per second), and a higher resolution video surveillance camera (4 megapixels, or 2250x1760 pixel resolution, at 15 frames per second). The imagery was analyzed manually to examine the density and speed of traffic along the main lanes of I-10 through the work zone. We also examined the queue lengths along the frontage roads and cross-streets from these images.

The imagery from the November and December flights was taken using the ANTAR platform, developed by the German Aerospace Center (Deutsches Zentrum für Luft- und Raumfahrt, or DLR). This platform included: (1) a high-resolution visual imagery camera which could obtain imagery of approximately 4 megapixels per image at 3-5 images per second; (2) a high-resolution infrared camera, capturing synchronous images with the visual camera; (3) a differentially-corrected GPS unit; and, (4) an inertial measurement unit (IMU) to capture the orientation of the helicopter and the camera platform. The ANTAR platform is illustrated in Figure 6.2.1-1.

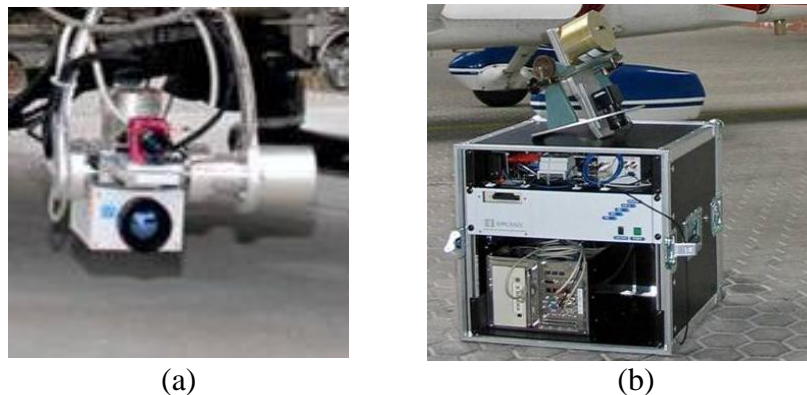


**Figure 6.2.1-1:** The ANTAR Platform. (a) The camera system with GPS and IMU; (b) the computer and communications infrastructure

The ANTAR system also includes a computer with a digital roadway database, allowing the platform to automatically register the imagery to geographic coordinates and to provide a reference roadway system for the analysis. Because the imagery included the latitude, longitude, elevation, and orientation of the camera, the roadway database could be used to geo-locate a vehicle found in the image onto the reference roadway system. In this way, the exact real-world coordinates of a vehicle in a given image could be identified. By comparing vehicle coordinates between images separated by a known period of time, the vehicle speed can also be determined.

## 6.2.2 Traffic Analysis Software

The DLR also provided a license to use two software tools that they created to analyze the ANTAR imagery. These include *TrafficFinder*, a software tool to automatically detect and record vehicle speeds and trajectories from the visual imagery, and *ClickTool*, a software tool that has similar features, but allows the user to manually specify the vehicles to be tracked in the imagery. The capabilities of ANTAR, TrafficFinder and ClickTool are shown in Figure 6.2.2-1. The imagery has been automatically geo-referenced; that is, the coordinates of all points in the image have been tied directly to coordinates on the earth. For this reason, the orientation of the images has been adjusted. In the ClickTool image, one may also note small markers in the image. These markers indicate vehicles that have been tracked across successive images.

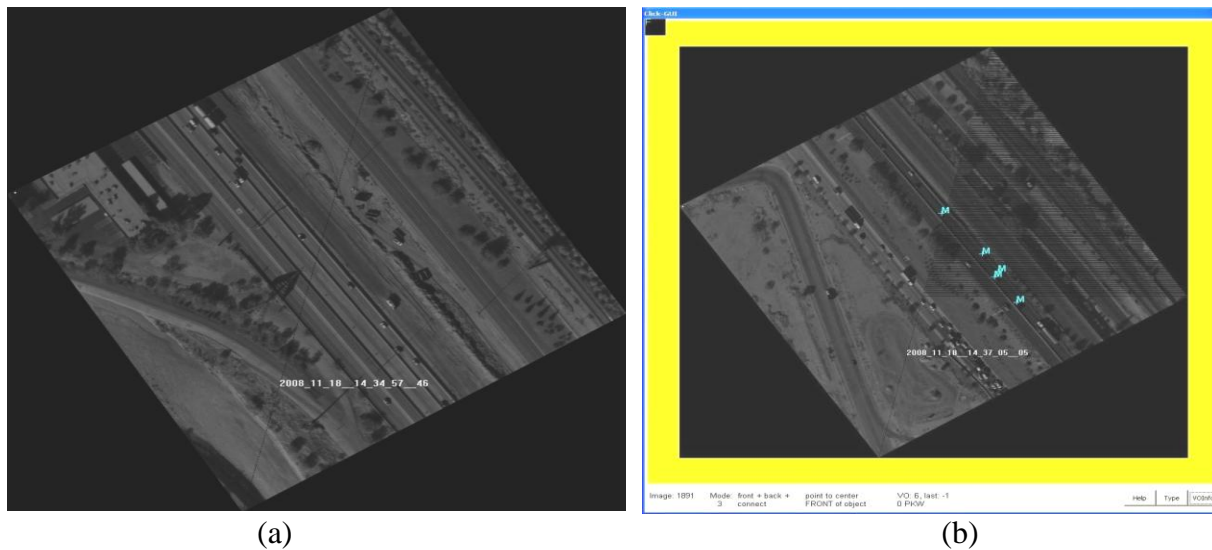


**Figure 6.2.2-1:** Registered imagery from the DLR’s ANTAR; (a) from TrafficFinder; (b) from ClickTool

## 6.2.3 Traffic Condition Measurement

### 6.2.3.1 Image Processing

TrafficFinder, ClickTool and an additional Python code are used to estimate the average speed of the vehicles on each segment of I-10 work zone from Prince to 29<sup>th</sup> Street. The automated vehicle tracking feature in TrafficFinder tracks the vehicles automatically, but not all vehicles are recognized initially. In contrast, ClickTool does not analyze the images automatically; rather, one has to click the vehicles in several successive images manually. In both cases, vehicle speeds can be estimated using the real-world coordinates of the vehicles, as the vehicle coordinates, which change from one image to the next, are automatically tied to a unique set of real-world coordinates through the geo-referencing capabilities of the system. With the output files

generated from TrafficFinder and ClickTool, a short Python code was developed to calculate the average speed of the vehicles using these coordinates and the time between successive images.

A digital street map of I-10, a digital terrain model (DTM) of the area, and a configuration file are created as input for TrafficFinder. The general steps to generate the digital street map of I-10 were those described in Table 6.2.3.1-1.

**Table 6.2.3.1-1:** Actions and results of steps used to generate the digital street map of I-10 used as input for the geo-referencing features of TrafficFinder and ClickTool

<b>Step</b>	<b>Action</b>	<b>Result</b>
1	Create I-10 northbound and southbound roads by placing a node every 20 meters along I-10 using Google Maps, as shown in Figure 6.1-1	.KML file which contains the longitude and latitude of each node, as shown in Figure6.2.3.1-1.
2	Copy the longitude and latitude of the nodes to an Excel file.	Excel file
3	Create a name file, node file and link file from the Excel file.	The name file contains the road ID's and road names, as shown in Figure 6.2.3.1-2. The node file contains longitude and latitude of each node, as shown in Figure6.2.3.1-3. Finally, the link file contains the Node_from,Node_to, length of the link, number of lanes, and selected additional information, as shown in Figure 6.2.3.1-4

```

I10 Nov 12th 2009 1.kml x
0 10 20 30 40
19 <name>I10 North Bound</name>
20 <description><![CDATA[]]></description>
21 <styleUrl>#style2</styleUrl>
22 <LineString>
23   <tessellate>1</tessellate>
24   <coordinates>
25     -110.974609,32.190392,0.000000
26     -110.974709,32.190517,0.000000
27     -110.974808,32.190666,0.000000
28     -110.974907,32.190815,0.000000
29     -110.974998,32.190952,0.000000
30     -110.975098,32.191105,0.000000
31     -110.975189,32.191250,0.000000
32     -110.975288,32.191402,0.000000
33     -110.975372,32.191544,0.000000
34     -110.975471,32.191708,0.000000
35     -110.975548,32.191833,0.000000
36     -110.975639,32.191986,0.000000
37     -110.975731,32.192135,0.000000
38     -110.975807,32.192272,0.000000
39     -110.975899,32.192421,0.000000
40     -110.975990,32.192581,0.000000
41     -110.976074,32.192707,0.000000
42     -110.976158,32.192852,0.000000
43     -110.976250,32.193001,0.000000

```

Figure 6.2.3.1-1: Excerpt from KML file for nodes placed along I-10

```

names.txt x
0 10 20 30 40 50 60 70
1 # NAME_ID2 NAME (last bit indicates the direction of the traffic flow)
2 600001 I10_Rd_S
3 600002 I10_Rd_N

```

Figure 6.2.3.1-2: Name file showing name of road segment

```

node_list_i10.txt x
0 10 20
1 # node list
2 5000 -11097461 3219039
3 5001 -11097471 3219052
4 5002 -11097481 3219067
5 5003 -11097491 3219082
6 5004 -11097500 3219095
7 5005 -11097510 3219111
8 5006 -11097519 3219125
9 5007 -11097529 3219140
10 5008 -11097537 3219154
11 5009 -11097547 3219171
12 5010 -11097555 3219183
13 5011 -11097564 3219199
14 5012 -11097573 3219214
15 5013 -11097581 3219227
16 5014 -11097590 3219242
17 5015 -11097599 3219258
18 5016 -11097607 3219271
19 5017 -11097616 3219285
20 5018 -11097625 3219300
21 5019 -11097634 3219315
22 5020 -11097643 3219329
23 5021 -11097652 3219344
24 5022 -11097660 3219359
25 5023 -11097669 3219373
26 5024 -11097677 3219388

```

Figure 6.2.3.1-3: Excerpt from node file with node numbers and coordinates (decimal degrees, x 100,000)

ID	Node	from	Node	to	length	vehicle	type	form	of	way	brunnel	type	street	type	speed	category		
1	50001	5000	5001	16.82851756	1000000000	3	-1	2	6	2	40	-1	600001	-1	-1	-1	1	-1
2	50002	5001	5002	19.05670164	1000000000	3	-1	2	6	2	40	-1	600001	-1	-1	-1	1	-1
3	50003	5002	5003	19.05670164	1000000000	3	-1	2	6	2	40	-1	600001	-1	-1	-1	1	-1
4	50004	5003	5004	17.52084786	1000000000	3	-1	2	6	2	40	-1	600001	-1	-1	-1	1	-1
5	50005	5004	5005	19.49241219	1000000000	3	-1	2	6	2	40	-1	600001	-1	-1	-1	1	-1
6	50006	5005	5006	18.3035288	1000000000	3	-1	2	6	2	40	-1	600001	-1	-1	-1	1	-1
7	50007	5006	5007	19.34920203	1000000000	3	-1	2	6	2	40	-1	600001	-1	-1	-1	1	-1
8	50008	5007	5008	17.70371125	1000000000	3	-1	2	6	2	40	-1	600001	-1	-1	-1	1	-1
9	50009	5008	5009	20.53092733	1000000000	3	-1	2	6	2	40	-1	600001	-1	-1	-1	1	-1
10	50010	5009	5010	15.71499688	1000000000	3	-1	2	6	2	40	-1	600001	-1	-1	-1	1	-1
11	50011	5010	5011	19.09564428	1000000000	3	-1	2	6	2	40	-1	600001	-1	-1	-1	1	-1
12	50012	5011	5012	18.74200615	1000000000	3	-1	2	6	2	40	-1	600001	-1	-1	-1	1	-1
13	50013	5012	5013	16.87260372	1000000000	3	-1	2	6	2	40	-1	600001	-1	-1	-1	1	-1
14	50014	5013	5014	18.74200615	1000000000	3	-1	2	6	2	40	-1	600001	-1	-1	-1	1	-1
15	50015	5014	5015	19.79586811	1000000000	3	-1	2	6	2	40	-1	600001	-1	-1	-1	1	-1
16	50016	5015	5016	16.127815	1000000000	3	-1	2	6	2	40	-1	600001	-1	-1	-1	1	-1
17	50017	5016	5017	18.00309878	1000000000	3	-1	2	6	2	40	-1	600001	-1	-1	-1	1	-1
18	50018	5017	5018	18.74224784	1000000000	3	-1	2	6	2	40	-1	600001	-1	-1	-1	1	-1
19	50019	5018	5019	18.30303383	1000000000	3	-1	2	6	2	40	-1	600001	-1	-1	-1	1	-1
20	50020	5019	5020	18.00309878	1000000000	3	-1	2	6	2	40	-1	600001	-1	-1	-1	1	-1
21	50021	5020	5021	19.03886596	1000000000	3	-1	2	6	2	40	-1	600001	-1	-1	-1	1	-1
22	50022	5021	5022	18.00309878	1000000000	3	-1	2	6	2	40	-1	600001	-1	-1	-1	1	-1
23	50023	5022	5023	17.60364165	1000000000	3	-1	2	6	2	40	-1	600001	-1	-1	-1	1	-1
24	50024	5023	5024	18.364061	1000000000	3	-1	2	6	2	40	-1	600001	-1	-1	-1	1	-1
25	50025	5024	5025	19.53674721	1000000000	3	-1	2	6	2	40	-1	600001	-1	-1	-1	1	-1

**Figure 6.2.3.1-4:** Link file showing segments connecting nodes

The steps to create the DTM file for the I-10 work zone involved downloading Shuttle Radar Topography Mission (SRTM) files from the US Geological Survey (USGS). The SRTM data were collected on previous US Space Shuttle flights and create a 3-dimensional surface describing the topography of various areas on the earth’s surface. For our purposes, it was necessary to stitch together two DTM files from the SRTM (in this case, N32W110.hgt and N32W111.hgt).

The configuration file contains all values that serve as major inputs to the TrafficFinder GUI, as shown in Figure 6.2.3.1-5, and many others can be specified in the configuration file, for example, the paths of input and output files, as shown in Figure 6.2.3.1-6.

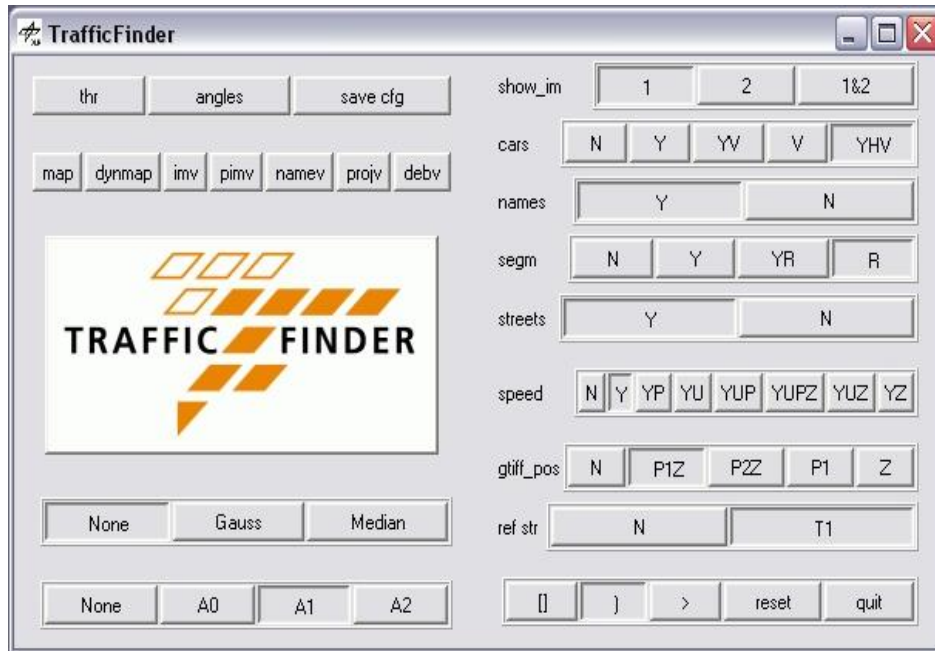


**Figure 6.2.3.1-5:** Traffic Finder GUI

```

tf_offline_i10.cfg x
0 10 20 30 40 50 60 70
127
128 # #####
129 # digital map for Arizona
130 # #####
131
132 dig_fpath = "C:\\TrafficFinder\\input\\i10\\street_files\\"
133 dtm_path = "C:\\TrafficFinder\\input\\i10\\dtm\\"
134 dig_fnamecoords = "node_list_i10.txt"
135 dig_fnamestreets = "link_list_i10.txt"
136 dig_fnamesplittedstreets = "splitted_links.txt" #dummy
137 dig_fnamestreetnames = "names.txt"
138
139 max_ews_str_type = 3
140 area = (-111.018845,-110.974609,32.19038,32.281403)
141
142 #geoid_height = 39.5 #berlin !!!
143 geoid_height = -29.1 #arizona !!!
144
145 dtm_filename = "N32W110.hgt"
146 dtm_width = 1201
147 dtm_height = 1201
148 dtm_raw_mode_s = "I;16BS" #"I;16"
149 dtm_orientation = -1 #hier war ich
150 dtm_lon0 = -110.
151 dtm_lat0 = 32.

```

**Figure 6.2.3.1-6:** Structure of TrafficFinder configuration file

There are several output files from Traffic Finder, namely geotiff files, infrared (IR) images in geotiff files, and files with speed information and navigation data. The geotiff and navigation data files are used as input files of the Python code to calculate the average speed of vehicles across a set of images. A geotiff file, an example of which is shown in Figure 6.2.3.1-7, are tiff

files with geo-referencing information, allowing the image to be located geographically and displayed according to specific map projections or coordinate systems. Through geo-referencing, the geotiff changes the orientation of the image, so that north always appears as the traditional “up” direction in the image.

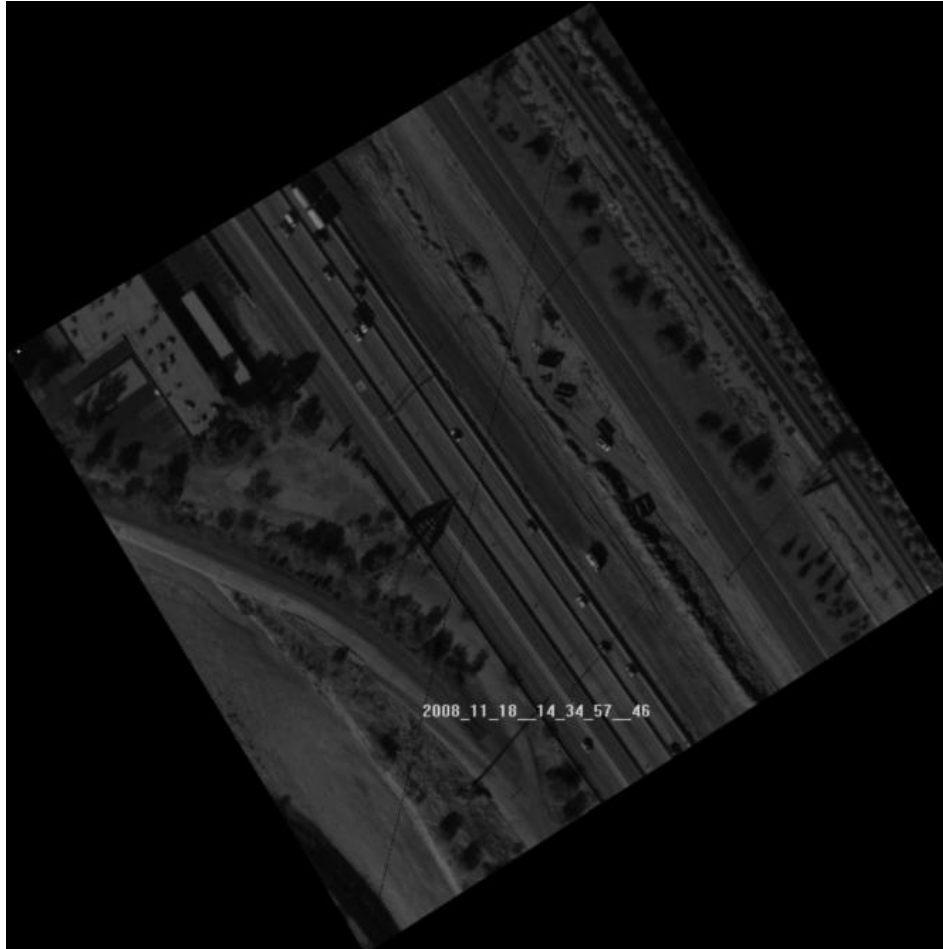


**Figure 6.2.3.1-7:** Example geotiff file

The following is an example of the entries in navigation data file, as shown in Fig 6.2.3.1-8:

```
001891.jpg g_2008_11_18_14_37_05_0589_001891.tif 2008_11_18_14_37_05_05
250625.05898 1.43000 1.13000 327.45000 32.273309 -111.011925 1260.320 0.00 0.00
0.00 -29.1 498876.99 3570730.66 498469.1058 0.9553 -0.0001 3571102.9184 -0.0001 -
0.9564 250625.05898. A description of the fields in this data file is given in Table6.2.3.1-2
```

all_nav_data.txt x											
0	10	20	30	40	50	60	70	80	90	100	J
1411	001879.jpg	g	2008_11_18_14_37_01	3088	001879.tif	2008_11_18_14_37_01	30	250621.30880	2.14000	1.420	
1412	001880.jpg	g	2008_11_18_14_37_01	6213	001880.tif	2008_11_18_14_37_01	62	250621.62131	1.86000	1.400	
1413	001881.jpg	g	2008_11_18_14_37_01	9347	001881.tif	2008_11_18_14_37_01	93	250621.93473	1.48000	1.400	
1414	001882.jpg	g	2008_11_18_14_37_02	2464	001882.tif	2008_11_18_14_37_02	24	250622.24641	1.04000	1.420	
1415	001883.jpg	g	2008_11_18_14_37_02	5589	001883.tif	2008_11_18_14_37_02	55	250622.55894	0.86000	1.470	
1416	001884.jpg	g	2008_11_18_14_37_02	8714	001884.tif	2008_11_18_14_37_02	87	250622.87143	0.90000	1.510	
1417	001885.jpg	g	2008_11_18_14_37_03	1838	001885.tif	2008_11_18_14_37_03	18	250623.18387	1.08000	1.490	
1418	001886.jpg	g	2008_11_18_14_37_03	4963	001886.tif	2008_11_18_14_37_03	49	250623.49638	1.30000	1.450	
1419	001887.jpg	g	2008_11_18_14_37_03	8113	001887.tif	2008_11_18_14_37_03	81	250623.81134	1.40000	1.420	
1420	001888.jpg	g	2008_11_18_14_37_04	1214	001888.tif	2008_11_18_14_37_04	12	250624.12140	1.72000	1.400	
1421	001889.jpg	g	2008_11_18_14_37_04	4338	001889.tif	2008_11_18_14_37_04	43	250624.43390	1.93000	1.260	
1422	001890.jpg	g	2008_11_18_14_37_04	7464	001890.tif	2008_11_18_14_37_04	74	250624.74642	1.65000	1.110	
1423	001891.jpg	g	2008_11_18_14_37_05	0589	001891.tif	2008_11_18_14_37_05	05	250625.05898	1.43000	1.130	
1424	001892.jpg	g	2008_11_18_14_37_05	3714	001892.tif	2008_11_18_14_37_05	37	250625.37147	1.27000	1.220	
1425	001893.jpg	g	2008_11_18_14_37_05	6839	001893.tif	2008_11_18_14_37_05	68	250625.68396	1.11000	1.300	
1426	001894.jpg	g	2008_11_18_14_37_05	9964	001894.tif	2008_11_18_14_37_05	99	250625.99647	0.80000	1.340	
1427	001895.jpg	g	2008_11_18_14_37_06	3089	001895.tif	2008_11_18_14_37_06	30	250626.30897	0.30000	1.360	
1428	001896.jpg	g	2008_11_18_14_37_06	6215	001896.tif	2008_11_18_14_37_06	62	250626.62157	0.16000	1.340	
1429	001897.jpg	g	2008_11_18_14_37_06	9359	001897.tif	2008_11_18_14_37_06	93	250626.93599	0.23000	1.310	
1430	001898.jpg	g	2008_11_18_14_37_07	2465	001898.tif	2008_11_18_14_37_07	24	250627.24657	0.40000	1.290	
1431	001899.jpg	g	2008_11_18_14_37_07	5591	001899.tif	2008_11_18_14_37_07	55	250627.55910	0.67000	1.330	
1432	001900.jpg	g	2008_11_18_14_37_07	8715	001900.tif	2008_11_18_14_37_07	87	250627.87160	0.96000	1.410	
1433	001901.jpg	g	2008_11_18_14_37_08	1840	001901.tif	2008_11_18_14_37_08	18	250628.18408	1.08000	1.540	
1434	001902.jpg	g	2008_11_18_14_37_08	4967	001902.tif	2008_11_18_14_37_08	49	250628.49671	0.96000	1.650	
1435	001903.jpg	g	2008_11_18_14_37_08	8125	001903.tif	2008_11_18_14_37_08	81	250628.81253	1.06000	1.750	
1436	001904.jpg	g	2008_11_18_14_37_09	1216	001904.tif	2008_11_18_14_37_09	12	250629.12164	1.16000	1.810	

**Figure 6.2.3.1-8:** Navigation data file

**Table 6.2.3.1-2:** Description of navigation file data elements

001891.jpg	Image file
g_2008_11_18_14_37_05_0589_001891.tif	Geotiff file name
2008_11_18_14_37_05_05	Date (yyyy_mm_dd), local time (Central European Summer Time)
250625.059	UTC time (sec from 1.1.1970)
1.43000 1.13000 327.45000	Roll, pitch, heading (decimal degrees)
32.273309 -111.011925 1260.320	Latitude, longitude (decimal degrees), elevation (in meters), using WGS84 ellipsoid
0.00 0.00 0.00	Position accuracy of latitude, longitude, and height (meters)
-29.1	Height of DTM over ellipsoid (meters)
498876.99 3570730.66	UTM coordinates of airborne camera (meters)
498469.1058 0.9553 -0.0001	Affine-transformation matrix for geotiff: GT(0), GT(1), GT(2)
3571102.9184 -0.0001 -0.9564	Affine-transformation matrix for geotiff: GT(3), GT(4), GT(5)

JPG files that are converted from the geotiff files and the navigation file generated by Traffic Finder, the .hkd file (a parameter file for the images, including image resolution), and the

configuration file for ClickTool, are input files for the ClickTool software. A software program, Geotiff2, was used to convert Geotiff files generated by Traffic Finder to JPG files for ClickTool. Finally, the configuration file for ClickTool is shown in Figure 6.2.3.1-9.

```

1 @DATADEF
2 {
3   Char  achShMemName      [128]; // Basename of Shared-Memory between Main- and GUI-Application
4   Char  achFileNameGUI    [256]; // .exe-filename of GUI-Application
5   Char  achResultDir      [256]; // Directory to write the Results
6   Char  achSessionFileName[256]; // Any filename (with full path-name)of an image in the to use session
7   Char  achDefaultType    [ 64]; // default vehicle type
8   Long  lToolMode;        // 1: static camera, 2: flying camera
9   Long  lMaxImageWidth;   // max. viewing width of an image in GUI-Window
10  Long  lMaxImageHeight;  // max. viewing height of an image in GUI-Window
11  Long  lFirstImageNr;    // Second lowest Frame-Number of all images in the folder
12 };
13
14 @LIST
15 {
16   Config;
17 };
18
19 @Config
20 {
21   achShMemName      = ClickTool;
22   achFileNameGUI    = D:\KlickTool_original_2007-03-20\ClickGUI.exe;
23   achResultDir      = D:\Clicktool\Results;
24   achSessionFileName = D:\KlickTool_original_2007-03-20\jpg\20081218_00\20081218_00_000004112.jpg;
25   achDefaultType    = PKW;
26
27   lToolMode         = 2;
28   lMaxImageWidth    = 1100;
29   lMaxImageHeight   = 800;
30   lFirstImageNr     = 4113;
31 };

```

**Figure 6.2.3.1-9:** Configuration file for ClickTool

The steps used to identify (“click”) vehicles using ClickTool are presented in Table 6.2.3.1-3.

**Table 6.2.3.1-3:** Steps used to identify vehicles using ClickTool

Steps	Actions
1	Choose mode 3, in which a vehicle is defined by selecting the front and the back of a vehicle, as shown in Figure 6.2.3.1-10.
2	Press the button “Type” to define the vehicle type and the lane of the vehicle.
3	Click on the front and the back of a vehicle with the left mouse button while pushing <shift> button (magnifying glass).
4	Connect the vehicle to its location in the previous image.
5	Press <tab> and move to the next vehicle in the image. Repeat Steps 2-4 to define next vehicle.
6	Press <page down> to move to next image. Repeat Steps 2-5 in the next images.

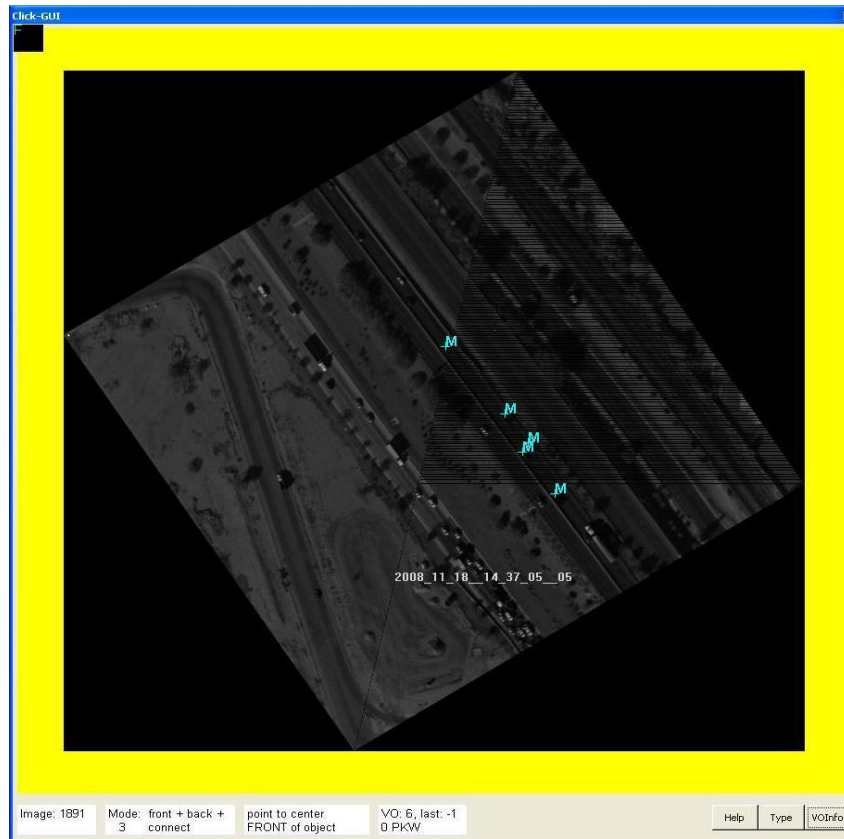


**Figure 6.2.3.1-10:** ClickTool GUI

The vehicles are clicked in each segment in each northbound or southbound run of the helicopter. In this case, three runs were made northbound (Westbound I-10), and two runs were made southbound (Eastbound I-10). To obtain speed estimates, vehicles were clicked in five successive images. The output file, Vehicles.log in Figure6.2.3.1-11, is used as input file of the Python code for the vehicle average speed calculation.

Finally, in the Python code, the longitude and latitude of the vehicle are calculated with the help of the result file from ClickTool and the navigation data file generated by Traffic Finder. If there is a clicked vehicle, its data will be written in the .log file, as shown in Figure 6.2.3.1-11. Only the coordinates of the front of the vehicle are used to calculate the distance that the vehicle has traveled.

```

Image_00001891_Vehicles.log x
0 10 20 30 40 50 60 70 80 90 100
37 @VehicleNr_1{
38   ulVehicleNr      = 1;                //Current vehicle number
39   ulVehicleNrLast = 1;                //Vehicle number in the last image; If there is no last number,
40                                           //"4294967295" is written.
41   ulStatus         = 0x00000003;      //lane; the fourth number after 0x describes the lane
42   ulVehicleType    = 0x00000010;      //type; the last two numbers describe the vehicle type
43   alTop            = 530, 497, 0x0001; //x and y coordinates of the top (pixel values)
44   alFront          = 530, 497, 0x0001; //x and y coordinates of the front (pixel values)
45   alBack           = 538, 508, 0x0001; //x and y coordinates of the back (pixel values)
46   alFrontLeft     = -32767, -32767, 0x0000; //Plausible numbers
47   alFrontRight    = -32767, -32767, 0x0000; //Plausible numbers
48   alBackLeft      = -32767, -32767, 0x0000; //Plausible numbers
49   alBackRight     = -32767, -32767, 0x0000; //Plausible numbers
50 };

```

Figure 6.2.3.1-11: Vehicles.log file

In addition, the following example entry can be found in the navigation data file:

```

001891.jpg g_2008_11_18__14_37_05__0589__001891.tif 2008_11_18__14_37_05__05
250625.05898 1.43000 1.13000 327.45000 32.273309 -111.011925 1260.320 0.00 0.00
0.00 -29.1 498876.99 3570730.66 498469.1058 0.9553 -0.0001 3571102.9184 -0.0001 -
0.9564 250625.05898

```

The bold numbers are affine-transformation matrix for geotiff: GT(0), GT(1), GT(2), GT(3), GT(4), and GT(5) in order. These six coefficients map the pixel coordinates into geo-referenced space based on the formula([http://www.remotesensing.org/gdal/gdal\\_datamodel.html](http://www.remotesensing.org/gdal/gdal_datamodel.html)):

$$X_{geo} = GT(0) + X_{pixel} * GT(1) + Y_{line} * GT(2) \quad (\text{Eq. 6.2.3.1a})$$

$$Y_{geo} = GT(3) + X_{pixel} * GT(4) + Y_{line} * GT(5) \quad (\text{Eq. 6.2.3.1b})$$

where  $X_{pixel}$  and  $Y_{line}$  are coordinates of the front of the vehicle.

The formula in (Eq. 6.2.3.2) is used to calculate the speed of the vehicle.

$$v = \frac{\sqrt{(X_{geo_c} - X_{geo_l})^2 + (Y_{geo_c} - Y_{geo_l})^2}}{T_c - T_l} \quad (\text{Eq. 6.2.3.2})$$

where  $X_{geo_c}$ ,  $Y_{geo_c}$  are geo-referenced coordinates of the vehicle in the current image,  $T_c$  is the time stamp of the current image,  $X_{geo_l}$ ,  $Y_{geo_l}$  are geo-referenced coordinates of the vehicle in the last image, and  $T_l$  is time stamp on the last image.

The Excel file produced by the Python code contains two sheets. Every row of first sheet corresponds to one vehicle and provides a reference to all images wherein the vehicle occurs. The second sheet contains calculation of the average speed, travel speed in the first image, and speed difference between travel speed in the first image and the average speed. Examples are shown below in Figure 6.2.3.1-12(a) and (b).

2. image						
Car_ID	TrafficLine	Image number	time (UNIX)	Xgeo	Ygeo	speed to last image [km/h]
1	3	001891	250625.059	498975.365	3570627.535	101.0
2	3	001891	250625.059	498941.935	3570674.402	125.0
3	4	001891	250625.059	498947.667	3570684.921	64.2
4	4	001891	250625.059	498923.788	3570717.442	69.4
5	3	001891	250625.059	498862.657	3570793.004	81.9

(a)

type	image number	first lane	last lane	average speed	travel speed	speed difference
Pkw	001890	3	3	91.2	96.6	5.4
Pkw	001890	3	3	102.6	128.9	26.3
Pkw	001890	4	4	75.9	82.1	6.2
Pkw	001890	3	4	78.9	76.8	2.1
Pkw	001890	3	3	102.9	98.4	4.5

(b)

**Figure 6.2.3.1-12:** Output Excel file containing (a) the vehicle and coordinates; and (b) the average vehicle speed

### 6.2.3.2 Traffic Density Calculation

In addition to vehicle speed, we also manually analyzed the imagery to produce estimates of density along the I-10 work zone. Determining density over roadway segments faces several somewhat subtle difficulties. In theory, in order to determine the density of vehicles, instantaneous images of the roadway segment are needed. However, covering the entire 4.5 miles of work zone roadway at a single instant is quite difficult and costly. In this study, the data consists of several sets of successive images over I-10, taken by a helicopter flying several times over the length of the freeway work zone. The problem with this set of data is that it takes a few minutes (and about 200 images) for the helicopter to cover the full segment.

The method we propose in this study is based on Daganzo's method of density calculation (Ch. 4 of Daganzo, 1977). In this method, vehicle trajectories are observed in a space-time area. The shaded portion in Figure 6.2.3.2-1 can be considered as the observation data set.

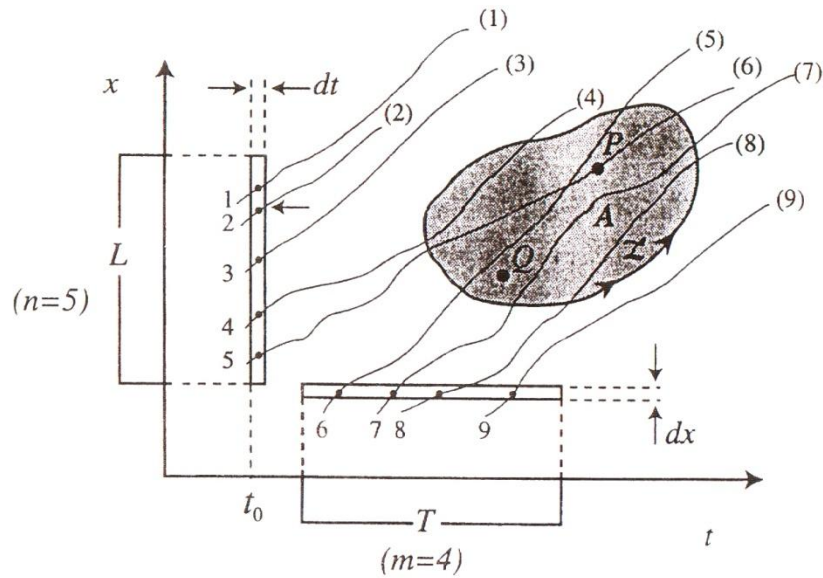


**Figure 6.2.3.2-1:** Vehicle trajectories and their intersection in time-space (Daganzo, 1977, Figure 4.1, p. 68)

This method uses an incremental approach and divides the observation region into small time and space increments to produce the density calculation formula:

$$Density = \frac{\text{Total time spent in space-time region by all vehicles (veh-hr)}}{\text{Area of the space-time region (mi-hr)}} \quad (\text{Eq. 6.2.3.2.1})$$

In order to apply this formula, one needs to consider the successive airborne images as the observation region, as shown in Figure 6.2.3.2-2. In this figure, the red bars illustrate the space-time regions captured by the various images. The number of vehicles observed in image  $i$  (number of intersections of trajectories with the red bar) is denoted by  $n(i)$ . The vehicle trajectories are shown as dashed lines.

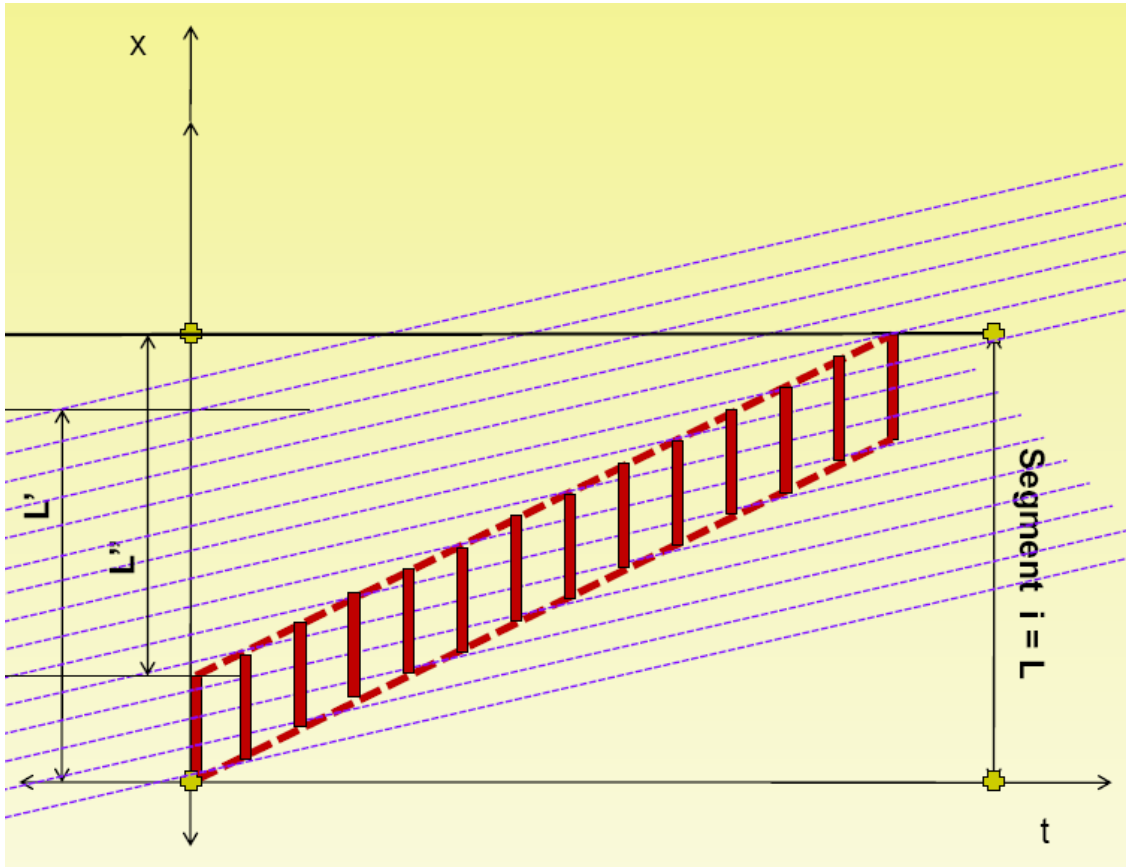


**Figure 6.2.3.2-2:** Images (red bars) in space and time across a set of vehicle trajectories

Considering a constant time interval of  $\Delta t$  between successive images ( $\Delta t = 0.33$  seconds in our study), we have:

$$Density = \frac{\sum_{i=1}^{N_s} n(i) \cdot dt}{L \cdot \Delta t} = \frac{\sum_{i=1}^{N_s} n(i) \cdot dt}{L \cdot \Delta t} = \frac{\sum_{i=1}^{N_s} n(i)}{L \cdot \frac{\Delta t}{dt}} = \frac{\sum_{i=1}^{N_s} n(i)}{L \cdot N_s} = \frac{1}{N_s} \sum_{i=1}^{N_s} n(i) = \frac{\text{Avg. number of vehicles in images}}{\text{Length of roadway in images}}$$

(Eq. 6.2.3.2.2)

where:

- Ns= number of images,
- n(i)= number of vehicles observed in each image,
- dt= constant time interval (0.33 sec in our study)
- L= constant span of images (0.16 mile in our study).

Based on (Eq. 6.2.3.2.2), the density can be directly calculated based on number of vehicles observed in each image.

The advantages of this method for calculating densities are three-fold. First, this method can be used for both traffic streams, the one moving in the same direction as the camera and the other moving in the opposite direction as the camera. Second, this method can be automatically applied when conducting image processing techniques for extracting data. Third, this method calculates the density independent of the speed of the camera and of the speed and direction of traffic. In this way there is high accuracy in the calculations of density resulting from the camera and traffic movements.

### **6.3 Selected Results**

In general, the I-10 work zone operated very efficiently during the construction. Primary sources of congestion were related to cross-street traffic along the frontage roads on either side of I-10. In these cases, it was anecdotally observed that the delays at these intersections were incrementally higher than before construction began. However, along the I-10 corridor itself, both along the freeway lanes and along the frontage roads, the level of congestion was significantly lower than expected. As will be shown below, the primary sources of congestion were at the endpoints of the work zone: at 29<sup>th</sup> Street, for traffic traveling westbound, and at Prince Road, for traffic heading eastbound. Much of the successful traffic performance has been attributed by local traffic engineers to an Interim Traffic Operations Center (ITOC) that was operated 24 hours per day, 7 days per week, during the project. Operators at the ITOC were able to monitor the full work zone using only freeway cameras. Nonetheless, the operators had access to more than 30 signal timing plans for operating the frontage roads, allowing great flexibility in enhancing through movements along the frontage roads. In total, the strategies for work zone management were considered highly successful for this project.

More quantitative evidence can be seen in the measures of speed and density from the flights made over the I-10 work zone. Table 6.3-1 and Table 6.3-2 show the average density over the roadway segments between interchanges in the work zone, for westbound and eastbound I-10, respectively. In addition, Tables 6.3-3 and 6.3-4 show the average speed over these same roadway segments, again for westbound and eastbound I-10, respectively. Westbound and eastbound runs 1-3 were made during the mid-day (assumed off-peak) period, while runs 4 and 5 and southbound 4 occurred later in the afternoon, during what is considered the PM peak period.

**Table 6.3-1:** Density of traffic (veh/lane-mi), Westbound I-10 (Runs 1-3 are in the mid-day; runs 4-5 are in the PM Peak)

Density	29 <sup>th</sup>	22 <sup>nd</sup>	Congress	St. Mary's	Speedway	Grant	Miracle Mile	Prince
Run # 1					29.6	34.7	52.5	36.7
Run # 2	28.5	23.9	15.2	22.6	49.3	54.5		
Run # 3	25.4	19.4	18.0	23.3	25.9	21.1	25.7	19.8
Run # 4	72.2	47.0	41.4	22.8	36.9	40.1	51.7	27.1
Run # 5	61.9	38.7	16.6	42.2	37.8	12.1	37.7	25.5

**Table 6.3-2:** Density of traffic (veh/lane-mi), Eastbound I-10 (Runs 1-3 are in the mid-day; run 4 is in the PM Peak.)

Density	Prince	Miracle Mile	Grant	Speedway	St. Mary's	Congress	22 <sup>nd</sup>	29 <sup>th</sup>
Run # 1	31.0	24.6	18.8	23.4	11.0	7.2	22.8	31.7
Run # 2			33.0	18.4	19.1	31.1	28.5	14.1
Run # 3	23.4	15.2	5.4	30.1	3.7	28.6	20.8	35.2
Run # 4	8.3	28.1	20.8	20.3	21.1	14.8	21.5	2.3

**Table 6.3-3:** Average speed of traffic (mph), Westbound I-10 (Runs 1-3 are in the mid-day; runs 4-5 are in the PM Peak.)

Average Speed	29 <sup>th</sup>	22 <sup>nd</sup>	Congress	St. Mary's	Speedway	Grant	Miracle Mile	Prince
Run # 1					69	49	49	57
Run # 2	62	72	82	66	57	55	46	
Run # 3	24	24	25	26	20	26	31	34
Run # 4	59	33	23	16	31	24	29	44
Run # 5	53	27	23	20	30	49	28	42

**Table 6.3-4:** Average speed of traffic (mph), Eastbound I-10 (Runs 1-3 are in the mid-day; run 4 is in the PM Peak.)

Average Speed	Prince	Miracle Mile	Grant	Speedway	St. Mary's	Congress	22 <sup>nd</sup>	29 <sup>th</sup>
Run # 1	81	68	84	81	70	69	68	66
Run # 2			42	47	30	22	15	32
Run # 3	36	45	41	36	35	24	29	26
Run # 4	43	53	52	44	47	36	38	34

By examining the results in the tables, one can see some interesting trends on traffic patterns. During the mid-day period (runs 1-3), the westbound traffic appears to move fairly smoothly up until Miracle Mile (run 1) or up to Grant and Speedway (run 2). This is reflected in the relatively high average speeds over these segments on the southern end of the work zone (Table 6.3-3), but with lower speeds and higher densities on the northern end toward Speedway, Grant, and Miracle Mile. While densities are relatively low during run 3 in the westbound direction (Table 6.3-1), the speeds are consistently low, hovering around 25 mph. This reflects perhaps a more substantive shift in the traffic regime in the work zone, where both densities and speeds are low.

During the peak periods (runs 4-5), the westbound traffic seems to move consistently slower, with lower average speeds over the whole work zone (Table 6.3-3). Also supporting this conclusion of higher congestion, there are relatively high densities of westbound traffic near 29<sup>th</sup> Street and 22<sup>nd</sup> Street, and again around Miracle Mile.

The densities of traffic through all the eastbound runs are consistently low throughout the work zone. This may be related to the time of day, in which the eastbound movements are in the off-peak direction. However, there are cases throughout the latter three runs (runs 2-4) where the average speeds are much lower, under 50 mph and in some cases even under 30 mph, particularly toward the southern end of the work zone (St. Mary's, Congress, 22<sup>nd</sup>, and 29<sup>th</sup>). At this southern end, it is not uncommon to have more significant traffic congestion in the PM peak, at the merger of I-10 and I-19 just south of 29<sup>th</sup> Street. Nonetheless, the results would suggest that conditions of both low speeds and low densities do exist in the work zone.

## **6.4 Conclusions**

Both the traditional camera platform system and the high-resolution ANTAR system allowed us to document queue lengths and determine traffic densities in the work zone. However, the ANTAR system also allowed vehicle speed information to be automatically generated from the geo-referenced imagery using automated vehicle detection and tracking. While proving the ability to produce these traffic measures and demonstrating the value of the better technology for airborne traffic data collection, no major work-zone induced congestions was observed in the empirical study, mainly because of successful traffic management in the corridor.

## Section 7. Conclusions

We were successful in using remote sensing and geospatial technologies to collect data on truck activity times at international border crossings and around work zones. The geo-fence approach employed at the Ambassador Bridge and Blue Water Bridge crossing sites was able to produce unprecedented level of detail on multiple activity times at these sites. Because the approach takes advantage of existing hardware, software, and communications systems that are already being used by some existing truck fleets, the activity time information could be obtained with minimal additional data collections costs. The added data communication fit easily in the carrier's budget and added no data transmission costs. Once we developed the concepts, the data processing, data cleaning, and trip chaining tasks were done with limited human intervention. These steps could be automated further if a system were to be developed for ongoing, operational use. In addition, because the geo-fences can be implemented remotely, no roadside hardware is required. Data can thus be collected on multiple activities without having to negotiate institutional barriers that may be imposed by the multiple agencies and industries operating the border crossing infrastructure and facilities. In addition, the geo-fences can be easily updated in the event that information on new activities is desired, refinements to existing geo-fences are warranted, or the physical infrastructure where activities occur changes.

Because of the ability to continually collect data, the geo-fence approach is also attractive for determining patterns in the activity times and for ongoing monitoring of activity times. We were successful in demonstrating patterns in overall crossing times and in queuing times that depended on crossing site, direction of travel, and time of day. The data also highlighted stability in the distributions of times associated with primary customs inspection. In addition, we demonstrated the usefulness of the data collected in this ongoing fashion in documenting decreased queuing times that resulted from improved traffic management at one of the crossing sites.

The primary deficiency of the geo-fence approach employed here is that it requires data from private carriers. The carrier's fleet must regularly traverse the border if the data are to provide a picture of activity time patterns, rather than anecdotal information on a single crossing. We were fortunate to have been entrusted with the data of CEVA Logistics, whose fleet regularly traverses the border crossing sites. However, since the trucks in the CEVA fleet are all FAST-certified, the CEVA times would not necessarily be representative of activity times of the broader truck population using the crossing. Indeed, comparisons with estimates of times produced from other data indicate that the CEVA times would likely provide good estimates of inspection and queuing time patterns for FAST-certified shipments, but would only yield rough estimates of patterns for general shipments.

The air-based data collections we undertook in a validation effort at the Ambassador Bridge and Blue Water Bridge crossing sites and as a primary data source at the Mariposa Port of Entry produce information on the broader truck population without a need to deploy any roadside

infrastructure. However, institutional arrangements must still be made to avoid suspicion that the aircraft is “loitering” near sensitive infrastructure while collecting data for an extended time. Of greater concern, the high cost of collecting data using airborne platforms (we used both fixed wing and helicopter) makes such an approach economically infeasible for continuous activity time monitoring. Nevertheless, we demonstrated how the airborne data can be used for one-time studies and for infrequent data collection. We also demonstrated how the airborne data can be used to complement less expensive ground-based data collection for special studies. With the airborne platform, more detailed activity times can be obtained between the locations that are observed with the ground-based surveillance. In addition, the aerial perspective offers a synoptic view of activities that can provide a general understanding of flow processes that aid in interpreting the data collected with traditional ground-based methods or with the geo-fence method.

Although not foreseen when developing the scope of work, we were able to conduct a preliminary comparison of overall crossing times determined from our geo-fence data with Transport Canada data obtained with another technology. The Transport Canada data were obtained from a set of trucks that represented a broader cross-section than the CEVA fleet used to produce our geo-fence data. There were also differences between the locations between which crossing times were measured. Despite these differences and the preliminary nature of the comparisons, there were enough similarities between the data sets to encourage further comparisons and possibly combining the data sets to produce improved estimates of activity times than can be produced from either set by itself or developing an approach that includes the salient features of each approach.

We also demonstrated that the data collected could be used with other data sources to estimate aggregate, macroscopic models of queuing time upstream of primary customs screening as a function of traffic volumes and number of inspection booths open. The coefficients were statistically significant and had the anticipated signs, but the explanatory power of the models does not appear sufficient for prediction and “what if” purposes. The inspection processes are likely too dynamic and too complex to be captured in such aggregate models. We illustrated the development of a microsimulation model to capture these dynamic and complex interactions. We used the data obtained from the aerial imagery to calibrate truck activity time distributions and the general patterns of truck routing for a model of the Mariposa Port of Entry. We did not have the extended data required to validate the models and, subsequently use them to explore “what if” scenarios, but collecting such data seems feasible with the geo-fence approach or with the air-based approach used in this study.

For the work zones, we consider our efforts to have been successful in using advanced remote sensing and spatial information technologies to monitor traffic conditions. The data collection methods can range from simple manual methods (*e.g.*, observing traffic densities) to much more sophisticated hardware and software tools for image processing (*e.g.*, estimating individual vehicle speeds). Surprisingly, the expected construction impacts failed to materialize in our study

zone. Thus, while we have ample results as a proof-of-concept, we do not have any major findings on the impacts of work zones on traffic behavior, or the effect of specific construction activities on traffic congestion.

We believe that we have been successful in showing that novel use of remote sensing and geospatial information technologies already in use by many carriers can produce truck activity time information at border crossing facilities. We also believe that we have been successful in demonstrating that imagery collected from airborne platforms can provide quantitative measures of traffic conditions in an around work zones.

## REFERENCES

- Ambassador Bridge Facts, [www.ambassadorbridge.com/IntlCrossing/BridgeFacts.aspx](http://www.ambassadorbridge.com/IntlCrossing/BridgeFacts.aspx), accessed on September 4, 2010
- Arc2Earth, <http://www.arc2earth.com/>, accessed on July 14, 2010.
- Ben Akiva, M. and S. Lerman, *Discrete Choice Analysis: Theory and Application to Predict Travel Demand*. MIT Press: Boston, 1985.
- Blue Water Bridge Info, [http://www.bwba.org/bridgeinfo\\_e.html](http://www.bwba.org/bridgeinfo_e.html) , accessed on September 4, 2010.
- Bradbury, Susan L., "An assessment of the free and secure trade (FAST) program along the Canada-US border," *Transport Policy*, Vol. 17: 367-380, 2010
- Canada Border Services Agency, NEXUS Highway and FAST Programs Evaluation Study, Ottawa, Canada, 2008, <http://cbsa-asfc.gc.ca/agency-agence/reports-rapports/ae-ve/2008/nf-ne-eng.html>, accessed July 27, 2010.
- Customs and Border Protection Agency, U.S./Canada FAST program, [http://www.cbp.gov/xp/cgov/trade/cargo\\_security/ctpat/fast/us\\_canada/](http://www.cbp.gov/xp/cgov/trade/cargo_security/ctpat/fast/us_canada/), accessed July 27, 2010.
- Daganzo, C.F., *Fundamentals of Transportation and Traffic Operations*. Pergamon: New York, 1997.
- Dong, Hao, Mark R. McCord, and Prem K. Goel, "Empirical Truck Activity Times and Excess Times at International Crossings using Electronic Geo-fences," *Working paper*, The Ohio State University, December 2009.
- Esmer, Berker, "An Analysis of Gamma Mixtures for Service Networks," *MS Thesis*, Department of Systems and Industrial Engineering, University of Arizona, 2009.
- Federal Highway Administration, *Work Zone Impacts Assessment: An Approach to Assess and Manage Work Zone Safety and Mobility Impacts of Road Projects*, Publication No. FHWA-HOP-05-068, 2006.
- Federal Highway Administration, *Traffic Analysis Toolbox Volume VIII: Work Zone Modeling and Simulation - A Guide for Decision-Makers*. Publication No. FHWA-HOP-08-029, August 2008.
- Federal Highway Administration, *Traffic Analysis Toolbox Volume IX: Work Zone Modeling and Simulation - A Guide for Analysts*. Publication No. FHWA-HOP-09-001, March 2009.
- Google Code, <http://code.google.com/apis/kml/documentation/>, accessed on July 22, 2010.

Google Maps,

<http://maps.google.com/support/bin/static.py?hl=en&page=guide.cs&guide=21670&topic=21676&from=21676>, accessed on July 22, 2010.

Jeannotte, K., A. Chandra, V. Alexiadis, and A. Skabardonis, *Traffic Analysis Toolbox Volume II: Decision Support Methodology for Selecting Traffic Analysis Tools*. June 2004.

Liang, Jinjian, Mark R. McCord, and Prem K. Goel, *Truck Screening Time Analysis of the U.S.-Canada International Border*, Working paper, The Ohio State University, September 2009.

Mannering, F., S. Washburn, and W. Kilareski, *Principles of Highway Engineering and Traffic Analysis*. 4<sup>th</sup> Edition, John Wiley and Sons, Hoboken, NJ, 2009.

McCord, M.R., P.K. Goel, P. Kapat, C. Brooks, R. Wallace, and H. Dong, *Empirical Evidence of Decreased Truck Queuing Times from Traffic Management Changes at the Blue Water Bridge using Geo-fence Derived Data*, Working paper, The Ohio State University, July 2010.

McCord, M., P. Goel, P. Kapat, H. Dong, and J. Liang, *Manual for Extracting Travel Information from 13 Geo-fence Database on International Border Crossings*, The Ohio State University, [http://www.stat.osu.edu/~pkapat/bc/CRESTA\\_Manual.pdf](http://www.stat.osu.edu/~pkapat/bc/CRESTA_Manual.pdf) , 2009, accessed on November 9, 2009.

McCullagh, P. and J.A. Nelder, *Generalized Linear Models*, 2<sup>nd</sup> Edition, Chapman & Hall, 1989.

Michigan Department of Transportation. *I-75 Gateway Project*. [www.michigan.gov/gateway](http://www.michigan.gov/gateway), accessed on July 1, 2009

Neto, O., Lee D. Han, and Myong K. Jeong, *Tracking Large Trucks in Real Time with License Plate Recognition and Text-Mining Techniques*. Paper presented at the 88<sup>th</sup> Annual Meeting of the Transportation Research Board, Washington, DC.  
<http://trb.metapress.com/content/7372g05382k11883/> 2009, accessed July 25, 2010.

PTV, *VISSIM 4.30 User Manual*, Karlsruhe, Germany, May, 2007.

PTV, *VISSIM 4.30-04 COM Interface Manual*, Karlsruhe, Germany, September, 2007.

RTI International, *The Economic Benefits of Expanding the Border-Crossing for Commercial Vehicles at the Mariposa Crossing in Nogales, Arizona*. Final Report, June 2007.

Sabean, J., and C. Jones, *Inventory of Current Programs for Measuring Wait Times at Land Border Crossings*. Transport Canada and Federal Highway Administration, for the U.S. Department of Homeland Security and Canada Border Services Agency. 25 pp.  
[http://www.thetbwg.org/downloads/Inventory%20of%20Current%20Wait%20Time%20Programs\\_May%2021%202008.pdf](http://www.thetbwg.org/downloads/Inventory%20of%20Current%20Wait%20Time%20Programs_May%2021%202008.pdf) , 2008, accessed February 11, 2009.

Shallow, T., *CV Border Wait-Time Measurement Project*, Presentation at the Transportation Border Working Group Data Workshop, Romulus, MI, June 2008,  
[http://www.thetbwg.org/meetings-archive-200806\\_e.htm/10](http://www.thetbwg.org/meetings-archive-200806_e.htm/10), accessed on August 15, 2010.

Szuch, Michael, Blue Water Bridge Manager for Michigan Department of Transportation, personal communications, Feb 20, 2010

Texas Transportation Institute and Department of Civil and Environmental Engineering, Univ. of Washington, *Developing Framework for Collecting and Sharing Data and Information*, Prepared for Office of Freight Management and Operations, FHWA and TBWG Travel and Trade Data Subcommittee, 2009.  
[http://www.thetbwg.org/downloads/TBWG\\_Data\\_Framework\\_Final\\_Report\\_052909.pdf](http://www.thetbwg.org/downloads/TBWG_Data_Framework_Final_Report_052909.pdf), accessed February 11, 2010.

Texas Transportation Institute and Battelle Memorial Institute. *Evaluation of Travel Time Methods to Support Mobility Performance Monitoring: FY 2001 Synthesis Report*.  
[http://ops.fhwa.dot.gov/freight/freight\\_analysis/brdr\\_synthesis/](http://ops.fhwa.dot.gov/freight/freight_analysis/brdr_synthesis/) 2002, accessed July 26, 2007.

TOLLROADSnews, <http://www.tollroadsnews.com/node/4825#attachments>, accessed July 28, 2010

Turnbull, K. F. *Performance measures to improve transportation systems*. Transportation Research Board, 2005.

US Customs and Border Protection, *Border Wait Times*, <http://apps.cbp.gov/bwt/>, 2010, accessed July 30, 2010.

U.S. DOT, Research and Innovative Technologies Administration, Bureau of Transportation Statistics, *America's Freight Transportation Gateways*, November 2009,  
[http://www.bts.gov/publications/americas\\_freight\\_transportation\\_gateways/2009/pdf/entire.pdf](http://www.bts.gov/publications/americas_freight_transportation_gateways/2009/pdf/entire.pdf), accessed June 7, 2010.

Villalobos, J.R., A. Maltz, O. Ahumada, G. Treviño, O. Sánchez and H.G. Garcia, *Logistics Capacity Study of the Guaymas-Tucson Corridor*. Report completed for the CANAMEX Corridor, 2006.

APPENDIX TO SECTION 1  
SUMMARY OF TECHNICAL EXPERT ADVISORY  
COMMITTEE MEETINGS HELD IN 2010

**Technical Expert Advisory Committee (TEAC)**  
**Southern Border Meeting Summary**  
**Consortium for Remote Sensing of Traffic Activities (CRESTA)**  
**April 27, 2010, 9:00 am-11:45 am**  
*The Brickyard, Arizona State University, Tempe, AZ*

Participants

Team Members: Pitu Mirchandani, Arizona State University  
Mark McCord, The Ohio State University  
Mark Hickman, University of Arizona

Committee Members: Scott Nodes, Arizona Department of Transportation  
Tom Buick, Independent Consultant  
Aichong Sun, Pima Association of Governments (on-line)  
David Gibson, Federal Highway Administration (on-line)

Other Participants: David Lucas, Arizona State University  
Monica Gentile, visiting scholar, Arizona State University  
Eileen Mandl, visiting scholar, Arizona State University

The meeting began at approximately 9:10 am with introductions.

Mark McCord, Principal Investigator, began the program with a review of the CRESTA activities. He described the background of the team in terms of its remote sensing expertise and experience. The scope of work was reviewed, covering truck activities at international border crossings and truck and traffic flows in major construction work zones. The project focused on site-specific studies of these truck movements, and involved different means of data collection: use of GPS-based truck tracking information at the northern border, and the use of airborne imagery from the southern border. Mark also covered the expectations for this meeting: that we would have the opportunity to present findings from the program, and that we would seek the advice of the TEAC in terms of potential spin-offs and continuing research moving forward from this point.

Mark McCord then proceeded to describe the major activities at the northern (US-Canada) border, looking specifically at two bridge crossings: the Ambassador Bridge and the Blue Water Bridge, between Michigan and Ontario. He outlined the cooperative work with CEVA Logistics and General Motors, allowing the team to monitor GPS locations of trucks as they moved through the border area. Specifically, he described the use of “geo-fences” to determine truck activity times. These “geo-fences” consist of a set of polygons that can be used to describe areas where specific activities occur (e.g. primary or secondary inspection). These geo-fences are downloaded to the trucks, and a record is sent to the fleet manager (CEVA Logistics) every time a truck crosses a geo-fence.

The presentation on the northern border then turned to a discussion of the results. These included estimates of the mean and distribution of truck crossing times, and the estimation of “excess time” (time in excess of free-flow travel time through the area). The results also include estimates of travel times and excess times for different activities, including primary inspection, secondary inspection, duty-free activities, and other related activities at the border. Finally, a validation of the data set using airborne imagery was also presented, discussing possible differences between the CEVA trucks (which are FAST-certified) and the universe of all trucks at the crossing.

Major questions on this presentation included: (1) the resolution of the GPS and of the geo-fences, and possible errors in determining crossing times; and, (2) the possible use of Transport Canada Bluetooth data as another source of data for travel time estimation or validation.

The second major presentation was made by Mark Hickman and discussed the data collection and findings from the southern border and from the I-10 work zone in Tucson. The presentation covered the use of airborne imagery as the primary form of data collection, using imagery to track truck movements and to measure queues at various locations at the border in Nogales, Arizona. The data collection also included complementary manual counts of truck movements on the ground, as well as license-plate tracking of trucks from one side of the border crossing to the other. The airborne imagery provides the primary data on truck arrival rates, inspection times, and truck diversion probabilities (i.e., the probability of being routed to different inspection stations in the port of entry). This in turn was validated using the license plate data and some statistical inference from those data. Also, the use of the ANTAR imaging platform from the German Aerospace Center (DLR) assisted in a second data collection effort. The ANTAR system allows for automatic registration and tracking of vehicles from airborne imagery.

The truck movement data from Nogales, and from the Blue Water Bridge on the northern border, were used to calibrate a truck simulation model for both border crossings. The simulation model uses VISSIM as a tool for simulating vehicle movements in and around the port of entry, and a software interface using Visual Basic (VB) allows one to establish various parameters for the inspection times and the truck routing probabilities. Both simulation models were demonstrated, although no “what-if” scenario analysis has been conducted to date.

Mark Hickman also presented results from the I-10 work zone study. In this case, standard airborne imagery as well as imagery collected with ANTAR were analyzed. The study investigated queuing on the side streets and frontage roads, vehicle speeds, and vehicle densities were measured. Originally, planners expected the I-10 reconstruction project to cause major disruptions to traffic on I-10, on the frontage roads, and on side streets crossing I-10. Surprisingly, the resulting traffic speeds and densities, and roadway queue lengths, indicate that there was little or no major changes in traffic conditions along I-10 or on neighboring roadways. These observations from the imagery mimic the overall consensus view of the successful traffic management during this construction project. However, this meant that little was learned through the I-10 monitoring as part of this project.

There were no additional comments or questions raised on this project at the conclusion of the meeting, and the meeting adjourned at 11:45 am.

**Technical Expert Advisory Committee (TEAC)**  
**Northern Border Meeting Summary**  
**Consortium for Remote Sensing of Traffic Activities (CRESTA)**  
**June 11, 2010, 8:30 am-1:00 pm**

*The Dave House Center, Michigan Tech Research Institute (MTRI), Ann Arbor, MI*

Participants

Team Members: Mark McCord, The Ohio State University  
Prem Goel, The Ohio State University  
Mark Hickman, University of Arizona  
Colin Brooks, Michigan Tech University – MTRI  
D. Eric Keefauver, Michigan Tech University – MTRI  
K. Arthur Endsley, Michigan Tech University – MTRI  
Greg Jordan, Skycomp

TEAC Members: Jim Phillips, General Motors  
Chris Dingman, Federal Highway Administration  
Dave Franklin, Federal Highway Administration  
Jim Schultz, Michigan Department of Transportation  
George Saylor, Ohio Department of Transportation  
Tony Shallow, Transportation Canada – Ontario Region

Local Stakeholders: Ray Cossette, CEVA Logistics  
Bill Anderson, University of Windsor  
Trevor Brydon, Southeast Michigan Council of Governments  
Tim Heideman, Blue Water Bridge – MDOT  
Jessee Gwilliams, Michigan Department of Transportation

The meeting began at approximately 9:00 am with welcome and introductions by Colin Brooks.

The meeting was led by a presentation from the CRESTA team leaders Dr. Mark McCord and Dr. Prem Goel. The geofence-based approach was outlined with an emphasis on the implementation specific to the northern border. As the concept of geofences was introduced, one TEAC member asked whether or not geofences can be changed “on the fly”? The CRESTA pointed out that the answer depends on the precise meaning of “on the fly” but that in general they can be changed when needed and had already been refined several times for this project. In discussing the data generated from the geofence-based approach, another question was raised about trip chaining, and a team member highlighted the necessity of figuring out, for each vehicle, what observations correspond to each of its trips across the border and how this was accomplished using trip chaining.

A virtual tour of the geofences used at the Ambassador and Blue Water Bridges was given with sufficient detail to communicate the procedure. Descriptive statistics were provided to illustrate the work that had been done so far and the valuable information on crossing times and excess times obtained from the team’s methods of applying geofences and Position, Navigation, and

Timing (PNT) data. The precise position of duty-free fences and the differences between accounting for and omitting that segment of truck trips was presented. The temporal patterns of crossing times, one interesting way to represent truck traffic data collected in this project, were displayed. As the definition of excess times was presented, a team member pointed out that, as expected, there is more queuing (excess) time going into the U.S. than going into Canada. The difference between queuing times before and after FAST-lane separation was highlighted and it was demonstrated to be a significant difference that could not be explained by differences in traffic volumes. When the subject of primary inspection screening came up, a TEAC member raised the question of whether there was any correlation between the Homeland Security threat level or bridge security and screening gap excess times. The discussion that followed indicated there is a great deal of interest in knowing the proportions of trucks selected for secondary inspection as well as the total number of trucks in using the FAST lane.

At the end of the presentation, other activities such as aggregate modeling and air-based visualization were detailed by Dr. Mark Hickman. The aggregate modeling involved correlation of excess times with traffic conditions with the ultimate goal of predicting excess times and included an attempt to determine what number of lanes are open based on excess times. At this point, CRESTA team members described they are not currently comfortable using the data for predictive modeling. Questions from the TEAC included whether or not finer-grained (i.e. better than hourly) truck observations are needed and whether or not the capacity of the bridge plaza itself has an effect on the crossing time. Team members communicated that data can be presented at finer-grained scales than an hourly basis. Following the presentation on aggregate modeling, initial correlations between SkyComp aerial data and the geofence-derived data were presented. The differences between the two methods of collection was emphasized for all meeting participants: SkyComp data was only available for 40 minutes at a time, whereas the geofence-derived data is available all hours of the day every day. The TEAC members showed considerable interest in what the SkyComp data had to say about FAST lane use at this time. Colin Brooks presented examples of using geospatial tools such as Google Earth, ArcGIS, and open source web mapping tools for visualizing and communicating study results.

Following the presentations, input was sought from the TEAC that generated ultimately generated a discussion about the potential audience for the results of this study or future studies. Some potential clients discussed included state DOTs, infrastructure operators, and freight carriers. Homeland Security and the State Department were also identified as potential clients, even though they are not freight stakeholders, because they may be interested in top-level, border-related applications. U.S. Customs and Border Patrol was identified as a potential user but, as one TEAC member pointed out, crossing times are not a top priority for them—in fact, for other potential users, as well, overall efficiency is not necessarily the top priority. It became apparent from the discussion that performance was going to be defined by the audience, and it would be extremely useful to quantify performance as it provides a sense of what can be improved.

Richard Wallace led the discussion of results and future potential applications of this study. A representative of the Southeast Michigan Council of Governments (SEMCOG) indicated they would benefit a great deal from a robust traffic volume/crossing time database, and that community members in southeast Michigan have an impression that crossing times are very long,

which discourages travel between the U.S. and Canada. U.S. Customs and Border Patrol or the Commercial Vehicle Safety Alliance might be amenable to make some changes (e.g. open more car lanes) if we were able to bring them some quantitative data in support of such a measure. As our Transport Canada TEAC member pointed out, the real value of the study is in this legacy of the time series and the level of detail that we are able to provide that reflects the commercial trucking activities along the route.

The sensitivity of the data was another issue brought up during the TEAC meeting. For instance, it is likely that some carriers will not want to release their data out of concern it will be used against them or shared in some way. Thus, the need to consolidate carrier data and insure anonymity was identified as a priority. The solution to such a problem may also involve outreach to carriers, perhaps performed by one of our existing partners such as CEVA Logistics, which may convince them to share their data in a secure environment. This issue came up again with regards to secondary inspections. A declining number of secondary inspection referrals would be good press for a carrier but they could also not want their secondary inspection rate to be known.

#### **Agenda – Northern Border TEAC Meeting, 6/11/2010**

8:30-9:00	Continental Breakfast
9:00 -9:10	Welcome and Introductions - Colin
9:10 -9:20	Meeting Overview and Expectations - Prem
9:20 -9:30	CRESTA Project Scope - Mark M
9:30--10:30	Geo-Fence Approach and Results at the Northern Border - Mark M
10:30 -10:45	Break
10:45-11:15	Results from the Southern Border and Microscopic Modeling -Mark H
11:15-11:30	Visualization - Colin
11:30-12:15	Discussions of Results and Future Potential -Richard
12:15-1:00	Lunch with Continued Discussion
1:00	Adjourn

APPENDIX TO SECTION 2  
TABLES IN SUPPORT OF SECTION 2.4.2

Note: Cells or column headings marked with a \* **in any Table in this Appendix are not applicable** because of Construction in the US Ambassador Plaza

**Table A2.4.2-1** Free flow speeds (mph) for various geo-fences at the Ambassador Bridge

Geo-fence name	US-to-Canada	Canada-to-US
Wtw amb usapproach**	55/62/25	-
Amb usdutyfree*	21	-
Amb usplaza toll2CA*	18	-
Amb usplaza toll2CAexit*	22	-
Amb usplaza tollfCA	-	12
Amb ustoll	-	10
Amb usplaza	-	25
Amb usbridge	41	37
Amb cabridge	71	37
Amb caplaza	24	29
Amb cadutyfree	-	15
Amb hurnchrchrd	44	43
Amb caapproach	55	57

\*\* Approaches from three directions. - Not used in this direction.

**Table A2.4.2-2** Free flow speeds (mph) for various geo-fences at the Blue Water Bridge

Geo-fence name	US-to-Canada	Canada-to-US
Wtw bwb 6994split	65	65
Bwb splitplaza	65	63
Bwb rte25collect	40	36
Bwb usplazabridge	40	36
Bwb caplazabridge	40	35
Bwb cadutyfree	-	15
Bwb caapproach	67	60

- Not used in this direction

**Table A2.4.2-3** Free flow speeds (mph) for roadway section including toll collection and customs inspection, in the US-to-Canada direction at the Ambassador Bridge

Geo-fence Name	Free flow speed for bounding geo-fences	Free flow speed for gap	Distance of gap** (mile)
Toll collection*			
amb_usplaza_toll2CA*	18	22	0.02
amb_usplaza_toll2CAexit*	22		
Customs inspection			
amb_caplaza	24	44	0.03
amb_huronchrchrd	44		

\*\* based on median of crossing records.

**Table A2.4.2-4** Free flow speeds (mph) for roadway section including toll collection and customs inspection, in the Canada-to-US direction at the Ambassador Bridge

Geo-fence Name	Free flow speed for bounding geo-fences	Free flow speed for gap	Distance of gap** (mile)
Customs inspection			
amb_usplaza	25	25	0.01
amb_ustoll	10		
Toll collection			
amb_ustoll	10	12	0.02
amb_usplaza_tollfCA	12		

\*\* based on median of crossing records

**Table A2.4.2-5** Free flow speeds (mph) for roadway section including toll collection and customs inspection, in the US-to-Canada direction at the Blue Water Bridge

Geo-fence Name	Free flow speed for bounding geo-fences	Free flow speed for gap	Distance of gap** (mile)
Toll collection			
bwb_rte25collect	40	40	0.02
bwb_usplazabridge	40		
Customs inspection			
bwb_caplazabridge	40	67	0.02
bwb_caapproach	67		

\*\* based on median of crossing records

**Table A2.4.2-6** Free flow speeds for roadway section including toll collection and customs inspection, in the Canada-to-US direction at the Blue Water Bridge

Geo-fence Name	Free flow speed for geo-fence	Free flow speed for the gap (mph)	Distance of gap** (mile)
Toll collection			
bwb_caapproach	60	60	0.02
bwb_caplazabridge	35		
Customs inspection			
bwb_usplazabridge	36	36	0.02
bwb_rte25collect	36		

\*\* based on median of crossing records

**Table A2.4.2-7** Activity times for various geo-fences ,US-to-Canada direction, Ambassador Bridge

	Amb usapproach	Amb* sdutyfree	Amb* usplazatoll2ca	Amb* usplazatoll2caexit	Amb usbridge	Amb cabridge	Amb caplaza	Amb huronchrchrd	Amb caapproach
#	9088	9186	4730	4722	9190	9195	9193	9189	8687
Mean	6.43	3.84	0.24	0.17	0.87	1.53	1.93	5.40	8.33
S.D.	13.31	13.64	0.53	0.58	0.64	1.78	3.06	2.40	4.32
Max	538.47	534.43	35.00	40.00	45.00	65.53	96.42	89.73	351.02
Min	0.18	0.10	0.10	0.10	0.13	0.12	0.17	0.92	1.28
90P	8.82	4.82	0.28	0.20	1.02	1.78	5.05	6.77	10.08
75P	6.65	3.68	0.25	0.17	0.90	1.40	2.48	6.00	9.00
50P	4.93	2.23	0.22	0.15	0.80	1.23	0.73	5.15	7.98
25P	3.57	0.85	0.18	0.13	0.73	1.10	0.37	4.43	7.12
10P	2.60	0.73	0.17	0.12	0.68	1.00	0.32	3.83	6.50
S.D./Mean	2.07	3.55	2.22	3.52	0.74	1.16	1.58	0.44	0.52
90P-50P	3.88	2.58	0.07	0.05	0.22	0.55	4.32	1.62	2.10
(90P-50P)/50P	0.79	1.16	0.31	0.33	0.27	0.45	5.89	0.31	0.26

**Table A2.4.2-8** Activity times for various geo-fences, Canada-to-US direction, Ambassador Bridge

Fence	Amb caapproach	Amb huronchrchrd	Amb caplaza	Amb cabridge	Amb usbridge	Amb usplaza	Amb ustoll	Amb usplaza tollfca
#	7446	7665	7670	7673	7666	7674	7512	7639
Mean	7.98	4.44	0.99	1.39	0.88	7.72	0.47	0.20
S.D.	2.70	1.63	0.71	0.77	0.87	7.08	1.77	0.75
Max	165.87	39.68	35.00	45.00	50.00	95.00	85.42	65.00
Min	0.67	0.78	0.22	0.42	0.10	1.32	0.08	0.10
90P	9.67	5.63	1.13	1.58	0.97	16.43	0.92	0.25
75P	8.73	5.13	1.00	1.43	0.85	10.12	0.43	0.22
50P	7.82	3.95	0.90	1.32	0.75	5.23	0.23	0.17
25P	6.95	3.65	0.83	1.22	0.68	2.78	0.17	0.15
10P	6.23	3.45	0.78	1.13	0.63	2.15	0.13	0.13
S.D./Mean	0.34	0.37	0.71	0.55	0.98	0.92	3.77	3.72
90P-50P	1.85	1.68	0.23	0.27	0.22	11.20	0.68	0.08
(90P-50P)/50P	0.24	0.43	0.26	0.20	0.29	2.14	2.93	0.50

**Table A2.4.2-9** Activity times for various geo-fences in the US-to-Canada direction at the Blue Water Bridge.

	Bwb 6994split	Bwb splitplaza	Bwb rte25collect	Bwb usplazabridge	Bwb caplazabridge	Bwb caapproach
#	3786	3788	3778	3797	3797	3783
Mean	1.28	3.73	1.30	1.35	1.99	5.85
S.D.	0.69	5.22	2.82	0.86	1.69	9.31
Max	26.82	146.18	79.15	40.00	45.00	353.17
Min	0.10	0.57	0.10	0.12	0.82	0.55
90P	1.37	3.58	2.22	1.52	3.00	5.92
75P	1.32	3.37	1.17	1.40	2.02	5.37
50P	1.28	3.23	0.72	1.28	1.53	5.08
25P	1.22	3.12	0.58	1.18	1.35	4.87
10P	1.05	3.02	0.52	1.10	1.23	4.70
S.D./Mean	0.54	1.40	2.18	0.64	0.85	1.59
90P-50P	0.08	0.35	1.50	0.23	1.47	0.83
(90P-50P)/50P	0.06	0.11	2.09	0.18	0.96	0.16

**Table A2.4.2-10** Activity times for various geo-fences in the Canada-to-US direction at the Blue Water Bridge.

	Bwb caapproach	Bwb caplazabridge	Bwb usplazabridge	Bwb rte25collect	Bwb splitplaza	Bwb 6994splt
#	2857	2860	2859	2857	2856	2853
Mean	7.38	1.90	5.48	1.52	3.65	1.28
S.D.	9.72	1.93	5.85	4.16	7.84	1.05
Max	124.70	40.83	49.90	81.90	418.88	55.00
Min	0.88	0.38	0.83	0.13	2.10	0.35
90P	7.07	2.02	13.03	1.30	3.85	1.38
75P	5.97	1.80	7.12	1.08	3.58	1.32
50P	5.47	1.65	3.07	0.93	3.40	1.27
25P	5.13	1.52	1.65	0.82	3.27	1.17
10P	4.88	1.42	1.38	0.73	3.17	1.08
S.D./Mean	1.32	1.02	1.07	2.75	2.15	0.82
90P-50P	1.60	0.37	9.97	0.37	0.45	0.12
(90P-50P)/50P	0.29	0.22	3.25	0.39	0.13	0.09

**Table A2.4.2-11** Excess times for various geo-fences in the US-to-Canada direction at the Ambassador Bridge.

	Amb usapproach	Amb* usdutyfree	Amb* usplazatoll2ca	Amb* usplazatoll2caexit	Amb usbridge	Amb cabridge	Amb caplaza	Amb huronchrchrd	Amb caapproach
#	4424	4424	4424	4424	4424	4424	4424	4424	4424
Mean	3.07	0.99	0.09	0.04	0.24	0.51	1.70	2.63	3.78
S.D.	2.78	5.06	0.13	0.07	0.45	1.56	3.11	2.30	5.69
Max	126.26	177.69	4.35	1.73	15.38	64.49	95.69	86.51	346.05
Min	0.76	0.00	0.00	0.00	0.00	0.00	0.00	0.09	0.25
90P	4.54	0.69	0.13	0.08	0.40	0.75	4.75	4.07	5.72
75P	3.40	0.46	0.10	0.05	0.28	0.39	2.29	3.27	4.41
50P	2.61	0.32	0.08	0.03	0.19	0.22	0.53	2.40	3.32
25P	2.04	0.22	0.05	0.00	0.12	0.10	0.15	1.63	2.40
10P	1.68	0.15	0.03	0.00	0.06	0.01	0.09	0.98	1.74
S.D./Mean	0.90	5.09	1.52	1.64	1.84	3.06	1.83	0.88	1.51
90P-50P	1.93	0.38	0.06	0.05	0.21	0.53	4.22	1.67	2.40
(90P-50P)/50P	0.74	1.18	0.78	1.93	1.13	2.39	7.98	0.70	0.72
Free flow time	2.54/1.67/1.42	0.54	0.17	0.11	0.64	1.04	0.25	2.95	4.82

**Table A2.4.2-12** Excess times for various geo-fences in the Canada-to-US direction at the Ambassador Bridge.

	Amb caapproach	Amb huronchrchrd	Amb caplaza	Amb cabridge	Amb usbridge	Amb usplaza	Amb ustoll	Amb usplaza tollfca
#	7277	7277	7277	7277	7277	7277	7277	7277
Mean	3.34	1.54	0.31	0.23	0.18	6.21	0.30	0.10
S.D.	1.97	1.56	0.58	0.53	0.62	7.05	1.57	0.08
Max	65.18	36.82	20.37	15.54	9.07	93.53	80.89	1.85
Min	0.00	0.00	0.00	0.00	0.00	0.00	0.00	0.00
90P	5.03	2.74	0.46	0.42	0.26	14.92	0.73	0.17
75P	4.11	2.25	0.32	0.28	0.14	8.59	0.26	0.12
50P	3.20	1.05	0.23	0.16	0.05	3.71	0.07	0.09
25P	2.32	0.75	0.16	0.06	0.00	1.29	0.02	0.07
10P	1.61	0.55	0.11	0.00	0.00	0.65	0.00	0.05
S.D./Mean	0.59	1.01	1.87	2.29	3.39	1.14	5.18	0.75
90P-50P	1.83	1.69	0.23	0.26	0.21	11.22	0.65	0.08
(90P-50P)/50P	0.57	1.61	0.99	1.60	3.78	3.02	8.89	0.97
Free flow time	4.62	2.89	.66	1.15	.70	1.51	.12	.10

**Table A2.4.2-13** Excess times for various geo-fences in the US-to-Canada direction, Blue Water Bridge

	Bwb 6994split	Bwb splitplaza	Bwb rte25collect	Bwb usplazabridge	Bwb caplazabridge	Bwb caapproach
#	3763	3763	3763	3763	3763	3763
Mean	0.10	0.94	0.91	0.43	0.91	2.19
S.D.	0.46	5.19	2.77	0.59	1.53	9.27
Max	25.61	143.40	78.76	18.74	29.20	348.48
Min	0.00	0.03	0.00	0.00	0.00	0.00
90P	0.15	0.80	1.81	0.61	1.92	2.28
75P	0.10	0.59	0.80	0.49	0.96	1.71
50P	0.07	0.46	0.34	0.37	0.47	1.43
25P	0.05	0.34	0.21	0.28	0.28	1.21
10P	0.02	0.25	0.15	0.20	0.17	1.04
S.D./Mean	4.68	5.51	3.04	1.38	1.68	4.24
90P-50P	0.08	0.34	1.47	0.24	1.45	0.85
(90P-50P)/50P	1.04	0.75	4.33	0.63	3.12	0.59
Free flow time	1.22	2.77	.38	.92	1.07	3.67

**Table A2.4.2-14** Excess times for various geo-fences in the Canada-to-US direction, Blue Water Bridge

	Bwb caapproach	Bwb caplazabridge	Bwb usplazabridge	Bwb rte25collect	Bwb splitplaza	Bwb 6994splt
#	2847	2847	2847	2847	2847	2847
Mean	3.04	0.60	4.47	1.00	0.72	0.11
S.D.	8.03	1.71	5.81	3.99	7.80	0.13
Max	120.70	34.62	48.90	80.54	415.78	2.79
Min	0.04	0.00	0.00	0.00	0.00	0.00
90P	3.07	0.72	11.97	0.80	0.94	0.19
75P	1.98	0.53	6.11	0.60	0.67	0.13
50P	1.46	0.37	2.06	0.45	0.48	0.09
25P	1.13	0.24	0.65	0.34	0.35	0.07
10P	0.89	0.16	0.39	0.26	0.26	0.04
S.D./Mean	2.64	2.87	1.30	3.98	10.82	1.11
90P-50P	1.61	0.35	9.91	0.35	0.47	0.10
(90P-50P)/50P	1.10	0.93	4.81	0.77	0.99	1.10
Free flow time	4.00	1.27	1.00	.48	2.90	1.19

**Table A2.4.2-15** Total crossing times in both directions at the two bridges, with and without duty-free times included

Crossing Time	With duty-free				Without duty-free	
	Ambassador Bridge		Blue Water Bridge		Ambassador Bridge	Blue Water Bridge
	US-to-Canada	Canada-to-US	US-to-Canada	Canada-to-US	Canada-to-US	Canada-to-US
#	9195	8619	3797	3892	7674	2860
Mean	13.58	24.90	10.29	16.93	24.93	16.13
S.D.	14.43	8.74	6.72	20.76	8.51	17.24
Max	543.30	181.18	158.63	543.52	181.18	386.65
Min	3.22	6.15	1.93	4.70	7.00	5.03
90P	19.73	35.17	12.13	26.07	35.22	24.93
75P	13.92	27.87	10.18	16.87	27.92	16.18
50P	11.12	22.55	9.10	11.77	22.63	11.62
25P	9.47	19.58	8.45	9.98	19.63	9.92
10P	8.38	17.68	8.05	9.18	17.72	9.17
S.D./Mean	1.06	0.35	0.65	1.23	0.34	1.07
90P-50P	8.62	12.62	3.03	14.30	12.58	13.32
(90P-50P)/50P	0.78	0.56	0.33	1.22	0.56	1.15

**Table A2.4.2-16** Total excess times in both directions at the two bridges

Excess Time	Ambassador Bridge		Blue Water Bridge	
	US-to-Canada	Canada-to-US	US-to-Canada	Canada-to-US
#	9192	7277	3763	2847
Mean	2.17	6.21	0.91	4.47
S.D.	3.70	7.05	1.53	5.81
Max	95.81	93.53	29.20	48.90
Min	0.00	0.00	0.00	0.00
90P	5.74	14.92	1.92	11.97
75P	2.67	8.59	0.96	6.11
50P	0.80	3.71	0.47	2.06
25P	0.32	1.29	0.28	0.65
10P	0.14	0.65	0.17	0.39
S.D./Mean	1.71	1.14	1.68	1.30
90P-50P	4.93	11.22	1.45	9.91
(90P-50P)/50P	6.14	3.02	3.12	4.81

**Table A2.4.2-17** Toll collection and customs inspection gap activity times in both directions at the two bridges.

Activity Time	Ambassador Bridge				Blue Water Bridge			
	US-to-Canada		Canada-to-US		US-to-Canada		Canada-to-US	
	Toll*	Customs	Toll	Customs	Toll	Customs	Toll	Customs
#	3356	9136	7632	6507	2044	3720	2821	2818
Mean	0.05	1.32	0.61	1.48	0.04	1.06	0.54	1.75
S.D.	0.06	0.87	0.25	0.89	0.48	0.53	0.27	1.18
Max	2.92	17.77	6.88	12.05	16.28	11.27	10.53	26.90
Min	0.02	0.02	0.07	0.02	0.02	0.03	0.07	0.03
90P	0.07	1.98	0.78	2.45	0.03	1.45	0.72	2.85
75P	0.05	1.45	0.65	1.80	0.03	1.13	0.58	1.95
50P	0.05	1.13	0.57	1.27	0.02	0.95	0.50	1.47
25P	0.03	0.90	0.48	0.93	0.02	0.80	0.43	1.15
10P	0.03	0.73	0.43	0.70	0.02	0.68	0.40	0.92
S.D./Mean	1.21	0.66	0.41	0.61	11.08	0.50	0.50	0.68
90P-50P	0.02	0.85	0.22	1.18	0.02	0.50	0.22	1.38
(90P-50P)/50P	0.33	0.75	0.38	0.93	1.00	0.53	0.43	0.94

**Table A2.4.2-18** Toll collection and customs inspection gap excess times in both directions, at the two bridges

Excess Time	Ambassador Bridge				Blue Water Bridge			
	US-to-Canada		Canada-to-US		US-to-Canada		Canada-to-US	
	Toll*	Customs	Toll	Customs	Toll	Customs	Toll	Customs
#	3343	3343	6478	6478	2026	2026	2790	2790
Mean	0.01	1.26	0.49	1.44	0.02	1.03	0.52	1.71
S.D.	0.06	0.85	0.25	0.89	0.28	0.47	0.27	1.19
Max	2.88	12.91	6.77	11.55	9.55	6.28	10.52	26.85
Min	0.00	0.00	0.00	0.00	0.00	0.02	0.03	0.00
90P	0.02	1.94	0.68	2.43	0.01	1.42	0.70	2.81
75P	0.01	1.39	0.54	1.76	0.00	1.10	0.56	1.90
50P	0.00	1.07	0.45	1.24	0.00	0.93	0.47	1.42
25P	0.00	0.85	0.38	0.91	0.00	0.79	0.42	1.11
10P	0.00	0.67	0.32	0.68	0.00	0.67	0.38	0.88
S.D./Mean	8.41	0.68	0.52	0.62	17.52	0.46	0.52	0.69
90P-50P	0.02	0.87	0.23	1.19	0.01	0.48	0.22	1.39
(90P-50P)/50P	19.49	0.81	0.50	0.97		0.52	0.48	0.98

APPENDIX TO SECTION 3  
FIGURES AND TABLES IN SUPPORT OF VALIDATION STUDY

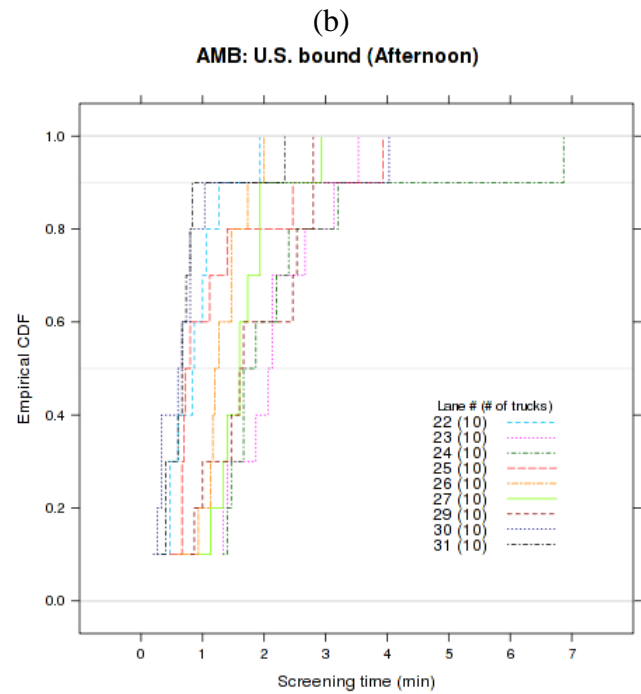
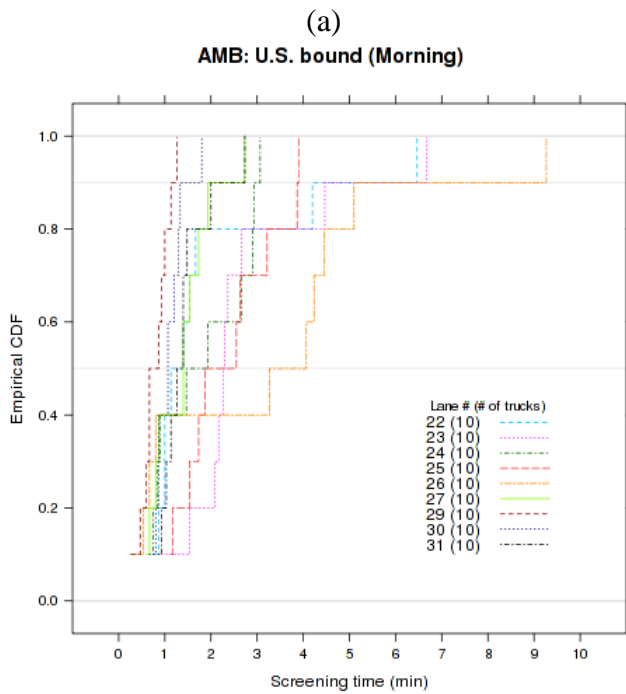
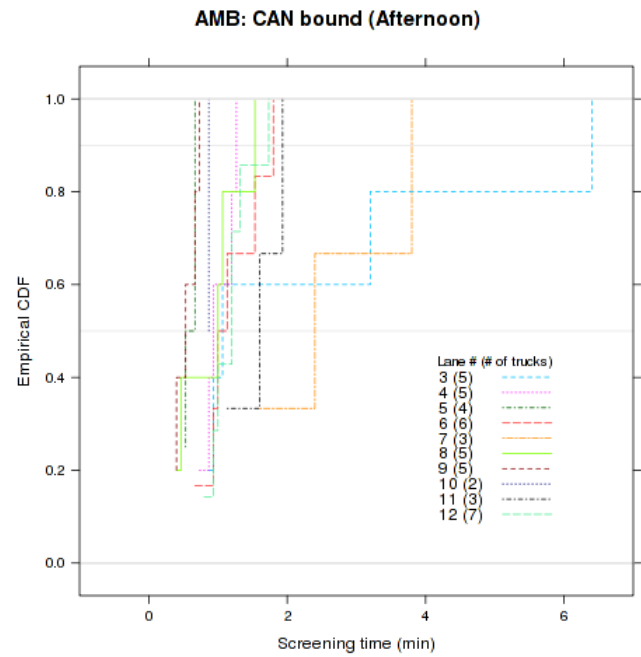
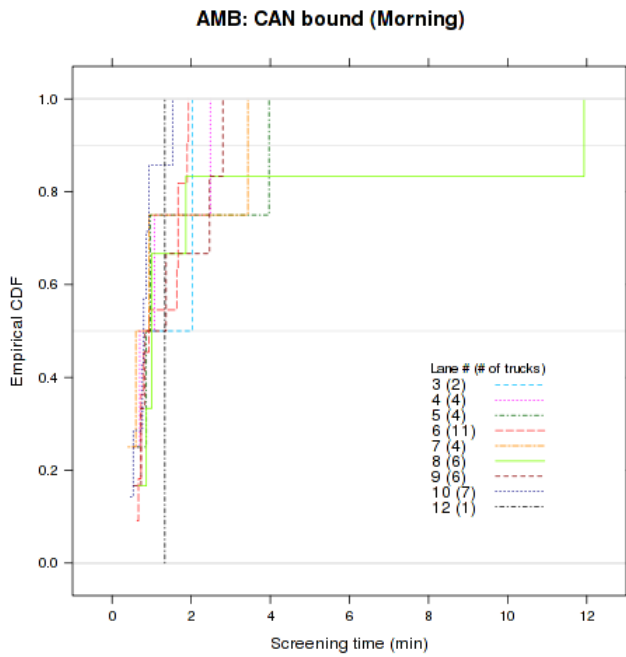


**Figure A3.2-1:** ECDF of screening times (min), by lane, derived from air photos at the Ambassador Bridge crossing

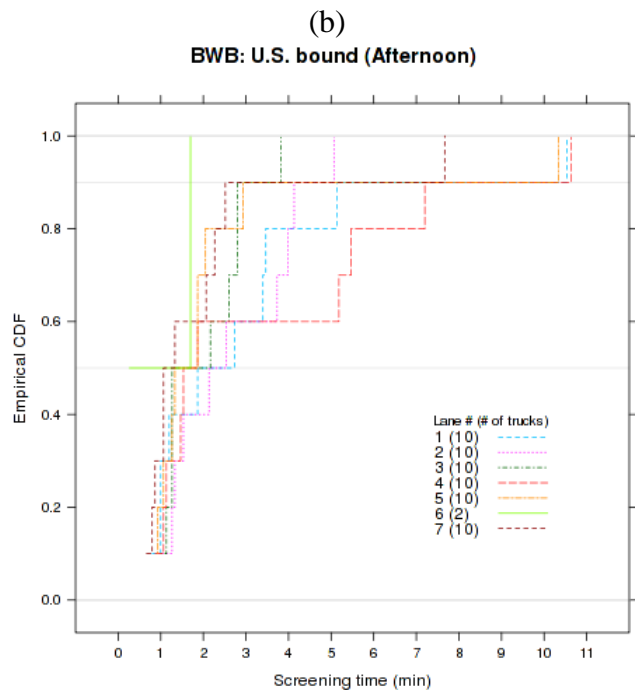
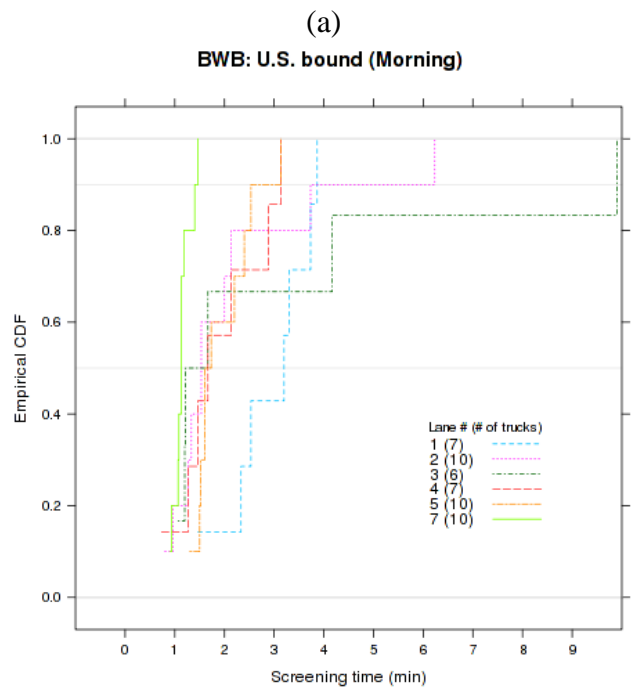
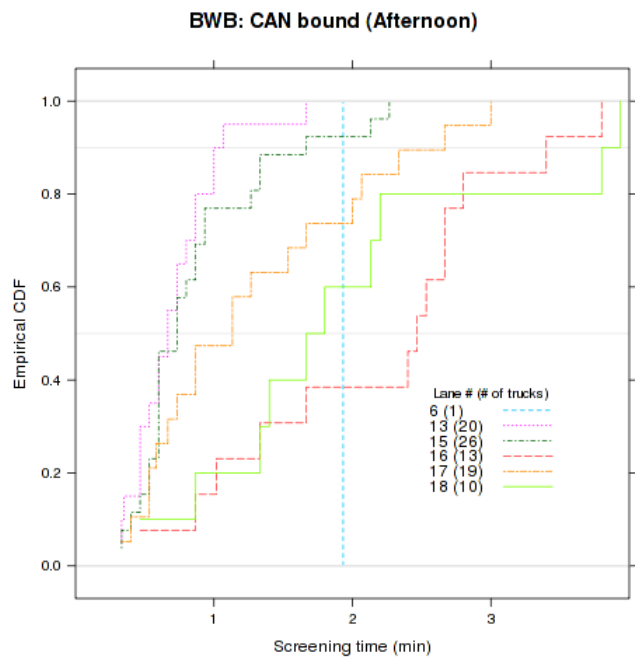
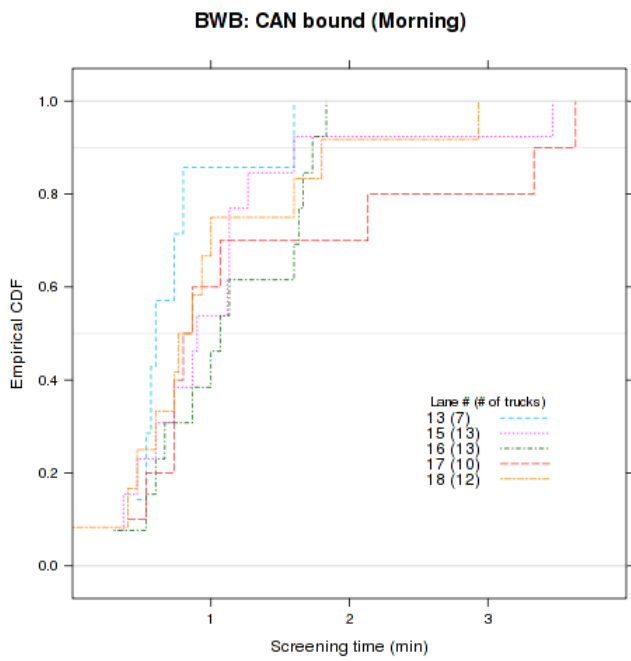


**Figure A3.2-2:** ECDF of screening times (min), by lane, derived from air photos at the Blue Water Bridge crossing

**Table A3.2-1: Summary statistics of screening times (min), by lane, derived from air photos**

**Ambassador Bridge**

**U.S. to CAN, Morning:**

Lane	n	mean	SD	10%	50%	90%	95%	90%-50%	95%-50%
3	2	1.52	0.73	1.10	1.52	1.93	1.98	0.41	0.46
4	4	1.20	0.89	0.58	0.88	2.06	2.27	1.18	1.39
5	4	1.58	1.60	0.63	0.92	3.07	3.52	2.15	2.60
6	11	1.21	0.54	0.67	0.93	1.90	1.92	0.97	0.98
7	4	1.34	1.41	0.46	0.77	2.68	3.06	1.92	2.29
8	6	2.89	4.45	0.77	1.00	6.90	9.42	5.90	8.42
9	6	1.46	0.96	0.63	1.10	2.63	2.72	1.53	1.62
10	7	0.84	0.35	0.51	0.80	1.17	1.35	0.37	0.55
12	1	1.33	NA	1.33	1.33	1.33	1.33	0.00	0.00

**U.S. to CAN, Afternoon:**

Lane	n	mean	SD	10%	50%	90%	95%	90%-50%	95%-50%
3	5	2.49	2.39	0.89	1.07	5.12	5.76	4.05	4.69
4	5	1.00	0.23	0.79	0.93	1.24	1.25	0.31	0.32
5	4	0.60	0.08	0.53	0.60	0.67	0.67	0.07	0.07
6	6	1.18	0.42	0.80	1.07	1.67	1.73	0.60	0.67
7	3	2.60	1.11	1.76	2.40	3.52	3.66	1.12	1.26
8	5	0.89	0.47	0.43	1.00	1.35	1.44	0.35	0.44
9	5	0.55	0.15	0.40	0.53	0.71	0.72	0.17	0.19
10	2	0.87	0.00	0.87	0.87	0.87	0.87	0.00	0.00
11	3	1.56	0.40	1.23	1.60	1.87	1.90	0.27	0.30
12	7	1.17	0.31	0.88	1.20	1.48	1.61	0.28	0.41

**CAN to U.S., Morning:**

Lane	n	mean	SD	10%	50%	90%	95%	90%-50%	95%-50%
22	10	2.01	1.85	0.86	1.27	4.43	5.45	3.16	4.18
23	10	2.75	1.65	1.47	2.28	4.69	5.68	2.40	3.39
24	10	1.82	1.00	0.75	1.70	2.95	3.01	1.25	1.31
25	10	2.36	1.04	1.16	2.21	3.87	3.88	1.66	1.68
26	10	3.27	2.82	0.51	3.67	5.52	7.39	1.85	3.72
27	10	1.37	0.67	0.66	1.40	2.01	2.37	0.61	0.97
29	10	0.79	0.31	0.45	0.77	1.15	1.21	0.38	0.44
30	10	1.10	0.33	0.79	1.07	1.38	1.59	0.31	0.52
31	10	1.43	0.56	0.93	1.33	2.07	2.40	0.74	1.07

**CAN to U.S., Afternoon:**

Lane	n	mean	SD	10%	50%	90%	95%	90%-50%	95%-50%
22	10	0.88	0.47	0.45	0.85	1.33	1.63	0.48	0.78
23	10	2.16	0.76	1.33	2.10	3.17	3.35	1.07	1.25
24	10	2.41	1.67	1.39	1.77	3.57	5.22	1.80	3.45
25	10	1.29	1.09	0.65	0.76	2.61	3.27	1.85	2.51
26	10	1.30	0.40	0.90	1.23	1.76	1.88	0.53	0.65
27	10	1.65	0.55	1.11	1.60	2.03	2.48	0.43	0.88
29	10	1.80	0.79	0.86	1.63	2.80	2.80	1.17	1.17
30	10	0.91	1.13	0.26	0.63	1.33	2.68	0.70	2.05
31	10	0.77	0.58	0.39	0.67	0.98	1.66	0.32	0.99

**Bluewater Bridge**

**U.S. to CAN, Morning:**

Lane	n	mean	SD	10%	50%	90%	95%	90%-50%	95%-50%
13	7	0.76	0.39	0.51	0.60	1.12	1.36	0.52	0.76
15	13	1.08	0.81	0.39	0.90	1.53	2.35	0.63	1.45
16	13	1.13	0.52	0.55	1.07	1.72	1.77	0.65	0.71
17	10	1.42	1.19	0.52	0.83	3.36	3.50	2.53	2.66
18	12	1.01	0.78	0.41	0.82	1.78	2.31	0.96	1.49

**U.S. to CAN, Afternoon:**

Lane	n	mean	SD	10%	50%	90%	95%	90%-50%	95%-50%
13	20	0.71	0.32	0.35	0.67	1.01	1.10	0.34	0.43
15	26	0.88	0.51	0.43	0.73	1.50	2.02	0.77	1.28
16	13	2.16	1.01	0.90	2.47	3.28	3.56	0.81	1.09
17	19	1.28	0.81	0.51	1.13	2.40	2.70	1.27	1.57
18	10	1.96	1.14	0.83	1.73	3.81	3.87	2.08	2.14

**CAN to U.S., Morning:**

Lane	n	mean	SD	10%	50%	90%	95%	90%-50%	95%-50%
1	7	2.92	0.86	1.99	3.20	3.79	3.83	0.59	0.63
2	10	2.15	1.65	0.95	1.53	3.98	5.11	2.45	3.57
3	6	3.20	3.48	1.13	1.44	7.03	8.47	5.59	7.03
4	7	1.90	0.87	1.05	1.67	2.98	3.06	1.32	1.39
5	10	1.95	0.59	1.48	1.67	2.59	2.86	0.93	1.20
7	10	1.14	0.18	0.93	1.13	1.41	1.44	0.27	0.30

**CAN to U.S., Afternoon:**

Lane	n	mean	SD	10%	50%	90%	95%	90%-50%	95%-50%
1	10	3.11	2.96	0.98	2.30	5.67	8.10	3.37	5.80
2	10	2.66	1.46	1.23	2.33	4.23	4.65	1.89	2.31
3	10	2.01	0.96	1.12	1.72	2.90	3.36	1.18	1.64
4	10	3.64	3.34	1.05	1.70	7.54	9.09	5.84	7.39
5	10	2.46	2.84	0.93	1.60	3.67	7.00	2.07	5.40
7	10	2.03	2.09	0.79	1.20	3.03	5.35	1.83	4.15

**Table A3.2-2: Summary statistics of queuing times (min), by lane, derived from air photos**

**Ambassador Bridge**

**U.S. to CAN, Morning:**

Lane	n	mean	SD	10%	50%	90%	95%	90%-50%	95%-50%
3	2	2.10	2.78	0.53	2.10	3.67	3.87	1.57	1.77
4	4	1.66	2.01	0.40	0.90	3.52	4.08	2.62	3.18
5	4	0.32	0.21	0.15	0.27	0.52	0.56	0.25	0.29
6	11	1.96	2.19	0.27	1.40	3.90	5.65	2.50	4.25
7	4	0.72	0.82	0.22	0.37	1.49	1.71	1.13	1.35
8	6	0.31	0.09	0.23	0.30	0.40	0.43	0.10	0.13
9	6	1.81	3.26	0.10	0.20	5.12	6.71	4.92	6.51
10	7	1.78	2.02	0.17	1.00	4.40	4.85	3.40	3.85
12	1	0.07	NA	0.07	0.07	0.07	0.07	0.00	0.00

**U.S. to CAN, Afternoon:**

Lane	n	mean	SD	10%	50%	90%	95%	90%-50%	95%-50%
3	5	0.43	0.41	0.16	0.27	0.84	0.99	0.57	0.72
4	5	0.27	0.16	0.16	0.20	0.43	0.48	0.23	0.28
5	4	0.20	0.09	0.13	0.17	0.29	0.31	0.13	0.15
6	6	0.19	0.07	0.13	0.20	0.23	0.25	0.03	0.05
7	3	0.20	0.07	0.15	0.20	0.25	0.26	0.05	0.06
8	5	0.23	0.04	0.20	0.20	0.27	0.27	0.07	0.07
9	5	0.27	0.05	0.23	0.27	0.31	0.32	0.04	0.05
10	2	0.27	0.09	0.21	0.27	0.32	0.33	0.05	0.06
11	3	0.18	0.04	0.15	0.20	0.20	0.20	0.00	0.00
12	7	0.27	0.05	0.20	0.27	0.33	0.33	0.07	0.07

**CAN to U.S., Morning:**

Lane	n	mean	SD	10%	50%	90%	95%	90%-50%	95%-50%
22	12	9.05	5.72	4.75	7.47	14.50	19.28	7.03	11.82
23	11	11.92	4.47	7.17	11.73	16.50	18.32	4.77	6.58
24	11	12.37	11.93	6.37	8.90	13.70	30.62	4.80	21.72
25	10	13.50	4.35	9.72	13.03	17.59	20.68	4.55	7.64
26	10	15.64	10.75	6.68	11.53	33.62	34.46	22.09	22.93
27	14	8.05	3.73	5.50	7.78	9.54	13.16	1.76	5.38
28	1	2.60	NA	2.60	2.60	2.60	2.60	0.00	0.00
29	23	5.98	2.94	4.13	5.10	7.26	7.36	2.16	2.26
30	15	5.57	1.88	3.92	4.60	8.39	8.76	3.79	4.16
31	15	7.67	8.38	3.72	5.13	9.03	17.52	3.90	12.39

**CAN to U.S., Afternoon:**

Lane	n	mean	SD	10%	50%	90%	95%	90%-50%	95%-50%
22	6	5.12	2.05	3.23	4.85	7.27	7.97	2.42	3.12
23	5	4.75	2.96	2.16	4.07	7.96	8.55	3.89	4.48
24	5	4.31	0.82	3.48	4.27	5.11	5.15	0.84	0.89
25	8	4.58	3.55	2.09	3.03	9.93	10.40	6.90	7.37
26	8	3.43	2.18	1.72	2.40	6.58	6.86	4.18	4.46
27	7	4.30	2.80	1.57	4.60	6.99	8.13	2.39	3.53
29	7	2.59	0.43	2.16	2.53	3.09	3.11	0.56	0.58
30	5	2.63	0.50	2.09	2.80	3.09	3.15	0.29	0.35
31	4	2.15	0.14	2.04	2.13	2.27	2.30	0.14	0.17

**Bluewater Bridge**

**U.S. to CAN, Afternoon:**

Lane	n	mean	SD	10%	50%	90%	95%	90%-50%	95%-50%
13	7	1.50	0.18	1.32	1.43	1.73	1.75	0.29	0.31
15	13	1.78	0.39	1.42	1.77	2.39	2.48	0.62	0.71
16	13	1.89	1.10	1.37	1.57	2.29	3.56	0.72	1.99
17	10	1.94	0.49	1.53	1.67	2.53	2.65	0.86	0.98
18	12	1.88	0.69	1.25	1.50	2.97	3.04	1.47	1.54

**U.S. to CAN, Afternoon:**

Lane	n	mean	SD	10%	50%	90%	90%-50%	95%-50%
13	20	1.86	0.54	1.37	1.63	2.77	1.14	1.21
15	26	7.69	3.90	2.98	6.60	12.03	5.43	5.74
16	13	8.77	4.53	3.47	9.30	14.21	4.91	5.37
17	19	8.66	6.04	3.35	5.77	17.75	11.99	12.62
18	10	11.88	6.71	4.90	9.27	19.39	10.13	10.85

**CAN to U.S., Morning:**

Lane	n	mean	SD	10%	50%	90%	95%	90%-50%	95%-50%
2	2	21.90	1.51	21.05	21.90	22.75	22.86	0.85	0.96
4	1	20.83	NA	20.83	20.83	20.83	20.83	0.00	0.00
5	1	22.37	NA	22.37	22.37	22.37	22.37	0.00	0.00
7	14	3.71	1.83	1.97	3.45	6.11	6.88	2.66	3.43

**CAN to U.S., Afternoon:**

Lane	n	mean	SD	10%	50%	90%	95%	90%-50%	95%-50%
1	8	11.00	2.41	8.17	11.14	13.60	14.26	2.46	3.12
2	13	9.70	2.81	6.43	9.37	12.47	13.76	3.11	4.39
3	7	9.14	3.05	5.91	10.20	12.03	12.83	1.83	2.63
4	4	6.49	5.84	3.23	3.88	11.84	13.54	7.96	9.65
5	3	12.63	1.35	11.51	13.17	13.54	13.59	0.37	0.42
7	5	4.93	4.10	1.35	3.27	9.39	9.51	6.13	6.25

This page left intentionally blank.